Digital Surface Representation and the Constructibility of Gehry's Architecture

by

Dennis R. Shelden
Director of Computing, Gehry Partners, LLP.
MS Civil and Environmental Engineering, MIT, 1997

Submitted to the Department of Architecture
in partial fulfillment of the requirements for the degree of

DOCTOR OF PHILOSOPHY IN THE FIELD OF ARCHITECTURE:
DESIGN AND COMPUTATION
AT THE MASACHUSETTS INSTITUTE OF TECHNOLOGY

SEPTEMBER 2002

Signature of Author: _____
Department of Architecture
August 9, 2002

Certified by: _____
William J. Mitchell
Dean of the School of Architecture and Planning
Professor of Architecture and Media Arts and Sciences
Thesis Supervisor

Certified by: _____
Stanford Anderson
Professor of History and Architecture
Chair, Department Committee on Graduate Students

READERS

William J. Mitchell
Dean of the School of Architecture and Planning,
Professor of Architecture and Media Arts and Sciences, MIT
Thesis Supervisor

John R. Williams
Associate Professor of Civil and Environmental Engineering,
Associate Engineering Systems, MIT

George Stiny
Professor of Design and Computation, MIT

Digital Surface Representation and the Constructibility of Gehry's Architecture

by

Dennis R. Shelden
Director of Computing, Gehry Partners, LLP.
MS Civil and Environmental Engineering, MIT, 1997

Submitted To The Department Of Architecture on August 9, 2002
in Partial Fulfillment of the Requirements for the Degree of
Doctor of Philosophy in the Field Of Architecture: Design And Computation

ABSTRACT

This thesis presents work in the development of computational descriptions of Gehry's architectural forms. In Gehry's process for realizing buildings, computation serves as an intermediary agent for the integration of design intent with the geometric logics of fabrication and construction. This agenda for digital representation of both formal and operational intentions, in the context of an ongoing exploration of challenging geometries, has provided new roles for computation in architectural practice.

The work described in this thesis focuses on the digital representation of surface geometry and its capacity for describing the constructibility of building enclosure systems. A particular class of *paper surface* forms – curved surfaces with minimal in plane deformation of the surface material – provide the specific object of inquiry for exploring the relationships between form, geometry and constructibility.

An analysis and framework for the description of Gehry's geometry is developed through existing theory of differential geometry and topology. Geometric rules of constructibility associated with several enclosure system strategies are presented in this framework. With this theoretical framework in place, the discussion turns to efforts to develop generative strategies for the rationalization of surface forms into constructible configurations.

Thesis Supervisor: William J. Mitchell
Title: Dean of the School of Architecture and Planning,
Professor of Architecture and Media Arts and Sciences, MIT

ACKNOWLEDGEMENTS

A work of this nature owes a heavy debt of gratitude to many persons. During the time that this thesis has been prepared, it has been my rare privilege to work closely with a number of enormously talented individuals, both members of Gehry's firm as well as those of associated engineering, construction and fabrication organizations. The products of their efforts are often referenced in this work, and the inspiration for this inquiry would not have occurred without their influence. In the interest of brevity, I can unfortunately only mention a few of their names.

The first and foremost debt of gratitude is owed to Frank Gehry himself. His design vision and exploratory energy have fostered the community of talent and ideas in which the work described in this document has occurred. The efforts to realize his design ambitions have resulted in a context of architectural and building practice for which there is perhaps no equivalent at this point of writing. Furthermore, his commitment to the achievement of these design intentions have translated into a support of computational efforts beyond that of his contemporaries, and have provided the environment for computational inquiry in which the work described in this document has taken place.

Jim Glymph has served as a mentor and inspiration on all matters architectural and computational during my time with the firm. The description of a reconstructed architectural practice presented in Part 1 of this document is largely attributable to many hours of formal and informal discussions with this visionary practitioner.

The opportunity to apply this research to the firm's projects has occurred through close collaboration with the senior designers and project architects on these projects. I gratefully acknowledge Partner Randy Jefferson, Project Designers Craig Webb and Edwin Chan, and Project Architects Terry Bell (Disney Concert Hall), Marc Salette (MIT Stata Center), George Metzger and Larry Tighe (Experience Music Project), Gerhard Mayer (Weatherhead) and Michal Sedlacek (Museum of Tolerance), for their support and willingness to accommodate these research efforts on their projects.

The firm's computational methodologies are similarly the product of many persons' efforts. The work of Rick Smith of C-Cubed, Kristin Woehl, Henry Brawner and Kurt Komraus on

projects is extensively referenced in this document, while the efforts of Reg Prentice and Cristiano Ceccato in the computing group have profoundly contributed to the development of the firm's computational practice. David Bonner of Dassault Systèmes Research and Development and John Weatherwax from Department of Mathematics at MIT assisted substantially in the formulation of the material simulation model described in Chapter VII.

On the academic front, I would like to thank the members of my Doctoral Committee, for their guidance and support of what has become a circuitous path to the completion of this thesis.

Finally, I thank the Reader, for taking the time and interest to review the thoughts contained herein.

TABLE OF CONTENTS

TABLE OF FIGURES

TABLE OF SYMBOLS

Topologies and manifolds

R ..... the set of real numbers, the real number line, the real number topology

$\mathbf{R}^n$ ..... n – dimensional Euclidean space, a Cartesian product of n real numbers

n, m, etc ..... the ordinality or degree of a Cartesian product space (e.g. $\mathbf{R}^n$)

I ..... the set of integers, the integer topology

Z ..... a set of discrete values, the discrete topology

α, β, ϕ, etc. ..... a mapping function of the form $\mathbf{R}^n \rightarrow \mathbf{R}^m$, e.g. curves and surfaces.

N, *M*, etc ..... a bounded region of space in $\mathbf{R}^n$, $\mathbf{R}^m$, etc.

a, b, c, etc. ..... a (typically scalar, real valued) variable

p, **q**, etc ..... a vector or vector field

i, j, *etc* ..... the index of a vector component (e.g. $\mathbf{p}_i$)

Curves and surfaces

t ..... a scalar parameter in the curve function $\alpha : t \rightarrow \mathbf{x}$

α', α'', etc, ... differentiation with respect to *t*

s ..... the unit arc length parameterization of a curve

$\dot{\alpha}, \ddot{\alpha}$, etc ..... differentiation with respect to *s*

u ..... a 2-dimensional position vector in $\mathbf{R}^2$ "parametric space"

u, v ..... the scalar components of $\mathbf{u}_i$

x ..... a 3-dimensional position vector in $\mathbf{R}^3$ "world space"

x, y, z ..... the scalar components of $\mathbf{x}_i$

Physical modeling

m ..... particle mass

M ..... the 3*n* x 3*n* particle mass matrix

t ..... time

h ..... time step (Δt)

n ..... vertex count

x ..... the 3*n* vector of particle locations

v ..... particle velocity

a ..... particle acceleration

$\mathbf{f}$ ..... force on a particle

$\mathbf{x}_i$ ..... $\mathbf{R}^3$ location of particle *i*

$\mathbf{x}^1, \mathbf{x}^2, \mathbf{x}^3,$ ..... the individual *(x,y,z)* coordinates

ϕ ..... the $\mathbf{R}^2 \rightarrow \mathbf{R}^3$ material mapping function

ω ..... the linear approximation of ϕ on a triangle

C ..... the behavior function

E ..... the system energy

K ..... a stiffness constant

REFERENCED PROJECTS AND ABBREVIATIONS

	Santa Monica Place, Santa Monica, CA 1973-80
	Gehry Residence, Santa Monica, California 1977-78; 1991-92
	Winston Guest House, Wayzata, Minnesota 1983-87
	Edgemar Development, Venice, California 1984-88
	Chiat Day Building, Venice, CA 1985-91
	Lewis Residence, Lyndhurst, Ohio, 1989-95 (unbuilt)
	Team Disneyland Administration Building, Anaheim, California 1987- 96
DCH	Walt Disney Concert Hall, Los Angeles, CA 1987-
Barcelona	Vila Olimpica, Barcelona, Spain 1989-92
Weissman	Frederick R. Weissman Art Museum, Minneapolis, Minnesota 1990-93
Bilbao	Guggenheim Museum Bilbao, Bilbao, Spain 1991-97
Prague	Nationale-Nederlanden Building, Prague, Czech Republic 1992-96
Dusseldorf	Der Neue Zollhof, Dusseldorf, Germany 1994-99
EMP	Experience Music Project, Seattle, Washington 1995-2000
Berlin	DG Bank Building, Berlin, Germany 1995-2001
Weatherhead	Peter B. Lewis Building, Weatherhead School of Management, Case Western Reserve University Cleveland, Ohio 1997-
MIT	Ray and Maria Stata Center, Cambridge, Massachusetts 1998-
OHR	Ohr-O'Keefe Museum, Biloxi, Mississippi 1999-
MOT	Winnick Institute Museum of Tolerance, Jerusalem, Israel 2000-

FOREWORD

Over the past decade, Gehry's firm has developed a unique and innovative approach to the process of delivering complex building projects. Computer based project information plays a vital and integral role in enabling this process. The concepts and strategies that have emerged though the development of the firm's methodologies offer profound lessons for the design community, not simply in the ways that computing may be applied to architectural practice, but in the ways by which computing methods can change the process of building. It is with an eye to providing further insight into this important example of computing and practice that this thesis has been prepared.

This thesis offers a view into Gehry Partner's computer aided design methodologies, based on the author's experiences with the firm over the past half decade. Rather than attempting to tell this story in a historical or encyclopedic fashion, this thesis takes as its object of inquiry a specific set of building intentions, and associated computational strategies, playing a fundamental role in the firm's work: *the design, engineering and fabrication of surface forms on Gehry's projects*. This set of issues is explored as a topic of substantial interest in its own right, while serving as an example of the larger sets of intentions exhibited by the firm's practice.

The qualities of materials and the role of craftsmanship as guiding intentions of Gehry's work have received considerable discussion[41]. These intentions have critical counterparts in project documentation and construction activities, and in associated computational constructs. The goal of adequately representing intentions of materiality and craft in digital form is perhaps the most important and complex aspect of the firm's computing efforts. These intentions are fundamental motivations of the firm's approach to digital representation of the geometry of project forms, and of the fabrication processes responsible for their realization. These are central themes of this thesis.

This body of this text is organized into three parts. Part 1 offers an introduction to the role of computing in Gehry's design and building delivery process. Computing is explored in its relationship to key project design, analysis and construction intentions. Important concepts guiding the development of the firm's computing efforts are presented, including the nature of geometric representations employed by the firm, and the role of analytically driven operations

on project geometry. A set of materially guided intentions fundamental to the generation of Gehry's surface forms are introduced. Examples and case studies are provided that demonstrate the application of these tenets on recent projects. This introductory section establishes the framework for the inquiry developed in the remainder of the text.

Part 2 focuses on developing a formal representation of materially guided surface forms. This section describes the firm's efforts to develop digital counterparts to the behavior of surface materials in modeling and fabrication. A review of the theory of topology and manifolds underlying representations of curved spatial objects is presented in Chapter V, followed by a rigorous formal exploration of the geometric structures employed by the firm and their applications to specific constructibility problems. A promising new approach to the representation of surfaces through physical modeling of material behaviors is presented in detail in Chapter VII. This Part establishes a unified geometric framework for the modeling, simulation and analysis of the elementary shape elements employed in the firm's designs.

Part 3 expands on this geometrical framework, in developing a formal methodology for considering assemblies of these basic surface elements. This extended framework has implications for the digital representation of project scale gestures, as well as utility for addressing localized surfacing system fabrication and assembly requirements. With a formal framework for the representation of surface organizations established, the discussion turns to operations on these assemblies. The potential is demonstrated for automaton of key processes addressing constructibility requirements of building systems. Several examples of these generative approaches to the design of surface systems are documented. The thesis concludes by presenting a computational framework for the generation of materially guided surface assemblies.

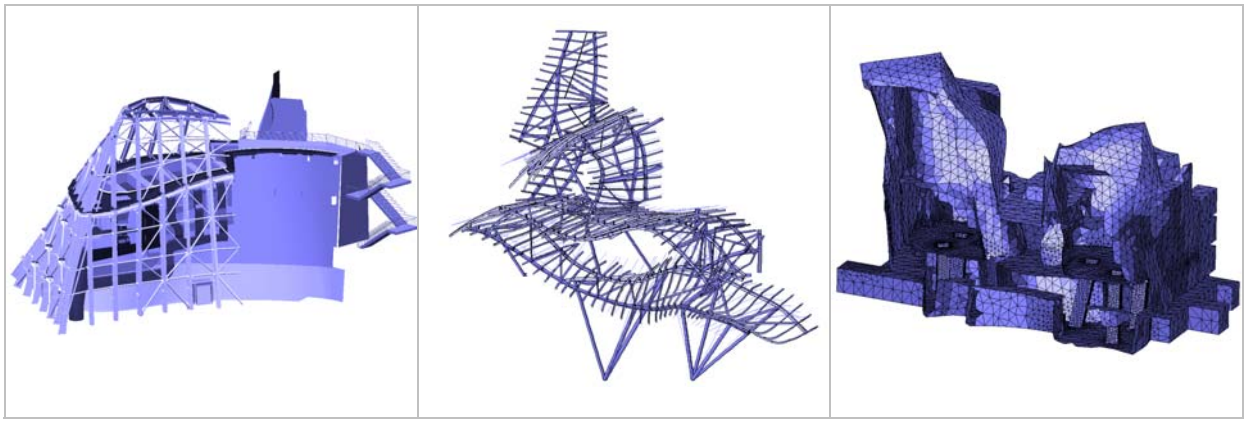

I. INTRODUCTION

It seems that Gehry's practice has become synonymous with cutting edge computing technology and CAD / CAM manufacturing processes. But the path to the firm's prominence in architectural computing applications has not been easy or straight forward. Gehry himself remains skeptical of computing as a tool for design[96]. He speaks with a certain degree of pride in his inability to operate a computer, and suggests that the quality of the digital image is dangerous and subversive to the designer's eye.

Gehry's design process is perhaps best characterized by its emphasis on physical objects as the principal artifacts on which design takes place. The firm places a unique emphasis on the development of designs through physical models, full scale mockups and other physical artifacts as the means for understanding and developing design intentions. These artifacts of include numerous sketch models, some undergoing active transformation while others wait on shelves or in storage, documented in photos, serving as records of design intentions at significant points in the process. These models are often deliberately developed to a rough, unfinished state, in order to allow suggestion of new directions of development as the designers contemplate the objects. The power of this design process springs in part from the ambiguity presented by this multiplicity of physical design representations.

These evocative qualities of the firm's designs persist in the further development of projects as they enter documentation and construction phases. Project engineering and detailing strategies are often developed that accommodate the real world indeterminacy of on-site construction events. Many building system strategies have involved in-situ fabrication and placement of system elements as a means for responding to on-site conditions. This reliance on the efforts of craftsmen, operating in the field, again reflects the profound concern for physical artifacts and events as driving elements of the design process and the aesthetic that results.

The role of computer-based methodologies in this fundamentally tactile, evocative process presents a dilemma. Contemporary CAD modeling capabilities seem to stand in marked contrast to these design intentions. CAD modeling strips away ambiguity, producing definitive geometric forms that "leave little to the imagination". These digital, logically founded

constructs stand in curious contrast to the indeterminacy of physical based activities and artifacts.

The physical / digital interactions, and the tension between these realms of the process have become fundamental to the success of the firm's design process. At the heart of the process is an ongoing affinity between a disparate set of design intentions, embodied in multiple physical representations, and a coherent set of computer based representations. The process utilizes the definitiveness computer representations at points in the process where it is appropriate, and draws these digital descriptions into the assemblage of representations. The computer based description represents the glue that ties the physical design representations together, and ultimately document their convergence. Computer representations allow the intentions embodied in multiple physical representations to be resolved, translations of scale to be performed, and incursion of system fabrication decisions to be resolved into the design intent.

Three dimensional computer aided design applications provide a critical characteristic relative to traditional building documentation, in the ability to translate design intentions from physical design artifacts to constructed objects without recourse to two-dimensional representations. On more "conventional" building projects, this direct translation is unnecessary and perhaps inefficient. Conventional two dimensional architectural documents, comprised of plans, sections, elevations and details, compress the full spatial and dimensional scope of a design into a set of inter-related representations. The regularity of an object whose dimensions may vary little or not at all from floor to floor can be efficiently described by a single floor plan background, repeated for each floor. Variations in fit out can be overlaid on this normalizing representation. Typical details may be specified as a single detailed drawing. Its application across the project is specified by annotation on floor plans or sections, or in specifications. For buildings with repetitive components, and regular floor plans, the necessity for individually describing each element as a three dimensional model correctly positioned in space would require substantial additional labor. The ability to mentally resolve multiple two-dimensional representations of a design into a coherent understanding of the three dimensional object and its methods of construction is a core part of traditional architectural training and heritage. Architects take a professional pride in the development of this mental ability.

The relationships between tools, process of making enabled by tools, and the objects produced by operating tools are subtle and deep. The operations enabled by a chosen tool guide the operator to make specific types of objects or products that the tool affords. The parallel rule and triangle, blue print and tracing paper overlay of conventional document production facilitated the design of orthogonally organized building designs. The compass allows circular arcs to be included in these compositions. When two-dimensional plans are extruded perpendicularly to the plane of the paper in a uniform fashion, a single drawing presents a slice through the designed objects whose applicability is invariant of where the cut is taken. The two dimensional drawing construction provides tremendous expressive power in describing this geometric regularity. In turn, the designer is subtly guided toward the development of designs for which the utility of this geometric construct holds. More elaborate geometries than simple extruded form are of course possible, by combining multiple sections either in parallel or orthogonally, but the “trace” of the tool is inevitably felt in the resulting designs.

The adoption of the tools of two-dimensional representation has provided a basis for the development of descriptive conventions unifying the building industries. This shared language has Euclidean geometric forms and their sectional representations as an underlying construct. Straight lines stand in for wall and floor planes, arcs represent cylindrical forms. Parallel bold lines represent vertical walls, dashed lines represent overhead elements, usually aligned with elements on a floor plan cut at a higher elevation. This common understanding among participants in a building project is so deeply shared that it eludes dissection. An architect and contactor can discuss the layout and construction of a building on the basis of a two dimensional floor plan without any discussion of what the elements in the drawing mean. In parallel with the development of this common language of Euclidean elements, numerous interwoven industries and industrial processes have been developed around the making of Euclidean objects and building components. Saw mills turn trees into straight lumber of square profile and flat, rectangular sheets of plywood, steel mills extrude molten steel into linear members with invariant profiles. Carpenters use plumb bobs, string, levels and 3:4:5 triangle measurements to produce straight, vertical walls and their perpendiculars. So pervasive has the “tyranny” of Euclidean geometry become in the building industries that any building designed without strict accordance to its rules is subject to characterization as impossible to build.

In Gehry's design process, physical model making is the principal design tool. This primacy of the construction of physical objects as the vehicle for design explorations in itself propels the firm's work beyond the constraints of the Euclidean rationale. In its place, a new set of guiding rules have been developed, directly related to the materials and operations available to the processes of object making. Viewed in isolation, the operations of physical modeling are insufficient to guarantee the constructibility of the full scale products that models are intended to represent. However, in Gehry's process, models serve not simply to describe the object in scale. Rather, the processes and materials of model making are brought into alignment with, and stand in for, those of craftsmen and fabricators on the resulting building construction. Materials and construction strategies are selected to emulate aspects of their full scale counterparts. This approach binds the operations of design directly to those of building, bypassing the filter of a common language of Euclidean geometry.

Prior to the firm's adoption of computing based practices, the firm's process suffered a key limitation in its methods of project documentation. While the firm could reasonably guarantee that the designs could be fabricated, the designs still required rendition into conventional two-dimensional description to support steps of the conventional construction process, including building permit submissions, bidding and on-site project layout. In order to bring the design back into the language of building industry convention, two dimensional plans, sections and elevations needed to be developed. Often, the forms of the models would require re-interpretation into conventional Euclidean forms of planes, cylinders and cones, simply to be consistently described through plans and sections.

Even with this painstaking development of project documentation, the geometry was still beyond the norms of conventional construction description. While fabricators could build the shapes, the process of bidding and coordinating the projects presented difficulty to construction managers. Accuracy of quantity takeoffs could not be guaranteed using conventional methods of measuring off of plans. Shop drawings – necessary for describing the detailed fabrication geometry – were difficult to render into orthogonal views. Spatial coordination of building elements became unmanageable as component details were developed. The limitations of understanding the project geometry through the lens of two dimensional views exacerbated perceptions of project complexity.

The history of the development of computer assisted building delivery by the firm in response to these limitations has been well documented[52]. Jim Glymph joined Gehry's firm in 1989. Glymph had substantial experience in the role of Executive Architect on several substantially complex building projects, including the San Diego and Los Angeles Convention Centers. At the time, 3D CAD was beginning to have application to architectural visualization, movie animation and automotive and aerospace design. Glymph realized that these technologies could be applied to the processes of *architectural documentation*, independent of the contemporary interest in the technology as a means for project visualization.

Initial forays into the technology were tentatively undertaken. The firm selected the Barcelona Fish sculpture – part of the Vila Olimpica project as an initial test of the approach. The fish sculpture – a 50 meter long sculpture of woven stainless steel mesh on a structural steel frame – provided a relatively safe test case for the use of digital representation as a vehicle for construction documentation. As a sculpture, with minimal life safety or building system issues, only the geometry of the project and the elements of fabrication needed to be represented digitally. Code compliance documentation requirements were minimal compared to that required for an inhabitable structure.

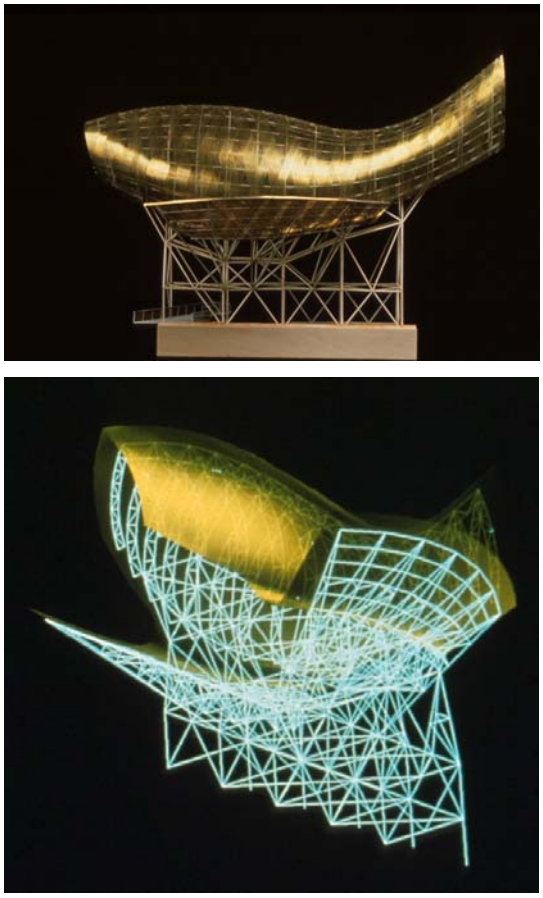

Figure I-1: Barcelona fish, physical and digital construction models.

The development of the surface mesh geometry presented substantial concern for the design team. The mesh was understood to have a resistance to forming in an arbitrarily curved fashion, and would buckle undesirably if certain constraints on the surface form were adhered to. Additionally, templates for cutting the shape of the mesh elements needed to be provided.

Glymph contacted William J. Mitchell, then Professor of Architecture at the Harvard Graduate School of Design, who produced an initial model of the design in the Alias software package with graduate student Evan Smythe. While the results of the study demonstrated the possibility of representing construction documentation in digital form, a critical limitation emerged in the Alias software's underlying representation of surfaces. Alias represented the surface of the sculpture through a tessellation of triangular faces. While this representation was sufficient to provide visual fidelity to Gehry's initial physical model, geometric operations on the surface required to produce the structural steel model were problematic. The sculpture's skeleton is constructed as a set of planar, vaulted truss "ribs", offset from the surface, and connected to a cross braced structural steel skeleton. Intersections of the rib planes with the tessellated surface resulted in segmented polylines. It was difficult to control the segmentation of the mesh surface produced by Alias to correctly produce the required segmentation of the steel trusses. Offsetting of curves to produce the bottom chord of the trusses and other geometric operations produced similar undesirable linearization of the geometry.

Realizing that this segmentation of smooth surfaces would be a critical limitation to its digital construction documentation process, the firm began to search for more advanced representational capabilities in other software packages. At the time, the CATIA software package was one of the few CAD platforms offering true smooth surface representations. CATIA – initially developed by Dassault Aviation as an in house CAD application for the development of the Mirage fighter plane – had recently been released as a commercial application through IBM and was gaining acceptance by the automotive and aerospace industries. At the time CATIA Version 3 had achieved a commercially viable CAD application based on Bézier curve and surface algorithms[28].

As an engineering tool, CATIA also offered capabilities for surface analysis not provided by Alias. While unable to provide a detailed assessment of the mesh behavior, capabilities for analyzing surface curvature were supported. Additionally, CATIA allowed curved surfaces to be flattened into shapes allowing a reasonable approximation of the mesh profiles required to cover the surface. These utilities, while representing quite loose approximations of the true mesh behavior, were sufficiently powerful to support the design and detailing of the mesh surface.

Rick Smith – proprietor of the consulting company C-Cubed - was at the time an independent IBM business partner, providing CATIA services to the southern California aerospace industries. Smith revisited the digital modeling of the fish, demonstrating the possibility of accurately creating the curved geometry of the surface and the construction of the structural steel geometry as offsets and intersections derived from the curved surface model. Construction of the sculpture was awarded to Permasteelisa, an Italian curtain wall fabrication company, for what would be the first of many successful collaborations between the two firms. Smith brought his model and CATIA station to Italy and worked directly with the Permasteelisa's engineers and fabricators to produce the shop drawings for the steel and layouts for the mesh elements.

Glymph characterizes the experiences of the Barcelona Fish project as a breakthrough in many ways. The fact that the project, with its admitted geometric complexity, was completed on time and on budget, while the conventional steel construction of the rest of the Pavilion complex was suffering construction delays and on site reworking of steel elements "showed that [the firm] was onto something" in identifying a new process for project documentation. Furthermore, the direct collaboration with Permasteelisa on the development of shop drawings - with the endorsement of the project owner - circumvented the conventional disassociation between architect and fabricator.

At the same time as initial experiments in digital project description were being conducted by the firm, Dassault Systèmes, the developers of CATIA, were developing a comprehensive methodology to support the design of Boeing's 777 aircraft line. Dassault termed this methodology Digital Mockup (DMU), with the intent to support design, detailing and CNC fabrication of the 777 aircraft and all components in an integrated, paperless fashion. This development effort resulted in software functionality within the CATIA product line beyond the limited functionality of curved surface description that Gehry's firm had initially sought. The story of these developments in the digital design of manufactured products presents a parallel history to Gehry Partners' efforts in developing similar methodologies for the support of building projects, and served as an important example closely observed by the firm. The parallel development of these manufacturing methodologies has also disclosed important differences in economies and supply chain organization between "vertically integrated" industries such as the aerospace industry, with opportunities afforded by economies of scale,

and the constraints of process imposed by construction industry. Comparisons between the methodologies of these industries are discussed below.

Applications to building projects followed shortly. The Nationale-Nederland Building in Prague and Team Disneyland Building drew on elements of the process proven on the Barcelona Fish. The development of the firm's process culminated with the opening of the Guggenheim Bilbao museum in 1997. While refinements of the process continue, the essential elements of the process and its applications were defined in the early successes of these projects.

It would seem, from the success of these projects, that digital representation is poised to free architecture from the constraints imposed by historically developed project description. Complexity of geometric representation and methods of constructibility are apparent in the design and construction of Gehry's projects, but digital technology seems to have proven up to the task of resolving this complexity. Digital modeling now allows free form, non-Euclidean shapes to be represented with exacting tolerances. Digital CNC fabrication technologies, developed to serve the automotive, aerospace, and Hollywood animation industries stand ready for application to building, faithfully rendering building components to similar exactness. The Boeing 777 project and other manufacturing processes have proven the viability of a fully digital design development process. To the delight of some critics and the dismay of others, digital technology seems poised to cast off the last relics of a historically developed building context, translating the designer's gesture effortlessly into final form through Hollywood animation software coupled to robotic production devices. As post modern historicism freed design from contextual constraints, digital representation seems poised to remove the remaining constraints imposed by historically developed conventions of building description and production.

It would be unfortunate to draw so simple a lesson from Gehry's work. The firm's ability to successfully realize innovative forms springs partly from its ability to bring these projects *within the context of conventional construction documentation and building process*. A view of the development of Gehry's body of work shows a formal language that originates in the forms and materials of conventional construction, and an ongoing experimentation to press these materials and methods to their limits. The succession of Gehry's built projects shows a gradual, continual coaxing of the conventions of fabrication and building, each work drawing

on the lessons learned from previous successes to push building method in new directions and to further limits. The power of Gehry's architecture springs partly from a struggle, negotiation and ultimate reconciliation with existing context and conventions.

Part of the role of digital technology in the firm's process has been to disclose simplicity within the geometric complexity, and to bring the description of building elements and processes within the conventional language of contemporary construction practice. This discipline is key to the success the firm has enjoyed in successfully completing projects. Perhaps surprisingly, much of the detailing of building components relies on extensions to conventional processes of building, and seldom relies on aerospace or Hollywood methods of object making. Rather, the firm strives to work with the existing processes of craftsmen and fabricators, and attempts to produce detailing and documentation strategies that reflect a deep understanding of the methods and constraints of existing fabrication processes. Two dimensional documentation, flat patterns, Euclidean cut edges and profiles are the norm in these fabrication methods. Digital technology is drawn on to render Gehry's forms within these conventions; is it not seen as an opportunity to discard the capabilities of traditional craftsmanship. Part of the reason for this approach is of course necessity. Even where fully digital fabrication technologies are available, the costs of these methods are frequently prohibitive. But part of this methodology seems to be drawn from Gehry's embracing of material qualities and craftsmanship, and an aesthetic that pushes conventions to their limits, rather than creating a design language from scratch.

Viewed from a geometric perspective, the methods drawn on in the digital description and documentation of projects are enabled by capabilities for developing project descriptions in full three dimensional, digital form, using non-Euclidean geometric constructs. However, the reliance on non-Euclidean geometric constructs in no way means that these structures are constraint free. Non-Euclidean, digital representations bring their own constraints and artifacts to description processes, in the forms that can be represented, the geometric operations that can be performed, and the fabrication processes that are enabled. This structuring of non-Euclidean geometry on surface representation and associated constructibility will be a central theme of this thesis. It will be shown that the non-Euclidean representational constructs at the heart of the firm's digital process can in fact be positioned as extensions of Euclidean constructs into a more general framework, in which Euclidean and a variety of non-Euclidean descriptive elements coexist on equal footing.

II. THE DEVELOPMENT OF GEHRY'S BUILDING PROCESS

In order to realize the innovations of Gehry's forms on built projects, corresponding innovations of design development and building process have been required. The firm's computational innovations have been developed parallel to, and as part of, these building process innovations. To understand the context in which the firm's digital process has evolved, it is appropriate to review some of the guiding intentions of the firm's building delivery methodologies that these digital representations serve.

A. PROJECT COST CONTROL

It may not be overstatement to say that project budget control – and the reconciliation of design intent with project financial requirements – are the most important driving forces behind the firm's design development phase decisions. Certainly, project cost control has been the most important factor in the development of the firm's digital building delivery process. This position may surprise readers. It is sometimes assumed that Gehry's practice engages predominately or exclusively in "budget less" projects, with clients for whom money is no object. This is far from the truth. The firm has achieved its successful track record of completed projects by providing buildings within clients' budgets, and within the rough per square foot costs of more conventional projects of similar building usage types.

Project costs can be broken down in a number of different ways. First, the distinction is often made between the "soft costs" of a project, including the design services of architects and engineers, versus the 'hard" costs attributed to actual construction materials and labor. Second, there is an important distinction to be made between costs identified prior to commencement of construction, roughly up the GMP (Guaranteed Maximum Price) bid phase, and cost overruns that can crop up during construction. Both of these distinctions are subject to further inspection in light of the new forms and processes championed by Gehry's firm.

It is often assumed by owners that the hard costs of a building are a fixed factor in building construction, while soft costs are an area for flexibility. This reasoning seems at a preliminary glance to be valid. In theory, a 2x4 stud is a 2x4, a cubic foot of concrete is a known quantity. The unit prices of these materials seem relatively fixed. Buildings of a certain size require

certain amounts of material. Metrics for these material quantities relative to square footages of given construction types are available in the industry. Quantity estimating on conventional construction is a fairly straight forward process. The estimator adds up linear wall lengths from the 2D drawings, multiplies this length by the height of the walls to determine square footages, throws in a percentage for material waste, and multiplies these quantities by established local costs for the building materials and per quantity estimates of hours and rates of construction labor, to arrive at a cost for the construction of a given building system. If the client is interested in higher quality materials or construction, these decisions can increase the cost of construction, but in theory the client “gets what he or she asks for” in terms of a higher quality product. In turn, it is perceived that the soft costs of the architectural and engineering services have some flexibility. If the architect spends less time in schematic design, the number of billed hours can be reduced, beneficially impacting the bottom line of the building construction budget. On many conventional building projects, the design services are seen as an area to squeeze some cost reduction.

The above distinctions between soft and hard costs of construction may be valid for conventional construction, where quantities and associated costs are relatively well established. On unconventional construction, where established industry costs for the type of construction are not available, the rules of the game are thrown wide open. Even the straight forward activity of quantity estimating can be difficult to accurately perform if these quantities can not be easily determined from conventional 2D documentation. Material waste factors can be difficult to estimate, since atypically shaped building elements can be more difficult to fit on industry standard sheets of material. The labor associated with unit quantities of unconventional construction systems can be difficult to anticipate.

Even on conventional construction, construction budgeting is less of a science than it first appears. For conventional construction, rough per unit cost rules of thumb are available in the industry, and are known to architects and construction managers. These unit costs vary widely from region to region, and are substantially impacted by short term localized economic factors. Factors contributing to the cost of a given system include local availability of materials and equipment, availability of skilled vs. unskilled labor and the influence of trade unions, and competition among projects in a given locale for certain elements of construction. A “hot” building market will drive up costs for most basic construction systems, as demand for sub-contractors is driven up. The history of Gehry’s projects is rife with

anecdotes of these local and temporary economic considerations. The economic feasibility of titanium for the Guggenheim Bilbao project is traced to a temporary glut of available titanium in the world market after the fall of the Soviet Union. The Big Dig project in Boston reduced the available concrete contractors in the local market during the construction of the Stata Center. Low demand for skilled carpenters in the Czech Republic after the fall of communism contributed to the development of a hybrid digital / manual fabrication process for concrete panels of the Nationale – Nederland project.

The premium on direct hard costs associated with unconventional project geometry is an important factor in preliminary project budgeting. This premium is acknowledged by clients as a cost associated with the acquiring one of the firm's designs. The rationale of cost associated with receiving a superior product is applicable to Gehry's buildings. Many budgetary tradeoffs are made throughout schematic design phase decision making. For example, Gehry's design aesthetic suggests more economical, conventional materials used in unconventional forms, in lieu of more expensive finishes applied to conventional geometry. Mixing project geometry to include conventional construction and geometry along with more highly shaped elements is an important element of the design process. These tradeoffs can be managed in schematic design in order to meet client budget requirements.

A more problematic aspect of project budgeting can be identified, in terms of *risk management*. In North America, construction sub contracts are typically awarded based on guaranteed price bids. Typically, construction sub contracts are awarded through a competitive bidding process, with the low bidder being awarded the contract. The recipient of the contract is obligated to perform the agreed upon services – specified through project documentation - for a contractually committed price. On conventional construction, sub contract estimators have a good understanding of their internal unit price costs for conducting work, and can make trade offs between competitive pricing and profit margin. On unconventional construction, where prior experience and industry established price points do not exist, cost estimation is difficult to conduct with any guarantee of successful completion of the project. The level of risk associated with contracting to perform the work at *any* specific price can be substantial. The result can be sub contractor bids containing large factors of safety, which ultimately represent premiums on the price of construction. Many sub contractors will simply elect not to consider taking on the work, reducing the competitive pool of providers and resulting in higher cost bids being accepted. The premiums cannot be

construed to be costs associated with a superior product, but simply represent higher costs for the same quality of construction. This price of risk can dwarf the premiums that can be expected due purely to additional labor or materials.

While the pre-construction pricing exercises can jeopardize the commencement of a project, lack of project and associated cost control during construction present even greater jeopardy to the project and participating organizations. The major risks in terms of cost overruns during construction can be traced to lack of dimensional coordination, and errors and omissions in construction documentation or their interpretation. Errors in dimensional coordination can result from mis-communication between trades, misunderstanding of dimensions of components, and complexities of routing equipment through tight spaces, such as duct runs of mechanical systems. Obvious errors of miscalculating dimensions on traditional 2D documents or not updating dimensions on plans when updates and changes are made occur all to frequently on conventionally documented construction drawings. When such errors escape notice until they are discovered in the field, at best re-work is necessary. More significantly, this rework can cause delays impacting many of the trades on the job. If these delays are significant enough, they can cause a “ripple affect” where subsequent trades are impacted. For example, the mis-sizing of a single primary steel beam, discovered in the field can delay the placement of adjoining members while the erroneous member is rebuilt and shipped. In turn, placement of any system to be attached to the primary steel system may be held up. If delays are significant, they can put in jeopardy guaranteed contracts with sub contractors, who may have other work scheduled in anticipation of completing their portion of the job by a certain date. The costs of running a large construction site per day can be substantial even without the subcontractor labor costs.

Improved project information provided by 3D CAD documentation has the potential to address many of these issues, allowing control of, and dramatically reducing, the so called “hard costs” of project construction. Much of the cost saving opportunities offered by information technology can be traced to reduction of risk. By facilitating improved unit quantity estimates early in schematic design, budget tradeoffs can be played out before detailed design has begun. Improved dimensional coordination can be a direct outcome of “virtually” constructing the building and its components to some level of detail prior to generating contract documents. Tricky or idiosyncratic conditions for typical system details – at corners or atypical interfaces with other systems – can be identified prior to committing

work contractually. Admittedly, this added information may give prospective bidders better insight into the complexity of the project, resulting in higher initial bids. However, if this complexity were to be discovered after the fact, disputes about the completeness of construction documents would need to be resolved, likely resulting in remediation.

Part of the successful design development practices of Gehry's firm results from the frequent use of conventional system detailing, applied to unconventional geometry. The firm is continually cognizant of the availability of locally available talented craftsmanship, and seeks to take advantage of the materials and practices of their local construction practices. This is part of the contextual aesthetic of Gehry's designs, and an aspect of the respect of craftsmanship for which the firm is known. One strategy for reducing project costs is to be able to provide construction information in a format familiar to these local trades. The 3 dimensional project database allows information to be "sliced and diced" to extract information supporting construction practices familiar to these local trades. If the description of complex geometry can be provided in a format that supports practices familiar to these trades, the risk factor can be reduced or eliminated. Complex geometry may still carry a premium in labor and material, but these factors can be understood in terms of real impact on the costs of construction, not buried in excessive cost contingencies to protect the contractor from unknown risks.

B. BUILDING TEAM ORGANIZATION AND INFORMATION FLOW

The conventions of contractual relationships among organizations participating in a construction project vary widely in different parts of the world. In many ways, the North American construction environment is among the most difficult for supporting unconventional building practices. It is partly for this reason that many of the early successes of the firm's digital building delivery process were achieved on projects outside North America. Much of the development of the divisions between design and construction teams can be traced to the increase in construction litigation that has occurred in America since the 1950s. To protect the various partners from litigation, strict boundaries have been defined for the scope of responsibility each party takes on, and the flow of information between parties.

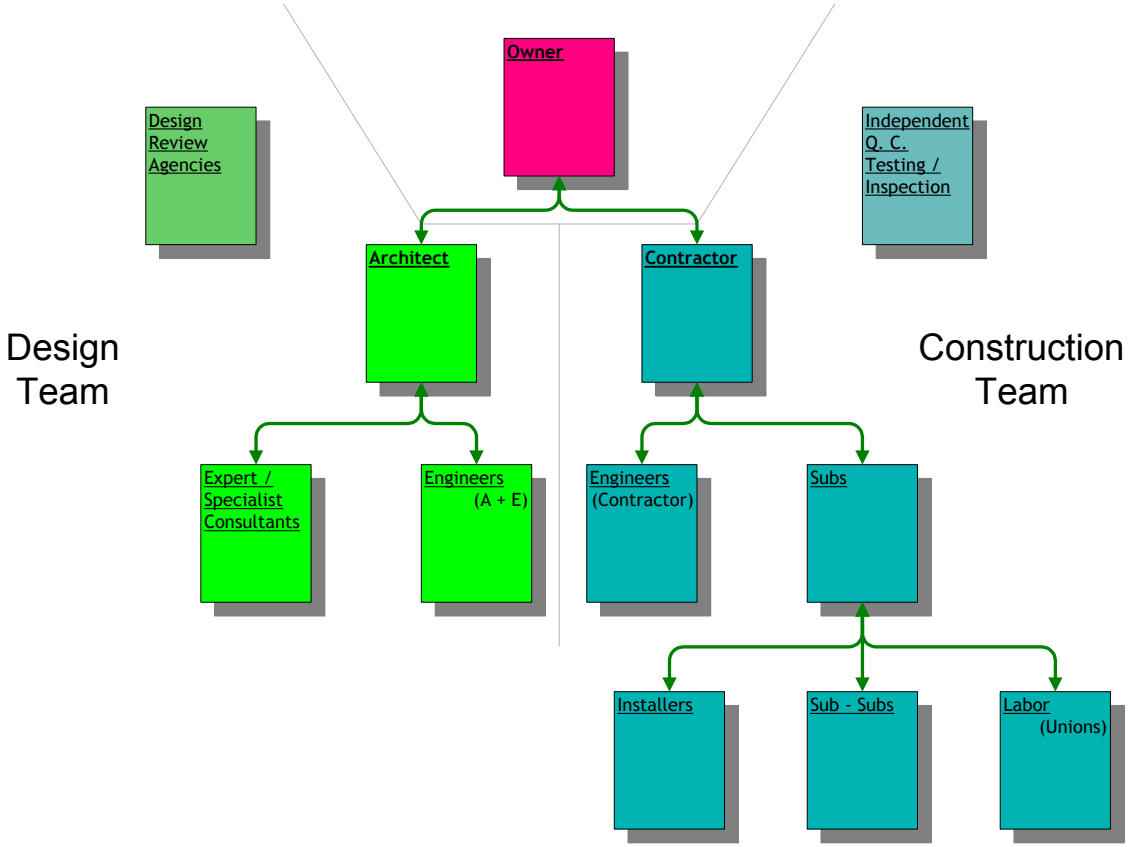

Figure II-1 Standard contractual organization

Figure II-1 diagrams the contractual relationship between organizations on a standard North American design – bid - build project. The contractual relationships are organized as a tree. The major contractual relationships are defined between the owner and architect, and owner and contractor. The architect is “prime contractor” for the design team, which specifies the scope of construction through construction drawings and specifications. The general contractor is responsible for the construction of the project per the construction documentation provided by the design team. All contractual relationships at the top of the hierarchy are with the owner; no contractual relationship exists between the architect and general contractor.

The architect sub-contracts for engineering services to structural, mechanical, acoustical, lighting and other consulting engineers. Various specialist engineers may be enlisted to perform peer review on the work of the engineering team. The design team completes the

specification of the project to demonstrate conformance with local building codes, and to sufficient level of detail to guarantee in theory that the project can be built without errors or conflicts between the activities of building trades.

The general contractor in turn apportions work, at their discretion, to internal resources or to subcontractors. These contracts need only to guarantee that the specifications of the design team are met; beyond these base line requirements the contractor is free to select any contracting organizations that can reasonably be expected to perform the work. The contractor will generally award sub contracts on the basis of lowest bid.

Sub contracting organizations “fill in the details” of the project specification through shop drawings that describe building systems and components to a level of detail necessary for actual construction. The sub contracting organizations have their own engineering teams that conduct detailed engineering of system components to verify that proposed fabrication meets the standards specified by the design team. Again in theory, the contract documents provided by the design team have anticipated all the geometric and coordination conditions that will occur as a consequence of the systems that have been selected for the project. In practice, the level of detail performed by the design team to define the resolution of typical conditions may not anticipate all the actual localized conditions generated by the specified systems. The level of detail provided by the shop drawing detailing may be necessary to disclose the full range of implications of a selected building system strategy. Any discrepancies between general and actual localized conditions can be a source of dispute between the design and construction teams. These shop drawings are submitted to the design team for review, comment or exception. The design team is usually responsible for guaranteeing that the details specified in the shop drawings can be dimensionally coordinated between trades. Note that dimensional conflicts between the work of different trades may not be apparent in any single trade’s shop drawing submissions. Coordination through integrating information contained on numerous shop drawings may be required for the design team’s review. Problems can be difficult to detect when this information is contained on disparate two dimensional documents.

When a condition is detected by the sub contractor that is beyond the scope of the details specified by the bid package, requests for information (RFIs) are generated by the sub contractor and sent through the contractual hierarchy to the architect - as head of the design

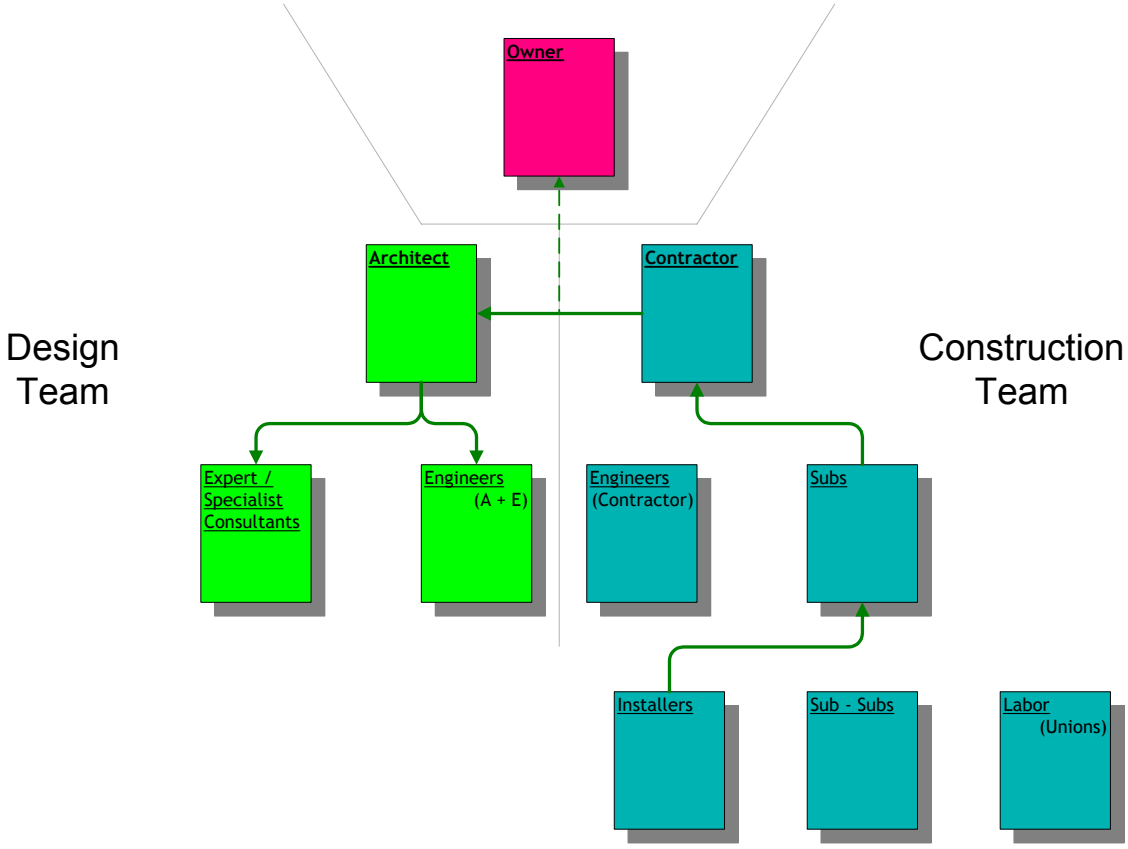

Figure II-2: Communication path and controls

team - for clarification of design intent. Depending on the severity of the condition, the design team may issue a supplemental information document (SI), indicating that the design team believes the condition is within the original intent of the contract documents. If the condition is determined to be outside the scope of the details specified in the contract documents, change orders may need to be generated. The generation of change orders indicate that resolution of the condition is in fact beyond the scope of the original construction documents and contract, and will frequently generate additional fees for the construction team. This change of contractual scope will necessarily require the approval of the owner.

Information flow between organizations is strictly controlled along the paths of contractual relationships (Figure II-2) . The parties higher up in the contractual tree are typically leery of allowing their sub contractor organizations to communicate or make decisions directly with other organizations, since they are ultimately responsible for the work of the subordinate organizations. Worse, the fear is, subcontracting organizations may “leak” information about internal decision making between contracting and sub contracting organizations to

organizations “on the other side of the fence”, who may use this information to their advantage if disputes arise.

When construction proceeds smoothly (which it seldom does, even on conventional construction!) this strict control of information generation and dissemination protects all parties from erroneous decision making that would jeopardize the intent of the project specifications that form the basis of the contractual relationships. For conventional construction, where the work of each party is fairly well defined by standard details and other conventions of practice, the process of design and construction decision making can be accommodated by this tightly contractually controlled process.

For innovative, complex or unconventional construction, the disaggregation of information and limitations imposed on communications between decision makers can virtually guarantee that problems will occur in project coordination. When they do occur during construction, resolution of problems can be difficult. Problems which could be quickly fixed on the spot - if the construction team had sufficient authority - require a chain of events and decisions, above all a determination of the party responsible for the condition. While the resolution of decisions are winding their way through the chain of command, construction delays can ensue, further aggravating the impact the condition has on the project schedule and cost. Communication technologies have been drawn on to assist in the speed of resolution of on site conditions, including simple technologies (such as emailed digital photos) and more elaborate technologies including information tracking Web sites.

More problematic for innovation of construction is that the true sources of fabrication innovation – and the parties ultimately responsible for execution of this innovation – are the fabricators themselves. These are the organizations that will ultimately be required to develop innovations of process necessary to efficiently construct innovative project geometries. This expertise is best included in the design process during design development decision making, before the contract documents have been completed. In the contractual scheme defined above, these entities are excluded from the decision making process. Worse, sophisticated fabricators may be better informed of the actual effort and cost required to perform sophisticated construction work. This knowledge may work to their detriment, since the bids they submit may reflect the actual cost required to complete the project. Their bids may be turned down by the general contractor in favor of less qualified fabricators, who

may turn out be unable to execute the work to which they have committed themselves. The specification and bidding process also can fail to turn the award of contracts in favor of fabricators who perform higher quality work.

Gehry's design aesthetic has always tended to favored innovation of fabrication and craft over that of engineering. These intentions would conspire to flip the standard contractual process around. Theoretically, the fabricators would work directly with the architect and engineers of the design team to provide the specification of the work to be performed. Unfortunately, this tight relationship between design team and craftsmen violates many of the contractual conventions of North American construction.

To address this issue, GP has occasionally – with the consent of owner and general contractor - entered into unconventional contractual relations with fabricators in the design development phase. These *design assist* contracts are forged between the architect and skilled fabricators. The fabricator serves as a quasi consulting engineer for the specification of a building system, and is compensated for this service. There is no commitment by the general contractor to ultimately award the contract to the particular fabricator; it may be awarded to the fabricator's competition, if the fabricator's bid is unreasonable. In practice, this is however seldom the case.

A second issue of potential impact on contractual relations is the availability of computing capabilities by the fabrication organizations. The accurate performance of shop drawing work requires the fabricator to dig into the master model database. Until recently, the skills necessary to operate CATIA, and familiarity with a 3D centric approach to detailing were unavailable outside of Gehry Partners. While the ability to fabricate the components existed in skilled fabrication shops, the necessary CAD expertise was not part of these organizations' services. When CAD expertise existed, data would still need to be translated into formats appropriate for the fabricator's work. This lack of availability of computational expertise has often required Gehry Partners to perform services as part of construction administration phase activities, well beyond those conventionally within the architect's scope. In order to address the contractual ambiguity of these services, C-Cubed – Rick Smith's CATIA consulting organization – has often been recommended as a sub contractor to general contractors and fabricators. C-Cubed provides both CATIA operator expertise, as well as familiarity with the firm's digital methodologies. C-Cubed has contracted directly to contractor

and sub contractor organizations to perform digital shop drawing services, removing Gehry Partners from any direct work and contractual relationship with these organizations.

On recent projects, 3D CAD capabilities have become more prevalent in fabricating organizations. Often these organizations have developed sophisticated digital methods of their own, or have acquired 3rd party applications whose development targets the specific activities of their trade. CAD activities to support these relationships have turned more toward translation of data between the CATIA master model and these proprietary formats. Often, Gehry Partners will engage in development of translation processes to serve particular contracting organizations. These capabilities are officially provided “for reference only”; the CATIA database remains the official format for 3D data on the firm’s projects. When appropriate, GP has provided these translation technologies to the general contractor, who becomes responsible for data coordination with their subcontractors.

C. FABRICATION ECONOMIES

Building projects are predominately singular endeavors. Site conditions, local building practices and codes, client specific requirements, and the need to work with locally based construction firms and their heavy equipment, all are conditions that contribute to the necessity for treating each project as a unique undertaking.

This characteristic is perhaps the single most important distinction between building construction and product manufacturing industries. The products of manufacturing industries vary widely in scale, complexity and cost. Airplanes are enormously complex design and engineering endeavors, and carry very high unit costs. Only a few hundred or thousand units may be produced over the lifetime of an aircraft product line. A toy is a relatively simple object to engineer and produce. Hundreds of thousands or even millions of identical toys may be produced in the lifetime of the product line.

Economies of scale unify the production these different manufactured products. There are many implications of mass production on the economics and opportunities afforded by product lines. With economies of scale, the up front cost of engineering and tooling design required to develop the product line is distributed over the cost of each unit. Even if these costs are high relative to the unit cost, substantial design and engineering activity can be

undertaken with limited impact on this unit cost. These implications impact the fabrication methods available to mass production, and in turn have consequences on the shapes that be manufactured. The tooling of dies for extrusion molding or stamping fabrication technologies often represent a high fixed cost of product manufacturing. Metal stamping requires the fabrication of a positive and negative dies. The manufacturing of these dies in manufacturing is often a multi-step process. A wax positive form may be constructed, or highly finished CNC routed positive is developed in foam. Then, a high strength negative form is cast from the sculpted positive form. Depending on the stamping process, a second positive in high strength material may be developed from the negative form, and a high strength steel die formed from this element. This elaborate process can be easily justified for large scale runs of identical parts. It is fairly obvious that application of such a process to one of a kind component runs would be drastically expensive. Yet, for fully free form surface forms, elements of a stamping or molding process are still required.

A more subtle implication of economies of scale – or lack thereof – is found in the *cost of information* required to develop a given component. This cost of information can be identified in the design, engineering, and modeling or drafting associated with the development of the component. With large product runs, the cost of engineering and modeling a component is again a small component of the cost of fabricating the individual unit. In the development of singular products and components, the relative cost of engineering to that of materials or fabrication labor can be high. It may be more economical to over design the specification for all units, adding more material and hence strength into the objects' designs, than to engineer each unit to a more optimal configuration. Similarly, it may be more cost effective to use additional fabrication effort - allowing the craftsman working on the component to figure out aspects of the component's configuration – than it would be to fully detail an individual component through computer based or traditional drafting.

Issues of mass production have been a topic for architecture since the industrial revolution[44]. While a full treatment of this topic is well beyond the scope of this thesis, some observations may be made on the geometric organization of building projects and its affordance of mass production. The regularized, Euclidean organizations of building layout strategies have historically provided the basis for incorporating mass produced elements. Modular systems based on grid layouts - repetition of rectangular dimensions in the organization of building designs – allow components of identical proportions to be mass produced and deployed

across the project. Countless examples of such designs exist, we note in passing much of the work of Mies van der Rohe and fellow high modernists. These strategies rely on dimensional repetition as a means for achieving geometric symmetries supporting the incorporation of identical elements. Rotatational symmetries afford similar dimensional repetition. Variations in localized performance requirements may exist across elements of identical dimensions. The wind forces on the glazing modules of high rise buildings are greater at the top than at the bottom. This localized performance variation may be trivially satisfied by over designing the unit to satisfy the worst case design conditions; the inefficiency of deploying materials in a less than optimal fashion may be vastly outweighed by the informational economy of engineering the unit a single time.

There is perhaps an even greater body of built work drawing on regularities of Euclidean geometry to support systems founded on mass produced raw materials. The conventional American 2x4 system is a key such example. This system does not require modular dimensions, but rather relies on easily formed raw materials with certain assumed constraints on the building geometry to which they will be applied. The obvious constraints of the 2x4 system are planar wall, floor and roof geometries. Straight, rectangular edges and perpendicular wall organizations are suggested by this system; however, the system can accommodate angles between planar elements and non-perpendicular edges with minor customization. Gehry's early work (Section IV.A) explored the limits of these building systems and materials.

The non-repetitive geometries that characterize Gehry's recent work afford neither modular dimensional regularities nor other regularities afforded by Euclidean systems. However, in order to satisfy budgetary and schedule requirements on the firm's projects, systematic building strategies are still required. This imperative has caused design development strategies and geometric modeling efforts to pursue the identification of geometric regularities that do exist in the design geometry, or can be imposed on the geometry with minimal impact on the design intent. The term *rationalization* (Section III.F, below) is used within the firm to describe this process of pursuing and incorporating geometric regularities in the building form. The disclosure and constructibility implications of geometric regularities in non-Euclidean geometry are a central topic of this thesis. Considerable discussion of different geometric forms present in Gehry's designs, the regularities inherent to these

geometries, and constructibility strategies that take advantage of these regularities will be provided in Parts 2 and 3 of this thesis.

D. MANUFACTURING TECHNOLOGIES AND METHODS

CNC (Computer Numerically Controlled) production methods hold promise to alleviate some of the geometric constraints on mass production strategies. CNC fabrication equipment can dramatically reduce the labor associated with controlled fabrication of custom components. CNC technologies include a variety of different technologies, including laser or plasma cutting of flat sheet materials, automated hole punching used in structural steel fabrication, 3 and 5 axis routing, automatic lathing, and full fledged robotic manufacturing. However, there are economic and formal considerations in applying these technologies. The cost of this equipment is substantial relative to more conventional fabrication equipment. This up front cost must be amortized over the life of the machine, which can in it self result in significant costs per cutting operation. Certain combinations of materials, sizes of elements and shapes have no current CNC solutions. For example, re-configurable mold technologies are currently being researched, but to date these technologies are unavailable in commercial applications for high quality fabrication of steel plate or other high strength materials. The cost of generating and processing the information necessary to drive the equipment must be considered as well. Long machine run times on expensive equipment (such as 5 axis milling) can make applications of these technologies prohibitively expensive. Computer based modeling requires highly skilled operators, frequently working on high priced workstations and software. The amount of information necessary to generate shop drawing information for CNC fabrication may be more than that necessary to generate equivalent shop drawings for manual fabrication. To date, few building fabrication shops have invested in these technologies. The limited competition among firms for this type of work has to date resulted in premiums for full CNC enabled approaches to building component generation. Certainly, we can expect to see continual reductions in the cost of these technologies over time. The automation of shop drawing production combined with the ongoing reduction in cost of computer hardware promises to beneficially impact the cost of generating building components with unique configurations.

Gehry's firm has promoted the use of CNC manufacturing technologies in these production processes. CNC technologies are utilized in the manufacturing process to produce the

custom geometry of individual components at exact tolerances. Manufacturing tool paths may be exported directly from the CATIA master model to the CNC production equipment, resulting in building components that conform to the local geometric requirements of the project. The building systems that result from this method offer tremendous flexibility in addressing programmatic or aesthetic considerations. Using CNC production methods tied directly to the definitive 3D project information additionally results in improved coordination of connection geometries throughout the project, fewer dimensional conflicts between building system components, and fewer costly modifications of components at the construction site.

In other situations, the more traditional methods associated with manual construction techniques have proven to be more cost effective. When traditional construction methods are adopted, the resulting systems are subjected to similar requirements of dimensional coordination with the three dimensional computer master model. To fulfill this requirement, manual fabrication is directed through the use of *loft drawings* - full scale construction templates. With the full three dimensional model in place, information may be extracted in forms appropriate for the support of traditional trade practices.

The processes that have been developed by the firm provide interfaces to both traditional manual construction practices, and to technical innovations associated with CNC manufacturing. For each building system, a manufacturing process is developed through close collaboration between Gehry's firm and partnering fabricators. The resulting process is rigorously substantiated through full scale mockups in conjunction with computer modeling and analysis, and subjected to value engineering assessment. The approach which is ultimately pursued can combine traditional, manual construction techniques with advanced computer based manufacturing methods, to arrive at an optimal solution both from the perspective of cost as well as the quality of the resulting system.

E. DIMENSIONAL TOLERANCES

Building construction neither provides nor requires the tight fabrication tolerances of aircraft and automotive manufacturing. The tightest tolerances that can be achieved through typical fabrication and construction techniques are on the order of 1/8" to 1/16". In practice many building fabrication systems have far lower tolerances. Primary structural steel fabrication in North America can be expected to have tolerances of no better than 1 inch. These tolerances

differ greatly from those expected in manufacturing industries, where tolerances tighter than 1 mil may be expected. CNC fabrication methods can offer higher tolerances of components to their corresponding digital description. However, CNC developed components often still require assembly through traditional manual methods, and the typical construction tolerances are often re-introduced into these systems during manual assembly. As a general rule, one can anticipate a premium for fabrication with tighter construction tolerances, and lower tolerances for one of a kind objects relative to those produced through machine automated mass production methods.

Construction tolerances are closely related to the issue of *dimensional control* of the project. The exacting numerical specificity of contemporary CAD modeling applications are of little utility if building components can not reasonably be expected to be accurately positioned in space in conformance with the digital model. On site digital surveying capabilities allow components to be positioned in space in tight conformance with the digital model. However, the labor involved with positioning building components through digital surveying is significant. Building system strategies that rely on sampling vast quantities of surveyed points can be expected to have associated project cost and schedule implications. Even if such exacting positioning of certain building system elements is presumed, the relative fabrication tolerances of adjoining building components can require adjustable connection strategies for resolving dimensional discrepancies.

An alternative strategy for positioning building components is to rely on one building system to serve as the positioning device or dimensional control mechanism for adjoining elements. The benefits of such a strategy are readily apparent. The dimensional control element serves simultaneously as building component, jig for the positioning of other elements, and structural support for the elements that join it. This requires, however, that the dimensional control element be fabricated to the construction tolerances required of the adjoining elements, with associated costs of a potentially high tolerance fabrication. Typically, the dimensional control component will be a more primary element than the elements that frame in. The costs for fabricating primary structural elements to tight tolerance may be far greater than that of fabricating secondary systems to similar tolerances. For example, primary steel can be used as the dimensional control for a stud framed wall system that it supports. The construction tolerances of the stud wall system are dictated by the requirements of the cladding system, while primary steel would normally be subject to more generous tolerances

than that required for the wall system. This generates a higher unit cost for the primary steel. On the other hand, only relative system conformance to the dimensions specified in the CAD model may be required. The positioning of framing members in the above example may need to tightly correspond to the edge geometry of the primary steel and to one another, but where this assemblage winds up relative to other elements of the project may be of little consequence. If so, then the tolerance requirements of the dimensional control system can be relaxed.

CNC fabrication technologies can often support the development of registration information as part of the fabrication process. Laser or plasma cutting tools, operated at lower power levels than required to burn through material, can allow dimensionally accurate registration marks and even textual annotation as part of the cutting process[66].

Issues of tolerance and dimensional control have profound implications for project cost and quality. Tolerance decisions can not be isolated from the system design and modeling strategies. These decisions will have implications for manufacturability, erection and project cost which can impact the design, coordination and site logistics with implications beyond the actual system on which these decisions are made. A judicious use of tolerance and flexibility in the dimensional control of project geometries has been an important part of the firm's success in realizing projects within reasonable construction budgets.

III. THE MASTER MODEL METHODOLOGY

A. INTRODUCTION

The master model methodology represents the technological core of Gehry Partner's digitally assisted building delivery process. Broadly stated, the project master model is an integrated repository for three dimensional CAD based descriptions of all aspects of project construction. The geometric nature of these descriptions, and the utilities it serves in guiding the development of the built project and the coordination of building processes will be considered in some detail.

The master model methodology grew out of early experiments in paperless shop drawing development discussed in the introduction provided in Chapter I. However, substantial development of both digital technologies and the building development methodologies that these technologies support has taken place, from the early, relatively simple applications on Gehry's sculptural projects to current iterations serving full design, engineering and construction activities on the firm's current major projects.

Although the master model approach has been developed on a specific technology platform – Dassault Systèmes CATIA software product line – and is informed by technologically driven methodologies developed by Dassault to serve large scale complex manufacturing projects, the firm's technological methodology is wider in reach than reliance on any specific software product would allow. Nor is the methodology exclusively 3D centric, since support of conventional two dimensional documentation remains a requirement for successful operation in current construction practice. Ultimately, the master model methodology is exactly that, a methodology and an associated set of practices oriented toward the integration of project data through digital representation. Some of the goals of this methodology are to:

- Provide an common, integrating framework for all geometric project data, regardless of source;
- Support the extraction of geometry necessary for completion of all engineering and construction activities, in geometric forms and data formats appropriate to these activities;
- Allow the extraction and re-integration of "traditional" two dimensional project documentation;

- Support high resolution description of continuously curved surface and curve representations, and operations on these geometries;
- Support a design methodology centered around the creation of physically based design artifacts;
- Support a design development process requiring the incremental geometric development of building systems descriptions and intentions, corresponding to the incremental development of project information associated with project phasing;
- Support information control mechanisms appropriate for the development of building projects in light of industry standard project control and contractual practices.

It is important to recognize that the innovative use of three dimensional digital models represents only one component of the firm's process. The firm's success in realizing its projects is due in no small part to the development of methodologies that integrate three dimensional digital models with two dimensional drawings and other conventional project information. The master model technologies represent an extension – not abandonment - of conventional project descriptions and processes. The rationale behind the development of this hybrid process are partly related to cost control. In the current construction environment, fully digitally capable construction and fabrication partners do not always exist. Where they do, the costs of advanced CNC fabricated components may be much higher than that of traditional processes. The hybrid process allows these economic and quality tradeoffs to be made on a case by case basis, even within the scope of a single project. More importantly, Gehry's building occurs within the context of traditionally based construction environment. Substantial existing conventions of practice have been developed around two dimensional construction documentation. On large scale projects, disregarding these conventions in favor of a wholly unprecedented approach would be both impractical and dangerous.

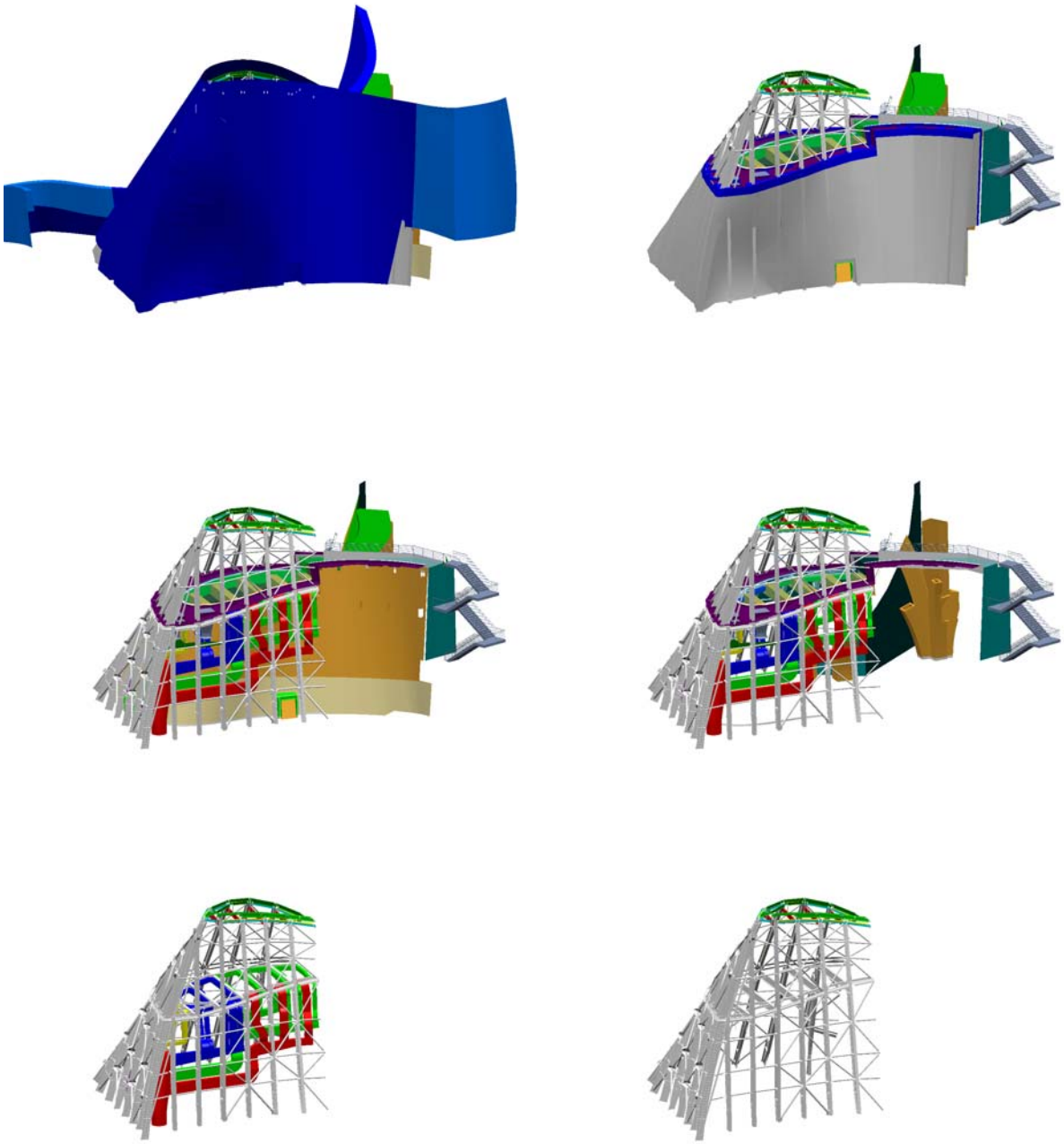

Figure III-1: Elements of 3D master model (DCH)

The ambitious agenda for digital project data raises questions of appropriate geometric representational formats, and the level of data development appropriate for each party's function in the building process. The full rendition of building components in 3-dimensional solid form would represent a level of effort well beyond that supportable even with generous

architectural fees. This is not simply a question of the firm's economics, but also a question of the level of project development and associated project responsibility allocated to the design team. As with conventional documentation, the architect developed project geometry to a certain level of detail, sufficient for other parties to build on and refine. The result is that project geometry provided as part of the architectural contract documents is surprisingly reduced and representational in terms of its level of geometric detail. However, the geometry that is shown provides the correct nominal dimensional control geometry for the indicated components.

An illustrative example is shown in Figure III-2. This model shows the 3D CAD component of the contract documents for the Experience Music Project's structural rib system. The model shows the location and positioning of the structural ribs and cross bracing, and the supporting concrete foundation. Each system is represented with a different geometric abstraction, reflecting the scope of detail provided as part of the design team's package. These abstractions provide the geometric information necessary to position the element in space and for the steel contractor to further develop the structural detailing. The structural concrete foundation is provided in full solid form, and correctly reflects the nominal surface of construction necessary for the development of concrete formwork. However, the structural ribs are for the most part shown only as a face cast between top and bottom curves. This representation provides only the dimensional information necessary for the structural fabricator to understand material quantities involved, and to geometrically guide the further development of the full rib geometry. The rest of the information necessary to satisfy the performance criteria of the ribs are found in conventional two-dimensional detail drawings and text based specifications. Text based rib numbering is

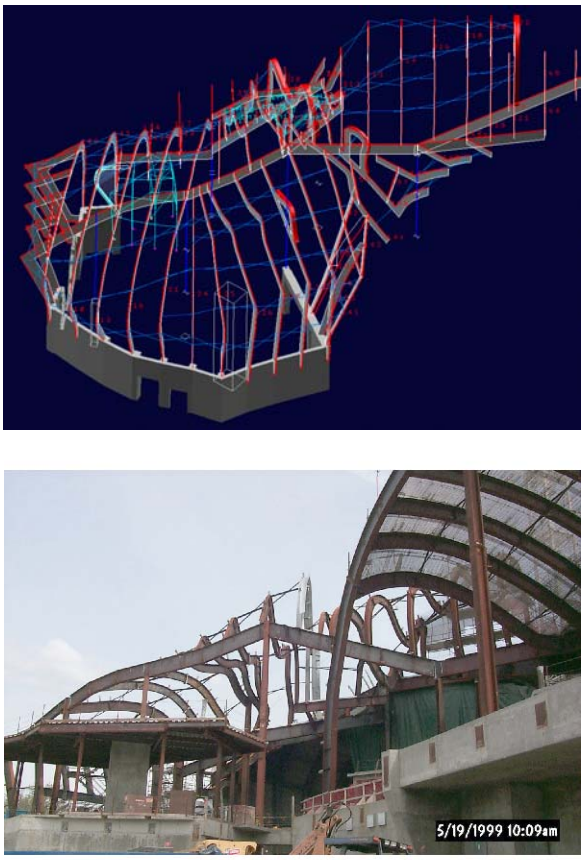

Figure III-2: Structural wireframe contract model (EMP)

provided in the model to allow cross referencing with schedules and other information in the conventional documentation. The cross bracing between ribs is provided in even simpler form, as single line elements cast between the top and bottom chords of the ribs.

Each of these geometric descriptions represent substantially impoverished abstractions relative to what one might imagine as a full geometric description of the structural elements. Much more information is needed to fully develop these systems in shop drawings: bolt holes, splices, weld specifications, etc. But this information is not typically considered to be part of either the architect or structural engineer's scope of work. The design team would not receive compensation for the effort or responsibility associated with providing this detailed information in the contract model. The level of geometric detail also reflects project phasing considerations, and the level project geometry known at the point in time of construction documentation. Providing additional geometry would likely be extraneous, since the structural detailer would likely request modifications of the geometry based on their more extensive knowledge of their fabrication process. These changes would then need to be carried forward by updating the master model geometry. More importantly, provision of excessive information by the design team would blur the boundaries of scope between the design and construction teams. If substantially detailed geometry were provided in contract documents, and then modifications of this geometry were required during shop drawing phase, these modifications would reflect changes relative to the construction documentation and hence to the contract itself. These changes could result in change orders or possibly invalidation of the contract. This re-opening of contractual agreements could ultimately result in additional fees to the construction team, even if the geometry and fabrication were simpler than that specified in the model.

This example serves to illustrate a critical point in the development of the master model methodology: the selections of geometric representation in the digital documents reflect the nature of the processes and relationships between parties of the project. These decisions are of enormous significance to the control of the construction process. Such implications are not new to a digital centric process; conventions in divisions of labor and associated project description exist in paper driven construction projects with conventional geometries and fabrication systems. However, in more traditional projects these conventions are well defined in the nature of existing practice. The scope of project development associated with each participating organization, and the descriptive conventions associated with performing this

work, are largely pre-determined. Legally binding standards for level of professional practice are defined relative to the information contained in conventional documentation.

The re-development of these practices in light of digital technology requires all of the conventions embedded in traditional documentation to be reviewed. The nature of each participant's scope of work in developing project definition is subject to reconsideration. Agreements between the parties regarding the type of information needed to perform allocated work, and the scope of responsibility assumed by parties in providing this information, need to be defined. Specifications need to be created to establish what these geometric abstractions represent, and the ways in which this information is to be used or not used. These decisions and agreements need to be revisited each time a new partnering organization is brought into the process, and each time a new building system is designed.

As a general rule in the firm's process, three dimensional models are provided as part of the legally binding project construction documentation. The 3D models specify the minimal dimensional information needed to develop spatially coordinated system components. Information necessary for quantity takeoffs is provided in these models, to some level of detail and abstraction. The specifications of component performance and connection detailing are provided through conventional two-dimensional documentation. The conventions established for these project descriptions are expressed in the (textually based) project specifications, including what each form of documentation provides, how the information is to be used, and which documentation governs in case of conflicts.

As the firm's digital process has matured, the level of detail represented in the jointly developed project database has dramatically expanded, and the amount of information provided solely in two dimensional form has diminished. Geometric abstractions have become less abstract; more geometric detail is provided as part of the design documentation. This expansion of geometric detail parallels an expansion of the firm's services from that of a design architect to full architectural services on many projects. Substantial experience with certain types of building systems often used on its projects has led the firm to provide increasingly detailed geometric specifications of these systems. Nonetheless, the mantra developed early in the firm's process development still applies as a guiding principal:

"Draw all - and only - the information necessary."

B. PROJECT CONTROL

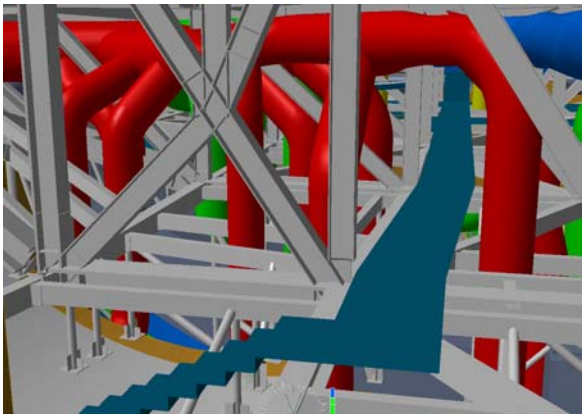

Figure III-3: Coordination model of ceiling space (DCH)

Beginning in design development phase, responsibility for development of portions of the project description begins to be turned over to partnering organizations – engineers, construction managers and fabricators. Elements of the 3D models are turned over to these partnering entities, who begin to develop the project information required for their roles in the process. The information developed by these organizations needs to be coordinated. Project coordination is within the traditional scope of the architect's role on a building project. Conventionally, this role is conducted by reviewing 2D drawing documentation provided by each partnering organization in format founded on conventions of their discipline. Coordination of the assembled body of documentation from these numerous partners in their native physical drawing formats is an extraordinarily difficult undertaking, and a major source of errors and omissions on construction projects.

The comprehensive 3D model that resides at the center of the firm's process provides an enormous aid for coordination. Even when two dimensional documentation is employed by a partner, this 2D documentation can be translated back into three dimensions, and oriented appropriately in 3D space relative to the other information on the project. When partners employ 3D documentation – as is increasingly becoming the case – this information may be directly imported and overlaid on the architectural models. The result is a comprehensive repository for all geometric data generated by the partners in the design process. By assembling and filtering this information, the process of system coordination is radically improved. System interferences may be detected, either via visual inspection or through tools that automate checking for spatial clashes or violations of system envelopes by other systems.

Time based visualization of construction sequencing has become a useful coordination tool on the firm's larger projects, including the Experience Music Project, the Disney Concert Hall, and the Stata Center at MIT. This detailed coordination of on site activities is part of the general contractor's responsibility. The enabling technology – developed by Disney Imagineering in collaboration with Stanford University's Center for Integrated Facilities Management (CIFE)[40] allows 3D project geometry to be associated with information from project scheduling software such as Primavera. Project managers and personnel responsible for on-site coordination can simulate the progression of activities on the construction site.

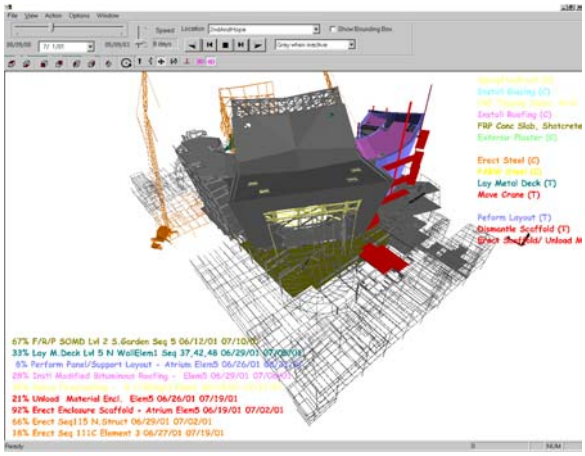

Figure III-4: CIFE's 4D modeling tool (DCH)

C. PERFORMANCE ANALYSIS

The ease by which specific engineering and other analytical models may be supported is a core benefit of the 3D project master model. The transfer of project information to and from formats satisfying the requirements of engineering and fabrication partners is a critical component of design development activities.

Numerous computational engineering analysis techniques have become available over the past two decades. Examples of such techniques include structural analysis, energy simulation and computation fluid dynamics based air flow studies, equipment performance simulation, as well as lighting and acoustic simulation. Much of this development has been through the use of finite element and finite difference techniques. These techniques approximate complicated geometric forms into assemblies of simplified elements. The global solution for the form is achieved by simultaneous solution of the individual elements' performances. These techniques are well suited to the analysis of the geometry on Gehry's projects. The feasibility of Gehry's recent projects is due in no small measure to the availability of these analytical approaches.

In conventional architectural processes, if such simulations are required, a special 3D model must be constructed, on the basis of 2D plans or other conventional documentation, and for the sole purpose of the particular analysis. Re-use of these models for other purposes in conventional architectural processes is generally not practical.

With the availability of a comprehensive, three dimensional project description, the level of effort required to provide specific analytical models becomes greatly reduced. In the firm's process, some representation of the system under inquiry is often available in the master model by the time that the analysis is required. Many of these techniques are undertaken relative to 3D geometric models in proprietary formats. However, software packages are continuing to improve their ability to import elements of these proprietary descriptions from neutral geometry formats.

Finite element structural analyses (FEA) have been conducted on virtually all recent Gehry projects, and are a critical part of project structural engineering activities. Often, the finite element models can be developed directly from the structural system wire frame from the master model. Typically, the project wireframe provides only the geometric definition of the positioning of elements. Additional information including materials, sectional properties and nodal degrees of freedom must be added to the engineering model. Currently, finite element structural software typically can not accept curved elements, a direct consequence of the geometries of finite elements that serve as the basis for these solution techniques. The project geometry must be rationalized (Section III.F) into segmented linear members and triangulated plate sections prior to import into the FEA solver.

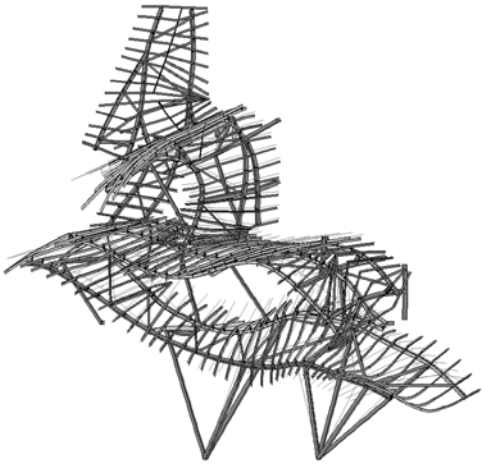

Figure III-5: Finite element analysis of frame (Riscal)

FEA structural analysis results in additional information pertinent to subsequent phases of structural system development, including the specification of member sections and load information at the connections. The firm's pursuit of comprehensive digitally based processes suggests that this information be translated directly back into the master model and on to

steel detailing and fabrication applications. To date, the full re-integration of FEA model information has been only partly successful. This is partly due to the “degradation” of project geometry that occurs in approximating curved project geometry into linearized elements, described above. The geometric approximations required for fabrication can involve different geometric abstractions than those required for FEA analysis. Translating critical, non geometric performance information between applications and across the division between the design and construction teams has to date been deemed to involve too great a risk to undertake without human oversight. Finally, the project geometry is typically not refined to the level required for structural detailing at the point in time of structural analysis. Structural analysis requires only fairly loose geometric tolerance relative to that required for fabrication. Dimensional approximations of frame elements of several inches have negligible effects on project loads, member sizing and modal analysis. This level of construction tolerance would obviously be unacceptable for final detailing. Nonetheless, many of these limitations are procedural more than any technical limitation of digital translation. Currently, geometry and sectional information are translated directly from the master model to both FEA and detailing applications. It can be anticipated that this digital integration of analytical and fabrication processes will continue to be expanded.

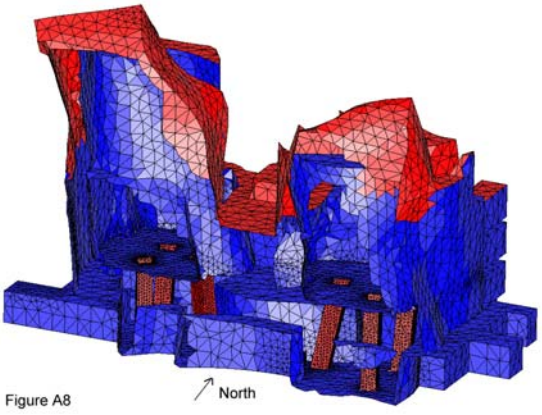

Figure A8

Computational Fluid Dynamics (CFD) techniques are becoming widely used in building energy and life safety applications. CFD can be used to model air, energy and particulate flows through spaces with complex shapes. In energy studies, these techniques are often combined with radiant analysis of solar gains to assess building heating and cooling strategies. Advanced building energy strategies such as displacement ventilation or natural heating and cooling can require this detailed analysis of air and energy flows in their design.

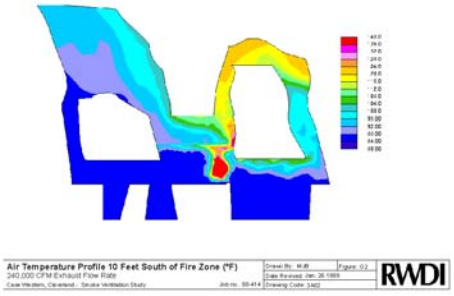

Figure III-6: CFD fire safety analysis (Weatherhead)

CFD is also used to simulate smoke and heat migration through atria and other interior spaces.

These applications are critical to the feasibility of Gehry's projects, since existing life safety codes are difficult to interpret in the context of Gehry projects. Codes typically allow variances in conditions where minimum safety conditions can be proven. Typically, the driving condition for fire safety is the time between the beginning of a fire event and the incursion of a specified density of smoke into occupied regions of the building. CFD applications allow specific fire events to be simulated. The dispersion of smoke through atria can be simulated, along with the behavior of fire doors, smoke dispersion fans and other fire safety equipment.

These simulation techniques require the generation of a negative space model delineating the boundaries of spaces enclosed by the building surfaces, which are readily extracted from the building geometry model (Figure III-6). Typically, adjoining walls, roof and floor surfaces must be extracted from the master model, then trimmed to each other to form a closed solid. The negative space model must then be tessellated into triangular facets to conform to the geometric requirements of the simulation technique.

Historically, the computational requirements of such techniques, and the necessity for trained engineering operators to run and interpret results, has relegated advanced performance simulation techniques to confirmation or final engineering assessment, conducted late in design development. The increasing speed of personal computing and availability of performance simulation software for personal computers has raised the possibility of drawing engineering simulation techniques into the set of tools available for schematic design iterations. The possibility of using performance analysis iteratively as part of the design process has been explored in many areas. Often, the level of accuracy required during early design development is at a much more qualitative level than would be required for the final, detailed engineering. These limitations on the required level of analytical detail can translate into corresponding reductions of computing complexity, fostering more interactive applications of these analytical techniques.

A variety of applications of such schematic performance simulations have found use on Gehry's projects. The use of CFD as an iterative tool to assess wind flow and associated pedestrian comfort was applied to massing studies on the MIT Stata Center Project[20] (Figure III-7). Visualization software is frequently used for shadow studies to assess natural lighting and energy performance (Figure III-8).

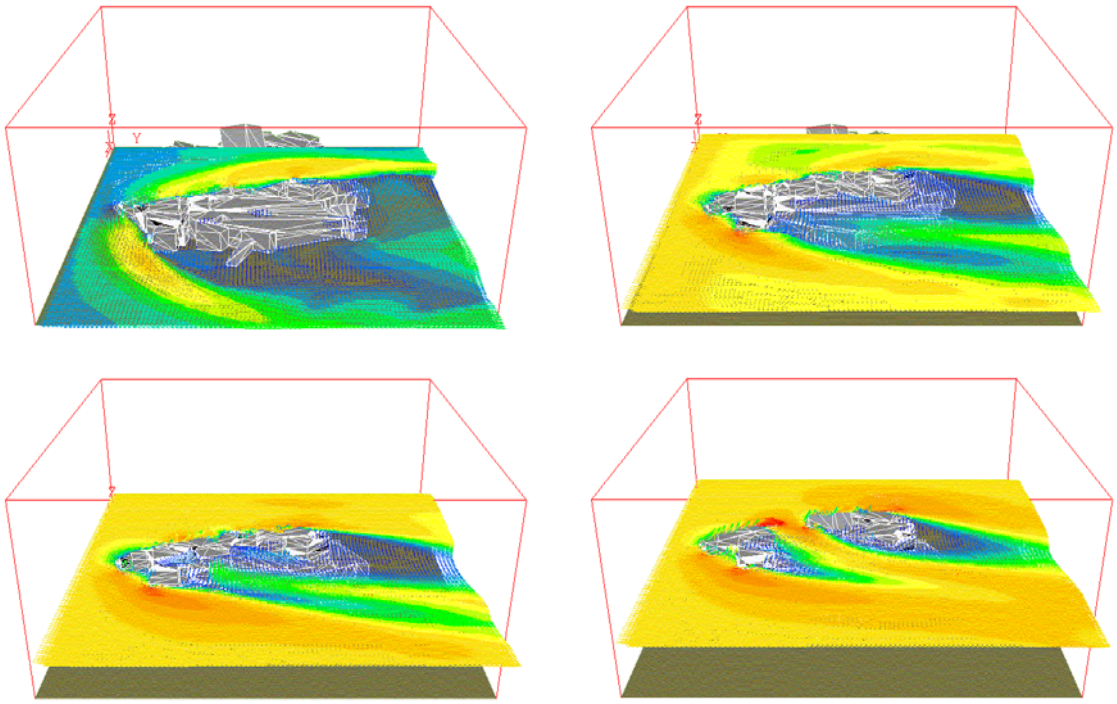

Figure III-7: CFD wind studies (MIT)

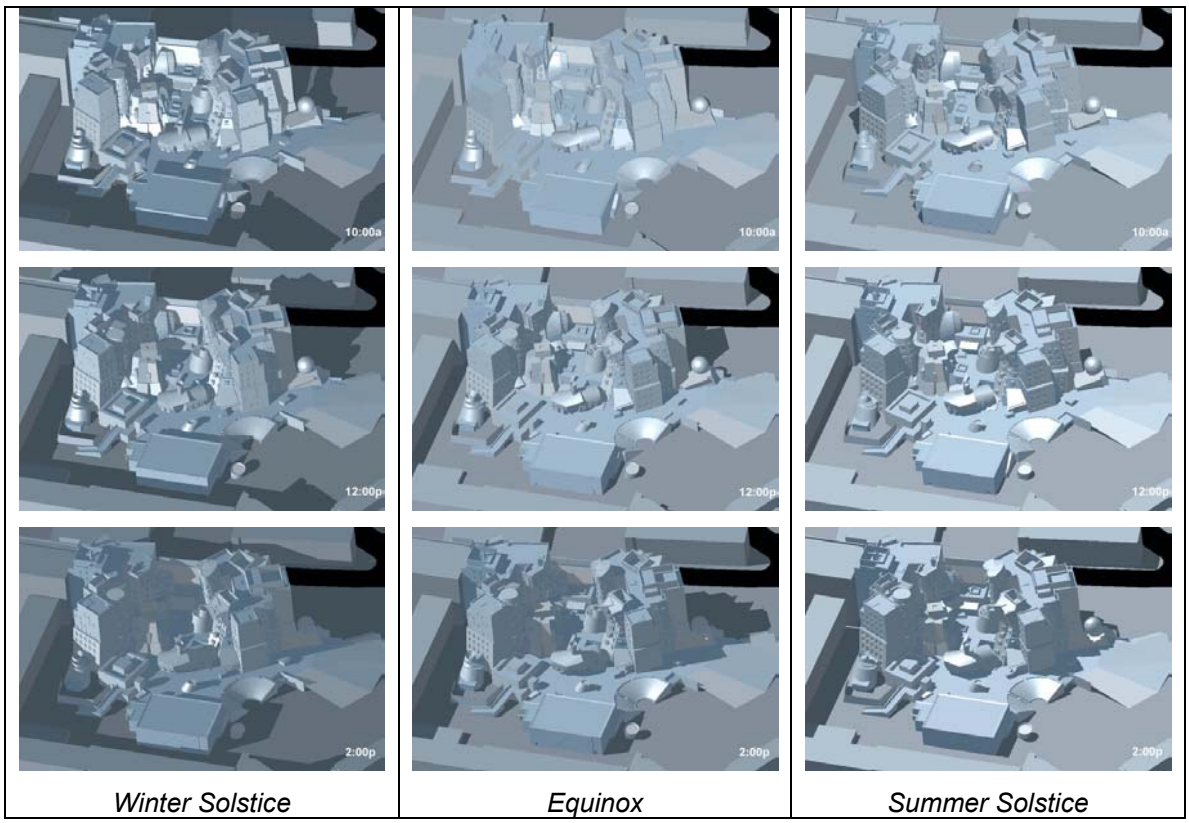

Figure III-8: Solar shadow studies (MIT)

The use of materials simulation techniques, described in Chapter VII, is a further example of the interactive performance applications that become available through tradeoffs between simulation accuracy and speed. This migration of performance analysis techniques from engineering to design applications is an important opportunity for the development of project design activities, and is again enabled through the existence of the building master model.

D. 3D – 2D INTEGRATION

The need to of carry both three dimensional and two dimensional descriptions of the project through the many design iterations and document submissions over the lifetime of a construction project has been one of the most difficult aspects of the firm's digital process. There are many reasons why two dimensional representations remain a necessary component of project descriptions for the foreseeable future:

- Interaction needs to occur with many organizations using traditional processes. Increasingly, technologically sophisticated partners are available who can provide favorable prices for services through efficiencies generated by technological advancement. However partners may, for regional cultural or economic reasons, provide the best price for services through traditional methods, or there may simply be no technologically enabled alternatives.

  It is largely the building agencies that remain most firmly entrenched in conventional documentation processes. These are the local governmental authorities that approve building permits, and review code compliance. These agencies need approval processes that serve the "lowest common denominator" for building projects within their jurisdiction. They also have neither direct financial incentives nor economic resources to justify technological advancements of process. Most building agencies will not accept even two dimensional CAD documentation.

- Building information is often symbolic in nature at points in the design process. Elements such as door swings, tile patterns and bathroom fixtures either do not merit full 3D geometric description, or the full geometric nature may not be known at a given point in time. The building description is facilitated by treating these elements as symbols on plans, rather than developing such abstract or trivial information into detailed three dimensional representations. As technology continues to be adopted industry wide, and

efficient standards for including and reviewing this information become available, this symbolic information may eventually be migrated to a three dimensional form.

- Many building components have important two dimensional qualities. Many of the efficiencies in building systems used on Gehry projects are derived from building components that are essentially two dimensional. CNC cut plate elements, flattenable surface elements, floor finishes, all have geometric natures efficiently expressed through appropriately oriented two dimensional views.

For these reasons, two dimensional project descriptions are likely to be an important element of design and construction processes for some time to come. The technical and procedural integration of 3D and 2D information is a substantial focus of technological development by the firm. At times, the process has had the flavor of maintaining a *dual database*: one database of three dimensional data, and the other embodied in two dimensional drawings. The process of integrating between these two representations, distanced by technological and representational conventions, is not yet ideal.

A number of technological approaches support this integration between 2D and 3D project representations. However, not all are applicable to complex non-Euclidean geometry. Until recently, brute force geometric operations were required to extract drawings from 3D models. Section cuts could be easily generated by intersecting the model geometry with a plane at the location of the cut. Utilities also existed for performing isometric or perspective projections. However, hidden line removal utilities did function correctly for all geometric objects. Laborious geometric operations were needed to remove hidden geometry such as pattern curves on surfaces. Creation of section / projection views required manually splitting the master model at the cut plane, and erasing geometry prior to drawing extraction! This two dimensional geometry was then exported to AutoCAD and cleaned up. Finally, annotation, text, and hatching, line weight correction and other two dimensional “dress up” were manually applied in 2D.

Even minor changes to the project geometry required redoing the entire process. Existing two dimensional annotations could be manually repositioned, rather than re-drawing. Any drawings unaffected by changes in geometry would of course not be re-processed. The whole process took enormous amounts of time for each revision. In times of project

deadlines, shorts would be taken. The 2D drawings might be manually changed, rather than modifying the 3D geometry and repeating the process. The result has been difficulty in maintaining the integrity of the dual database. This difficulty was exacerbated as the detail in project models has grown.

This dual 2D / 3D nature of project geometry, and the necessity for its integration has been known to software developers for some time. Various approaches to the 2D / 3D integration, and the integration of symbolic expressions of project information with geometric representations, have been proposed by researchers and vendors. The support of automatic 3D to 2D geometric extractions has improved. Other approaches involving the "intelligent" re-writing of the building objects in various contexts have been proposed as well. For example, AutoDesk's Architectural Desktop software allows walls, and other project objects to be drawn in 2D, while retaining knowledge of their behavior and representation in 3D. This approach works satisfactorily for conventional, Euclidean project geometry, but is ill suited to Gehry's geometry, where the 3D behavior of building geometry can not easily be predicted from simple two dimensional views. The firm's strategy has been to find ways to easily embed necessary project information in 3D representations, then draw on more powerful geometric and symbolic extraction mechanisms to produce 2D representations.

Recent enhancements in the CATIA modeling platform promise to streamline this process. The software allows parametric definitions of geometric drawing extractions to be defined in a persistent manner. Section cuts can be defined in the 3D model space. When project geometry is modified, drawing extraction is achieved through a simple (though slow in terms of computer time) update request. These improvements have allowed an approximately 90% increase in operator efficiency for generating backgrounds for two dimensional documentation from the 3D model. Opportunities for automated extraction to 2D of annotation from non geometric attributes defined on 3D objects are also being pursued. Figure III-9 provides views of this drawing extraction process. These developments promise an eventual integration of two- and three- dimensional information into a single, comprehensive project database.

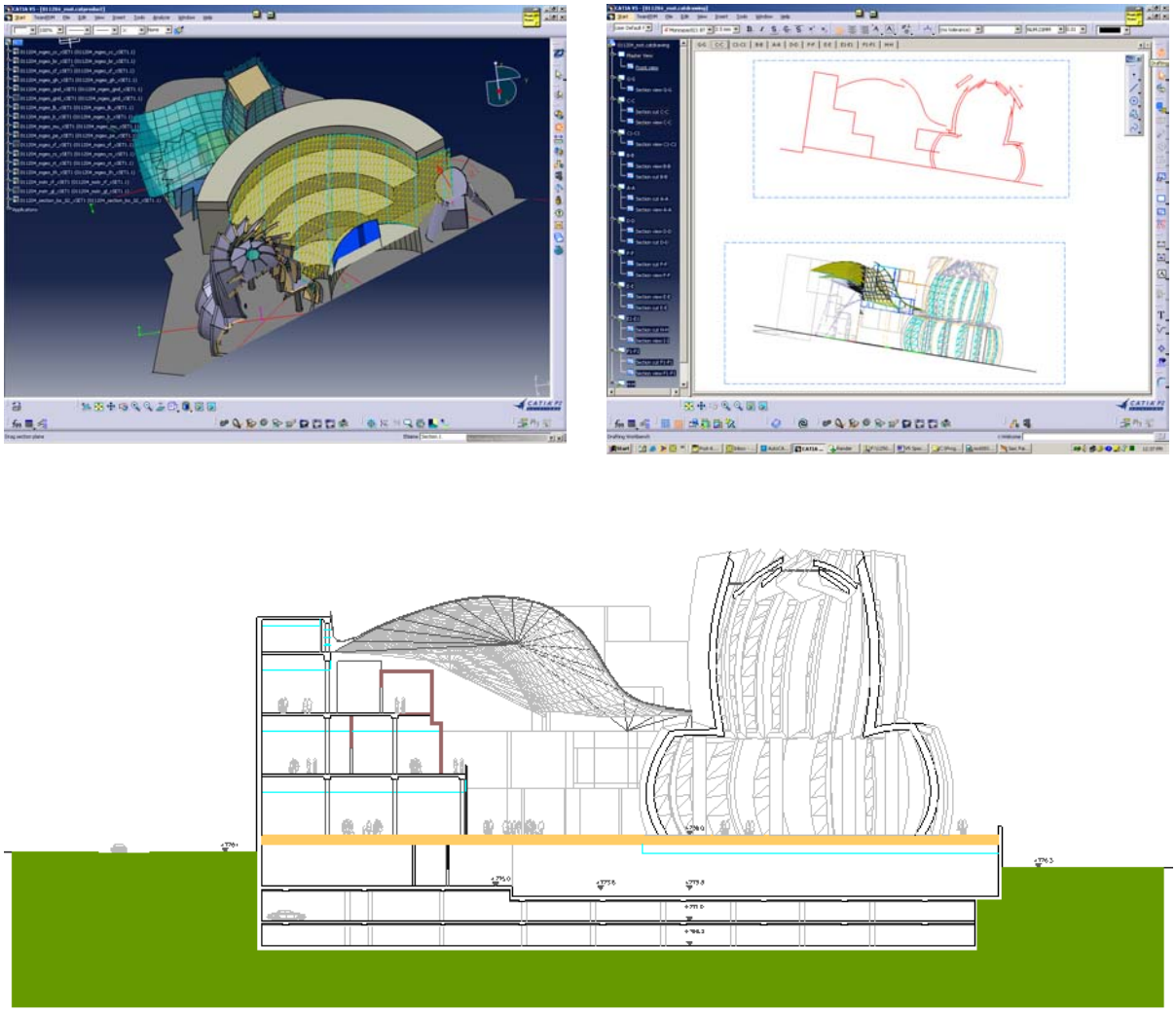

Figure III-9: Drawing extraction from the CATIA master model (MOT)

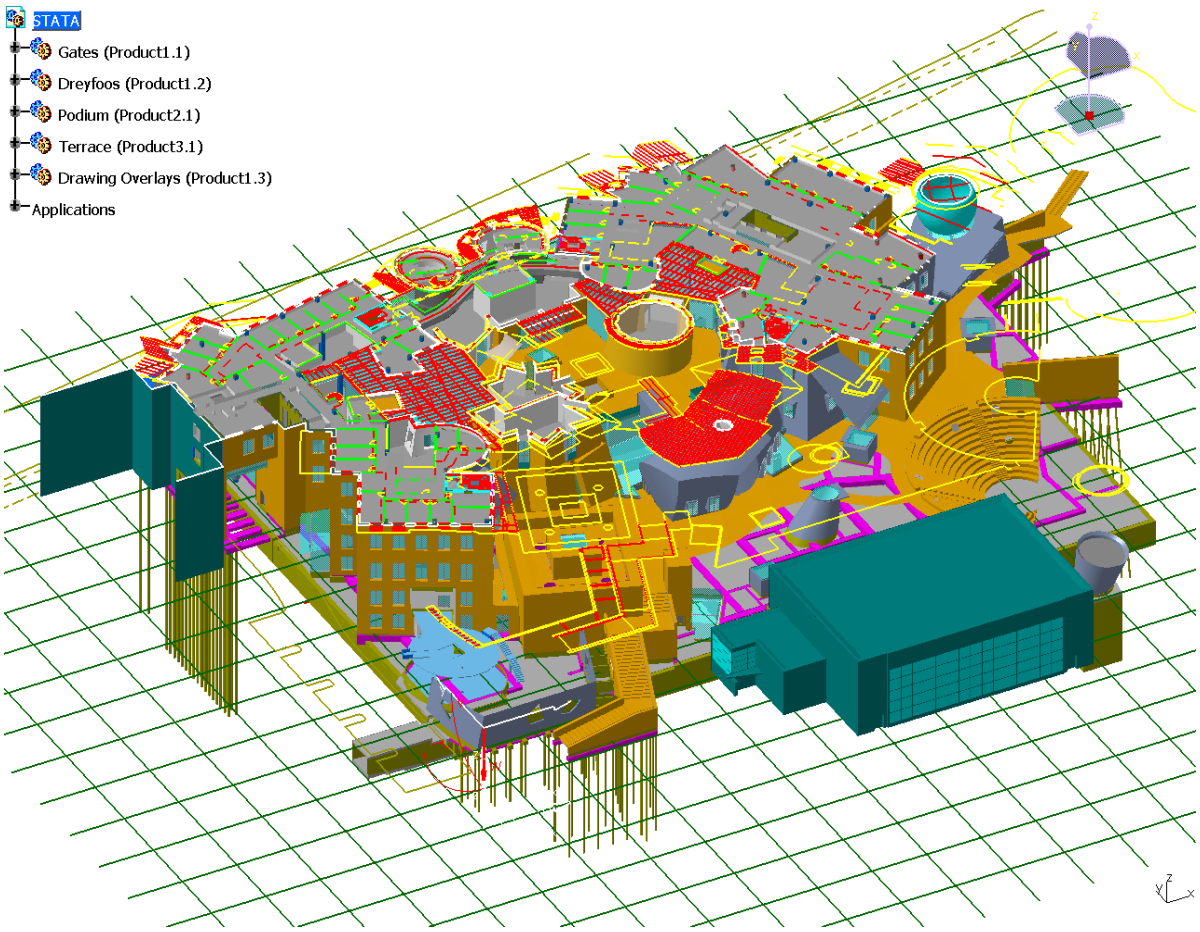

Figure III-10: Re-integration of two dimensional information in 3D (MIT)

Once these two dimensional extractions and annotations have been developed, it is of great benefit to be able to integrate this data back into the master project geometry, to allow review and coordination. This is easily achieved by importing the 2D CAD documents into the 3D environment, then moving and rotating the geometry back into alignment with the plane of the original cut. CATIA now allows AutoCAD files – exported through IGES format – to be permanently fixed to a location and orientation in space. Changes in the 2D drawing are thus automatically updated in the master model. Figure III-10 shows this overlaid 2D geometry – including projections of the geometry below – oriented with the project master model, which in turn has been cut at the level of the 2D drawing.

Many other applications of two dimensional extractions need to be supported in addition to the comprehensive documentation required for architectural documentation. The generation of shop drawings for certain systems can require numerous two dimensional extractions. For

example, concrete detailing requires many simple plan and section cuts of small areas of the project for detailed layout of re-bar. The utility of simple sketch drawings is preferable to the detailed generation of 3 dimensional layouts in this case. These simple cuts are easily achieved by planar intersections with the project geometry. Usually, these operations are performed either by the fabricator or by the general contractor as a service to the fabricator.

E. THE PHYSICAL / DIGITAL INTERFACE

The role of physical objects in Gehry's design process has had a profound role in the development of the firm's digital process. In any architectural or product design process, this relationship exists, since the products of the process are ultimately physical objects. Other firms do on occasion generate presentation models using CAD / CAM prototyping. The unique aspects of the physical / digital interaction in Gehry's process stem from the authority bestowed on physical objects and processes of making. Physical models are the primary elements of the process where the project design is developed. These physical objects define and embody the formal design intent as it is developed over the course of the project. Digital representations serve to capture this intent and allow for its processing and communication.

On more conventional project geometry, this division between physical and digital representation might not be so problematic. There are perfectly adequate ways of digitally and physically modeling orthogonally configured planar objects, and great geometric affinity between these digital and physical forms. Digitizing such conventional geometries is straight forward. A few dimensions can be measured, and then orthogonal planes can be positioned in digital space and intersected to form boundaries of surfaces. It is even arguable that the digital representation of such assemblies is a "better" representation of the design intent. Physical modeling necessarily introduces fabrication errors relative to pure Euclidean geometry. Materials warp, elements are cut too short or too long, edges are not perfectly straight, corners are not completely tight. While these imperfections might be imperceptible on well constructed scale models, when fully scaled these imperfections would likely be outside of construction tolerances. A gap at a corner of $^1/_{32}$" on an $^1/_8$" scale model represents a 3" hole at the corner of the construction! CAD modeling allows these imperfections to be cleaned up to within machine tolerances, well below the tolerances of construction. It is thus arguable that, if the design intent of a project is concerned with Euclidean geometry, digital

modeling can provide a more exact representation for the description of this intent than any scale physical representation. 3D CAD can even be a more efficient interface for generating this geometry, as the digital tools for performing cutting, positioning, moving, and editing of planar geometries can be easier than corresponding operations on physical modeling materials.

Gehry's process introduces a number of problematic issues into this clean relationship between physical and digital representations. Gehry's design models also contain imperfections of construction. However, unlike Euclidean geometries, established reference formalisms that serve to define the "true" geometry behind the shape do not necessarily exist. The geometry of the physical model provides the only definitive reference of design intent that digital representations must strive to emulate.

Highly accurate digitizing technologies exist that can sample points in tight conformance with physical objects. However, these representations still need to be cleaned up, to remove imperfections in the physical object and to simplify digital geometry to a form that can be manipulated. These operations introduce artifacts of the geometric representation underlying the CAD system – representational constructs whose characteristics may be radically different than those of the modeling materials. Distinctions between features of the physical object that are desired and those that are model imperfections or noise are qualitative, and must be undertaken through the filter of the CAD system's geometric representation.

A closely related issue emerges in comparing the "user interfaces" afforded by physical and digital modeling operations. Physical materials afford the development of certain forms, guided by the behavior of materials and operations that are facilitated by these materials. In the development of non-Euclidean geometries, these behaviors can be subtle and complex, as materials are driven to deformation at the limits of their material behavior. These effects generate formal qualities in the physical models important to the designers. The natural and intuitive operations of designers operating on these physical objects can be difficult to even approximately reproduce in digital form. As a result, either digital operations can result in subtly but critically different geometries, or the development of shapes with similar qualities can take substantial skill, time and attention by operators.

In Gehry's architecture, the physical models do not simply represent the geometry of the project. Modeling materials and operations on these materials have a certain representational relationship to qualities of the full scale materials and fabrication processes. Digital modeling substitutes mathematically founded constructs for physically based processes. In the process of taking a form from physical model to physical construction through the filter of digital representation, elements of the physical correspondence that binds model making to fabrication can be lost. The development of digital constructs that emulate and can retain these important physical qualities are a core part of the firm's computing research, and are explored in depth for specific materials and associated processes in the latter parts of this thesis.

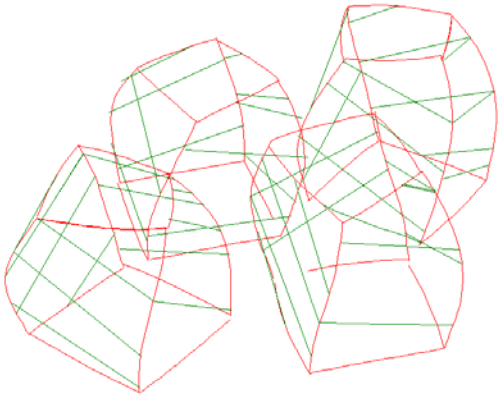

A. Digitized features

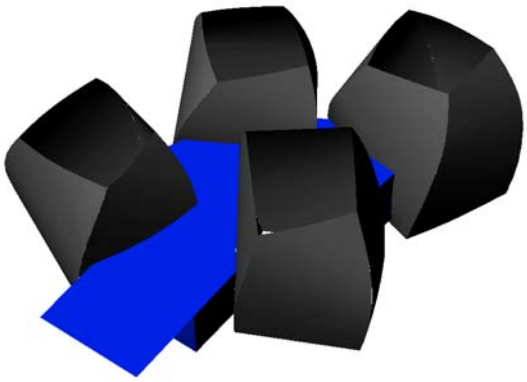

B. Digital "sketch" surface model

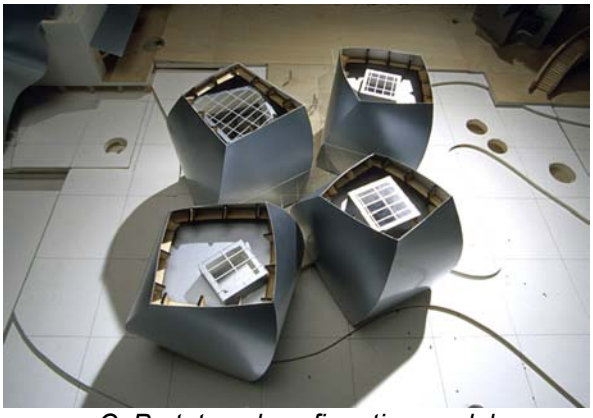

C. Prototyped confirmation model

Figure III-11: Digitized data, CAD model and prototyped model. (Ohr)

Despite the complexity of these issues, relatively simple technology is at the heart of the firms' digitizing process. The firm has relied on a FARO digitizing arm for the past eight years. This device allows points to be individually selected by the operator from the model. Segmented polylines can be generated by stringing sequences of these sampled points together. The arm is calibrated for each digitizing session so that samples from physical models can be registered with existing digital representations in "full scale" digital space. Many more elaborate digitizing technologies have been assessed over the years, such as cloud of points digitizing capabilities used by the automotive and animation industries. These technologies have until now been rejected due to practical

limitations, including cost, speed, visual occlusion issues and problems with the capturing of specific materials used in the firms' physical models.

The geometry sampled from the physical models is relatively sparse (Figure III-11A). This geometry captures critical *features* of the form to be observed in the digital reconstruction of the geometry, rather than a comprehensive sampling of the physical form. Critical features of the geometry vary depending on the material of the physical model. The edges between intersecting surfaces are often the most important manifestations of the designers' formal intentions. These edges include both those representing breaks in the surface form between surfaces of the model (shown in red in Figure III-11A), as well as the pattern of edges between sheets forming a single surface shape. Intermediate curves representing the flow of surfaces inside their boundaries are also captured to serve as guides for surface modeling efforts. On surfaces constructed from paper and other sheet materials, straight lines of ruling can be approximated from the surface material, shown in green in Figure III-11A. The geometric existence and implications of these features are discussed at length in Section VI.B below.

On the basis of these digitized features, a CAD surface model is developed using conventional NURBS modeling techniques (Figure III-11B). The result of this digitizing and re-construction process represents a "sketch" of the project geometry. It is far from a final representation, but rather serves as a background to the rest of the modeling process, providing the medium for production activities that resolve the shape into constructible form. Basic geometric operations such as closure of the surface into a "water tight" configuration can only be performed in the idealized geometric environment afforded by computer modeling.

The completed sketch model still represents a rudimentary representation of the building. It mirrors the level of detail of the physical sketch models, and may represent only the exterior envelope of the building. This digital sketch model will be in acceptable dimensional conformance with the physical model, such that preliminary architectural development exercises may be conducted relative to this digital artifact.

Verification models will be constructed from the CAD model so that designers can confirm that digital project representation does not deviate significantly from the form of the physical

models. Typically, “low tech” prototyping techniques are used by the firm to produce these models. In early versions of the process, “pancake models” were the preferred method for generating confirmation models. These models are made from layers of foam core, manually cut from the digital surface model. Planar intersections of the geometry generate profiles for these layers. The layers are manually cut from foam core, then re-assembled and glued together, and finally sanded and finished. These solid representations of the surface form can be physically modified by cutting into the foam core or layering on additional material. These modifications are then re-digitized, and the digital surfaces modified to reflect the changes.

As the process has developed and more intensive modeling operations are conducted earlier in design, more detailed and accurate verification model generation processes have become the norm. Frequently, verification models are now developed from intersecting sections of the surface geometry, organized as a “jig saw” puzzle of parts representing orthogonal sections though the surface geometry. These parts are developed in 3D as sections through the exterior and interior surfaces of the project geometry. Cut outs are inserted to allow elements to be connected together at their intersections. These parts are then flattened into 2D and cut out using flat bed laser cutting. The parts are re-assembled into a spatial framework, then covered with modeling materials (Figure III-11C). This process both allows a tighter conformance to the project geometry than the pancake method, and provides a model supporting the definition of both exterior and interior surfaces.

Occasionally, more elaborate technologies are drawn on, both for digitizing and prototyping. Layered object manufacturing (LOM, Figure IV-5), stereo lithography and material deposition (Figure III-17) techniques have been used on various projects. However, these techniques have important implications on the qualities of the resulting models, both in the forms produced and the modeling materials compatible with these techniques. Although these techniques result in models that are highly accurate dimensional representations of the digital models, they remove aspects of fabrication process from the model generation process, and rely on materials that may not retain qualities of either the generating physical models or the final fabrication methods. These prototyping techniques have typically been reserved for project elements whose ultimate fabrication materials are either molded materials such as concrete, or relatively free form fabric materials such as fiberglass or other composites.

More elaborate digitizing techniques have been attempted when the physical model would prohibit use the firm's feature digitizing and reconstruction process. CAT scanning of physical models was used on the flower sculpture on the DCH project[95], where the form and complexity of the physical model would have prohibited feature sampling using a digitizing arm (Figure III-12).

A. Physical model

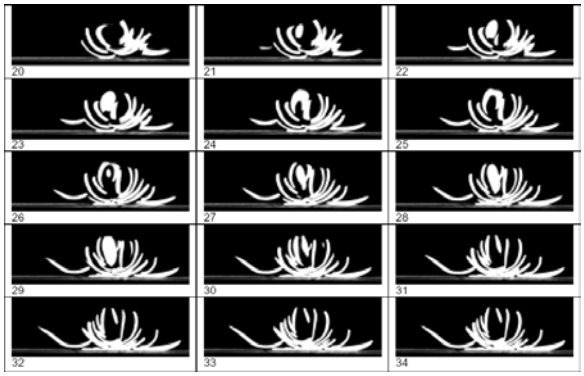

B. Sections through the physical model

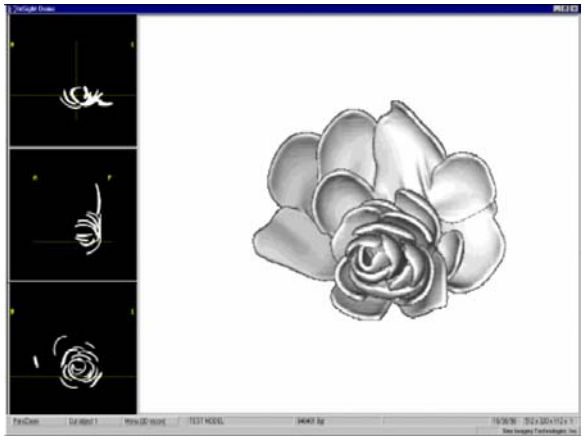

C. Model in medical imaging software

D. Digital reconstruction

Figure III-12: CAT scan and reconstruction of a complicated physical model (DCH)

The digital project models are developed in parallel with physical design modeling. At the end of design development, there exists a master physical model of the project and a corresponding digital model that are the in tight dimensional correspondence and together represent the master project geometric representations. The digital model is then carried forward through to construction. If there are changes to the geometry required to address construction issues, these changes will be made to both the physical and digital master models.

Figure III-13: The physical master model and its digital counterpart (MIT)

As the design progresses in its definition of constructibility intentions, the relationships between physical and digital elements take on new forms. The integration becomes less concerned with the capabilities of digital representation to capture form, and rather to come to an understanding of issues of constructibility. Gehry projects often adopt fabrication systems that have no exact precedent, and apply these systems to forms for which the full impact of geometry on fabrication can not easily be anticipated. Often building performance codes and analytical methods have been developed with the assumption of more conventional geometric conditions. Physical mockups of building systems provide valuable information for their development.

Schematic level studies of potential construction systems are conducted in both physical and digital form early in the design process. The level of detail of early systems exploration is intentionally limited. These studies may serve to test the feasibility of a system strategy, and provide a vehicle for communication with partnering organizations Figure III-14 shows examples of schematic physical and digital structural studies.

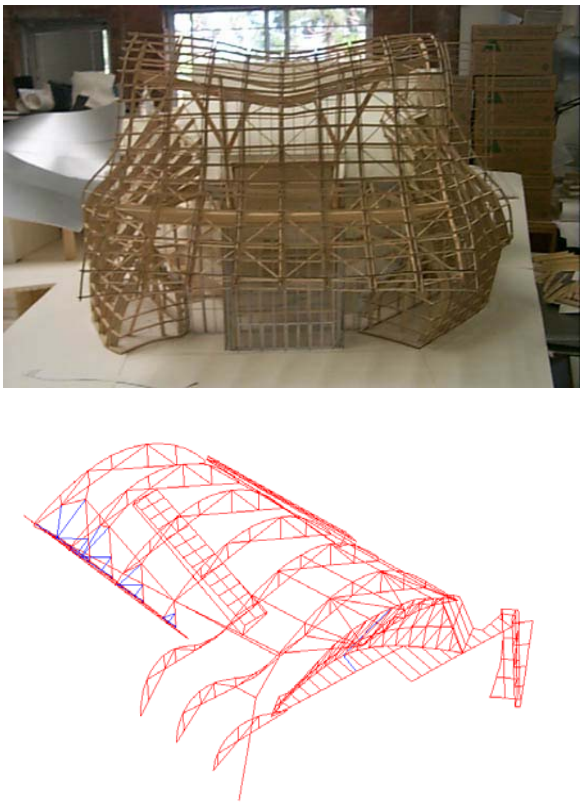

Figure III-14: Schematic design phase physical and digital structural studies

Larger scale physical mockups may be constructed of portions of the project geometry, and clad using potential materials of the final construction. These early mockups identify qualities of construction materials that may impact the aesthetic qualities of the project. During early design development, these mockups are constructed by the firm's internal modeling resources, and the actual correspondence to the final systems – in terms of fabrication or assembly components – is limited. Rather, the mock-ups at this point are utilized to explore the qualities of potential construction materials, and to expose some of the relationships between fabrication methodologies and the qualities of the shapes that are being considered. The full system detailing may not be employed; these mockups serve simply to test whether the assumptions about the relationship between project geometry and finish material qualities are valid. One main consideration to be tested is whether the finish system can actually assume the form specified in the digital model without warping, cracking or localized distortion around fasteners.

Later mockups become more elaborate. Fully detailed digital studies are conducted of small portions of the project, to fully test system detailing strategies in the CAD environment. These studies are conducted on selected portions of the project deemed representative of typical geometric conditions. These *digital mockups* are developed to a level of detail where

the organization of components – and special cases that may result from the deployment of a selected building system – can be understood. Issues identified in these selected portions of the facility will be extrapolated to the rest of the project. The level of detail undertaken will be up to that which would suggest that full completion of shop drawings could be undertaken. Figure III-15 shows design development phase digital mockups of several approaches to the construction of the "Kiva" element of the MIT Stata Center project. This element was considered to represent the geometry and construction of several areas of the project.

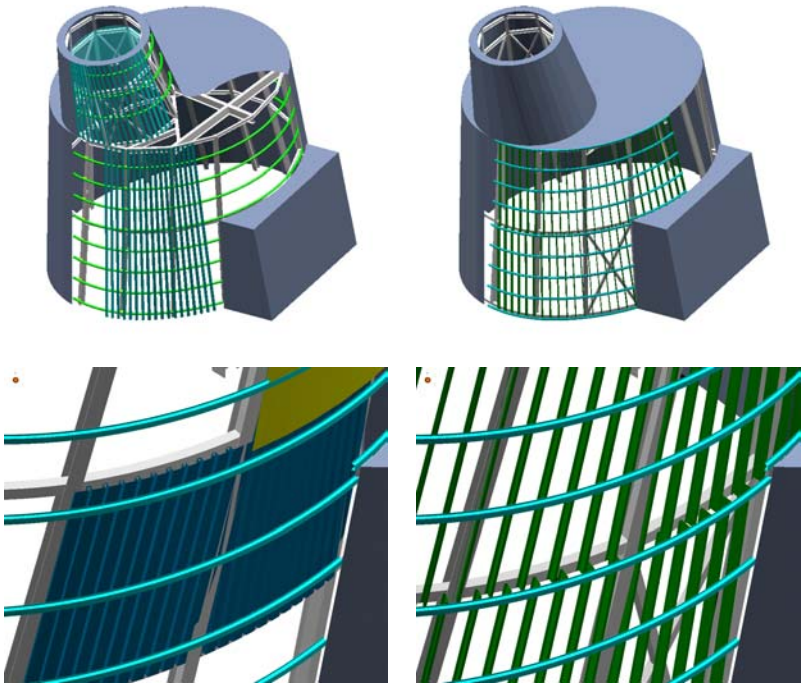

Figure III-15: "Digital Mockup" studies of cladding systems, Kiva element, Stata Center

Ultimately, full scale performance mockups may be constructed to allow full engineering testing of proposed building systems. These mockups test the full digital – physical construction process of the design and construction teams, including hand offs of geometric information. These mockups are typically developed for cladding systems to allow full engineering testing. Tests may include structural and wind loading performance, water penetration, and response to frame racking that might occur as a result of seismic events. Figure III-16 shows an example from the Disney Concert Hall project, in which a performance mockup was developed using the actual geometry of a small corner of the project from the project master model. This geometry served as the basis for developing a mockup comprising three major cladding systems: the typical cladding system, skylights and vertical glazing. The mockup was subjected to testing under simulated wind and rain conditions, in initial state as well as after frame racking was imposed.

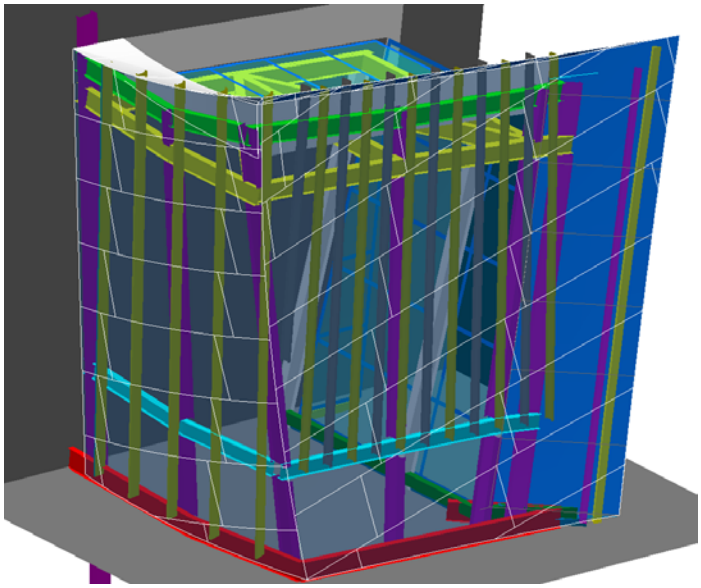

A. Digital shop drawing of mockup

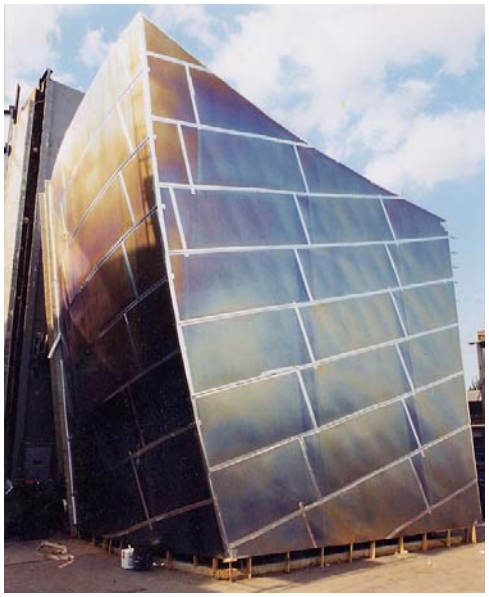

B. Typical cladding system

D. Testing under simulated wind and rain conditions

C. Glazing system and knife edge, skylight beyond

Figure III-16: Performance mockup of DCH cladding systems

.

F. RATIONALIZATION

The concept of rationalization is at the heart of Gehry Partner's computing and construction methodologies. Broadly stated, rationalization is *the resolution of rules of constructibility into project geometry*. The concept encompasses broad applications in the firm's process. Many of these applications can have substantial impact on the formal qualities and design intent of the project architecture. Others can have dramatic effects on the cost and control of construction, and hence can determine the feasibility of building strategies.

This issue of problem description through mathematics and geometry, and the fitness of a mathematical / geometric model to a given solution approach is of course nothing new in engineering and physics applications. In Gehry's building process, geometric representation and its role in providing the syntax for describing the project design intent, and supporting its translation into constructibility and building intentions deserves some inspection.

Mitchell makes reference to the role of rationalization on constructibility decisions in his comparison of the Sydney Opera House and Guggenheim Bilbao projects[57]. The Sydney Opera House (1957-73) designed and constructed just before the advent of digital geometric modeling, required the designed form to be rationalized into spherical elements simply to be describable using contemporary drafting and engineering methods. With the advent of digital curved surface modeling, these limitations on designer's descriptive capabilities seem to have largely been addressed. However, experience by the firm indicates issues of project description and geometric constraints are still very much in play.

Simply the operation of rendering a physical shape into digital form implies a structuring through the geometric representations of the CAD application. A broad palette geometric forms with various characteristics – one, two or three dimensional, Euclidean or other differentiable forms – are available to serve as representational bases for the surface geometry or any other element of the building. Selection of a set of geometric elements as a basis for the digital representation in itself imbues the digital description with certain characteristics. In the process of rendering the project design surface into digital form, variations between the shapes produced by physical modeling and that produced through digitizing occur. This is not so much due to any specific, substantial deviation in the sampling of geometry, but rather more subtly due to the qualities of the smoothing functions embodied

in NURBS representations, relative to that provided by physical materials. NURBS modeling tends to produce a more uniformly varying surface smoothness. Localized variations of the surface form generated through the forming of physical materials are lost in the process. Slight imperfections of the model geometry need to be "fixed" in order to close the project surface into a tight form. Loss of these nuances of form is apparent to the project designers, and the control of form as it passes between physical and digital representations is of substantial concern in design phase. While certainly digital modeling represents a vast improvement over traditional drafting methods in capturing non-Euclidean design forms, qualities of these digital geometric representations still have an impact on the description of forms.

Figure III-17: Physical model rationalized by digital modeling

The impact of geometric representation on project form is more apparent when representational constructs associated with fabrication are considered. The notion of congruence between a geometric representational form and the requirements of a system may seem unfamiliar on the basis of "conventional" construction. However, such decisions are made, even if standard conventions of project documentation make these decisions seem implicit. In conventional framing, a stud seems to be naturally described by one form: that of a line or linear extrusion. However, different views of the project (plans, sections, details) are based on other geometric constructs. Within these disparate representations, even a simple object such as a stud might assume a variety of geometric forms.

In the documentation of Gehry's forms, the issues involved in selecting geometric representations for project elements is more readily apparent. Numerous mathematical forms are available for representing curved objects in space. Each of these approaches introduces a de facto set of constraints on the shapes that can be represented. The activity of selecting a digital representation for spatial system components – in congruence with the physical constraints on the fabrication of these components – is a core aspect of the rationalization process

One motivation for rationalization efforts is ultimately project cost, reflected in the unit costs of available fabrication and construction systems. Fabrication efficiencies can pose substantial constraints on project geometry. Building systems come with rules or constraints that have direct bearing on the qualities of forms that can be accommodated. Low cost systems may highly constrain the forms that can be produced. Many contemporary fabrication processes rely on equipment geared toward the generation of Euclidean shapes: straight line break cutting and sawing, bending of extrusions to arc shapes on spindles. Alternatively, construction methodologies with great degrees of flexibility can represent prohibitive unit costs. Where competitive CNC enabled processes offering support of fully curved geometries exist, these processes often imply fabrication costs that would overwhelm reasonable construction budgets. Engineering and performance criteria can impose constraints on eccentricities in geometric positioning even if curved geometries can be fabricated.

In Gehry's work, new construction systems are frequently developed to support specific project forms. However, these systems will necessarily bring formal and organizational requirements that can require some modification of the project forms. The project design development and associated systems engineering strategies must be able to accommodate these requirements individually, and negotiate between the geometric impacts of differing systems' requirements as they interact. Computer modeling is the principal medium through which this geometric rationalization occurs. Digital project descriptions are the design artifacts in which detailed dimensional descriptions occur, where heuristics regarding the behavior of the design geometry can be made, where geometric rules organizing project elements can be represented, and where tools exist to perform operations that can bring project elements into conformance with these rules.

The identification of appropriate geometric constructs for a given system is fundamental to the development and deployment of building systems that support complex geometry. At best, if there is a tight conformance between the construction constraints of the system and the constraints of the geometric construct, simply generating shapes with this geometric construct guarantees constructibility of the shapes. Computational tools may be developed to support a rapid and intuitive generation of shapes based on the selected geometric form. The underlying logic presented by the geometric form – and its synergy with that of the construction system - may be drawn on to support automation of descriptive activities.

Consideration of these geometric and system decisions is ideally begun early in design, while the initial gestures of the project are still being developed. These rules, representing both formal and practical qualities of proposed systems, are developed in collaboration with engineers and fabricators. The development of system rules and operations occurs along a similar time line to that of the project form. Initially, only general notions of the selected systems and their associated constraints may be understood. This initial understanding may influence the selection of materials to be used during physical model explorations. The design's formal and system decisions are refined together as the project develops. A tighter level of understanding of the qualities of the design form the basis of more detailed system strategies, which in turn present more specific rules for the spatial organization of the project.

A simple example serves to illustrate the point. Many building systems used on Gehry's projects involve components whose shapes are curves generated from planar intersections with the design surface or offsets of this surface. This curve will derive the structuring of its geometric description from the intersected surface, typically a NURBS curve from a NURBS surface (Section V.D.3). This curve is smoothly and continuously varying in shape and curvature.

For much of the project, the element may remain represented in the master model in this original geometric description as a simple planar curve in space, even as details of its performance, materials and fabrication are being defined. The structural frame may be carried in the master model through to construction documents simply as a wireframe. During shop drawing production and fabrication, the geometry of the elements' descriptions will likely need to be refined. Economies of fabrication may dictate that performance criteria for the system can be satisfied most economically through systems which impose some constraints on the geometry of elements, relative to ideal curve generated from the model geometry.

Often, these smooth planar curves are ultimately rationalized into sequences of Euclidean sub-elements, either straight lines, constant curvature arc segments, or some combination of the two. Rationalization of curves into line segments is straightforward (Figure III-21B). A set of points on the curve is selected through some criteria; these points are joined together by line segments. This simple segmentation has obvious correlations to fabrication applications

(Figure III-18), and fairly obvious impacts on the tolerance of the resulting system relative to the ideal geometry expressed by the input curve. Segmented members can be constructed out of extruded profiles, including I beams or custom channels. The selection of segmentation points can be dictated by a number of criteria, including connection relations to other project geometry, maximum or minimum efficient material lengths, angle criteria, maximum distance deviation from the ideal curve, etc. These fabrication efficiencies can be expressed as geometric rules and encoded in the segmentation strategy. Numerous systems on Gehry projects have employed this geometric rationalization strategy, driven by widely different fabrication criteria and corresponding geometric rules.

Figure III-18: Segmented construction of planar curves (DCH)

Figure III-19:Arc Segment generated primary structure (MIT)

There are several limitations of a straight line segmentation approach from the perspective of constructibility. Segmentation produces angles between segments; which will cause kinks in the system that may disadvantageously affect the architectural form. The resulting angles may need to be resolved through complicated beveled connections. The deviation between the ideal curve and the linear segments can result in conflicts with other systems. Of course, the deviation can be controlled by increasing the number of segments, but this will also increase the number of parts and connections, which can drive up the cost of fabrication.

A second approach, used on several projects, rationalizes planar curves into sequences of arc segments, with tangency constraints imposed between the segments (Figure III-19). This can ameliorate some of the limitations of the linear segmentation strategy above. The connections between elements will be smooth, so no kinking of the system or the resulting connections results. The relationship between number of segments and deviation from the design curve is improved. Of course, bending material into an arc is likely to be more

expensive than leaving it straight, but the in reduction of the number of connections, and the resolution of connection geometry into straight connections can more than justify the expense of curving material.

Figure III-21C illustrates the geometry of this rationalization approach. Two points on the design curve – and the corresponding tangents to the curve at the points – are provided as input to the rationalization. These input location + tangent vector pairs can be joined through a *biarc* – two arcs joined in tangency[97]. In fact, a given input point / tangent pair generates a one parameter family of biarcs. Within this family of biarcs, the arc pair closest to the input curve can be determined by optimization. If the deviation between this optimal biarc and the input curve is outside of the desired tolerance for the system, the approach can be recursively applied by selecting a point somewhere in the middle of the design curve. The biarc solution can be applied to each of these ranges, resulting in a total of four arc segments (Figure III-21D). The process can be repeated recursively until a satisfactory solution is achieved.

In pipe bending, fabrication requirements have sometimes suggested including a straight line connection of pre-determined length between adjoining arcs (Figure III-21E). The reason for this is that the bending equipment can not bend the material all the way to its ends; a ”grip” section is required at the termination of the pipe bend. The rationalization strategy can be amended to accommodate this requirement by first casting a biarc over the curve as described above, then “backing off” the curve along lines of tangency at the ends and the biarc connection the required distance from both ends, and finally constructing arc segments from these new points.

Figure III-21F shows this approach on a study of the Weatherhead pipe system. The recursive biarc optimization algorithm, along with minimal straight line joining segments, was developed into a custom geometric modeling program. The program includes automation of dimensioning on arcs and straight segments of interest to the pipe bending fabricator.

Figure III-20: Curved, planar pipe system (Weatherhead)

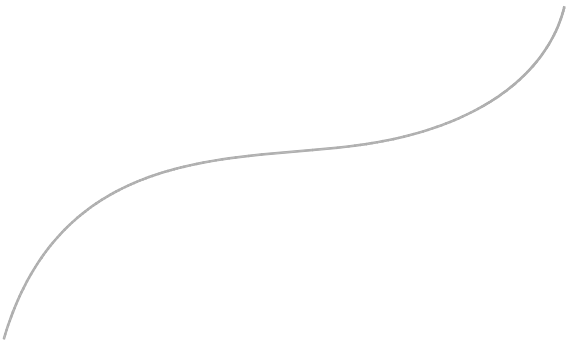

A. Input planar curve

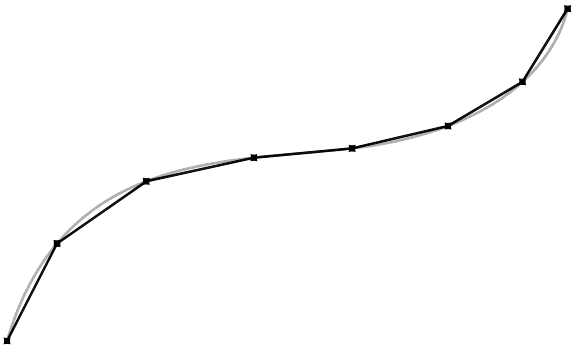

B. Linearized rationalization

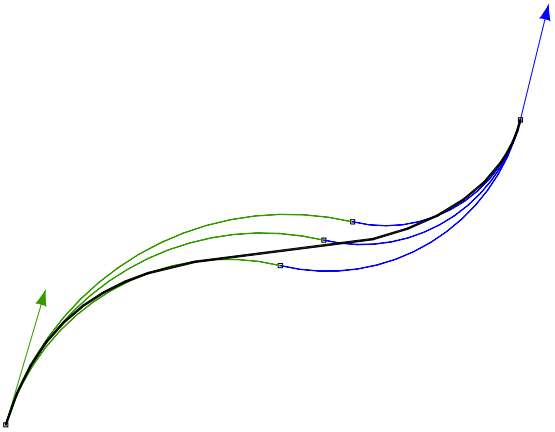

C. Biarc rationalization

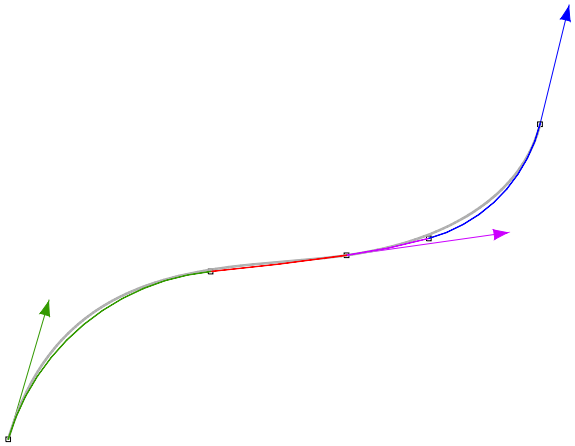

D. Recursive biarc rationalization

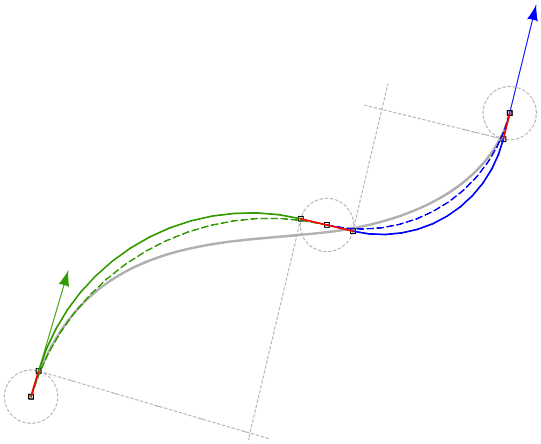

E. Biarcs with linear connections

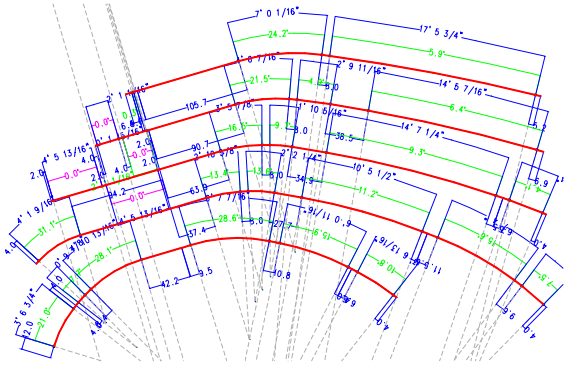

F. Automated rationalization results

Figure III-21: Rationalization methods for planar curves

This example presents a quite simple application of rationalization methods to the fairly simple geometry of planar curves. Even in this context, it is apparent that differences in the designs of building systems can profoundly affect the strategy of geometric representation. The rationalization algorithms described above are substantially deterministic. Given a planar curve, a geometry rationalization algorithm embodying constructibility rules can be identified through which successful solution can usually be guaranteed.

Rationalization considerations can become substantially more complex when system organizations move “off the plane” to full three dimensional spatial organizations. Additional degrees of freedom imposed on problems of geometric elements in 3D space can quickly render such deterministic solution strategies unachievable, or at least introduce geometries with more complicated fabrication requirements. This is illustrated in the development of global structural strategies on Gehry projects. A variety of primary structural systems have been employed; we compare two relatively typical approaches on the Experience Music Project and the Walt Disney Concert Hall, both projects with a primary structural strategy developed around a steel frame (Figure III-22).

A basic difference can be detected in the geometry of the structural scheme employed on these two projects – a distinction that represents an extension of the rationalization operations discussed in the above example. DCH represents a more “conventional” braced steel frame constructed from straight stick steel extrusions. These extruded members are formed from conventional AISC steel sections[1] – predominately I beam and column sections.

AISC section steel is mass produced by commercial steel mills, and represent a quite economical “raw material” for construction. However, in order to approximate the curved surface geometry of the DCH surface, the structural frame presents a “tessellation” of the curved surface geometry. A relatively tightly framed grid of columns and beams – approximately 10’ on center – was required to accommodate the curved surface geometry to tight enough tolerances. This relatively fine grain tessellation of the frame geometry results in a relatively large number of connections between primary structural elements.

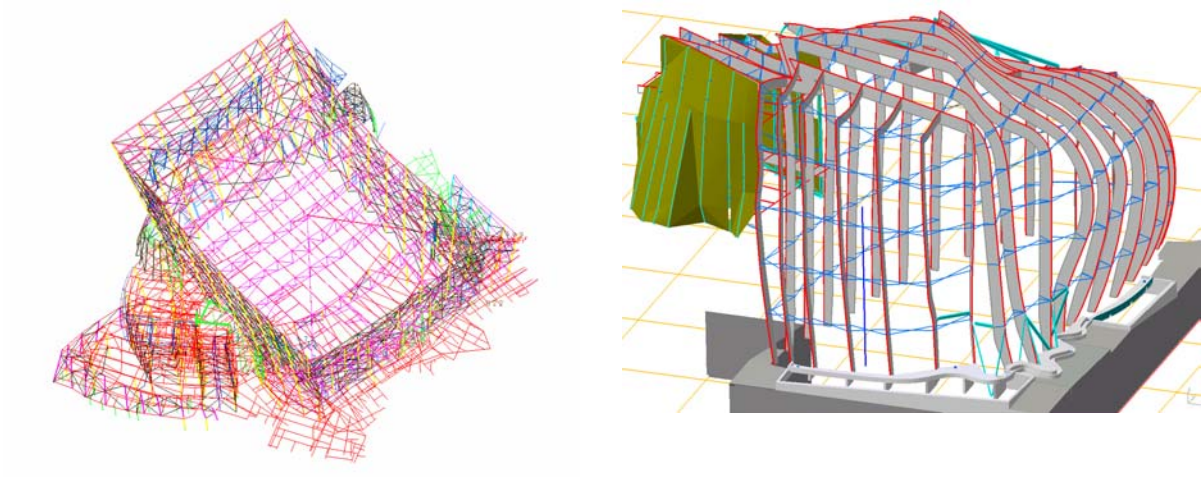

A. Frame geometry in the master model

B. Geometry of on site construction

Figure III-22: Comparison of DCH and EMP structural schemes

More importantly, the geometry of these connections is relatively complicated. Members do not frame together orthogonally, requiring difficult end bevels and complicated plate and clip assemblies (Figure III-23). The number and complexity of member connections has made the steel frame on DCH a difficult and expensive detailing job, offsetting the benefits of using straight, stock section members.

Figure III-23: Connection geometry on DCH

The frame design of the Experience Music Project takes a radically different approach[66]. The structural strategy results from plate built ribs, essentially curved I beams built up from custom cut plate elements. The frame is initially laid out as intersections between the design surface and a pattern of parallel, vertically oriented planes, spaced 10' on center The resulting planar curves are offset inward 24" from the finish surface to accommodate the curtain wall system (described in detail in Section IX.A below). Finite element modeling by the engineer (Skilling, Ward, Magnussun, and Barkshire) determined the necessary stiffness for each rib. On the basis of these performance criteria, the depth of the I-beam profile was determined for each rib. These depths were reflected in the CAD model of the system by simply offsetting the external curve of the rib the calculated distance.

In some highly curved areas of the structure, exactly following the planar intersection curve of the surface form would have imposed excessively tight curvatures in the rib profile. These curved regions would have disrupted the load path through the curve, producing excessive bending forces. In these highly shaped areas, the rib geometry was rationalized further, bringing the rib geometry away from the surface. The deviation between the surface and the rib was accommodated through additional secondary steel.

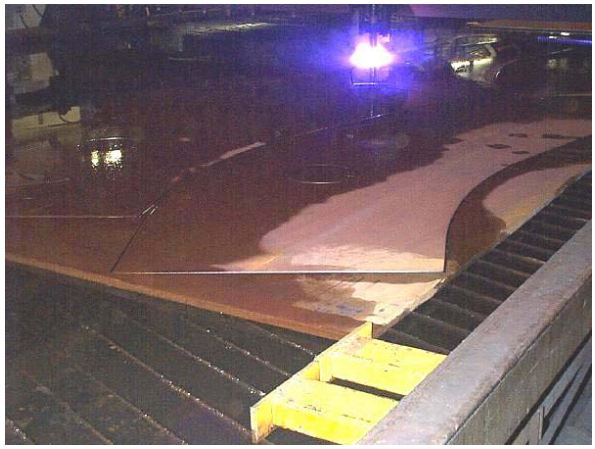

A. Plasma CNC cutting of rib web

B. CNC rolling of rib flanges

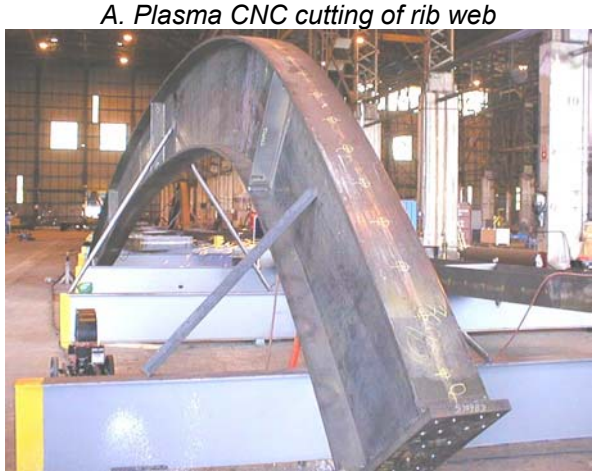

C. Completed rib in shop

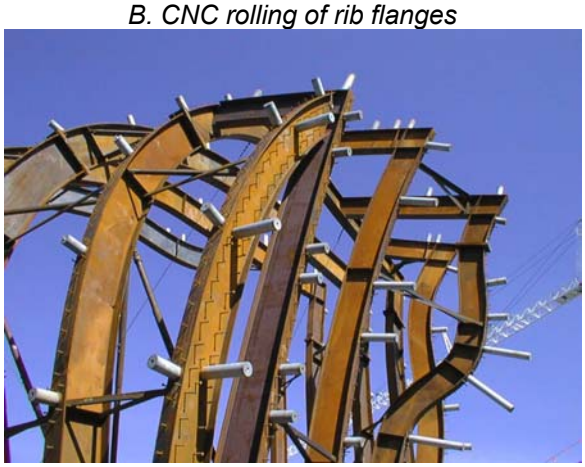

D. Rib assembly on site

Figure III-24: Steps in the CNC fabrication of EMP structural ribs

In the EMP system, a fully curved edge representation was retained through to fabrication. The curves were brought into AutoCAD, re-oriented, and flattened in 2D for shop drawing detailing. Curves defining the boundary of each rib's web were created, then sent to plasma cutting equipment (Figure III-24A). In a second step (Figure III-24B), the edge curves were passed to a custom built CNC plate rolling machine, which rolled plate steel for the top and bottom flanges of the ribs into shape.

Rationalization operations can be required simply as a consequence of the collaborative computational process. Translations from the NURBS surface based CATIA environment to other trade specific software applications can necessitate rationalization of the form described, just to achieve continuity of process. Currently, few of the steel analysis and detailing applications available accept curved elements. Finite element structural analysis programs still typically require linear elements for solution. While rationalized FEA models are not usually transferred directly to fabrication modeling, these linearized formats have

become the standard translation format for most steel translation. New additions to standards such as SDNF[51] allow the translation of elements comprised of constant curvature arc segments (Figure III-19). This enhancement of translation format still dictates rationalization of curved geometry into arc segments.

Figure III-25: Two dramatically different fabrication systems for curved glass forms

It should not be surprising that the toughest rationalization problems on Gehry's projects often derive from the fabrication of the surface envelope itself. The qualities of materials, and potential efficiencies in fabricating enclosure systems guided by material properties again present a wide range of geometric constructs, and constraints on the geometry and architectural intent determined by these constructs. The rationalization of surface forms adds another level of complexity to the digital process. Considerable attention will be paid to the geometric constructs underlying these systems' development in latter parts of this thesis. Figure III-25 provides a cursory introduction to the topic, in the geometric variation of curved glass fabrication systems.

G. MODEL INTELLIGENCE, AUTOMATION, AND PARAMETRICS

Substantial operator effort is involved in developing detailed system geometry in 3D CAD form. Since the geometry of each system element is often unique on Gehry projects, substantial repetitive geometric operations are required to instantiate the description of system elements. This level of effort, coupled with the cost of relatively high priced CAD operator labor, can have a significant impact on design and detailing costs. Furthermore, the project geometry is often in flux well into design development. The product of modeling effort invested early in the process can need to be reworked as changes to project geometry occur. On the other hand, building system development often requires studies of system geometry

to be conducted to some level of detail early in design, to ensure that system strategies address varying local geometric conditions. These issues of modeling effort have been addressed in the firm's process in several ways. Earlier in the development of the firm's digital process, virtually all CAD modeling was deferred until late in the design process, when the project designers had "closed" or finalized the building form. Prior to that point, only digital sketch models – rough surface models corresponding to the basic form of the physical models – were developed, usually only to provide geometry for cut extraction associated with specific document packages.

A general decline in the cost of computer modeling hardware, software and labor has allowed greater application of digital modeling earlier in the design process. However, issues of labor associated with large scale instantiation of system component definitions persist. The costs associated with this effort are partly addressed by limiting the level of detail of component geometric representations, and by performing detailed system studies or "digital mockups" on only small portions of the project geometry.

The dual goals of increasing efficiency of 3D digital documentation efforts, and supporting re-use of this information as variations in the building form occur, have been topics of research and development efforts by the firm and its partners. Much of this work as been centered around the development of procedural CAD modeling scripts to automate repetitive geometry generation tasks. Often a simple geometric operation requires several intermediate constructions to produce the required geometry. These operations are typically performed relative to some existing geometry of the model. Scripting of these tasks can reduce the time required to generate geometric descriptions of building components. For example, commercially available steel detailing packages such as X-Steel and SDS-2 provide macros for the generation of categories of steel connections. These macros perform cut backs, fillets, bolt holes, and other difficult geometric operations on steel members in 3D form, in addition to placing plates, clip angles and other connection components. Unfortunately, these applications have often been shown to make orthogonality and other geometric assumptions that do not necessarily hold on Gehry project geometry. These macros have required re-coding to support the geometric conditions in the firm's projects.

Sophisticated fabricators have developed their own programs to support the automation of repetitive geometric tasks during shop drawing generation. One example, A. Zahner

Company's Automated Panel Layout Application (ZAPLA), is described in Section IX.A below.

While these examples of procedural or scripted automation provide an element of modeling efficiency, they can not address requirements for updating information in response to changes in project geometry. The geometric scripts and any associated manual interactions must be re-applied on any modified input geometry. Toward the goal of addressing this limitation of scripted approaches to automation, the firm has recently begun intensive efforts to incorporate parametric technology into its digital process.

Parametric technology allows relationships among geometric elements to be encoded in the model as part of operations on these elements. For example, when a curve is generated as the intersection of a surface and a plane in space, the nature of this curve as a geometric relationship between the surface and plane is retained in its digital description. Changes to the input geometry – by modifying the surface or moving the plane - will flag an update and regeneration of the curve. Variables may be included in the descriptions of geometries; changes to the values of these variables can also be used to trigger updates of geometry.

Parametric modeling capabilities have existed in commercial applications for more than a decade. The technology has been the focus of architectural computing research in describing design typologies[55]. However, until recently, these applications were unmanageably slow for large scale geometric models. Furthermore, the user interface requirements for generating geometric associations between elements were unwieldy. The mathematical models underlying curved object representations add substantial computational requirements to the geometric description of objects, further slowing the updating of models.

Parametric technology has had substantial application in mechanical design applications, where changes to product definitions can be limited to dimensional variations of the product. Marc Burry's efforts to develop parametrically based models of elements on the Sagrada Familia construction project over the last ten years[15] provide a notable example of the application of parametrics in an architectural setting.

Recent improvements in the user interfaces to parametric modeling applications, and the inexorable advances in computational power, seem to have finally brought applications of

fully parametric modeling within the horizon of building construction applications. A pilot project to develop a fully parametric master model for the Museum of Tolerance (MOT) project was begun in January 2002, using Dassault Systèmes' most recent release of the CATIA product, Version 5. This initiative has produced promising results, although not without difficulties. One example from the project illustrates the potential of parametric approaches to constructibility issues.

Gehry Partners is currently collaborating with the engineering office of Schlaich Bergermann and Partner on the development of a free glass roof covering the atria of the Museum of Tolerance project. Several Gehry projects have included large curved surface elements comprised of triangular facets, including the DG Bank Headquarters skylight, a previous collaboration between the firms (Figure IV-2), and the entry façade of the Guggenheim Bilbao museum (Figure III-25).

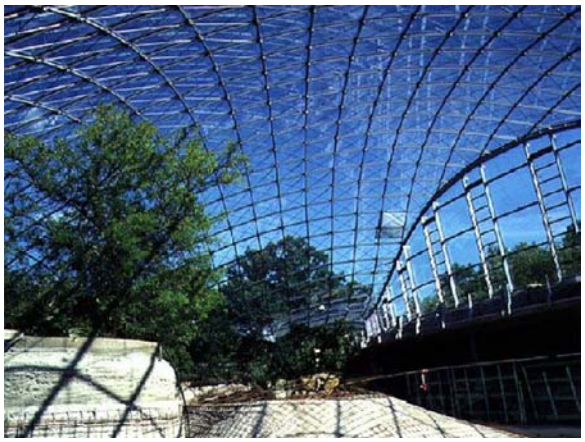

Figure III-26: Curved surface glazed roof (Berlin Zoo, Schlaich Bergermann & Partner)

A curved surface can be rationalized into an assembly of triangular facets with little difficulty. However, prior experience with large glazed roof structures by the engineer (Figure III-26) has suggested great economic advantage to constructing these structures from compositions of rectangular, as opposed to triangular, glazing elements. This requirement, while beneficial from a cost standpoint, imposes a substantial constraint on forms that can be constructed. While any surface can be tessellated into a closed composition of triangular faces, the surfaces that can be covered with a quadrilateral tessellation are highly constrained to configurations whose characteristics are not immediately obvious.

Independent study of the problem by both firms has identified the class of translation surfaces[18], which adhere to the geometric constraints necessary to allow quadrilateral tessellation. These are surfaces generated by a curve (the *generatrix* curve), swept in space without rotation along the path of a second curve (the *directrix*). It can be demonstrated that points, invariantly positioned along the resulting family of curves, can be joined by facets that

are necessarily both quadrilateral and flat. Figure III-27 shows elements of this construction. The vectors **A** (equivalently **B**) can be shown to be uniformly parallel, guaranteeing that a face lofted between any successive pair of these vectors is necessarily planar. This class of translation surfaces can be further extended by allowing the generatrix curve to be scaled as it is translated along the directrix. While certainly not all forms can be generated as translation surfaces, there is considerable freedom to the set of surfaces that can be described or closely approximated by a surface of this construction.

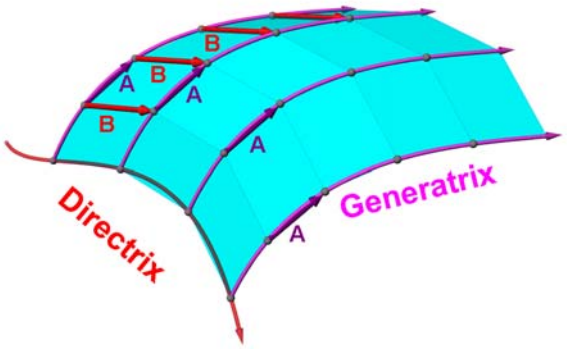

Figure III-27: Construction of the translation surface

The translation surface construction solves the problem of defining surfaces that can be approximated with quadrilateral tessellations. However, the generation of these surfaces requires a number of intermediate geometric constructions. Using conventional CAD approaches, the geometry must be re-constructed each time the generating curves are modified. This presents a substantial impediment to the interactive design of translation surfaces.

Parametric technologies allow these geometric operations to be encapsulated into a persistent, “intelligent” translation surface object that retains the structuring of its geometric construction. The inputs to, or handles on, this object are the generatrix and directrix curves, and a third curve that establishes the scaling of the genetrix as it is translated along the directrix. This dramatically simplifies the construction and modification of the surfaces, while still guaranteeing adherence to the constructibility constraints. Figure III-28 shows elements of this parametric construction, results of editing the surface by manipulating the input curves, and the resulting planar quadrilateral composition. It is anticipated that many of the firm’s constructibility problems can be attacked through similar definitions of parametric objects, which encapsulate the intelligence necessary to solve the given problem.

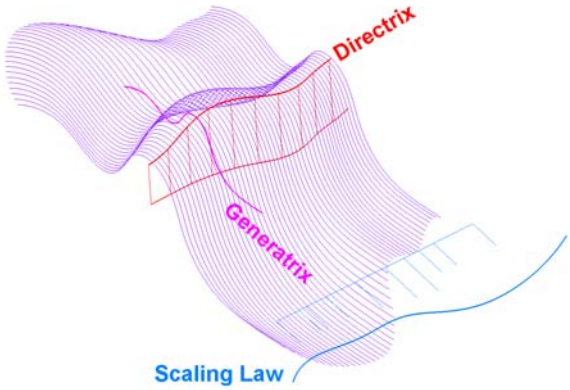

A. Controls and curve array

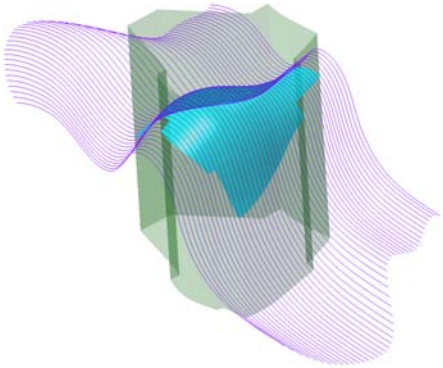

B. Clipping surface

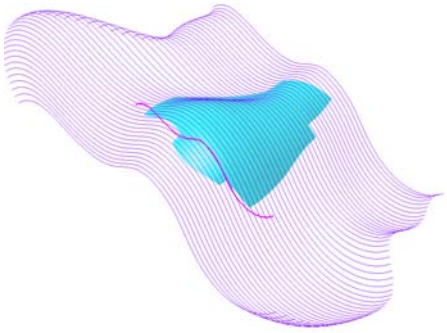

C. Modification of generatrix curve

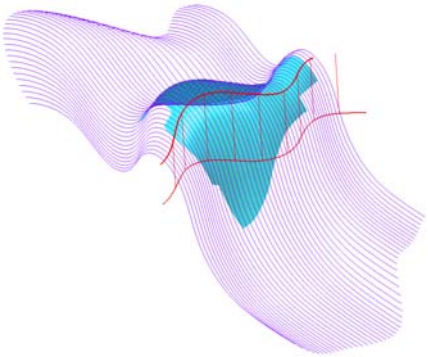

D. Modification of directrix curve

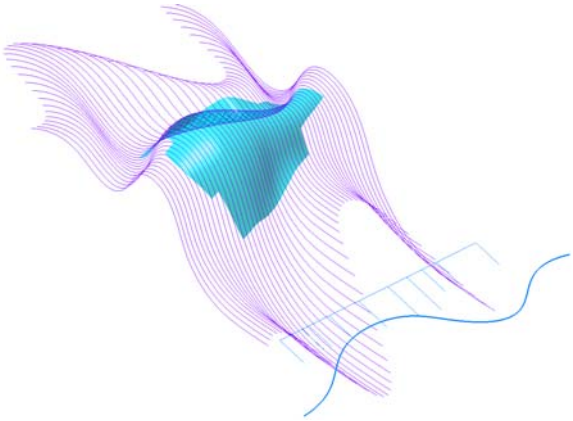

E. Modification of scaling law

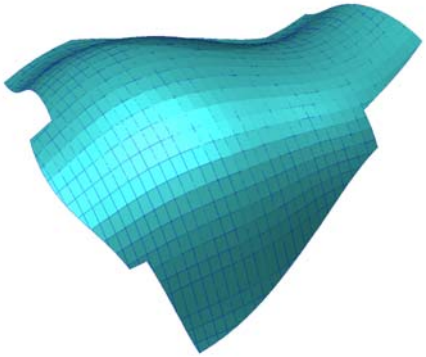

F. Resulting quadrilateral glazing assembly

Figure III-28: Parametric modeling of MOT roof system.

More limited applications of associating intelligence with project geometry have been employed by the firm for some time. Various mechanisms exist for associating non-geometric or “semantic” information with geometry. Layering and coloring constructs ubiquitous in CAD applications provide a trivial example of such capabilities. The establishment of project layering and coloring standards is a simple but important element of the master model definition. These standards are included in the project specifications and annotated in schedules on the two dimensional project documents. Maintenance of this attribute information during translation between the various CAD applications on the project is an important and not necessarily trivial aspect of the firm’s computational process development in general, and an element of the collaborative computational process developed with any new project partner.

One limitation of layering schemes for supporting model semantic information is that layer information represents only one “axis” or field for such information. There are many non geometric aspects of elements’ definition on a project that may be of interest, and that should be included in the project description along side geometry. These attributes may exist in many permutations. For example, on the Disney Concert Hall (Figure III-22B), attributes tracked in the structural steel wireframe model included primary vs. secondary steel, cardinal point (top of steel, center, etc.), steel grade, finish (galvanized, architectural finish quality), curved vs. straight elements, and provisional vs. released for construction. Each valid permutation of these attributes had to be tracked as a unique layer. While this scheme worked on this limited application, the strategy is not scalable as the number of systems and associated attributes in the master model are increased.

During the past three years, more advanced mechanisms for tracking of attributes have been attempted. CATIA V4 provides capabilities for developing *attribute schema*, named variables with defined values associated to the variable. The variables can be instantiated on any geometric object in the project master model. Queries can be run to identify elements of the project geometry with selected attribute combinations (Figure III-29A, B).

Similar capabilities provide support for associating attributes of structural steel elements with geometry. Attributes such as section profile, cardinal point, and material properties may be tied to a parametric description of structural elements’ position in space (Figure III-29C, D).

These developments promise to eventually achieve the firm's vision for an intelligent, fully integrated digital database of all project information. To date, this integration has been achieved by a mix of automated integration with substantial amounts of operator effort and project manager diligence. The scale and variety of information to be tracked on a project through its development presents an enormous computational task. Project information is not completely coherent until well into design development or construction documentation phases. Often, known conflicts or omissions of design information are carried in the project until the information necessary for resolution of these gaps in the information are available. Project designers can accommodate an ambiguity of information that might be difficult for an integrated database to process. Nonetheless, the firm's digital process and technologies offer elements of what can be imaged to be the future of digitally integrated project information.

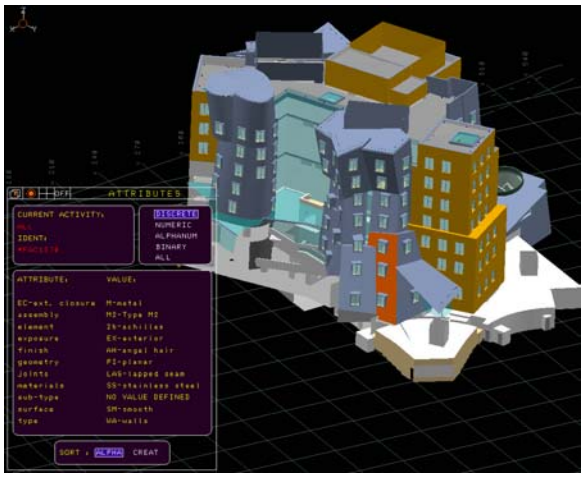

A. Listing of an element's attributes

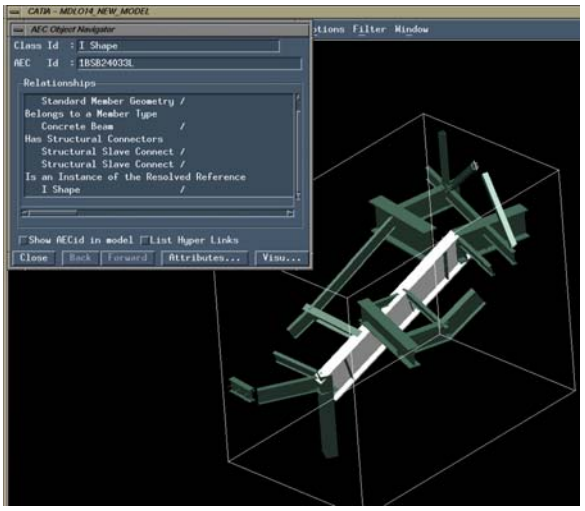

B. Searching for an element by ID

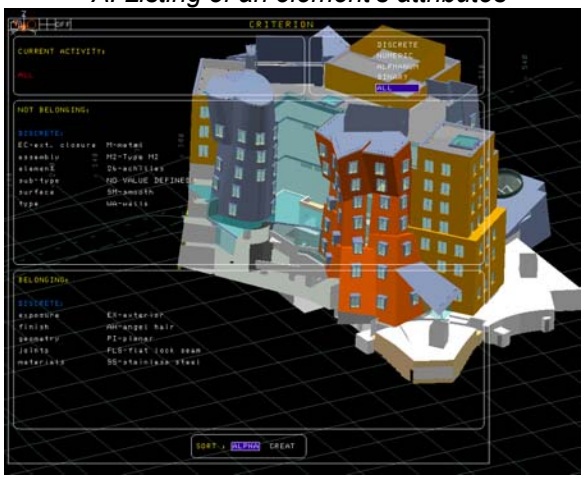

C. Query by attribute set

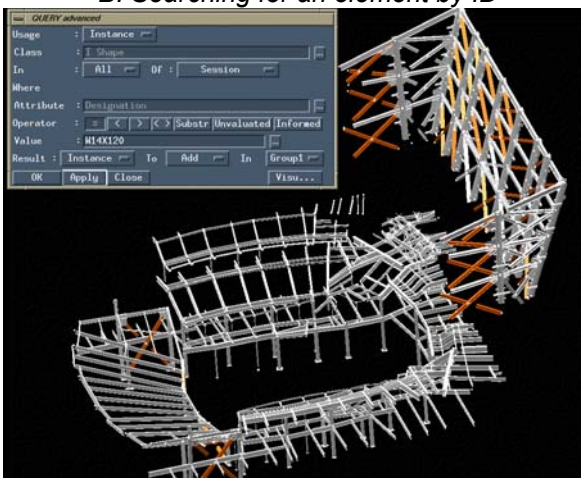

D. Query by member section

Figure III-29: Attributes on enclosure system model (MIT), structural frame model (DCH)

PART 2: THE REPRESENTATION OF SURFACE CONSTRUCTIBILITY

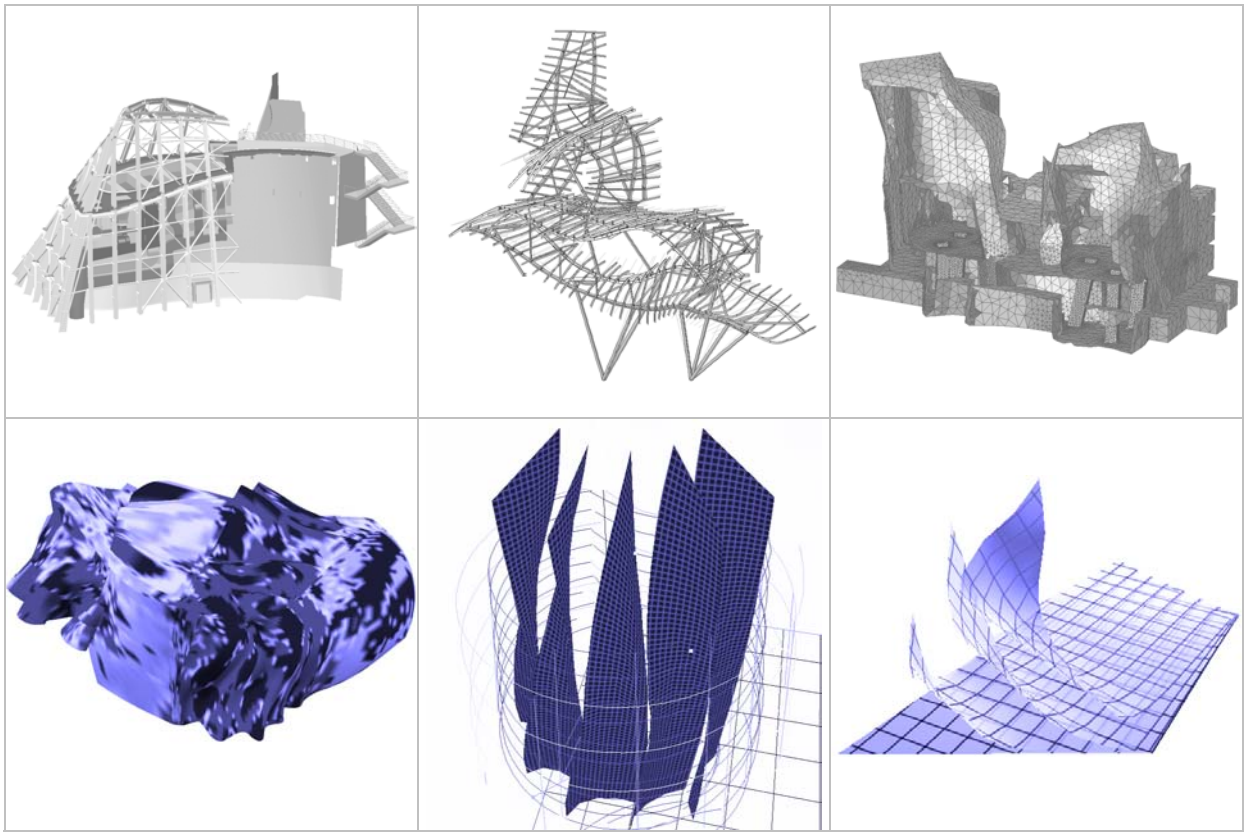

In Part 1 of this thesis, issues in the development of Gehry's Partners' building delivery process and associated computing methodologies were presented. Important relationships between the representation of project geometry and the operations of fabrication and construction were introduced. The concept of rationalization was introduced, through which requirements of constructibility are interpreted into geometric constraints on the project form. Examples of rationalizing geometric strategies were discussed in relationship to the building systems on which they have been applied.

While these issues impact the development of all building systems on Gehry projects, the most profound impacts are realized in the development of projects' exterior surface forms, and the corresponding building envelope systems that ultimately realize these forms. This exterior project geometry sets the stage for all subsequent constructibility strategies. It is here that subtleties of geometric interpretation can have the most profound consequences on the aesthetic qualities of the project.

The variety of geometric forms presented in Gehry's works eludes the development of a comprehensive taxonomy. However, in the body of work being developed by Gehry's firm at the current point of writing, there are a set of qualities which are identifiable and largely unique to Gehry's work: the smoothly curved surfaces which create the energetic, undulating forms on many projects. In these shapes there exists an important set of common building intentions, unified by similar approaches to the manipulation of surface materials, and guided by a common set of constructibility constraints and associated economies. The research presented in the remainder of this thesis is directed toward a geometric analysis of these forms, toward the goal of supporting the definition of constructibility requirements in computational form.

This discussion focuses on the set of shapes constructed from sheet materials, shaped in space without large scale material deformations that would require forming through molding or stamping. These shapes have been termed *paper surfaces* by members of the firm. The term "paper surface" is employed in this thesis in a deliberately pre-analytic and evocative sense, to reflect the wide range of formal and tectonic issues embodied in this class of shapes. Other more formal terms will be employed to characterize specific geometric constructs within this general class of surface forms.

This section is introduced through a qualitative survey of the surface geometries and associated formal, material and constructibility issues of Gehry's projects, provided in Chapter IV. Following this introduction, a review of the mathematical foundations of differential geometry underlying the description of curved spatial forms is provided. This mathematical foundation forms the basis for the definition of specific representational constructs supporting the description of paper surface forms. The definition of these constructs is provided in Chapters VI and VII, along with examples of their application to the definition of constructibility requirements on the firm's past and current projects.

IV. Materiality and its Geometric Representations

The previous chapters described the relationships between constraints on project forms introduced by economies and methods of fabrication, and corresponding constraints on the physical and digital representations of these forms. In Gehry's process, these constraints are represented in parallel: through the selection of physical modeling materials in the construction of scale models, and the selection of digital elements, defined by specific geometric constructs. We may consider the confluence of these physical, digital and fabrication constraints to define a class of surface forms.

It is possible to view the historical progression of Gehry's built projects as a progressive development of these classes of surface forms. The possibility of building the ambitious geometries exhibited in Gehry's recent work did not occur spontaneously. Rather, one can witness in his work the progressive development of an increasingly ambitious geometric vocabulary, beginning with the fairly conventional forms of his early commercial and residential projects, through to the extreme geometric forms of the Experience Music Project. Each project pushes the successful precedents and experiences developed on prior projects to new limits. On contemporary projects, Gehry often includes elements with geometries reminiscent of previous projects, as well as elements with ambitious extensions of prior geometries and, occasionally, elements for which no particular precedent yet exists. Corresponding to this formal development is a progressive development of engineering, fabrication and digital description techniques. While the progression of Gehry's gestural intentions may be difficult to decipher over the distance of time, the development of the underlying geometry can be discerned directly from the traditional and digital representations that document his works.

A. PLANAR SURFACES

The point of departure for this inquiry into classes of surface forms is the simplest and most obvious such class, embodied by planar surfaces. The basis for physical modeling of these surfaces are rigid sheet materials such as foam core or stiff cardboard, which may easily be formed into planar shapes. One can inquire what the geometric limits of these physical materials are. Non-planar shapes such as spheres or other curved surfaces are of course inappropriate for modeling with flat foam core. There are ways that this can be done, by

cutting and stacking, or wetting the material to achieve a paper-mache quality. But undertaking these activities using rigid flat materials seems to be qualitatively different than simply cutting out a piece of rigid material and positioning it in space. One may capture this observation as a rule regarding the behavior of stiff sheet materials, that “rigid sheet materials enable - and are constrained to - planar geometries”. As one works with rigid materials in scale, it is possible to “read through” the behavior of these modeling materials and to infer that, by working with these materials in an appropriate fashion, one is guided by these materials’ spatial behaviors to produce shapes within a vocabulary of planar forms.

Having built in model form an assembly of planar objects, one may have reasonable confidence that the assembly may be constructed using certain real world construction systems. There are of course a wide variety of construction systems supporting planar forms, from stud framing to glass curtain walls to concrete formwork. The economical deployment of these fabrication systems again suggests their application to, or enables, the construction of planar surface geometries. Notably, from the perspective of geometric performance, planar modeling materials may be used interchangeably to represent any of these construction systems. Although one may choose foam core of various thicknesses to represent concrete block or stud framing construction, or plexiglass to represent glazing systems, this selection impacts the perceptual fidelity with their represented constructions, not any further geometric conditioning on the modeled forms imposed by these materials. In extending this discussion to other geometric forms, this simplicity of geometric equivalence among physical modeling representations will no longer necessarily be the case.

Simple, precise mathematical descriptions exist for these Euclidean geometries, conducive to formulation in digital modeling applications. There are in fact multiple such descriptions. A plane in three dimensional space can be described as a relationship between three points in space, as a relationship between two intersecting lines or vectors, or through an implicit function of four variables[14]. A plane may be completely described by – and is “dual to” – a specially chosen point in space[10]. Each of these representations affords particular utility to specific geometric operations. However, these representations are equivalent, in the sense that we can translate between them explicitly; no loss of geometric information is incurred through this translation.

With the definition of this basic class of planar constructible forms in hand, one can begin to explore the limits of forms that respect the constraints of planar geometry. In typical construction, planar forms are organized orthogonally: vertical, perpendicular walls, horizontal floors. We may consider geometries of such orthogonally positioned planar elements to be a more highly constrained subclass of the general planar surface class. There are various fabrication and engineering efficiencies afforded by adoption this further restriction on geometries. Eccentric loading conditions are largely eliminated on vertical walls. Detailing of connections between orthogonally positioned wall and floor systems is simplified.

On conventional framed construction, pitched roofs provide an exception to the conventions of orthogonal, planar construction, and establish a precedent for the exploration of more ambitious planar forms. The geometry and corresponding detailing of hip or gable roof forms[63] is somewhat more complicated and expensive than that of the floors and walls below, but the documentation, engineering and fabrication associated with these geometries is well established in conventional wood frame construction practice.

Gehry's early works demonstrate precisely this exploration. The radical proposition or "violence"[21] of this early work is precisely in its demonstration that conventional, industrial materials and constructions could generate unconventional forms, applied unconventionally to non-industrial architectural programs. Along the way, the economies associated with this relatively conventional geometry and associated fabrication efficiencies are realized[42].

These geometries have persisted on elements of Gehry's more recent projects, even as his geometric vocabulary has expanded. Partly, this is a result of a budgetary strategy employed on Gehry's designs. These geometries remain inexpensive to construct, relative to the more recent additions to the vocabulary of geometric forms. Judicious use of conventional construction in concert with less constrained geometries has allowed the firm to meet project programmatic requirements within allocated budgets.

A. Planar forms re-adapted in Gehry's early work. (Gehry Residence, Wagner Residence)

B. Planar forms on contemporary projects, (MIT),

Figure IV-1: Examples of planar forms on Gehry project

In geometric terms, these planar forms are a highly constrained class of surfaces. This fact is evident by the trivial simplicity of its mathematical description. We can posit a metric for the freedom – or lack there of – of a class of surface forms by regarding the degrees of freedom in their mathematical descriptions. Planes in three dimensional space can be fully specified by three real numbers; the permutations of these three variables describe the positions of every possible plane in space. Of course, this is still an infinite set of potential configurations, and this representation does not take into account the possible configurations of boundaries that provide additional possibilities for planar forms. The simplicity – and rigidity - of this mathematical constraint system has a direct correlation with the both the simplicity and the geometric limitations of the corresponding fabrication systems.

B. "FREE FORM" SURFACES

At the opposite end of the geometric / constructibility spectrum, one can identify free form, virtually unconstrained surface geometries and associated fabrication methods. We may

construct scale physical models from materials that may be formed in an almost completely unencumbered fashion, such as one might do with clay. Here we are free to form virtually any shape, including the planar shapes enabled by rigid materials. Note, however, that smoothly planar forms are actually more difficult to form using clay than they are using rigid materials, where the planar forms are “at hand” in the form of the raw materials themselves. The freedom enabled by clay like materials seems disadvantageous if one is to engage in constructing planar forms. As one forms these materials, one may again “read through” the material to consider types of construction systems that might enable the shapes produced: molded systems such as concrete or cast metals, stamped technologies such as those utilized by automotive fabricators, or possibly even hand built up forms associated with indigenous construction. However, it should be apparent that these types of systems will typically involve other constraints, including cost of materials or labor, difficulty of producing molds necessary for casting, and complexities in describing these shapes in a mathematically rigorous, dimensionally controllable fashion.

Until relatively recently, geometric descriptions for such arbitrarily shaped forms did not exist. The basic mathematics for describing the localized shape characteristics of smoothly curved surfaces has existed in the theory of differential geometry since the 18th century[12]. However, applications of this general theory were limited to the representation of specific, canonical shapes, such as spheres, helices, tori, for which explicit, differentiable formulations could be provided. In design applications, constructive approaches were required to render curved geometries, through the use of French curves and ship splines. These techniques had limited capabilities for representing forms to accurate tolerances.

Practical capabilities for the accurate representation of arbitrarily curved surfaces are directly attributable to advances in computing. The curved descriptions that form the basis of contemporary CAD systems were developed specifically for the purpose of digital representation by Bézier, Coons, and others during the 1960s and 1970s[74]. The solution of positional information from these shape description formulations require intensive computational operations that are practical only through the use of computing.
Although these modeling techniques provide tremendous power and flexibility in representing many curved surface geometries, they are still constrained by their mathematical definitions. The base equations of Bézier and NURBS surfaces provide certain characteristics of smoothing between the controlling geometry. These functions can be used to cast curved

surface representations over sampled spatial data. But in between this sampled data, the surface formulations assume forms guided by their own functional characteristics. Tighter conformance to digitized data from physical forms requires additional information, as well as additional computational complexity of the surface description and associated user interaction. At their limit, mathematical descriptions of curved surfaces can accommodate any smooth surface form. But this limit condition is unachievable in practice. Increasing levels of precision in the affinity between physical forms and their digital counterparts often come with increasing costs in modeling and fabrication effort. The topological structuring of NURBS surfaces –defined through sheet like elements (discussed further in Section V.D.3 below) do not map readily to the structuring of clay or other formed materials. While we can imagine that designers working with rigid sheet materials intend to design constructions of planar geometries, this logic does not extend to curved surface geometries. We can not suppose that when designers work with clay they “really mean” to be manipulating NURBS surfaces objects.

There exists a more important potential discrepancy between digital and physical renditions of form. The digital constructs of curved surfaces do not in themselves exhibit any affinity with the behaviors and characteristics of project materials. Unlike the tight conformance between rigid sheet materials and planar geometries, there is typically little or no direct correlation between operations on free form modeling materials and operations on NURBS surface nets. The operations of physical modelers and those of their digital colleagues guide these parties toward the generation of forms with perceptibly different qualities. The nuances of physical forms - impacted by the behaviors of modeling materials during forming – can be lost during translation to digital form, or require substantial operator skill and diligence to re-impose on the digital model.

The impetus behind the early development of spline mathematics was in fact to approximate the physically founded behavior of ship splines, thin metal strips used in the delineation of ship hull forms, whose curvature characteristics were generated by material bending, and loosely approximated the corresponding bending of wooden laths on the ship hull. In the interim, however, the development of digital curved surface representation has diverged from this material nature, to one more abstract, guided by the feasibility of operations on the mathematical formulations themselves.

Truly free form shapes – constructed through CNC driven molded or stamped fabrication technologies – have had a relatively minor role in Gehry's work. The reasons for this limited role are largely practical and economic. Currently, molding or stamping of materials requires a unique, custom mold to be developed for each surface element. The labor and material required to develop the mold can at the very least add a premium to the cost of the system. This mold making process can ultimately be vastly more expensive than the typical costs of cladding systems, particularly in metal stamping process, where high strength materials must be formed (Section II.C). Specific examples exist, notably the conference room of the DG Bank Headquarters project (Figure IV-2), formed from stamped plate steel. A second version of this form was developed for the Gagosian gallery (Figure IV-3), this time through a manual labor process of forming of sheet lead – highly malleable material.

Figure IV-2: Horse's head (DG Bank)

Figure IV-3 Horse's head (Gagosian gallery)

This issue was elegantly addressed in the Neue Zollhof project in Dusseldorf (Figure IV-4), where recyclable Styrofoam molds were developed as part of an innovative CNC based process for forming cast concrete. The feasibility of this process resulted directly from efficiencies found in the CNC mold forming process. The low strength of Styrofoam allowed it to be routed at extremely high speed, reducing the machine time cost. Relatively low tolerances and allowable roughness of the mold finish allowed the routing to be done with a single pass of a large (approximately 2") bit. The Styrofoam was recycled after the concrete panel was formed, further reducing the material costs associated with the molding process.

Figure IV-4: CNC fabrication of cast concrete (Dusseldorf)

It is suggested that a second reason for the limited role of unconstrained, free form shapes in Gehry's designs: these shapes are simply "too easy", and reflect the loss of correlation between process and form in the qualities of the resulting shapes. This relatively open class of shapes, supporting substantially unencumbered opportunities for form generation, lose the "toughness" of form making as a consequence of this relatively open ended opportunity. It is partly for this reason, in addition to the economic realities of constructibility, that even forms initially modeled through the use of built up materials are eventually rationalized into compositions of more highly constrained materials.

Gehry has shown an ongoing interest in the use of fabric or mesh materials, beginning with early works including the Gehry Residence, Edgemar Development, and Santa Monica Place. As with other forms and materials, these materials have remained part of his vocabulary, even as they have been pushed to more extreme forms on recent designs. These materials in unrationalized form have been successfully realized on several sculptural projects, including the Barcelona Fish and Guggenheim retrospective installations (2001, discussed in Section VII.J below). To date the use these materials have not been achieved on building projects, in part due to the lack of available materials satisfying performance and life safety criteria. For example, fiberglass was initially considered as a building material for the Lewis Residence (unbuilt, 1989-95), but was rejected in part because no products could be found that satisfied fire safety requirements. The class of shapes represented by the forming of fabric presents what at first glance appears to be a quite open, unconstrained vocabulary of potential forms. However, again, on closer inspection, we can see behavior of these materials guiding generated forms in subtle but important ways. Features such as folds and creases generated by the subtle rigidity of the material are discernable in the shapes produced. The geometric definition of this behavior is not easily captured by contemporary NURBS modeling. Mesh materials are closely related to other sheet based materials that will be described in depth below.

A. Fabric and wax design model (Lewis residence)

B. Layered object manufactured (LOM) prototype

Figure IV-5: Geometries based on fabric materials

C. PAPER SURFACES

A. Weatherhead School

B. Telluride Residence

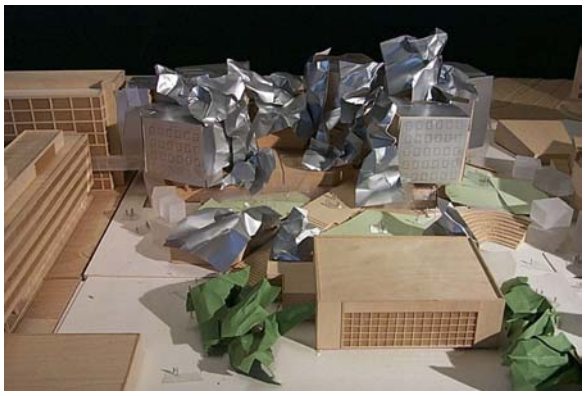

C. MIT Stata Center

D. OHR Museum

Figure IV-6:Paper surface constructions – physical models

Somewhere between the highly constrained class of planar geometries and the general class of curved surface forms lies the broad class of paper-like shapes that are the central focus of this inquiry. We may loosely describe this class of paper surfaces to be those constructed by smoothly bending flat, flexible sheet materials in space, and assembling these surfaces into closed shapes at their boundaries. In this thesis, this class of geometries will be referred to synonymously as either paper surfaces or sheet material surfaces, with the assumption that certain constraints on the method of forming these sheet materials are observed. In Gehry's current work, paper surfaces represent perhaps the most prevalent and important class of surface forms, encompassing a constellation of formal intentions, materials, fabrication economies and methods, physical and digital representations, and rationalizing operations. The importance of this class of surfaces in Gehry's current work, and complexities in the development of corresponding, sufficiently facile digital representations, are the impetus for

the research described in the remainder of this thesis. A qualitative description of their role in Gehry's design and building processes will serve as an introduction to the formal description of their geometric representations in subsequent sections.

The forms assumed by paper and other sheet materials in scale physical models have important counterparts in full scale construction. Many materials of construction have analogous constraints that at least qualitatively constrain full scale fabricated building elements to assume sheet like forms (Figure IV-7). These materials may be readily formed by manual methods into curved shapes in space, so long as these forms do not require stretch forming of the material that would produce plastic deformation in the plane of the surface material. This relationship between the material constraints of modeling materials in scale and the constraints of fabrication may only be approximate. However, for schematic design purposes, this approximate correspondence may be sufficient to guarantee the constructibility of designed forms.

Paper surface shapes are obviously less constrained than the class of planar Euclidean shapes, and may be viewed as a super-set of these forms. This is easily, albeit qualitatively, demonstrated by positioning a sheet of paper flat on a table, then lifting up one of its corners. The paper surface class encompasses the flat configuration and the final configuration of the sheet, as well as of the intermediate states between.

At the same time, the class is clearly quite constrained. While there is a broad class of shapes that may be constructed from a single sheet of paper positioned in space, there is certainly a much larger set of shapes (spheres, airplanes, Walt Disney characters, etc.) that can not be tightly covered by a paper sheet. Attempting to force the sheet tightly onto these shapes will be only partly successful, as wrinkling, creasing or ripping of the sheet will occur.

Unlike planar geometries, where the shapes formed by rigid materials are independent of the actual materials of construction, shapes formed from flexible sheet materials are highly conditioned by the material. Paper, rubber sheet, plate steel, plaster board, aluminum foil, all of these materials impose significantly different constraints on their corresponding set of constructible shapes. Some will break before they achieve the shapes enabled by others, some will assume shapes with a more less continuous or smooth form. Of course, if such features as creases, wrinkles and rips are desired, a potentially larger class of shapes is

enabled. Similarly, one may construct increasingly complex shapes by attaching sheets together, perhaps while allowing gaps, overlaps or creases between the sheets, introducing interior cuts or “dodges” at the edges of sheets, etc. Changing the boundary shape of a sheet of paper will radically affect its corresponding set of possible shapes. Generally, assemblies of a large number of smaller sheets allow more highly curved shapes those that can be formed by a few larger sheets.

In light of this expanding list of qualitative characteristics, the development of simple geometric representations that captures these qualities appears to be a difficult proposition. Geometric formulations representative of this class are likely to be much more difficult to establish than those governing Euclidean planar shapes. At the same time, these surfaces are highly constrained relative to the free form surfaces. It can be postulated that the definition of paper surface geometries could be formulated as a constraint condition imposed on the description of freely formed surfaces, and thus represent a sub-class of this more general class of surface descriptions.

The role of the material itself in guiding operations of designers constructing physical paper forms cannot be overstated. The designers respond to the behavior of these materials as they work with them in a direct, tactile fashion. Through this interactive process, designers are naturally guided toward feasible configurations of the materials. The designs produced through this active, physical process naturally obey the constraints of material behavior. The physicality of this direct tactile interaction shields the designer from the vast world of possible configurations just outside the surface class.

A surprisingly large set of building systems are governed by constraints of flexible sheet materials (Figure III-17). The most obvious such systems are those actually clad with sheet materials such as sheet metal or plywood (Figure III-17A). However, even within this typology there is a considerable range of materials, aesthetic and fabrication requirements, the qualities of which will have implications on the set of admissible surface forms. Examples range from overlapping shingled systems to continuous welded metal back pan systems. The materials, geometry of inter-panel seams, and perhaps most importantly the size and organization of sheets comprising the system all affect the qualities of feasible surfaces that may be constructed.

A. EMP – Cladding System

B. Concrete form work – Weatherhead School

C. Slumped Glass – Conde Nast

D. Snake Sculpture (Serra) Plate Steel

Figure IV-7: A wide range of "paper surface" materials and assemblies

Beyond purely cladded systems, numerous other construction systems may require shapes exhibiting paper surface geometries. Although concrete is a molded material, the form work which generates the shape of poured concrete shapes is often built from plywood, which in turn can assume a paper shape (Figure III-17B). Glass can be slumped into curved surface formwork, but there are limitations on the in plane deformation that can be accommodated without residual stress in the glass when cooled (Figure III-17C). Paper surface forms have been shown to provide a reasonable predictor of these constraints.

With this wide variety of construction materials, methods and assemblies to be considered, the utility of scale paper sheet materials to accurately represent the allowable forms is somewhat questionable. However, for many types of construction, paper modeling materials have been shown to at least qualitatively represent the forms that may be constructed, and in fact establish more conservative constraints than those permissible by the full scale fabrication.

In the following development of digital modeling representations for sheet surface fabrication constraints, it will be useful to keep in mind some of the qualitative features that characterize these systems and contribute to these constraints.

The overall, global shape of the surface assembly is the point of departure for considering qualities contributing to the form's constructibility. It is here that the initial physical modeling and materials used in this process contribute to an understanding of the shape's constructibility. Individual sheets employed on physical models vary in character and size, from full height wall size sheets to smaller panels perhaps 10' in scale. Critical issues such as the shape of boundaries of these macro scale sheets and the ways in which they are attached together have enormous implications on the types of forms that may be feasibly generated.

Localized smoothness of form is an inherent characteristic of the paper shape class. Again, while "catastrophic" operations- such as crumpling, ripping or stretching by stamping - can be undertaken, these operations and the forms that are generated represent extensions or violations of the rules of construction and corresponding definition of the class. Sheet materials respond to externally applied forces and actions by assuming smooth variation between these externally applied constraints. However, sheet materials have limits on the magnitude of deformation they can respond to. Beyond those limits, the material will either refuse to go, perhaps popping fasteners intended to hold the material into shape, perhaps buckling or tearing. The intentional introduction of discontinuities into a smoothly continuous surface can alleviate the materials' resistance to being positioned in a given way. If the design intent for the form allows discontinuities in the material's shape, then considerably more flexibility in the global nature of the shape is possible.

As a trivial example, spheres of any size can be constructed by tessellating the surface into triangles, resulting in a geodesic dome[31,32]. The panels of the dome do not necessarily have to be flat, but rather could assume some limited degree of curvature. The remainder of the sphere's curvature would continue to be made up at the panel seams. In this simple example, the tradeoffs between surface curvature, tangency discontinuities and fitness to the "design" surface are readily apparent (Figure IV-8).

The introduction of discontinuities in the smoothed form of global scale paper surface gestures is a key activity of rationalization activities on global shapes. The design intent will introduce a system of constraints on the nature of these rationalization operations, where they may occur, the layout and pattern of these discontinuities and the degree to which these discontinuities may appear in the surface form.

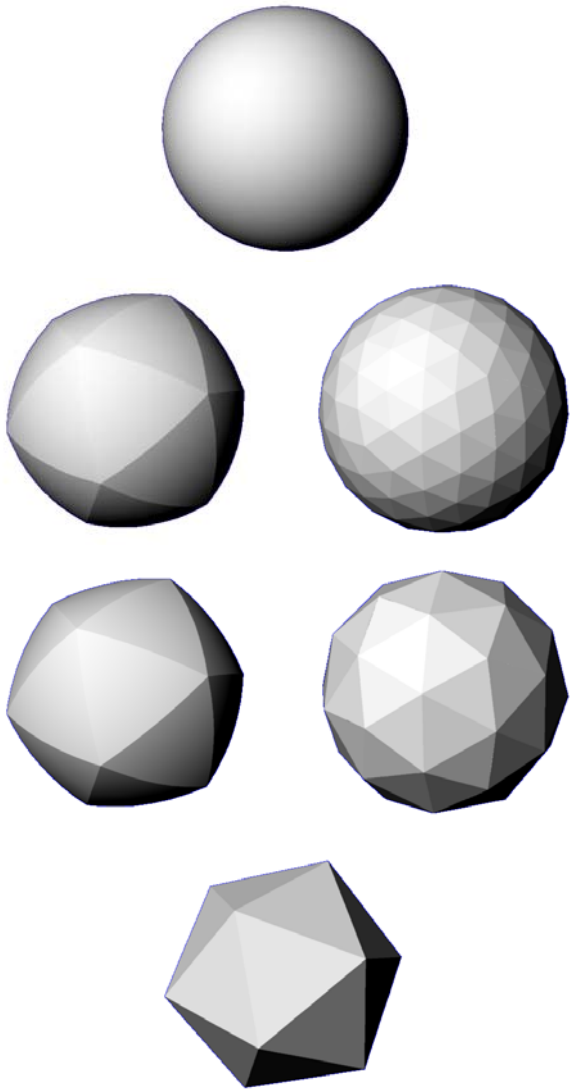

Figure IV-8: Rationalization of a sphere

The issues encountered at the macro scale of the project form play out at a variety of scales. Cladded systems are ultimately constructed from individual facing sheets of material. Similar considerations regarding the shapes of these panels and their assembly with one another occur at this level. In a sense, it is at this level that the ultimate determination of whether or not a surface is constructible occurs. The macro scale form of a wall or roof shape is propagated down to this face sheet level. However, modification of face sheet sizes, shapes and organizations can have dramatic implications on the types of shapes that are possible. Economic considerations in fabrication processes may limit the sheet sizes and edge conditions. Specific materials will be limited to certain maximum sheet sizes. Break forming of panels – a relatively inexpensive forming process - will limit edges to straight cuts, as opposed to the extended possibilities for sheet boundaries available using CNC cutting techniques.

Many cladding systems are built up of more than one layer of material (Figure IV-9). For example, a typical cladding strategy may adopt a back pan serving as the substrate for the actual waterproofing layer, while a rain screen or shingle system is positioned outside of this layer as the actual finish surface. Either of these systems may present the more highly constrained layer of the assembly. Frequently it is the waterproofing layer that presents the more rigid requirements in terms of continuity, material sheets and sizes, fastening strategies, etc. Alternatively, aesthetic requirements of the finish surface such as smoothness of appearance may govern.

Figure IV-9: Macro and element scale sheet forms (Bilbao)

The presence of seams between individual assembly sheets contributes substantially to differences in behavior between macro level shape studies and the shapes feasibly constructed out of panelized systems. Panels naturally introduce opportunities for introducing overlaps between individual sheets, slight or substantial discontinuities in the smoothness of the overall shape, and the possibility of slight warping of the material sheets. These effects are not identifiable at the macro level. This potential relaxation of constraint conditions as design heads toward actual fabrication is of course beneficial to the design process, and provides in essence a factor of safety in the schematic design of the project forms.

A rigorous understanding of the implications of panel system edge conditions is difficult to achieve, since subtle features of the physical geometry of panel-to-panel joints can have substantial effects on the geometry of the ensuing form. For example, the force of attachment of individual fasteners such as screws, which fix surface panels to supports, can affect the degree of shape discontinuity at panel edges.

Material qualities play a significant role in the qualities of surfaces that will be formed when deforming sheets of these materials into paper surface shapes. These qualities include the

actual material properties such as stiffness and brittleness. Material thickness and forming activities will affect the behavior of these materials. Thick plywood sheets will behave differently under deformation than layered assemblies of thin plywood sheets with the same thickness. Where titanium panels have been used, these sheets have typically been used with a thinner gauge than stainless steel or aluminum panels. Titanium is resistant to ductile deformation, and will thus typically be resistant to being forced into shapes with any in plane deformation. In contrast, lead and pewter sheet materials are highly ductile, and will readily assume shapes that would require molding or stamping of more conventional surfacing materials. Stainless steel has been used on different projects with a wide variety of gauges, from thin sheet to plate steel, with large differences in the limitations on shapes that can be produced.

Strategies for the organization of system components will have many implications on the surface qualities of paper surfaces. Similarly, the design intent in terms of the desired surface qualities will guide the selection of surface fabrication strategies. Surface fabrication systems will introduce a host of constraints presenting rules for the organization of surface components. Patterning strategies for sheet layouts will obviously be affected by the organization of sub-framing systems. Systems using straight members organized in an undulating form have been successfully applied to the construction of paper surface forms (Chapter V.B.). The economics of specific fabrication strategies that generate the constraints of paper surface forms will likely include specific additional implications for the way in which the systems components are organized, and the types of shapes that may be economically constructed using a given fabrication system. It is also possible for several different systems to be employed on different regions of a project, depending on the complexity of the localized surface form. For example, less curved surface areas may afford more straight forward construction, while more highly curved areas of are addressed with a more forgiving, less economical fabrication approach.

The formidable role of paper surface systems in Gehry's work and the complexity of these systems' formal constraints have placed a substantial demand on CAD modeling efforts. The geometric controls and operations by which paper surfaces are constructed in digital form are radically different than - and in many ways impoverished compared to - the flexibility and intuitiveness of direct material manipulation. For this reason, the process of faithfully re-constructing the physically generated forms in a digital context has been a time and labor-

intensive process. More troubling is that these surface modeling techniques may introduce constraints on the digital surface forms that are different than those of physical modeling materials or their fabricated counterparts.

This dichotomy between physical objects and their analytical counterparts is not new. In traditional engineering, limitations of analytical approaches to perfectly represent real world conditions are addressed implicitly by introducing factors of safety: backing away from the true limits of the materials and engineering in a more conservative manner than might be possible. Changes in analytical methods have at times allowed less conservative approaches to similar systems, such as the introduction of plastic deformation considerations into steel frame design in the 1980s.

These issues play out in the engineering and construction of paper surface forms as well. Many of the techniques for modeling paper surface systems include notions of factors of safety, constraining the surface form somewhat in order to be able to guarantee constructibility. Other approaches rely on rationalizing paper surface forms into canonical shapes such as cylinders and planes whose constructibility may by nature be guaranteed. Both of these approaches present obvious drawbacks, in that the qualities of shapes generated by rationalizing may be qualitatively different than the ideal surfaces, and may also not truly represent the limits of what can be fabricated. This discrepancy between the initial physically modeled forms, those that can possibly be fabricated, and the rationalized forms representing the limits of our predictive capabilities may not be completely resolvable. Nonetheless, an ongoing goal of computational research by the firm is to achieve greater parity between these three worlds as materials are pushed further toward their limits.

In the context of Gehry's digital building delivery process, the limits imposed by digital representation present an ultimate constraint on the inclusion of forms in the design vocabulary. If forms can not be described in the project documentation in a manner through which their constructibility can be substantiated, then they can not feasibly be accommodated in construction, regardless of the actual abilities of craftsmen to perform the work. This limiting condition creates urgency for developing representations of sheet materials, which accurately reflect fabrication constraints without imposing additional constraints resulting purely from limitations of the geometric representation itself.

V. Mathematics of Curved Spaces and Objects

The remainder of this thesis will develop descriptions of paper surfaces through geometric and mathematical formalisms. This chapter reviews the essential formalisms of non-Euclidean geometric constructs that are at the heart of virtually all curved object representations found in contemporary CAD applications. The development of paper surface representations will be developed within this general formalism. The discussion in this chapter follows the derivations in classical texts on differential and non-Euclidean geometry such as Kresig[47], Bonola[12], and O'Neil[60], and discussions of manifolds provided Bishop and Goldberg[7].

A. SPACES IN MATHEMATICAL FORMS

Readers familiar with the basic operations of CAD systems will have an understanding of the conventional representations of primitive objects, as being defined in terms of coordinates. The notion of a point, residing in 3D space, as being defined by an ordered set of number **p** = (*x*,*y*,*z*) should be readily apparent. The description of more complex objects in terms of basic functions on coordinates should also be readily apparent. We may describe a line segment in terms of an ordered pair of points, (**p**,**q**), which are may in turn be described by their coordinates as above. It should be recognized that this basic description is not the totality of the behavior of a line segment in space, rather, the end point coordinates form the basis for a *function*, which describes a set of points on the interior of the line segment (Figure V-1A). The end points of the line segment form one representation of these conditions; there are alternative descriptions of the conditioning of points on the line segment as well. For example (Figure V-1B), we may equivalently describe this same line segment through a starting point

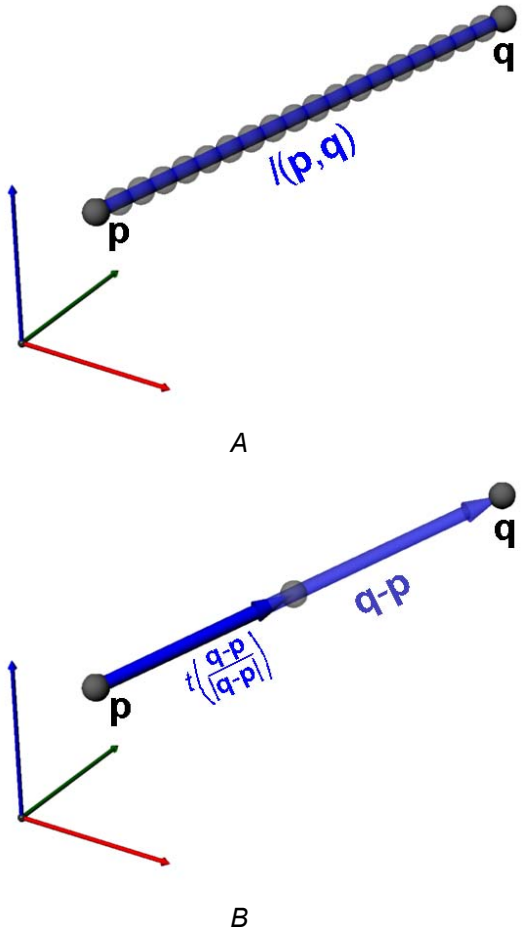

Figure V-1: A line as a function on end points

(**p**), a vector describing a direction in space (**q** - **p**), and a range of distances along this vector from the initial point which represent the range of the line segment ($0 \leq t \leq |\mathbf{q} - \mathbf{p}|$).

These examples rely on a common, unifying coordinate representation of 3-space, where a point in the space may be uniquely described by its ordered triple of coordinates. Two points in this space are equivalent if and only if their coordinates are equivalent:

$\mathbf{p} = \mathbf{q}$ iff $(x_\mathbf{p} = x_\mathbf{q}, y_\mathbf{p} = y_\mathbf{q}, z_\mathbf{p} = z_\mathbf{q})$

While this representation of space suffices for basic Euclidean primitives, such as points, lines, and planes, this representation of a space and the elements that reside in it becomes problematic for more complicated spatial elements. For example, a curve in space may be construed as being comprised of a set of points in space similar to that of a line. However, the description of the curve through an analogous function on its interior points will be more difficult.

Additionally, it is often useful to consider objects from the perspective of other spatial constructs than a homogenous 3-space representation. For example, architectural drawings typically consider the objects of their inquiry in terms of two dimensional representations such as plans and sections. These representations are inherently two dimensional, and may be read as such. The observer of these configurations may vary her frame of reference on these objects, alternating between considering the represented objects as two dimensional objects in the space of the drawing, as well as "reading through" to the three dimensional counterparts represented by these artifacts. A rigorous, formal description of spatial representations which allows translation between these interpretations is of benefit, rather than considering the two dimensional form of the drawing as some sort of emaciated abstraction relative to the "true" nature of the objects in some preferred, integrative 3-D space.

To circumvent the limitations of descriptive capabilities of a common 3-D descriptive space, we will need to turn to more general representations of spaces, which allow multiple spatial representations to co-exist. Such a system should support the development of spatial organizations as independent constructs – allowing the objects within a given spatial representation to be considered, while additionally allowing opportunities for associations

between spatial organizations to be supported. Such a structure will allow individual objects such as curves and surfaces to be considered from a spatial perspective that highlights the invariant qualities of the object, while in turn allowing its consideration relative to other objects that may in turn have spatial structuring in their own terms.

To expand on this notion of mathematical spaces, we must initially disregard some of the innate notions of physical space, and rather consider spaces whose character is simply based on permutations of numerical values. A space, in mathematical terms, is simply an ordered set of variables, e.g. (x_1, x_2, . . . , x_n). A point in this space is equivalent to a specific instantiation of values for these variables, such as (x_1= c_1, x_2= c_2, . . . , x_n= c_n). The specific values as (c_1, c^2, . . . , c^n) are termed the coordinates of the point. A space with this structure is termed a Cartesian product space of *n* real variables or $\mathbf{R}^n$.

Such mathematical spaces, developed simply as a description of ordered sets of variables, may be naturally combined into higher order constructs. Our definition of a line as defined by two points may be constructed as an ordered set of *two* $\mathbf{R}^3$ Cartesian product spaces – one for each set of the possible coordinates of each end point. The set of all possible line segments is defined in the ($\mathbf{R}^3 \times \mathbf{R}^3$) space, instantiated by the specification of six parameters: ($x_{1\mathbf{p}}$= c^1, $x_{2\mathbf{p}}$= c^2, $x_{3\mathbf{p}}$= c^3, $x_{1\mathbf{q}}$= c^4, $x_{2\mathbf{q}}$= c^5, $x_{3\mathbf{q}}$= c^6).

Cartesian product spaces provide much of the structuring required for the description of geometric objects. However, geometric spatial constructs often require the definition of an additional metric on the relationship between locations defined in the space. In and of themselves, Cartesian product spaces do not establish any notion of proximity or nearness between elements defined in the space. While it seems obvious that the point (0,0,0) is nearer to the point (1,0,0) than it is to the point (10,0,0), this is not a property of the simplistic notion of ordered sets of numbers. The establishment of a *metric* or *distance function* on members of a Cartesian product space allows notions of nearness, neighborhoods and continuity of spatial elements between coordinates in space to be defined. A metric function is a (symmetric, positive, nondegenerative) function of the form

$$\delta : \mathbf{R}^n \times \mathbf{R}^n \rightarrow R \qquad \text{(V.1)}$$

that takes two locations (equivalently, points) in the space and returns a real valued distance between them. One obvious such metric function is the Euclidean distance function:

$$\delta(\mathbf{p},\mathbf{q}) = \sqrt{(\mathbf{q}_1 - \mathbf{p}_1)^2 + (\mathbf{q}_2 - \mathbf{p}_2)^2 + (\mathbf{q}_3 - \mathbf{p}_3)^2} \qquad \text{(V.2)}$$

The specification of this Euclidean distance function on a Cartesian product *n*-space provides the structuring of the familiar Euclidean descriptions of elemental elements such as lines and points. Since this function is true also of simple permutations of real numbers, Euclidean space and Cartesian product n-spaces of independent or *orthogonal* variables are often used interchangeably. In the following discussion, we will encounter spaces representing parameters on objects for which this simple metric function no longer holds.

B. VECTOR SPACES

Spaces of numbers are expanded by considering spaces of vectors. The notion of a vector may be considered initially to be a primitive object, characterizing the spatial concept of directedness in space. For each variable, (x^1, x^2, . . . , x^n), we may assign a vector in space, and assign the corresponding coordinate as representing a multiple of this vector. A set of *n* linearly independent vectors serve as a basis for the space; by linearly independence we can simply state that no vector of the set may be expressed as a combination of any others of the set. In R^3 this simply means that the 3 basis vectors may not be co-planar.

Euclidean spaces may be characterized as vector spaces, where an obvious set of basis vectors exists: the unit vectors $\hat{\mathbf{e}}_i$, representing a unit length in each of the directions of the axes. It is important to keep this dual nature of Euclidean *n* space firmly in mind, as an ordered set of *n* scalar values, and as a vector space characterized by the unit vectors $\hat{\mathbf{e}}_i$. In Euclidean spaces, the basis vectors $\hat{\mathbf{e}}_i$ are orthogonal and invariant, in that their magnitude and direction remain constant over the space. The notion of a point in space is equivalent to that of a vector in space, since

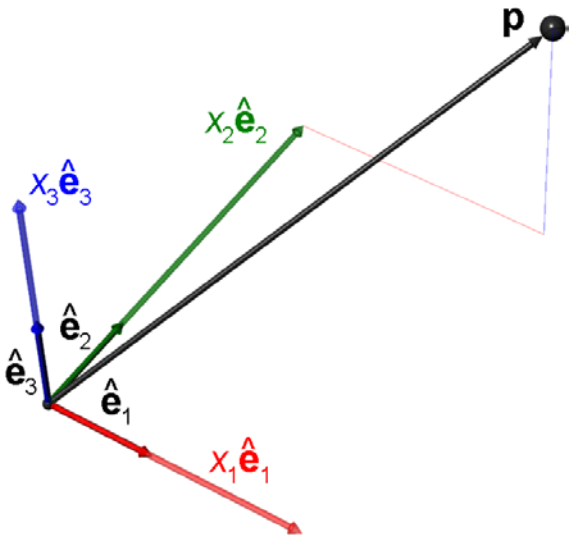

Figure V-2: Euclidean space basis vectors

we can describe the point **p** = (x_1, x_2, x_3) as a vector from the origin, defined as the sum of *i* vectors of length x_i in the direction of $\hat{\mathbf{e}}_i$:

$$\mathbf{p} = \sum x_i \hat{\mathbf{e}}_i \tag{V.3}$$

In representing curved objects, we must draw on spatial constructs whose characteristics are substantially more complicated than those of Euclidean spaces. By way of departure, we may consider affine vector spaces (Figure V-3), characterized by *n* basis vectors, whose directions are not necessarily orthogonal, and whose magnitude is not necessarily unit. Euclidean space may be considered to be a special case of affine space.

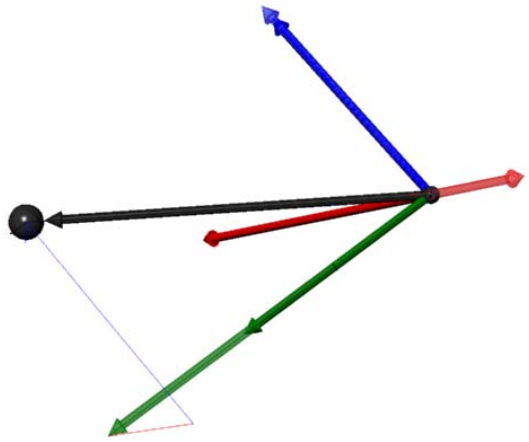

Figure V-3: Description of a point in an affine vector space

1. Vector Fields

The notion of a vector field may now be introduced. Consider the application of a *tangent vector* $\mathbf{v}_p$ at a point **p** in $\mathbf{R}^n$ space: the tail of the vector begins at the point **p**, while the direction of the vector is described by *n* ordered coordinates, indicating the direction and distance described by the vector. A tangent vector $\mathbf{v}_p$ is thus described by two ordered sets of *n* variables: the point of application **p**, and the *vector part* **v**.

The set of possible vectors with application at **p** thus may be characterized as a Euclidean space in its own right. We may consider each such vector to be equivalent or dual to a point in this vector space, associated with the point of application **p**. By extension, we may consider the combination of all points and all tangent vectors to these points in $\mathbf{R}^n$ to be Cartesian product space of character $\mathbf{R}^n \times \mathbf{R}^n = \mathbf{R}^{2n}$, a *six* dimensional Cartesian product space for tangent vectors in $\mathbf{R}^3$. Often, however, in considering deformations of spatial objects, we will be concerned with multiple vectors emanating from a single point of consideration. We may thus consider these vectors from the perspective of a coordinate system with its origin at the common application point of the vectors **p**. In doing so, we

diverge from the simple framework of a single coordinate system defined over the entire space.

A vector field is a function $F: \mathbf{p} \rightarrow \mathbf{v}(\mathbf{p}) | \mathbf{p} \in M,$ that assigns a tangent vector to each point **p** of some region *M* of $\mathbf{R}^n$. Specifying a region *M* allows the construct of a general vector field to be applied only to domains of $\mathbf{R}^n$ of interest to a given application, such as curves or surfaces, where the vector field may be undefined for regions of space outside of the domain.

2. Coordinate Fields

With the construct of vector fields in place, the basis is established for defining non-rectilinear coordinate systems in $\mathbf{R}^n$. Vector fields may be combined to construct general coordinate systems on $\mathbf{R}^n$, by establishing an *n* –part function:

$$\phi_i : \mathbf{p} \rightarrow \mathbf{v}_i(\mathbf{p}) \mid i \in (1 \ldots n), \mathbf{p} \in M \qquad \text{(V.4)}$$

The vectors $\mathbf{v}_i$ form a basis of *M* provided that $\mathbf{v}_i$ are linearly independent for each point **p** in *M*. Thus any vector whose point of application is **p** may be resolved into components in terms of the basis vectors $\mathbf{v}_i$. We will limit ourselves to consideration of vector basis functions that are differentiable over *M*, allowing assumptions such as continuity and smoothness to be assumed.

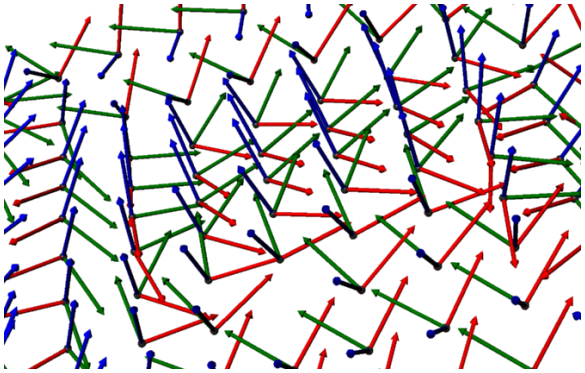

Figure V-4: a vector field in $\mathbf{R}^3$

The notion of a coordinate system varying at every point of application may cause some initial concern, since it seems incongruous with initial notions derived from the usual conventions of coordinate systems on Euclidean *n* space. For example, we can not directly determine the coordinates of a point p_2 from the coordinate field at p_1 by mapping the vector $p_2 - p_1$ onto the basis vectors at p_1, the way one could in the natural coordinate system. However, again, in considering curved objects in space, we will principally be concerned with the local character of the object, “near” a point under consideration. The localized coordinate field will provide a structure for considering this localized character of the object.

3. Frame Fields

The previous section established the notion of a coordinate system defined by basis vectors, continuously varying over a region of space. This coordinate system was established in terms of a set of *n* linearly independent basis vectors, whose direction and magnitude was dependent on the given point in space. While this construct provides broad generality for coordinate systems, this generality comes at some computational complexity. Even a simple operation as resolving a vector into its components in a general basis requires solution of a set of inter-dependent, linear equations.

With one important constraint on the basis vectors, the complexity of the coordinate system can be dramatically reduced. A frame field is a set of mutually orthogonal, unit length vectors $\hat{\mathbf{e}}_i$, applied to every point in a region of $\mathbf{R}^n$. Since these vectors are orthogonal and unit length, the dot product between any pair of these vectors, $\hat{\mathbf{e}}_i \bullet \hat{\mathbf{e}}_j$, is 0 unless *i=j,* in which case the dot product is equal to 1. We may introduce the important short hand notation of the Kroneker delta δ:

$$\hat{\mathbf{e}}_i \bullet \hat{\mathbf{e}}_j = \delta_{ij} \qquad \text{(V.5)}$$

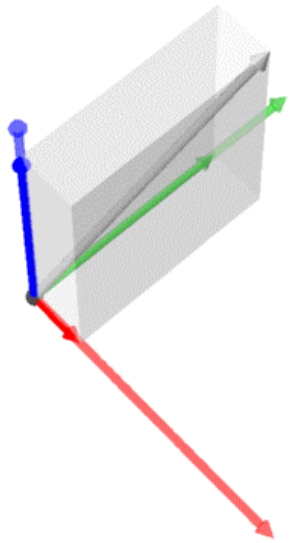

Figure V-5: Expansion of a vector by orthonormal basis vectors.

where:

$\delta_{ij} = 0$ if $i \neq j$,
$\quad 1$ if $i = j$,

The components of a vector **v** in the coordinate system defined by basis vectors $\hat{\mathbf{e}}_i$ are simply the dot product of the vector with the corresponding basis vector: The coordinate of **v** in the terms of the basis vector $\hat{\mathbf{e}}_i$ is simply the real value:

$$c_i = \mathbf{v} \bullet \hat{\mathbf{e}}_i \qquad \text{(V.6)}$$

Therefore, the i^{th} component of **v** is the vector $c_i \hat{\mathbf{e}}_i$ the basis vector $\hat{\mathbf{e}}_i$ scaled by length c_i. **v** is then the sum of these *n* components:

$$\mathbf{v} = \sum (\mathbf{v} \bullet \hat{\mathbf{e}}_i)\hat{\mathbf{e}}_i \qquad \text{(V.7)}$$

The process of resolving a vector into its components in terms of the frame vectors is termed *orthonormal expansion*.

Having previously established the notion of a general coordinate field in Section 6, the frame field represents a "step backward" to a less general construct. Note that the "natural" coordinate system (x,y,z), is a special, additionally constrained frame field whose basis vectors are invariant over the space. Frame fields enjoy some of the simplicity of Euclidean space, but only at local points of application. In investigating the shape of curved spatial objects, we will be establishing appropriate frame fields on these objects that highlight their localized characteristics.

C. MAPPINGS

We will next consider mappings between spatial representations - the means by which disparate spaces and objects expressed in these spaces may be integrated. A mapping may be defined between pairs of spatial representations. A mapping from a space $N = (x^1, x^2, \ldots, x^n)$, to a space $M = (y^1, y^2, \ldots, y^m)$ is a set of m functions, that expresses the relationships between the coordinates of the two spaces:

$$(y^1, y^2, \ldots, y^m) = \left(\phi^1(x^1, x^2, \ldots, x^n),\ \phi^2(x^1, x^2, \ldots, x^n)\ ,\ldots,\ \phi^m(x^1, x^2, \ldots, x^n)\right)$$

We may consider this mapping both in terms of the individual coordinate mapping functions:
$\phi^j \in (\phi^1 \ldots \phi^m)$,

or simplify our notation in considering the set of functions to be a single multi-part function, of the form:

$\phi: N \rightarrow M$ (read: ϕ maps N to M)

Similarly, we should expect that if such a mapping function exists, then an inverse function exists, mapping from the space *M* back into the space *N*, of the form:

$\phi^{-1} : M \rightarrow N$ (read: the inverse of ϕ maps *M* to *N*)

For the purposes of exploring curved spatial objects, we will presume that these mapping functions are differentiable to the degree appropriate for the required application, i.e. that rates of change in the coordinate variables of the space *M* can be determined by considering the rates of change in the variables of the space *N*. A mapping function is infinitely differentiable if each of the coordinate mapping functions ϕ^j possesses valid derivates up to infinite order. Typically we will be interested in mappings that present derivatives at least up to some finite order.

In considering the forms of curved spatial objects, the structure presented by these differentials will often have greater significance than the actual mapping functions themselves. While we may of course be interested in the actual placement of objects in space, the geometric nature of these objects are frequently invariant, should the object be subject to some translation in the space. In such an event, the localized rates of change of the mapping function between the parametric and embedding space will be preserved, while the specific functions mapping coordinates between these spatial representations may not. We will from time to time consider the structure of curved spatial objects in terms of these derivative functions, without explicitly stating the characteristics of the mapping functions themselves.

Mapping between frame fields is a straight forward computation. Given a vector ***v*** with components $\mathbf{v}_i = c_i \hat{\mathbf{e}}_i$, we wish to determine its components $\mathbf{v}_j = d_j \hat{\mathbf{f}}_j$ in some second coordinate system, whose basis are the orthogonal, unit length vectors $\hat{\mathbf{f}}_j$. The transformation is found by resolving each basis vector $\hat{\mathbf{e}}_i$ into its components in the frame $\hat{\mathbf{f}}_j$. These components are found by conducting an orthonormal expansion of each vector $\hat{\mathbf{e}}_i$:

$a_{ij} = \hat{\mathbf{e}}_i \bullet \hat{\mathbf{f}}_j$ (V.8)

The j^{th} component of $\mathbf{v}$ in the coordinate frame $\hat{\mathbf{f}}_j$ can then be found by summing the contribution of each of its components in the directions $\hat{\mathbf{e}}_i$, as they are resolved into the direction of $\hat{\mathbf{f}}_j$:

$$d_j = \sum a_{ij} c_i \qquad \text{(V.9)}$$

$$\mathbf{v}_i = \sum_i (a_{ij} c_i) \hat{\mathbf{f}}_j$$

1. Manifolds

The above discussion has used the term space in a fairly unformulated manner. We have seen the term applied to ordered sets of numbers, and alternatively have discussed the concept of vectors spaces. The concept of a *manifold* allows a rigorous definition of geometric objects and their occupancy in space through mappings between a local coordinate system, intrinsically defined on spatial object and Euclidean in nature, and some extrinsic, containing space. We will refer loosely to the intrinsic space of the object as the *parametric* or *embedded space* of the object, and the space into which this object is mapped as the *containing* or *embedding* space. The topological characteristics of the object are determined by the orders of each of these spaces. In turn, the shape of the object in the containing space is largely determined by the mapping function.

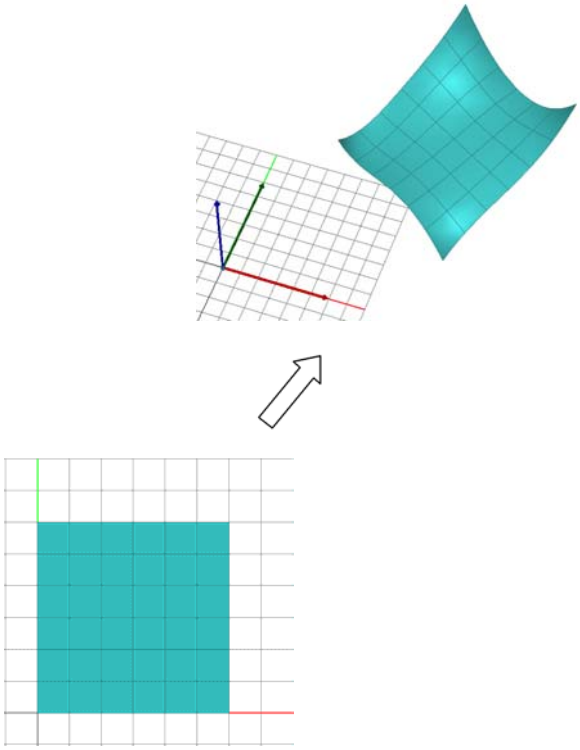

Figure V-6: A manifold, defined as a mapping between parametric and containing spaces

A manifold is properly defined as a topological space in which some neighborhood of each point admits a coordinate system. The passage between coordinate systems at neighboring points is smoothly continuous, allowing notions of differentiability of the space and bodies

described in the space. If X is a topological space, a chart at $\mathbf{p} \in X$ is a function $\mu : U \rightarrow R^d$, where U is an open set containing **p**. The concept of a manifold allows notions of elements of a space to be constructed independently of an particular coordinate system, and provides the basis for establishing mapping between coordinate systems. Additional structuring appropriate for modeling of physical systems, such as distance and other spatial metrics may be overlaid on the structure of manifolds, whereas notions of continuity, smoothness, and differentiability are part of the structure of manifolds themselves.

2. Submanifolds and Imbeddings

With the structure of vector spaces and mapping functions between these spaces in place, we have the formal basis necessary to discuss the means by which spaces – and the objects defined in these spaces – can be integrated.

In contrast to the "conventional" spatial structure of simple CAD systems, where the structuring of objects occurs through a single, principal, 3-D Euclidean space, we instead consider a notion of space constructed from multiple manifolds of differing dimension, with equal weight in the total description of spatial objects, integrated by mapping functions between these objects. Given a manifold N of dimension n, we will consider the means by which other spatial constructs may be embedded within this space.

A manifold M is imbedded in N if there is a invertible, differentiable map Φ: $M \rightarrow N$, which supports a invertible coordinate function for every point $\Phi(m)$ in N. A proper imbedding of M into N requires that the image of M in the space of N not self intersect, since this would prohibit the unambiguous mapping backward of certain points in N. This limitation can be addressed by considering the imbedding to be valid on regions of M that are not mapped to points of overlap in the image.

This section has presented some of the mathematical foundations necessary for describing curved objects in space. In particular, we have moved away from space as being defined by a global coordinate system, and objects in this space as being merely functions on points in this space. Instead, both space and spatial objects are resolved through the concept of manifolds. Manifolds are not simply coordinate functions, but rather objects and sets of objects, spatial, numerical or other. Their structure and relationships are determined by the ability to map these objects to others, through mapping functions on their ranges, and their

variation in these ranges. The imbedding of objects in spaces, or spaces into other spaces, is achieved strictly through notions of imbedding.

The subsequent sections will describe general applications of these principals to two important classes of deformable objects: curves and surfaces.

D. CURVES AND SURFACES

1. Curves in $\mathbf{R}^3$

In contrast with the above sections, we will focus on the special cases of objects in 3D space, and replace the above inquiry of an n dimensional space with the special case of $\mathbf{R}^3$.

A curve is a mapping from an interval I in the (one dimensional) real line **R**, to its image in $\mathbf{R}^3$. A manifold description of a curve in $\mathbf{R}^3$ is a function which maps a single parameter on an interval I of the real number line to locations in 3-space, of the form:

$$\alpha(t) = \left(\alpha_1(t),\ \ \alpha_2(t),\ \ \alpha_3(t)\right) \mid t \in I$$

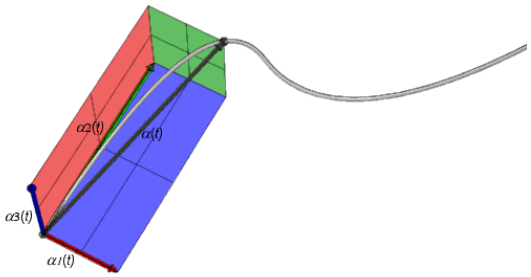

Figure V-7: A space curve as three mapping functions

where $\alpha_1(t)$, $\alpha_2(t)$, and $\alpha_3(t)$ are some as yet unspecified functions which produce a value for the corresponding coordinate, given a value for t. The functions are valid on some interval I for t such that $t_1 \le t \le t_2$, where t_1 and t_2 specify the limits of the interval. This curve function may be succinctly stated as:

$$\alpha\colon I \rightarrow \mathbf{R}^3 \qquad \text{(V.11)}$$

We assume that the functions $\alpha_i(t)$ are differentiable. The nature of α as a function and as a curve in space is indistinguishable from a mathematical perspective.

The parameter t is sometimes considered analogous to time; one can imagine the function α sweeping a curve in space as it maps points to t, while t, a parameter independent of the

space $\mathbf{R}^3$, structures this sweeping through space. In keeping with this temporal analogy, we may consider the first derivative of the function α at a particular value of *t* to be the velocity vector of α at *t*, of the form:

$$\alpha'(t) = \left(\frac{\partial \alpha_1}{\partial t}(t), \quad \frac{\partial \alpha_2}{\partial t}(t), \quad \frac{\partial \alpha_3}{\partial t}(t) \right)_{\alpha(t)} \tag{V.12}$$

This function determines the instantaneous direction of travel of the curve at a specific point in space, in much the same way that the velocity of an object passing through space indicates the instantaneous direction of the object's travel. Geometrically, this derivative with respect to *t* is the tangent of the curve α. The vector $\alpha'(t)$ also has a length or *magnitude*. This magnitude is derived from the parameterization of the function α, and is not discernable from the geometric shape of the curve itself. As this discussion of curved objects progresses, the distinction will be explored between the parametric, functionally derived qualities of a curve on one hand, and the purely spatial properties of the curve on the other.

By way of progression to discussing these purely geometric properties of curves, we consider the fact that the specific parameterization of the function α does not uniquely describe the curve in space; rather, there are a potentially unlimited number of parameterizations which can describe the same path through space. Drawing on the temporal analogy, a given path in space may be traversed by any number of speeds, and variations of speed along the path. This *reparametrization* of the curve α may be constructed as follows:

Let α: $I \rightarrow \mathbf{R}^3$ be a curve. Let η: $J \rightarrow I$ be a differentiable function on an open interval *J* of **R**. The function:

$$\beta = \alpha(\eta(s)) \tag{V.13}$$

is a reparametrization of α by η. The function η imbeds the interval *J* into *I*, and is of the form $\mathbf{R} \rightarrow \mathbf{R}$. The velocity vector β' is related to α' through the chain rule:

$$\beta'(s) = \frac{d\eta(s)}{ds}\alpha'(\eta(s)) \tag{V.14}$$

Since $\alpha'\eta(s)$ is simply the tangent vector of α at the reparameterized location $\eta(s)$, and $d\eta(s)/ds$ is the derivative of a scalar, the tangent vector of the two parameterizations differ only by magnitude. This maps to real world experience, where the same path taken with differing velocities differ in their instantaneous velocities at a location in speed, but not direction.

The second derivative of α with respect to the parameter *t* is - in our temporal analogue – the acceleration of the curve, and takes the form:

$$\alpha'' = \left(\frac{d^2\alpha_1}{dt^2}, \frac{d^2\alpha_2}{dt^2}, \frac{d^2\alpha_3}{dt^2} \right)_\alpha \tag{V.15}$$

In contrast with velocity, the acceleration vector is not generally tangent to the curve except for the trivial case of a straight line. Additionally, unlike the tangent vector, whose direction was independent of the particular parameterization, the acceleration vector's direction will depend on the parameterization chosen. This, again, maps to temporal experience. A vehicle traveling at constant velocity around a circle will experience centripetal acceleration toward the center of the circle. If, however, the vehicle is simultaneously accelerating, the acceleration felt by the passengers will be the composite of both the centripetal acceleration and that in the tangential direction. Thus the direction of the acceleration experienced will be dependent on the velocity function. It is apparent that the specific choice of a parametric space and mapping function has a large implication on our "experience" of the curve from the perspective of the parametric space. At the same time, different parameterizations and mappings can produce the same curve in space. One might ask if there is an improved representation of the curve that illuminates its shape properties, independent of the chosen parameterization. To achieve this, an important, canonical coordinization of the space curve will be developed in terms of a frame field that is defined by the shape of the curve itself. We postulate a reparametrization of the curve $\beta(s)$ such that the magnitude of the velocity vector at each point is 1:

$$\beta : I \to \mathbf{R}^3 \mid \left\| \beta'(s) \right\| = 1 \text{ for all } s \in I \tag{V.16}$$

In principle, any curve can be reparameterized as a unit speed curve. We can establish this reparameterization for any curve initially defined by some arbitrary parameter *t*. We first define the *arc length*, or distance along the curve as:

$$s(t) = \int_{t0}^{t} \sqrt{\dot{x}^2 + \dot{y}^2 + \dot{z}^2}\, dt = \int_{t0}^{t} \sqrt{\dot{\alpha} \bullet \dot{\alpha}}\, dt \qquad \text{(V.17)}$$

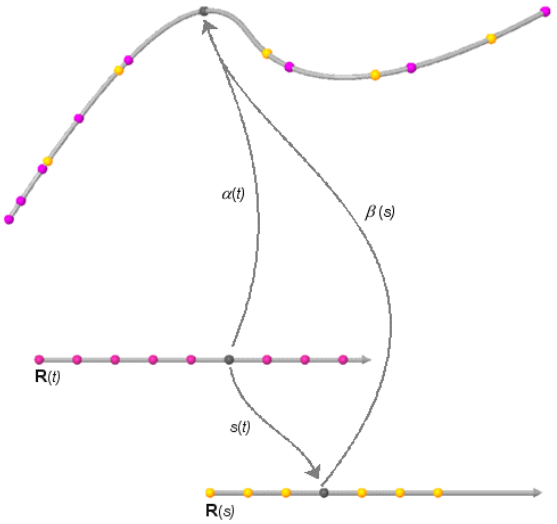

Figure V-8: Mapping of a curve to a unit arc length parameterization

i.e., the integral of the change of position in the original curve function. We will adopt the notational convention that derivatives of the curve function with respect to some general parameter *t*, will be denoted $\dot{t}$, and derivatives with respect to the arc length *s* by *s'*. We may map between these derivatives as follows:

$$\dot{s} = \frac{ds}{dt} = \sqrt{\dot{\alpha} \square \dot{\alpha}} = |\dot{\alpha}|$$
$$\ddot{s} = \frac{d\dot{s}}{dt} = \frac{\dot{\alpha} \square \ddot{\alpha}}{\sqrt{\dot{\alpha} \square \dot{\alpha}}}$$
$$t' = \frac{dt}{ds} = \frac{1}{|\dot{\alpha}|} \qquad \text{(V.18)}$$
$$t'' = \frac{dt'}{ds} = -\frac{\dot{\alpha} \square \ddot{\alpha}}{(\dot{\alpha} \square \dot{\alpha})^2}$$

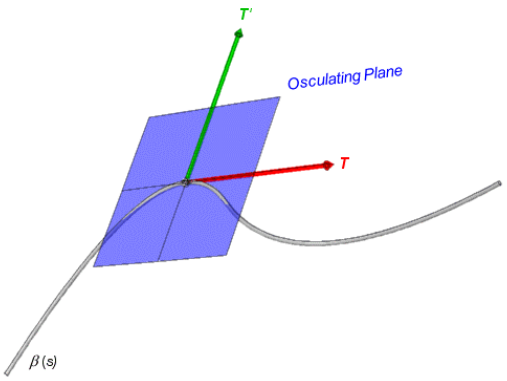

Figure V-9: Osculating plane of a curve

We call **t** = β' the *unit tangent* vector field on β. All vectors normal to **t** at $\beta(s)$ lie in a place called the *normal plane* to the curve β at *s* [*].

[*] Note that the vector **t** is not in any way directly related to the parameter *t*; the choice of the letter 't' used for both quantities is coincident

Since **t** is constant length, its derivative **t**'=β" has no tangential component, and therefore reflects purely the variation of the curve's direction due to turning of the curve. Differentiation of **t** • **t** = 1 yields 2(**t**' • **t**) = 0. Therefore the dot product of **t** and **t**' is 0, and **t**' is always orthogonal to **t**, hence normal to the curve β. Since the point of application of **t** and **t**' are the same – namely the point of application **p** = $\beta(s)$= $\alpha(t)$, these two vectors determine a unique plane for the curve at the point of application, termed the *osculating plane* (Figure V-9). Spatially, this is the plane that the curve "lies in" at the infinitesimal neighborhood of **p**. The unit vector in the direction of **t**' is termed the *normal vector* to the curve, and will be referenced by the bold letter **n**, where:

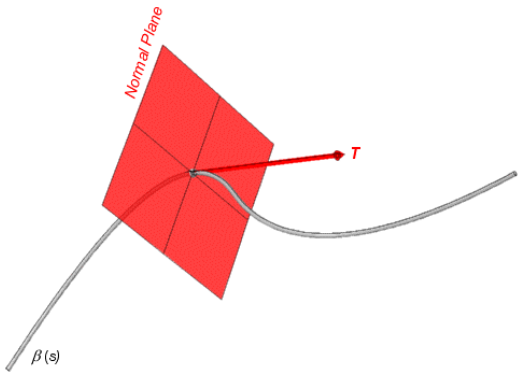

Figure V-10: Normal plane of a curve

$$\mathbf{n} = \frac{\mathbf{t}'}{|\mathbf{t}'|} \tag{V.19}$$

Similarly, the tangent vector **t** defines a second plane, normal to the curve at **p**, called the *normal plane* (Figure V-10). The length of the vector **t**' determines a numerical measurement of the curvature of β. The function:

$$\kappa(s) = \|\mathbf{t}'(s)\| \tag{V.20}$$

is called the *curvature function* of β. This scalar function provides a metric for the way in which the curve deviates from a straight line at any point. The function $1/\kappa(s)$ has a spatial sense, in that it is the radius of a circle of curvature equivalent to β at **p**. A circle whose center is located a distance positioned $1/\kappa(s)$ in the direction of **t**' will be pass through **p**, and follow the curve $\beta(s)$ as it curves in the neighborhood of **p**.

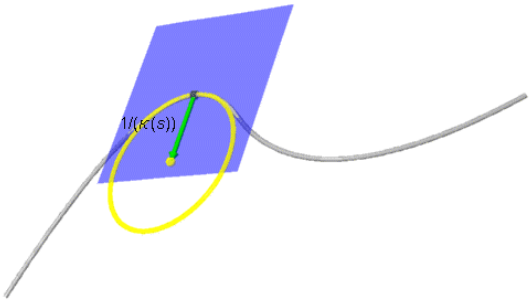

Figure V-11: Curvature of a curve

A third canonical vector completes the axis system at **p**. The *binormal vector* **b** is perpendicular to both **t** and **n**. This vector is defined by the cross product **b** = **t** × **n** and is thus normal to the osculating plane. The three vectors **b**, **t**, and **n** are mutually orthogonal, satisfying the relations:

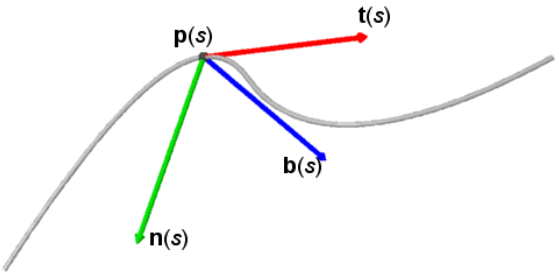

Figure V-12: The Frenet frame vectors

$$\mathbf{b}\cdot\mathbf{b}=1 \qquad \mathbf{n}\cdot\mathbf{n}=1 \qquad \mathbf{t}\cdot\mathbf{t}=1 \qquad \text{(V.21)}$$
$$\mathbf{b}\cdot\mathbf{n}=0 \qquad \mathbf{b}\cdot\mathbf{t}=0 \qquad \mathbf{t}\cdot\mathbf{b}=0$$

Differentiation of $\mathbf{b}\cdot\mathbf{b}=1$ and $\mathbf{b}\cdot\mathbf{t}=0$ yields

$$\mathbf{b}'\cdot\mathbf{b}=0 \qquad \text{(V.22)}$$

since, again, **b** is a unit vector, and

$$\mathbf{b}'\cdot\mathbf{t}=-\mathbf{b}\cdot\mathbf{t}'=-\mathbf{b}\cdot\kappa\mathbf{n}=-\kappa(\mathbf{b}\cdot\mathbf{n})=0 \qquad \text{(V.23)}$$

b' is thus orthogonal to **b** and **t** , and is therefore parallel to **n**. We define the *torsion* τ of the curve $\beta(s)$ as:

$\mathbf{b}' = -\tau\mathbf{n}$ (V.24)

The torsion of a curve at a point $\mathbf{p} = \beta(s)$ measures the twisting or winding of the curve, the rate at which the curve diverges from the osculating plane at the point. We may extend the discussion of curvature at a point by describing the curve in the infinitesimal neighborhood of **p** as having a shape equivalent to a helix with equivalent curvature to $\kappa(s)$ and torsion $\tau(s)$.

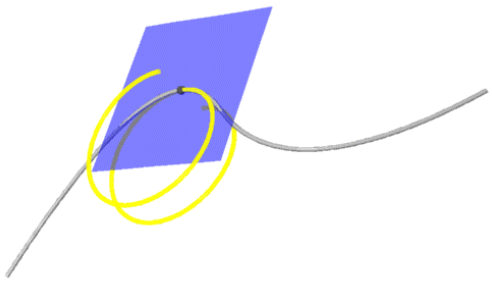

Figure V-13: Torsion of a space curve

A plane curve in $\mathbf{R}^3$ is a curve that lies in a single plane in $\mathbf{R}^3$. Intuitively, such a curve never leaves its osculating plane; its torsion must therefore be uniformly 0.

The derivative **n**' of the vector **n** is similarly orthogonal to **n**, again by virtue of the fact that **n** is by definition a unit vector over β. The vector **n**' may therefore be expanded into components in the directions of **t** and **b**. Differentiation yields[61]:

$\mathbf{n}' = -\kappa\mathbf{t} + \tau\mathbf{b}$ (V.25)

These derivatives of **t**, **n**, and **b** may be summarized through the Frenet formulas:

$$\begin{aligned} \mathbf{t}' &= \kappa\mathbf{n} \\ \mathbf{n}' &= -\kappa\mathbf{t} + \tau\mathbf{b} \\ \mathbf{b}' &= -\tau\mathbf{n} \end{aligned} \qquad \text{(V.26)}$$

and may be succinctly stated in terms of the skew symmetric *matrix of connection forms* [62]:

$$\begin{bmatrix} \mathbf{t}' \\ \mathbf{n}' \\ \mathbf{b}' \end{bmatrix} = \begin{bmatrix} 0 & \kappa & 0 \\ -\kappa & 0 & \tau \\ 0 & -\tau & 0 \end{bmatrix} \begin{bmatrix} \mathbf{t} \\ \mathbf{n} \\ \mathbf{b} \end{bmatrix} \qquad \text{(V.27)}$$

The above discussion has focused on the special case of unit speed curves - parameterizations of the form $\beta(s)$ where $\|\beta'(s)\| = 1$. The correction factor for general curves is imply $v = |ds / dt|$, the scalar speed of the curve $\alpha(t)$:

$$\begin{bmatrix} \mathbf{t}' \\ \mathbf{n}' \\ \mathbf{b}' \end{bmatrix} = v \begin{bmatrix} & \kappa & \\ -\kappa & & \tau \\ & -\tau & \end{bmatrix} \begin{bmatrix} \mathbf{t} \\ \mathbf{n} \\ \mathbf{b} \end{bmatrix} \tag{V.28}$$

The Frenet formulas determine a unique and significant frame field for the curve $\beta(s)$. Drawing on the discussion of (Section V.C.2), a curve in $\mathbf{R}^3$ may be an imbedding of the 3×1 manifold of $\mathbf{R}^3$ vectors ($\mathbf{t}_{(t)}$, $\mathbf{n}_{(t)}$, $\mathbf{b}_{(t)}$) into the $\mathbf{R}^3 \times \mathbf{R}^3 \times \mathbf{R}^3$ Cartesian product space of all 3-vectors in $\mathbf{R}^3$. The Frenet frame field is specifically adapted to discussion of problems concerning the shape of a curve. The functions $\kappa(s)$ and $\tau(s)$ that are disclosed by adopting this particular frame field fully describe the shape of the curve, such that these functions are preserved over isometric transformations of the curve in $\mathbf{R}^3$.

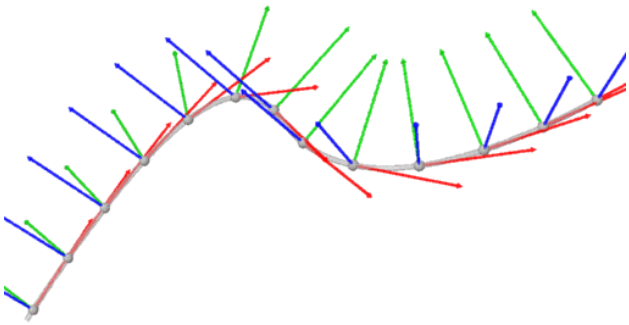

Figure V-14: The vectors **t**, **n**, *and* **b** *as a vector field*

This section has described a particular type of non-Euclidean construct – the curve, and its imbedding into Euclidean 3-space. Viewed from the perspective of the embedding space, the curve is a special subset of this space, whose topological structure is obtained by the ability to map points in this set back to a bounded region *I* of the real number line **R**, in a smooth manner, i.e. continuous and continuously differentiable. As such the curve exhibits the qualities of a manifold of single dimension, embedded in an $\mathbf{R}^3$ space.

Furthermore, the concept of shape functions on the curve were developed. Curvature and torsion are such shape functions, metrics inherent to the shape of the curve and independent of the specific parameterization or mapping responsible for the curve's generation. These

metrics were brought to light by establishing a suitable frame field over the curve in $\mathbf{R}^3$, a frame field defined by reparameterizing the curve by a function of distance along the curve – the arc length. Finally, the moving frame field was shown as an embedding of a vector space in $\mathbf{R}^3$. These concepts are further extended in considering surfaces, below.

2. Surfaces in $\mathbf{R}^3$

A surface in $\mathbf{R}^3$ is defined through a one-to-one regular mapping σ: $M \rightarrow N$ of a region M of $\mathbf{R}^2$ into a region N of $\mathbf{R}^3$. By convention, we will call the coordinate parameters in $\mathbf{R}^2$ u and v, or equivalently elements of the 2-dimensional vector $\mathbf{u} = (u, v)$, and state that:

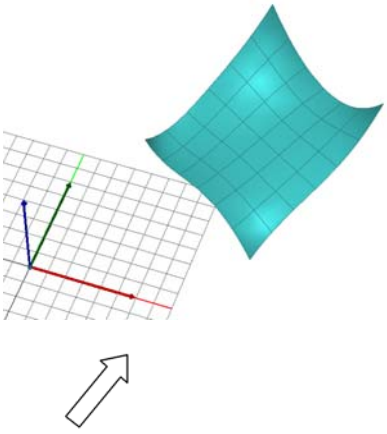

$$\mathbf{x} = \sigma(\mathbf{u}) \qquad \text{(V.29)}$$

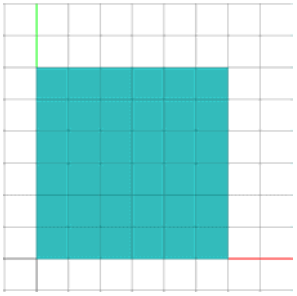

Figure V-15: Parametric definition of a surface

We again consider the Euclidean space $\mathbf{R}^3$ to be the Cartesian product of the real numbered variables $\mathbf{x} = (x_1, x_2, x_3)$. We will colloquially refer to the $\mathbf{R}^2$ specification of the surface as its *parametric space* definition, and its mapping into $\mathbf{R}^3$ as its occupancy of *world space*. For the purposes of defining the localized structure of the surface, this mapping must be regular and one-to-one: derivatives must be available, and the surface must not self intersect in $\mathbf{R}^3$. These restrictions may in turn be overcome by removing portions of the surface that do not exhibit these properties (critical points, self intersections, etc.) from consideration in discussing properties of the surface requiring regularity. As in our discussion of curves in space, the concepts discussed in this section will again spring from a localized consideration of the surface in a neighborhood of some point on the surface.

Given a mapping function σ and its inverse σ^{-1}, we can uniquely determine a u and v parametric values for any point on the image of the surface in $\mathbf{R}^3$. This one-to-one, invertible mapping of parametric coordinates onto the surface in $\mathbf{R}^3$ provides a coordinate map on the surface patch; the parameters (u, v) form a coordinate system on the points of the surface

embedded in $\mathbf{R}^3$. This definition of a surface specifies the local properties of a point in $\mathbf{R}^3$ necessary for its inclusion in a surface. In order for the properties of the surface in $\mathbf{R}^3$ to be understood and defined, it is necessary to work backward from $\mathbf{R}^3$ to $\mathbf{R}^2$, ensuring that localized properties for the inverse mapping hold for each point in $\mathbf{R}^3$ considered to be on the surface. A surface in $\mathbf{R}^3$ is a subset M of $\mathbf{R}^3$ such that for each point $\mathbf{x} \in N$ we can define a point in M whose image contains a neighborhood of $\mathbf{x}$ in $\mathbf{R}^3$.

On one hand, the relationship between coordinate patches and points in $\mathbf{R}^3$ is considered from the perspective of $\mathbf{R}^2$, where its behavior is essentially consistent with the Euclidean nature of a bounded region of $\mathbf{R}^2$ space. On the other hand, a surface is specified by considering its structuring in the neighborhood of points embedded in $\mathbf{R}^3$ space.

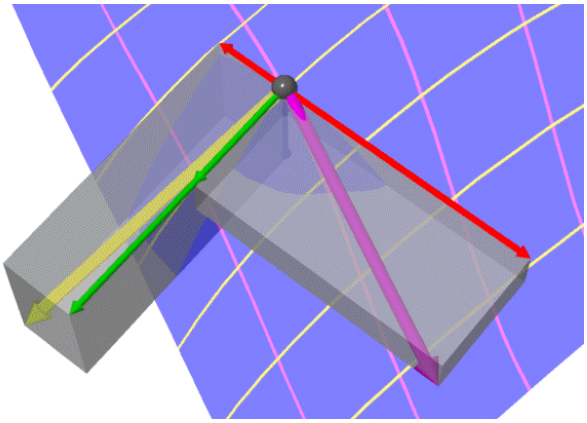

Figure V-16: The partial derivatives of the surface function

We will analyze the shape of surfaces from the localized perspective of individual points mapped between $\mathbf{R}^2$ and $\mathbf{R}^3$ spaces as they survey the structuring of their neighborhoods in these spaces, and defer on considerations of the surface's global nature and properties until such localized understanding is achieved. The essential tool for considering the shape and structuring of a surface will be to survey its variations of position and other vector based metrics near a point on of the surface as other quantities in both parametric or world space representations are varied. An obvious point of departure for consideration is the variations of points' positions in $\mathbf{R}^3$ as variations of their dual positions in $\mathbf{R}^2$ parametric space are undertaken. Other more interesting properties of the surface such as curvature and other shape metrics will in turn be defined on top of these simple variations. This variation among spatial parameterizations is comprised of six linearly independent functions, one for the variation produced in each coordinate in the three dimensional vector space $\mathbf{x}$ as either of the Euclidean 2-space parameters u and v are varied. Numerically, these values are limits of 6 ratios:

$$\frac{d\mathbf{x}_i}{d\mathbf{u}_j} = \lim_{u_{i1} \to u_{j0}} \frac{\Delta \mathbf{x}_i}{\Delta \mathbf{u}} = \frac{\mathbf{x}_{i1} - \mathbf{x}_{i0}}{\mathbf{u}_{j1} - \mathbf{u}_{j0}} \qquad \text{(V.30)}$$
$$\left| \mathbf{x}_i \in (x, y, z), \quad \mathbf{u}_j \in (u, v) \right.$$

of each component of the vector $\Delta\mathbf{x} = (\mathbf{x}_1 - \mathbf{x}_0)$ from a point $\mathbf{x}_0$ to a second point $\mathbf{x}_1$ as $\mathbf{x}_1$'s parametric coordinates (u_1 and v_1) are varied toward those of $\mathbf{x}_0$. The terms σ_u and σ_v refer to the two $\mathbf{R}^3$ vectors $d\mathbf{x}_i/du$ and $d\mathbf{x}_i/dv$,. These vectors are imagined to radiate outward from the point $\mathbf{x}_0$ in $\mathbf{R}^3$ (Figure V-17).

These functions may be organized in a 2X3 matrix (the *Jacobian matrix*) of the function σ, which may be viewed as an orthonormal expansion of the vectors $d\mathbf{x}/du$ and $d\mathbf{x}/dv$ in some Cartesian coordinate field, e.g. a "global coordinate system" $\mathbf{x} = (x, y, z)$.

$$\begin{bmatrix} \sigma_u \\ \sigma_v \end{bmatrix} = \begin{bmatrix} \frac{\partial \mathbf{x}}{\partial u} \\ \frac{\partial \mathbf{x}}{\partial v} \end{bmatrix} = \begin{bmatrix} \frac{\partial x_1}{\partial u} & \frac{\partial x_2}{\partial u} & \frac{\partial x_3}{\partial u} \\ \frac{\partial x_1}{\partial v} & \frac{\partial x_2}{\partial v} & \frac{\partial x_3}{\partial v} \end{bmatrix} \tag{V.31}$$

The surface is *regular* at $\mathbf{x}_0$ provided that the location of $\mathbf{x}$ in $\mathbf{R}^3$ does in fact vary continuously as u and v vary in the $\mathbf{R}^2$ neighborhood of $\mathbf{x}$'s map in D. The derivatives $d\mathbf{x}/d\mathbf{u}$ may not of be 0 magnitude at any point in this neighborhood. Furthermore, the vectors σ_u and σ_v must be linearly independent: they may not be parallel.

If these conditions are met, then σ_u and σ_v define a plane, tangent to the surface at $\mathbf{x}$, and a vector $\mathbf{N}$ normal to the surface at $\mathbf{x}$. The vectors σ_u and σ_v, and any linear combination of these vectors, are similarly tangent to the surface at $\mathbf{x}$. The magnitudes (lengths) of these vectors represent the "speeds" or *partial velocities* of a point $\mathbf{x}$'s travel in $\mathbf{R}^3$ as u and v are varied with unit speed in parametric space.

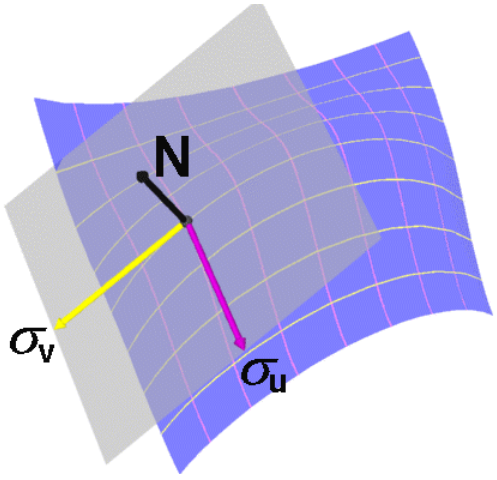

Figure V-17: Tangent plane defined by the differentiating the surface function

Note that while the vectors u and v are by definition orthogonal in parametric space (by virtue of being aligned with the correspond parametric space coordinate axes), the same need not be true in world space: the vectors σ_u and σ_v at $\mathbf{x}$ do not necessarily compose a right angle in

the plane they define. Significantly, any other parameterization of the surface of the form $(\bar{u},\bar{v})$, would have partial velocities $\sigma_{\bar{u}},\sigma_{\bar{v}}$ at **x** that would necessarily be linear combinations of σ_u and σ_v. Thus $\sigma_{\bar{u}}$ and $\sigma_{\bar{v}}$ would comprise an identical tangent plane in $\mathbf{R}^3$ at **x**, albeit with a different parameterization of the plane.

In Section V.D.1, curves in space were presented through a family of parameterizations, tracing the same curve through space and differing by the speed of the curve's trajectory through space as a function of the parameter *t.* The re-parameterization of these functions to one based on a unit arc length was identified. Normalizing the curve and its variations with respect to arc length defined a unique frame field (the Frenet frame) whose variations yielded shape metrics of the curve (curvature and torsion). These metrics in turn proved to be characteristics of the shape, invariant over parameterizations. Our consideration of the metrics defining the shape of a surface will take place along similar lines. We will look for qualities of the shape independent of its parameterization, and canonical frames of reference by which to view important shape variations of the surface. The shape of a surface is specified by qualities defined by its mapping function, viewed through its variations at localized points on the surface. In contrast to the single value parameterization of the curve, a surface is described by two parameters. The analogous shape metrics will necessarily take place by considering variations of these two parameters, both singly and in relation to one another.

We can extend the analysis of curves from Section V.D.1 to an analysis of surfaces by considering a member of the family of curves lying on the surface passing through a point **x**. The definition of this family of curves is dramatically simplified by considering the curve initially as lying in the $\mathbf{R}^2$ parametric space of surface, then mapping this parametric space curve into world space by the surface mapping function σ. The curve in parametric space is represented simply as:

$$u = u(t) \qquad \text{(V.32)}$$
$$v = v(t)$$

The parameter *t* thus sweeps a set of points in parametric space, which in turn are provided as input to the mapping function of the surface. We may equivalently say that the $\mathbf{R}^1$

manifold of the curve's parameter is transformed and embedded into the $\mathbf{R}^2$, Euclidean parametric space by the mapping function $\mathbf{u} = \alpha(t)$. In turn, the embedded curve $\alpha(t)$ in $\mathbf{R}^2$ is embedded in $\mathbf{R}^3$ world space as

$$\sigma(t) = \sigma(\alpha(t)) \tag{V.33}$$

Holding either $u(t)$ or $v(t)$ constant – the equivalent of defining a parameter t that varies in one parametric variable only – produces a "vertical or horizontal" line in parametric space and an *isoparametric* curve in $\mathbf{R}^3$. The set of isoparametric curves traces out a coordinate grid in space. The tangent to these isoparametric curves is provided by σ_u and σ_v, the 1st derivatives of σ with respect u and v, equivalently the tangent vectors of the isoparametric curves $\sigma(u(t))$ and $\sigma(v(t))$.

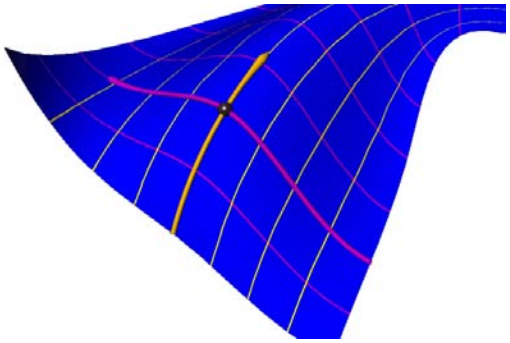

Figure V-18: Isoparametric curves on surface

The vectors σ_u and σ_v naturally determine a vector *normal* to the surface and tangent plane, orthogonal to both σ_u and σ_v, by the cross product $\mathbf{n} = \sigma_u \times \sigma_v$:

$$\mathbf{n} = \sigma_u \times \sigma_v = \begin{bmatrix} \hat{\mathbf{e}}_1 & \hat{\mathbf{e}}_2 & \hat{\mathbf{e}}_3 \\ \frac{\partial x_1}{\partial u} & \frac{\partial x_2}{\partial u} & \frac{\partial x_3}{\partial u} \\ \frac{\partial x_1}{\partial v} & \frac{\partial x_2}{\partial v} & \frac{\partial x_3}{\partial v} \end{bmatrix}$$

Any parameterization of an equivalent surface will determine a normal vector in the direction of **n**. This surface normals established by various surface parameterizations at a point will be parallel but differ in magnitude, a consequence of the speeds of travel along the surface established by the specific parameterization. To refine the surface normal's invariance over parameterizations, we define a unit length vector normal to the surface:

$$\mathbf{N} = |\mathbf{n}| = \frac{\sigma_u \times \sigma_v}{|\sigma_u \times \sigma_v|} \tag{V.34}$$

This unit normal vector is the first important invariant of surface shape we will encounter. Its variation over the surface forms an vector field on the surface, providing one component of an invariant coordinate frame field on the surface, similar to the Frenet frames developed for space curves in Section V.D.1. To complete this invariant frame field, we will need to seek out appropriately invariant directions on the surface provided by the shape of the surface as well.

The parameterization of a curve on the surface through a point **x** on the surface forms a basis for the considering the variation of surface metrics. We can trace variations of the surface's shape as we move along a curve. Then, drawing on the coordinate framework established on the surface, we can consider the expansion of surface properties from our knowledge of how the surface acts in these orthogonal parametric directions.

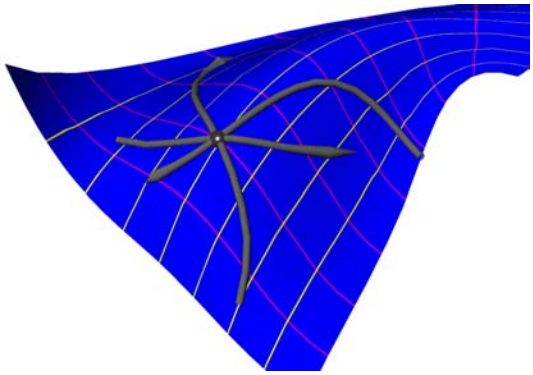

Figure V-19: The family of surface curves through a point

The arc length of a curve on the surface is found by integrating

$$ds = \sqrt{dxdx + dydy + dzdz} = \sqrt{d\sigma \bullet d\sigma} \tag{V.35}$$

The vector $d\sigma/dt$ tangent to the curve may be expanded in terms of the curve's parameterization:

$$\frac{d\sigma}{dt} = \sigma_u \frac{du}{dt} + \sigma_v \frac{dv}{dt} \tag{V.36}$$

Combining (V.35) and (V.36) results in the first important metric of the shape of surface at a point:

$$I = ds^2 = d\sigma \bullet d\sigma = (\sigma_u du + \sigma_v du) \bullet (\sigma_u du + \sigma_v du)$$
$$= (\sigma_u \bullet \sigma_u) du^2 + (\sigma_u \bullet \sigma_v) du dv + (\sigma_v \bullet \sigma_v) dv^2 \quad \text{(V.37)}$$

Note that while *ds* represents the notion of infinitesimal arc length along a curve, the quantity ds^2 represents an infinitesimal area on the surface between two neighboring pairs of isoparametric curves on the surface, joined by path taken by a curve on the surface $\sigma(t)$. The scalar quantities

$$e = \sigma_u \bullet \sigma_u$$
$$f = \sigma_u \bullet \sigma_v \quad \text{(V.38)}$$
$$g = \sigma_v \bullet \sigma_v$$

represent measures of this variation of the surface in the neighborhood of **x**. *e* and *g* represent the rate of stretch or shrink of the surface as one moves in the direction tangent to *u* and *v* at **x**, while f measures the rate of shear between these two space vectors.

The quantities *e, f,* and *g* represent the *first fundamental form* of a surface. The quantity

$$eg - f^2 = (\sigma_u \bullet \sigma_u)(\sigma_v \bullet \sigma_v) - (\sigma_u \bullet \sigma_v)^2$$
$$= (\sigma_u \times \sigma_v) \bullet (\sigma_u \times \sigma_v) \quad \text{(V.39)}$$
$$= \left|(\sigma_u \times \sigma_v)\right|^2$$

is the magnitude of cross product between the tangent vectors σ_u and σ_v.

The first fundamental form gives a metric of the surface, appropriate for considering the variation of the surface's shape from the myopic perspective of an "inhabitant" of surface situated at point on the surface **x**. As the inhabitant surveys the terrain of the surface in its neighborhood, important variations *in the plane of the surface* may be detected from the metrics in (V.38), allowing local variations of surface features such as arc length, angle and areas to be determined.

This localized variation of properties in the plane of the surface is however only part of description of its shape. The surface form must be considered from the perspective of variations out of the surface plane as well. We approach this by again considering the path

through space of a curve on the surface. In this step, we will consider the relationship of the Frenet field on the curve at **x** to the frames established by the surface plane and normal. The tangent vector to the curve **t** will lie in the plane of the surface. However, the normal vector of the curve's Frenet frame **n** will likely be in a direction independent from the surface normal vector **N** at the point. This stems from the fact that the curve may not only curve with the direction of the surface, but may simultaneously curve in the plane of the surface as well. In order to use this curve to establish metrics on the surface's curvature, we isolate the normal and tangential components of the curve's shape from the perspective of the embedding surface.

We may define an angle γ between the unit length normal to the curve **n** and the unit length normal to the surface **N**, as:

$$\mathbf{n} \bullet \mathbf{N} = \cos(\gamma)\left|\mathbf{n}\right|\left|\mathbf{N}\right| = \cos(\gamma) \qquad \text{(V.40)}$$

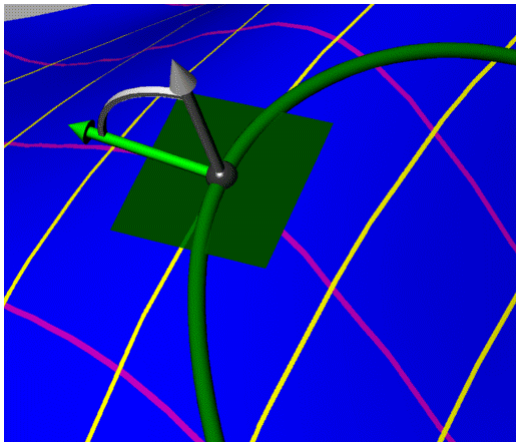

Figure V-20: The angle between surface and curve normals

The vector **n** points in the normalized curvature direction **t**′ of the curve σ (*t*). Correspondingly, the vector **N** normal to surface provides what seems intuitively a similar role on the surface. The relationship between surface normal and surface curvature is disclosed by considering the component of the curvature of $\sigma(t)$ lying in the plane formed by **N** and the vector **t** tangent to curve**.**

We decompose the curvature of $\sigma(t)$ into this *normal* component and the component in the plane of the surface, and may visualize this decomposition locally as two curves in these planes. Curvature in the plane tangent to the surface is termed the *geodesic* curvature of the surface. The normal curvature, out of the tangent plane and in the plane described by the tangent to the curve and the surface normal, will be the focus of consideration in establishing metrics for

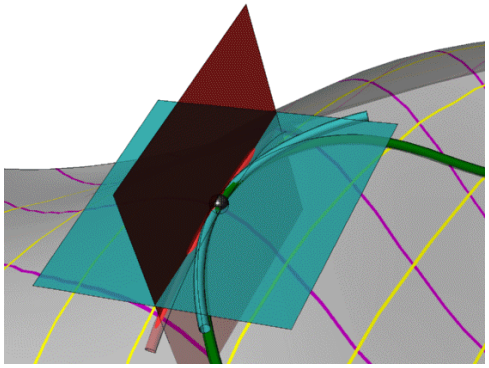

Figure V-21: Decomposition of surface curve into normal and geodesic components

the surface's curvature. The invariance of this component should be evident; any curve on the surface with an equivalent tangent at **x** will be constrained to share this component of curvature, by virtue of being constrained to the surface at that point. In contrast, the geodesic curvature of like curves at **x** will be distinct.

The valuation of the normal curvature at **x** with a unit tangent vector **t** is simply the component of the surface curve's curvature κ, projected onto the surface's normal **N** at **x**. This factor is computed as the surface curve's curvature, multiplied by the cosine of the angle γ :

$$\kappa \cos(\gamma) = \kappa \mathbf{n} \bullet \mathbf{N} \tag{V.41}$$

t', the 1st derivative of the curve's unit tangent vector with respect to arc length is defined as $\kappa \bullet \mathbf{n}$; therefore (V.41) may be expanded as:

$$\begin{aligned} \kappa \cos(\gamma) &= \kappa \bullet \mathbf{n} \bullet \mathbf{N} \\ &= t' \bullet \mathbf{N} \\ &= \sigma'' \bullet \mathbf{N} \\ &= (\sigma_u du + \sigma_v dv)' \bullet \mathbf{N} \\ &= (\sigma_{uu} dudu + 2\sigma_{uv} dudv + \sigma_{vv} dvdv + \sigma_u d^2u + \sigma_v d^2v) \bullet \mathbf{N} \end{aligned} \tag{V.42}$$

Since σ_u and σ_v are the tangent vectors to the isoparametric curves on the surface, **N** is by definition orthogonal to these vectors and $\sigma_u \bullet \mathbf{N} = \sigma_v \bullet \mathbf{N} = 0$. Therefore the last two terms in (V.42) equal 0, and the equation reduces to the *second fundamental form* of a surface:

$$\begin{aligned} \kappa \cos(\gamma) &= (\sigma_{uu} dudu + 2\sigma_{uv} dudv + \sigma_{vv} dvdv) \bullet \mathbf{N} \\ &= l\, dudu + 2m\, dudv + n\, dvdv \end{aligned} \tag{V.43}$$

where

$$\begin{aligned} l &= \sigma_{uu} \bullet \mathbf{N} \\ m &= \sigma_{uv} \bullet \mathbf{N} \\ n &= \sigma_{vv} \bullet \mathbf{N} \end{aligned} \tag{V.44}$$

The normal curvature of a curve on the surface κ_n may now be expressed by the components *e*,*f* and *g* from the 1st fundamental form (V.38), and the components of the second fundamental form *l*,*m* and *n*:

$$\kappa_N = -\frac{l\,dudu + 2m\,dudv + n\,dvdv}{e\,dudu + 2f\,dudv + g\,dvdv} = -\frac{l + 2m\lambda + n\lambda^2}{e + 2f\lambda + g\lambda^2} \qquad \text{(V.45)}$$

where $\lambda = dv/du$, the tangent of the angle curve $\sigma(t)$ prescribes *in the parametric coordinate* plane of σ at **u**.

Note that the above discussion has reduced our initial consideration of the family of all curves lying on σ to consideration of the family of curves formed by the intersection of the surface with the *pencil* of planes in which the surface normal **N** lies. The normal curvature component of any curve on the surface passing through **x** will be locally equivalent to the curvature formed by the intersection of the surface with the plane formed by the tangent to the curve and the surface normal.

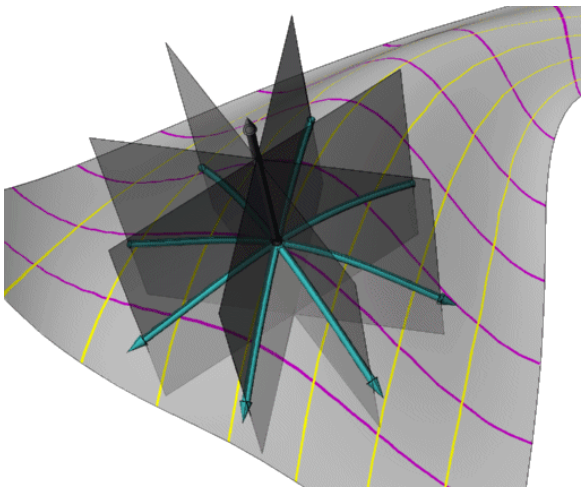

Figure V-22: The normal curves at a point

As this plane is rotated about **N**, the normal curvature κ_N will vary. Through this rotation, a maximum and minimum value for κ_N will be attained for some values of λ. The maximum and minimum values of κ_N are termed the *principal curvatures* of σ at **x**, and in combination they uniquely define the local shape of the surface at **x**. The principal curvatures may be determined by recognizing that the maxima are when the derivative of κ_n with respect to λ equals 0. Differentiating (V.45) with respect to λ yields:

$$\frac{d\kappa_N}{d\lambda} = 0 = (e + 2f\lambda + g\lambda^2)(2m + 2n\lambda) - (l + 2m\lambda + n\lambda^2)(2f + 2g\lambda) \qquad \text{(V.46)}$$

Therefore, at the directions of principal curvature:

$$(e + 2f\lambda + g\lambda^2)(2m + 2n\lambda) = (l + 2m\lambda + n\lambda^2)(2f + 2g\lambda) \tag{V.47}$$

and

$$\frac{(2f + 2g\lambda)}{(e + 2f\lambda + g\lambda^2)} = \frac{(2m + 2n\lambda)}{(l + 2m\lambda + n\lambda^2)} \tag{V.48}$$

Since

$$\begin{aligned}(e + 2f\lambda + g\lambda^2) &= (e + f\lambda) + \lambda(f + g\lambda) \\ (l + 2m\lambda + n\lambda^2) &= (l + m\lambda) + \lambda(m + n\lambda)\end{aligned} \tag{V.49}$$

substituting (V.45) into (V.48) and undertaking the substitutions in (V.49) yields the equation for the normal curvatures κ_N:

$$\kappa_N = -\frac{l + m\lambda}{e + f\lambda} = -\frac{m + n\lambda}{f + g\lambda} \tag{V.50}$$

Re-ordering yields the two equations, when κ_n is at its extreme values:

$$\begin{aligned}(l + \kappa_N e)du + (m + \kappa_N f)dv = 0 \\ (m + \kappa_N f)du + (n + \kappa_N g)dv = 0\end{aligned} \tag{V.51}$$

The roots of this simultaneous solution are:

$$\begin{aligned}\kappa_{N_{max,\,min}} &= H \pm \sqrt{H^2 - K} \\ K &= \frac{ln - m^2}{eg - f^2} \\ H &= \frac{2fm - en - gl}{2(eg - f^2)}\end{aligned} \tag{V.52}$$

K is the *gaussian curvature* , defined as:

$$K = \kappa_{N_{max}} \kappa_{N_{min}} \tag{V.53}$$

From (V.52) the equation for *H* can be determined to be $H = \frac{\kappa_{N_{max}} + \kappa_{N_{min}}}{2}$, the *arithmetic mean* or average of the principal curvatures.

The square root of absolute value of this gaussian curvature:

$$\sqrt{K} = \sqrt{\left|\kappa_{N_{max}} \kappa_{N_{min}}\right|} \tag{V.54}$$

is a useful valuation, representing the *geometric mean* of the principal curvatures' magnitudes. Note that on a sphere:

$$\sqrt{K} = \sqrt{\left|\kappa_{N_{max}} \kappa_{N_{min}}\right|} = \sqrt{\kappa_N{}^2} = \left|\kappa_N\right| \tag{V.55}$$

since $\kappa_{N_{max}} = \kappa_{N_{min}}$. The value $1/\sqrt{K}$ provides the radius of a sphere with equivalent gaussian curvature, a useful reference when considering what a particular gaussian curvature value represents.

We now consider a number of local surface conditions discernable from the valuation of gaussian curvature. First, we may identify three distinct local conditions of the surface depending on the sign of the gaussian curvature at the point. When the sign of κ_{Nmax} and κ_{Nmin} are the same (either both positive or both negative) the sign of the gaussian curvature will be positive. Geometrically, this means the surface curves in the same direction in the two principal directions. Qualitatively, this corresponds to a shape similar to a "dome" (if the surface curves away from the normal direction under consideration) or a "bowl" (if the direction of curvature is toward the surface normal). The term *elliptical* is used to describe this type of localized surface curvature configuration. The absolute values of the principal curvatures will thus take on a maximum and minimum. The surface will thus have directions of tightest and weakest curvature, corresponding to the greatest and least absolute values of the two principal curvatures.

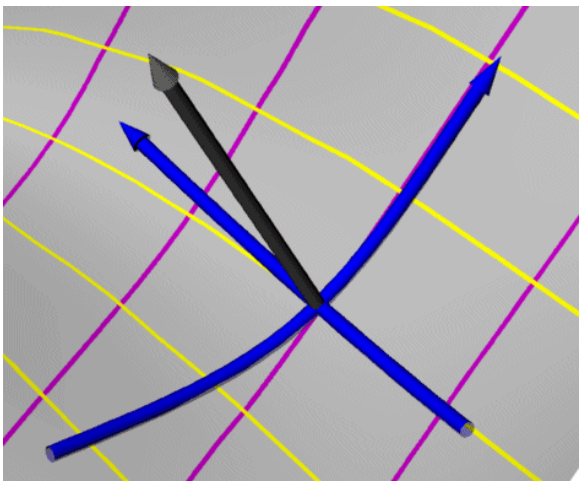

Figure V-23: Positive gaussian curvature - "bowl" configuration

The sign of the curvatures κ_{Nmax} and κ_{Nmin} will be dependent on the parameterization of the surface. If the parameterization is inverted (where u and v are reversed), the surface normal $\mathbf{n} = u \times v$ will be inverted. The direction of curving will thus be in the opposite direction relative to **n**, thus the sign of κ_{Nmax} and κ_{Nmin} will be inverted. However, the sign and valuation of the gaussian curvature $K = \kappa_{Nmax} \times \kappa_{Nmin}$ will remain constant regardless of parameterization. We may also recognize conditions where the principal curvatures are in the same direction and of equivalent value. In this case, κ_N is constant as the direction around the point is considered. The point is an *umbilical point*, locally spherical.

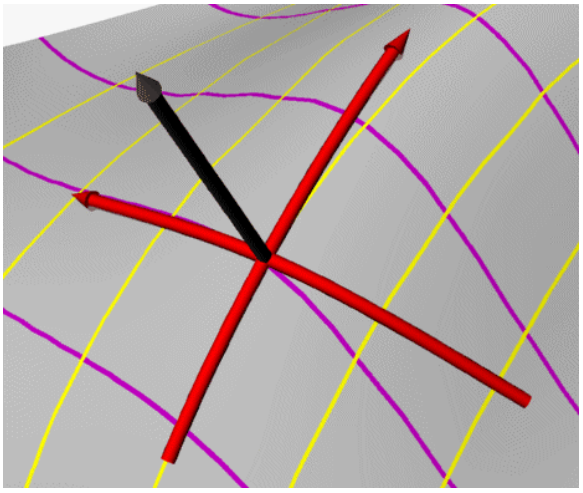

Figure V-24: Positive gaussian curvature - "dome" configuration

The surface takes on a qualitatively different shape at points of negative gaussian curvature. Here the principal curvatures κ_{Nmax} and κ_{Nmin} are necessarily of opposite sign. The surface curves in opposite directions along the two principal directions: one direction will curve in the direction of the surface normal, the other in the opposite direction. The local shape will have the characteristics of a "saddle" and is *hyperbolic* at the point. The principal curvatures are in the opposite sense. Consequently, the principal directions both represent directions of tightest curvature, the two extremes of the curvatures taken on by normal curvatures at the point.

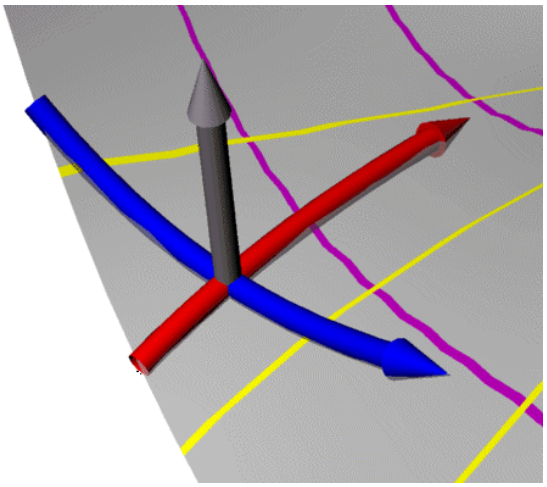

Figure V-25: Negative gaussian curvature configuration

Since the principal curvatures are of opposite signs, and the curvature of the normal sections vary continuously as the direction of consideration proceeds around the point, there must be two normal sections where $\kappa_N = 0$; i.e. the normal section is locally linear.

Finally, the gaussian curvature may be locally of magnitude 0. Since $K = \kappa_{Nmax}\ \kappa_{Nmin}$ this condition means that either one of either κ_{Nmax} or κ_{Nmin} are of magnitude 0, or they both are. Recall that a curve of curvature 0 is locally straight; The latter case, where both κ_{Nmax} and κ_{Nmin} are of magnitude 0, corresponds to the condition of a surface that is locally planar; the normal sections in the principal directions, hence in every direction, is straight.

Zero gaussian curvature is also the result when one of the principal curvatures is of magnitude 0, but the other is not. The normal curvature κ_N at the point never changes sign, but varies between the 0 and the maximum curvature established by κ_{Nmax}. This is referred to as a surface that is locally *parabolic*. Since $\kappa_{Nmin} = 0$, the surface corresponds locally to a line in one of the principal directions. The other principal direction must necessarily be orthogonal to this direction on the surface. Parabolic surface conditions will have a great role in the discussion of developable surfaces, to be presented in great detail in Section VI.B.

We can view values of gaussian curvature as defining a relationship between pairs of κ_{Nmax} and κ_{Nmin} values. Figure V-26 shows a chart graphing constant values of gaussian curvature, with the axes representing the two principal radii. Note that this graph is symmetric about the axis of equivalent radii. Similarly, we can view a constant value of gaussian curvature as defining a family of localized surface curvature conditions (Figure V-27).

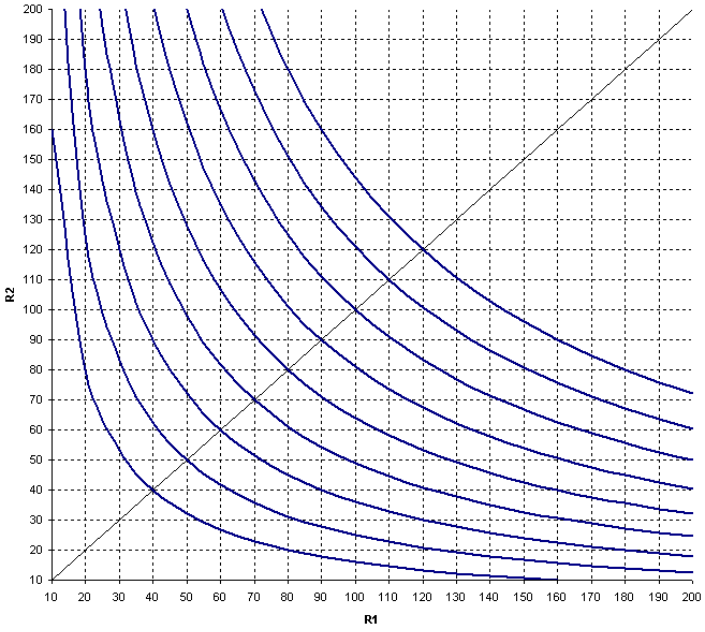

Figure V-26: Gaussian curvature as a relationship among principal curvatures

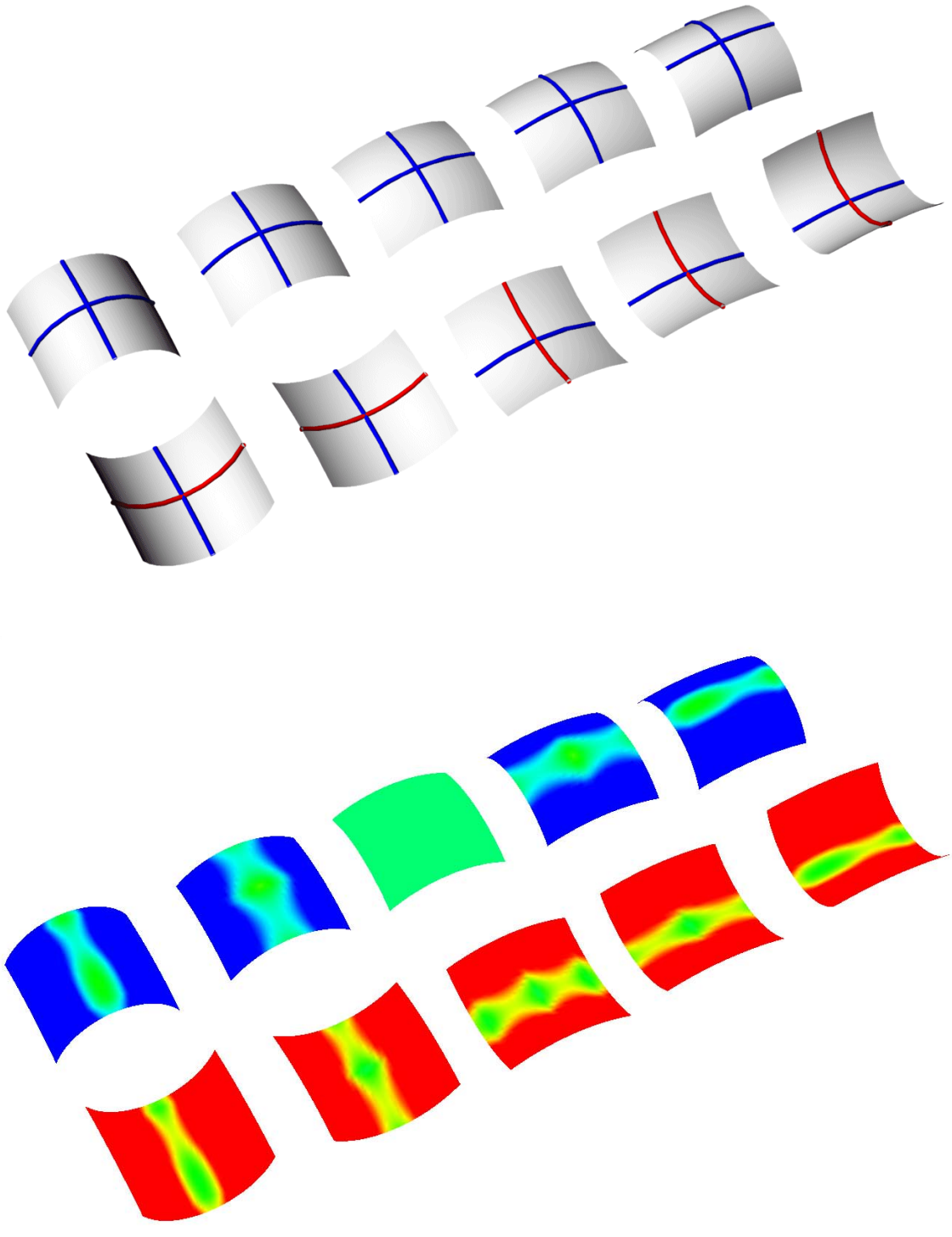

Figure V-27 Equivalent gaussian curvature family

The directions of maximum and minimum curvature, along with the normal, present three vectors on the surface that are each orthogonal to the other. This fact provides the conditions for a frame field (Section V.B.3) on the surface. This frame field is an analogue of the important Frenet frames (V.26) found on curves: a unique coordinate system on the surface, occurring purely as a result of the shape of the surface at local points and independent of the parameterization of the surface.

The notion of shape metrics - established on curves through the definition of curvature and torsion – were extended to surfaces through the definition of principal curvatures and gaussian curvature. These metrics are properties of the shape of the surface, independent of parametric description that generates the surface. These properties take the form of vector fields, defined across the surface manifold. Shape metrics will be drawn on in following sections to establish criteria for the constructibility of the designed shapes.

3. Bézier / NURBS formulations

This chapter has established curves and surfaces as special types of topological objects: manifolds embedded in 3-dimensional space through a mapping from an intrinsic parametric space that is locally Euclidean. From these topological conditions, shape metrics resulting from the differential properties of these mappings were identified. These principles were developed without regard to the specific formulations of the mapping functions, other than positing assumptions on the order of the mapping function and its differentiability.

In order to interpret these findings into numerical valuations, or simply to describe a specific object's inhabitation of $\mathbf{R}^3$, numerically evaluatable mapping functions will need to be to defined. In this section, parametric mapping functions of utility to computer aided design will be presented, and their ability to support differentiability and other conditions necessary for shape metric evaluations will be demonstrated.

Classical texts on differential geometry[87,47,36] typically present examples of spatial objects in terms of simple polynomial and trigonometric functions for which differentiation can be undertaken in a fairly straightforward fashion. For example the curve mapping function:

$$\alpha(t) = \begin{bmatrix} t \\ t^2 \\ t^3 \end{bmatrix} \tag{V.56}$$

is easily differentiable with respect to *t*:

$$\dot{\alpha} = \begin{bmatrix} 1 \\ 2t \\ 3t^2 \end{bmatrix} \tag{V.57}$$

The curve definition in (V.56) can be extended to describe a family of curves, by introducing additional variables in polynomial definition:

$$\alpha(t) = \begin{bmatrix} at \\ bt^2 \\ ct^3 \end{bmatrix} \tag{V.58}$$

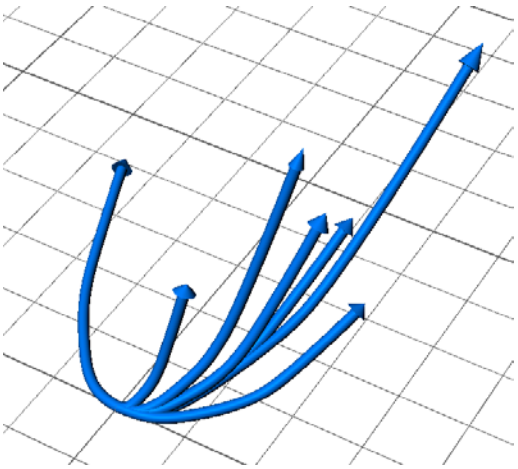

Figure V-28: A family of polynomial curves

Figure V-28 shows members of this family of curves, generated through variations of the variables *a, b,* and *c.* However, the utility of any such specific polynomial curve or surface formulation is rather limited. The curves in Figure V-28 all have roughly the same shape. If we are interested in a curve with an even minimally different configuration in space, we need to adjust the polynomial description of the curve, an operation that is not likely to be conducive to interactive editing for this simple polynomial approach.

The search for polynomial parametric expressions of more general utility, and improved user interaction, has resulted in the development of the Bèzier equations, and extensions of these equations including NURBS (Non-Uniform, Rational B-Splines)[64,74,29]. These formulations allow curves and, by extension, surfaces, or any order, embedded in spaces of arbitrary dimension. The basic equation of a Bèzier curve is:

$$\alpha(t): \mathbf{R} \rightarrow \mathbf{R}^3 = \sum_{i=1}^{n+1} \mathbf{b}_i B_{i,k}(t), \qquad \text{where } t_{\min} \le t \le t_{\max}, \qquad 2 \le k \le n+1 \tag{V.59}$$

The variable *i* denotes the order of the curve, while the vectors $\mathbf{b}_i$ are the positions of control point in the embedded space, $B_{i,k}$ are B-Spline basis functions.

$$B_{i,n}(t) = \frac{n!}{i!(n-i)!} u^i (1-t)^{n-i} \tag{V.60}$$

These basis functions provide a smoothing or averaging function on the locations of the control points, that varies as a function of the parameter *t*. for the simple case of an order 1 curve, or line, equation (V.59) reduces to simply:

$$\alpha(t) = (1-t)\mathbf{b}_0 + (t)\mathbf{b}_1 \tag{V.61}$$

The B-Spline basis functions may be extended into higher dimensions. The equation for a Bèzier surface is:

$$\sigma(u,v) = \sum_{i=0}^{n} \sum_{j=0}^{m} B_{i,n}(u)\, B_{j,m}(v)\, \mathbf{b}_{i,j} \tag{V.62}$$

Where the control points $\mathbf{b}_{i,j}$ define an ordered mesh of control points in size *i* x *j.*

Parametric curve and surface representations represented through B-spline equations form the basis for virtually all commercially available CAD representations at this point in time. The descriptions of paper surface representations currently used in Gehry's process are similarly founded on these underlying parametric descriptions. However, it should again be noted that these representations only specific examples of the set of potential manifold representations of curved spatial objects. Other representations will be considered in latter parts of this thesis.

VI. Differential Forms And Applications to Surface Constructibility

In Chapter V, shape metrics were defined as differential properties on shapes, useful for describing characteristics of the shape. In this chapter applications of shape metrics to issues of surface constructibility on Gehry projects are discussed. Two substantially different methodologies for applying shape metrics to guide the development of constructible surface forms are currently applied in the firm's digital modeling process. These different approaches have substantially different implications, both on the qualities of the resulting forms, and the fabrication systems that are supported.

As a general introduction to the approach, we are interested in establishing some surface metric that provides a measure of acceptable constructibility conditions. With this measure in hand, we can assess the project form in terms of its constructibility. If localized unacceptable conditions are determined, rationalization operations can be conducted to improve the form, until the constructibility metric on the form is satisfactory. In Section I.A, techniques used by the firm to apply gaussian curvature metrics as one such measure of constructibility are described.

Alternatively, we can look to constrained surface representations that by nature guarantees certain constructibility conditions. By interpreting the project form into assemblies of these surface elements, the identified constructibility conditions are guaranteed. The processes of describing the project form through these surface elements is thus unified with the processes of rationalization. In Section VI.B of this chapter, one such class of surface forms, the *developable surfaces,* are described, and their relationship to constructibility requirements are presented.

A. CONSTRAINED GAUSSIAN CURVATURE

1. Introduction

The application of gaussian curvature (Section V.D.2) as a heuristic for surface constructibility was first used on the Bilbao project, was substantially extended on the Experience Music Project, and has been in use on projects since that time. These projects represent paper surface constructibility problems, as described in (Section IV.C). On these

projects, fabrication strategies were adopted based on cladding the surface with metallic sheets, either stainless steel, aluminum or, in the case of Bilbao, titanium. For reasons of project economics, the assumption was made that the surface form should be fabricated through assemblies of sheet elements, positioned on a sub-framing system, without requiring expensive working of the sheet materials through stretch forming or other labor intensive methods.

At a first, qualitative glance, the notion of surface curvature as a metric for constructibility of these systems makes some sense. Experience by the firm has shown that some degree of macro scale surface curvature can be accommodated by these fabrication strategies. Within some limit of surface curvature, sheet materials can be fastened to a framing system with insignificant deviation between the sheets and the framing. Within this limit, the effects of surface curvature on the behavior of the sheets can be ignored.

The qualities of the gaussian curvature metric have a reasonable affinity with what can be observed in forming sheets in space. We can for example construct a cylinder of quite tight radius from a metal sheet, by simply rolling it into a form. Analysis discloses zero gaussian curvature for cylindrical forms. Other canonical forms such as cones have similar properties. Of course, at some point the material properties of the sheet metal begin to impact this qualitative assessment of form, since we can not manually roll a thick sheet of plate steel into a cylinder of any substantially tight radius. But with certain assumptions regarding the stiffness of the sheet material in place, the sheet's material behavior can be discounted for surface forms with zero gaussian curvature. By extension, we presume that some limited, non-zero surface curvature can be supported by sheet materials as well, and look to identify a measure of surface curvature that is acceptable given the surface construction.

On further inquiry, this intuitive assumption seems to unravel, when we look to identify precisely how this surface curvature is assumed by the system, and attempt to determine empirical metrics for this behavior. An analysis of the behavior of sheet materials seems to defy the proposition that any substantial curvature can be assumed by sheet elements. However, a curved surface of substantially large proportions can be covered by relatively small sheet elements. The ability of the system to "make up" this curvature is difficult to assess empirically. Some limited curvature may be assumed by in pane stretching of the material under manual forming. This claim is substantiated by observing the residual

deformation of the sheet if it is released from the substrate to which it is fastened. However, this manual stretch forming is only a small part of the story. Additional macro scale surface curvature is assumed by the sheet's buckling into complex configurations with minimal gaussian curvature as it is forced onto the framing system. The sheet does not assume the surface form exactly, but deviates somewhat, in a manner dictated by its internal resolution of the bending forces. Without conducting substantial material analysis for each sheet, the exact resolution of these forces by the sheet is difficult to predict. However, the results of these effects can be observed as the sheet is forced onto framing configurations that impose increasing gaussian curvature. At some point, the edges of the sheet will begin to display visible buckling. This phenomenon is highly dependent on sheet dimensions, fastening strategies, and material properties. Efforts to control these imperfections by orienting panels either with or against the direction of maximal surface curvature have been inconclusive.

Macro scale gaussian curvature may also be resolved in the fabricated assembly by discontinuities between adjoining sheet elements. Neighboring sheets will deviate slightly from one another in continuity or tangency. Small scale buckling independently assumed by each of the sheets will result in some discontinuity between the sheets. This discontinuity may have system fabrication or performance implications, and must remain within established construction tolerances for the system.

As difficult as it is to establish the precise mechanisms by which surface curvature is resolved by the fabrication system, the degree of imperfection allowable in a surface system is similarly difficult to determine. When sheet materials are part of the waterproofing strategy for the project, the allowable discontinuities between sheets must be kept to a minimum. On many of the firm's projects, surface fabrication strategies are employed that use several layers of sheet materials, each with different material behaviors, sheet sizes, and performance requirements.

In practice, it has often been the desired aesthetic qualities of the finish surface that have determined the tolerance for imperfections of surface smoothness and the corresponding degree of allowable surface curvature. The wrinkling of the titanium shingles on the Bilbao project was part of the desired aesthetic; the curvature considerations on this project were driven by constructibility requirements of the steel back pan sub-system. On the Experience

Music project, curvature considerations were driven largely by the desire for a smooth finish surface.

An empirical analysis of this wide range of phenomena and performance requirements – as they play out on the infinitely variable local conditions of the project form has not been practical on Gehry's projects to date. In practice, gaussian curvature has proven to be a reasonable heuristic of surface constructibility, encompassing all of these complex phenomena into one simple metric. Part of the strategy in adopting gaussian curvature to measure surface constructibility assumes a factor of safety in developing a gaussian curvature metric. Typically, mock up studies of a surface system will be conducted on the basis of maximum anticipated gaussian curvature. The mockups are tested for conformance to performance requirements, and the qualities of the finish surface are inspected. If the mockup is deemed successful on the basis of this assessment, the gaussian curvature exhibited by the digital rendition of the mockup provides a bench mark. The maximum acceptable surface curvature for the project at large may be stepped back to more conservative values, to allow a factor of safety.

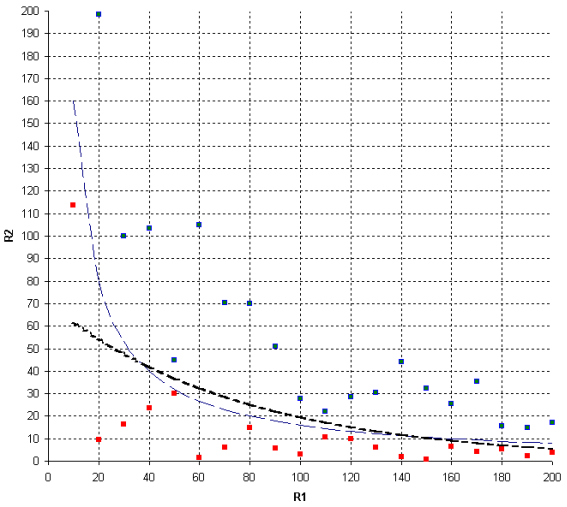

Figure VI-1: Gaussian curvature samples and curve

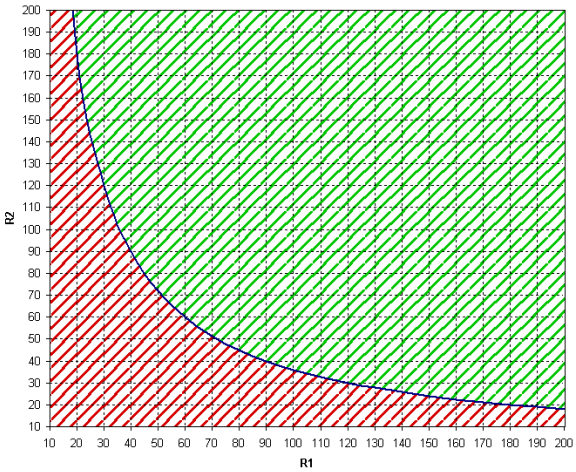

Figure VI-2: Acceptable and unacceptable curvature configurations

When surface curvature is detected in the design surface that exceeds the established curvature values for the project, the project form must be rationalized to reduce this curvature. Several techniques have been developed to address surface conditions where curvature constraints are not met. The simplest and most effective of these techniques is to break the surface and introduce tangency discontinues. These tangent discontinuity features

are addressed in fabrication as breaks between neighboring panels (Figure VI-3). This tangency discontinuity will have potential design and constructibility implications. A detail for the connection of surface sheets across a tangency discontinuity must be established. This detail may be more expensive than the typical condition of surface continuity, and there may be fabrication limitations on where this condition can be applied. The introduction of tangency discontinuities will of course have an impact on the design qualities, so rationalization exercises must be conducted with the input of project designers.

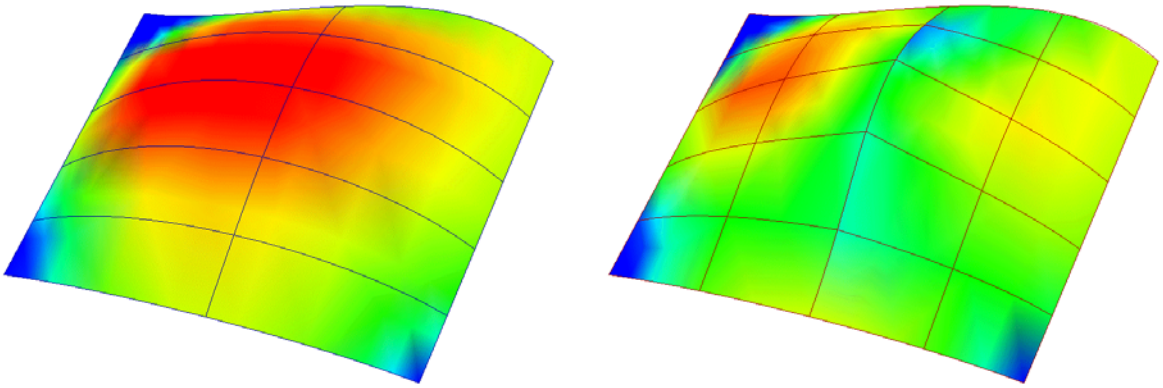

Figure VI-3: Control of gaussian curvature by introduction of tangency discontinuities

2. Applications on the Experience Music Project

The Experience Music Project (EMP, 1995-2000) represents the clearest and most ambitious example of the constrained curvature approach to surface rationalization. EMP was begun by Gehry Partners in 1995, with construction completed in May, 2000. The story of the project's surface form development and subsequent rationalization stems from a sequenced resolution of the project's design intent with constructibility decisions, undertaken on a fast track construction schedule.

Figure VI-4: EMP site model

The project is a multi-use facility, incorporating exhibits and multimedia rides surrounding the theme of music, as well as facilities for a music archive and foundation, as well as a variety of programs for music education. Initial discussions with the client focused the direction of the design on themes surrounding the energy and imagery of rock & roll. An important reference to the client was to pay homage to Jimi Hendrix, a Seattle native and founding influence of 1960s rock and roll. The theme of the electric guitar and in particular the image of Hendrix' smashing guitars on stage in the 1960s became one of the guiding references for the project. Gehry responded to the mixed use nature of the by disaggregating the facility into seven distinct objects. Each of the elements takes on the colors of a historically significant type of electric guitar.

As is typical in Gehry's design process, several alternative schemes were presented to the client during schematic design. Among the options presented were sketch models fabricated from plasticene materials, with more smoothly continuous surfaces than had previously been attempted by the firm. The client expressed a strong preference for these "swoopy", free form shapes. With this design direction in hand, the architectural team began a series of feasibility studies intended to develop surface fabrication systems supporting these highly curved shapes.

The design team initially established a fabrication strategy using terrazzo, covering relatively large (10' X 20') panels of pre-fabricated concrete. The terrazzo material would be colored and finished with embedded glass aggregate to approach the glittery finish of guitars. During this time, the final shape of the building was being completed and project computer models were produced from the physical design models (Figure VI-6). These computer models were generated on the assumption that the final surface would take on the form of generally continuous surfaces over the body of each element.

Figure VI-5: Terrazzo mockup (EMP)

The project schedule required that the primary structure be engineered before the relatively difficult problem of engineering the building surface system was completed. The structural engineer elected to construct the primary structural system out of curved, plate built up ribs, which would follow the general form of the finish surface. The structural ribs sliced the elements in an orthogonal arrangement, spaced 10' apart. To accommodate the as yet undetermined cladding system, a 24" offset zone was left between the outside finish surface and the exterior of the structural rib assembly. In highly formed areas, the rib system broke away from the outside surface form, anticipating a potentially substantially thicker surface assembly in these regions.

Mid way through design development, the terrazzo on concrete paneling approach was abandoned. This decision was largely based on economic factors. The terrazzo finish system was deemed to be prohibitively expensive, largely due to the labor intensive finishing of the terrazzo material. Instead, the decision was made to develop the building enclosure system based on a sheet metal cladded finish, similar to the systems that had recently proven successful on the Guggenheim Bilbao. However, unlike the Bilbao finish, the surface quality desired of the EMP project was to be smooth, recalling the imagery of the curved metal finish on airplane bodies. The architecture team considered the fabrication techniques of airplane bodies, where portions of the skin shapes are produced by limited deformation of sheet metal

surfaces, while other more highly shaped areas (such as the nose cone of an airplane) are mass produced by stretch forming.

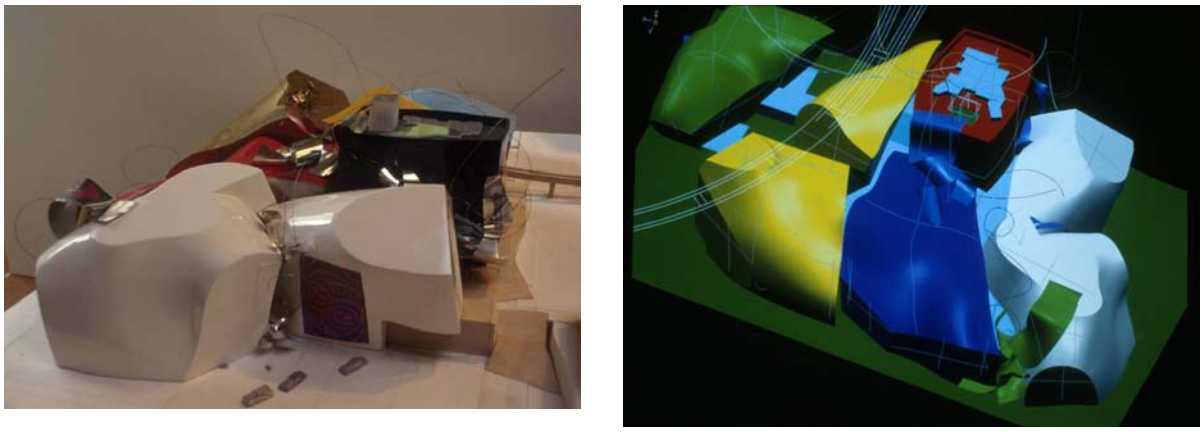

Figure VI-6: EMP design prior to selection of cladded surface system

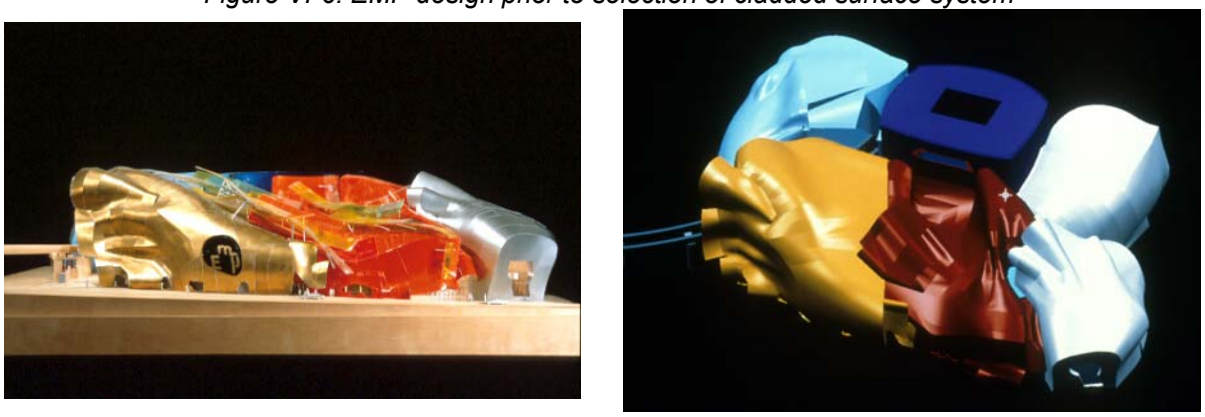

Figure VI-7: EMP design after rationalization for cladded surface construction

At this point, the sheet metal fabricator A. Zahner & Company (AZCO) was brought on to the construction team. Discussions ensued between the architecture team and the fabricating engineers to re-interpret the building shape into fabricatable sheet metal elements. It was known at the time that the CAD models – incorporating continuous free form surfaces – would have to be modified to substantially remove the double curvature in the form. However, the team had limited heuristics for determining what would be acceptable curvatures, and the economic implications of varying types of double curved surfaces. In the bid documents[33] provided to AZCO, a distinction was made between two types of surface systems: a “typical system” where presumptions of limited surface curvature could be made and where the project form would be subjected to the limitations of simply folded sheet metal materials, and “highly shaped areas” which might require additional forming of the metal material.

AZCO began a series of tests to determine the limits of gaussian curvature that could be supported on the typical system. A test bed was built, allowing combinations of surface curvatures to be evaluated. On this test bed, a series of threaded rods were positioned relative to pre-cut templates defining arcs of a given radius. Once the test bed was set up with a given combination of radii, sheets of finish metal were pressed on the surface of the bed. Based on the buckling of the material during the test, a pass or fail grade was established for each curvature combination.

With this data of acceptable and unacceptable curvature pairs in hand, a function representing the cut-off between acceptable and failed curvatures was developed. Three categories of surface conditions were tested: a “dome” condition corresponding to convex positive curvature, a “bowl” condition representing concave positive curvature, and a “saddle” configuration representing negative curvature. The distinction between convex and concave positive curvatures was established due to AZCO’s perception that concave configurations would be more difficult to force the sheet material onto than convex forms. Figure VI-8 shows the results of these studies. Ultimately, the ease of using gaussian curvature analysis capabilities available in CATIA led the team to select a gaussian curvature metric slightly more conservative than the function established directly by AZCO’s studies.

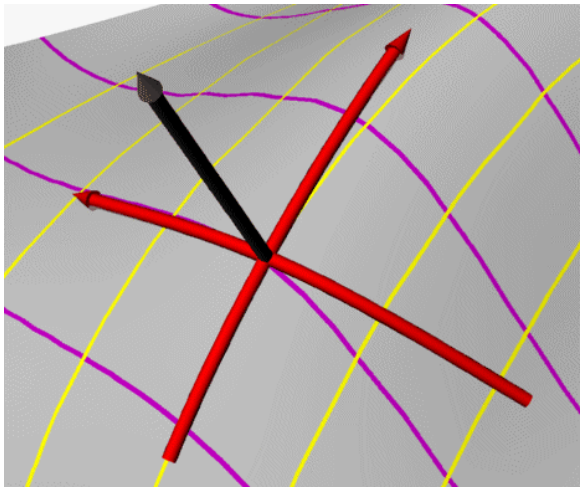

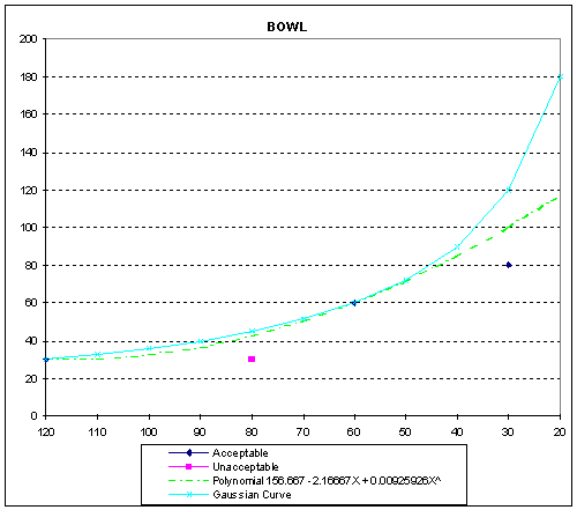

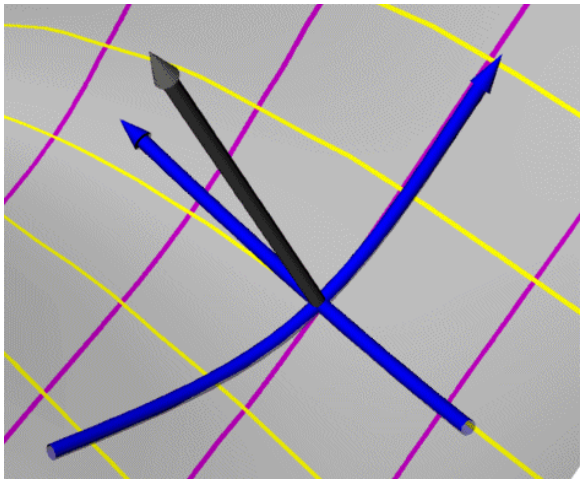

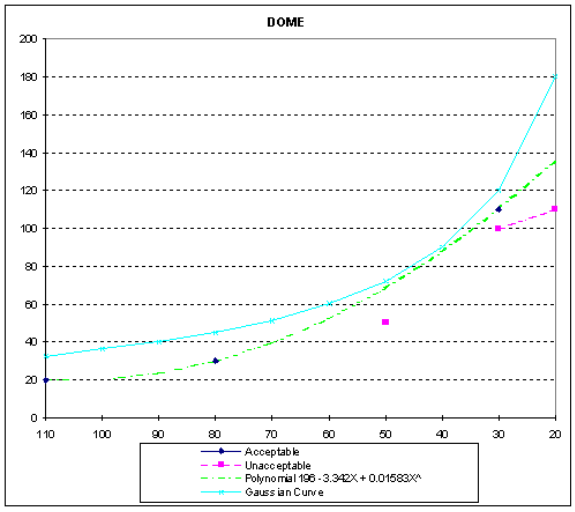

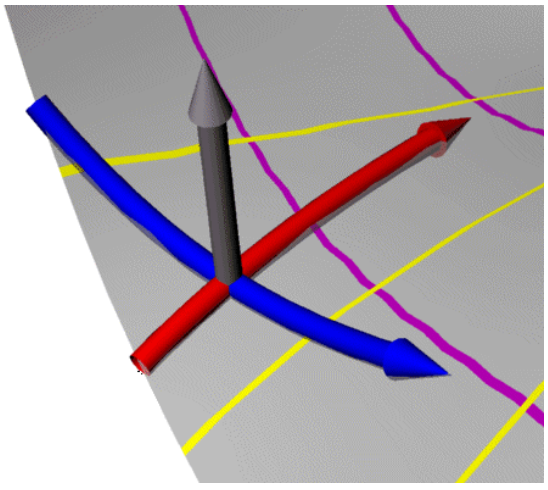

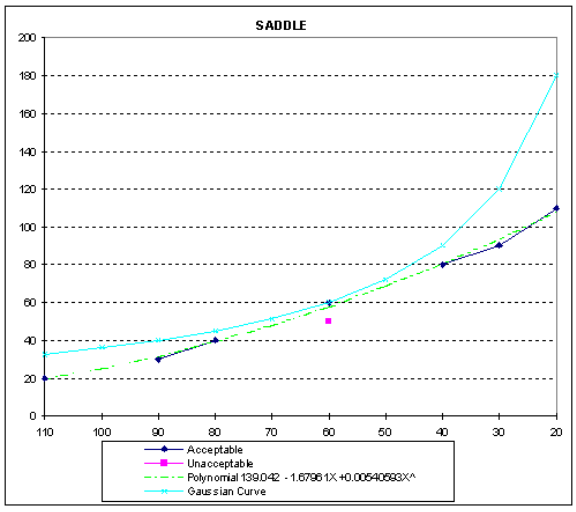

Figure VI-8: Surface geometry conditions and associated test results (EMP)

Gehry Partners' CATIA modelers were thus faced with the task of rationalizing the original, smooth surface model into conformance with the gaussian curvature test. The team went back to the physical model, digitized the edge curves of the actual paper panels on the physical model, and projected these curves onto the computer surface model. These curves served as guidelines for the locations of tangent discontinuities for breaking up the CAD model to reduce curvature where necessary. Figure VI-9 shows the results of this rationalization operation on the typical system areas for Element 7.

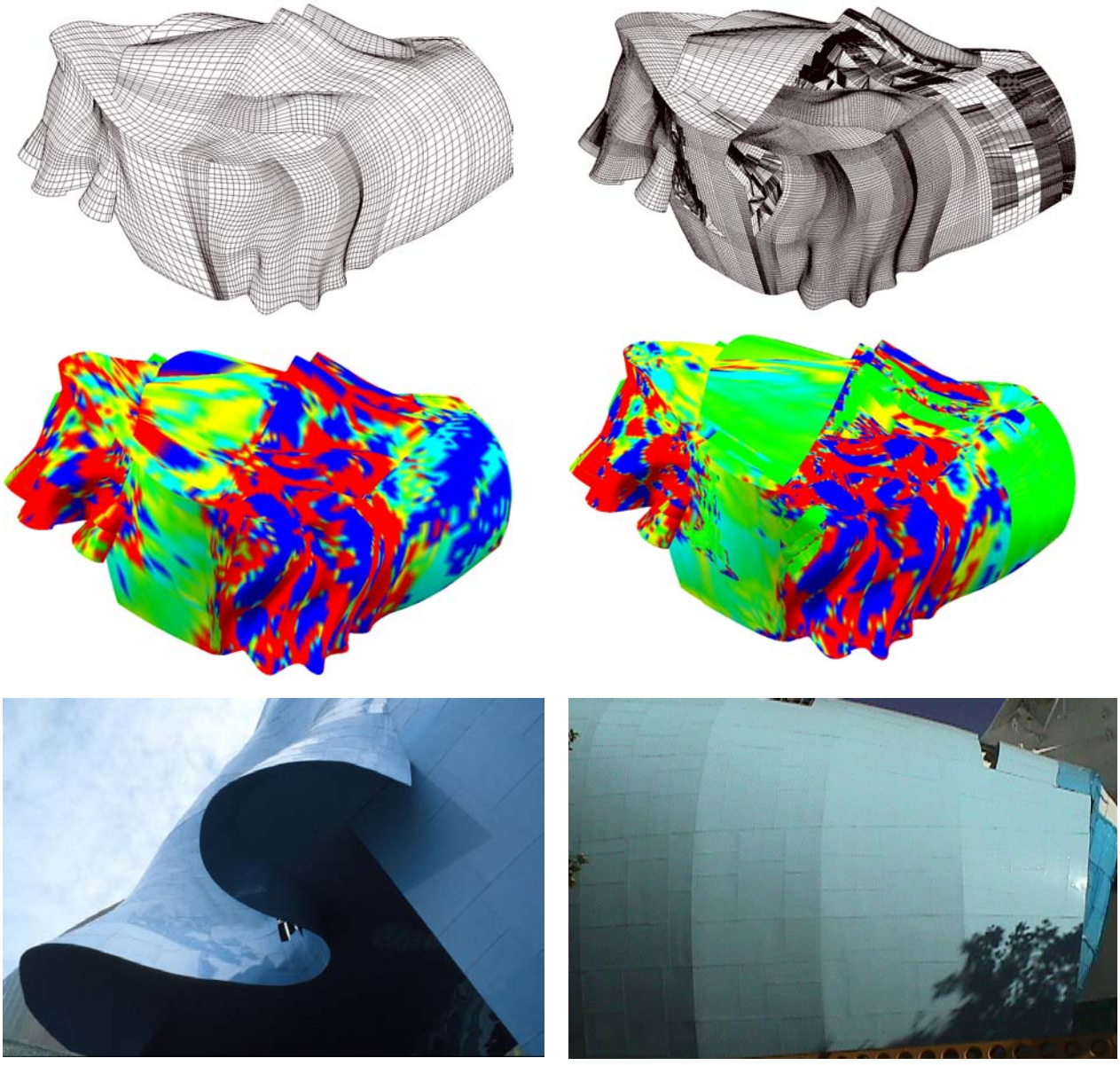

$|\kappa_{GAUSS}| > c$ $|\kappa_{GAUSS}| \leq c$

Highly curved areas *Rationalized regions*

Figure VI-9: Gaussian curvature rationalization (EMP)

3. Summary

By in large, the gaussian curvature metric established for the project has served its intended function. The typical system areas required no additional forming of the finish materials, and generally the fabrication assumptions in the design of the panel system posed few unanticipated complications. However, a few unanticipated problems were encountered on relatively high curvature areas when pre-punched holes did not line up correctly on neighboring face sheets. Fabrication strategies where sheet materials form the waterproofing membrane must obviously require a heightened level of attention to poor inter-sheet continuity.

There are some important characteristics inherent to any fabrication strategy adopted on constrained curvature forms. These surfaces are by nature bi-directionally curved, even if this curvature is limited. Thus, framing strategies for supporting the surfacing materials must be curved in at least one direction. On several projects including EMP, panel assemblies have provided the sub-framing technology (Figure VI-10). On EMP, these panels were developed from planar sheet materials. The top edge of each framing member or "fin" is CNC cut to reflect the curvature of the surface along its profile. Thus, the panel itself provides the dimensional control of the surface, on the basis of surface dimensional data provided by the digital master model. Additional discussion of the development of the panel system and layout are presented in Part 3, below.

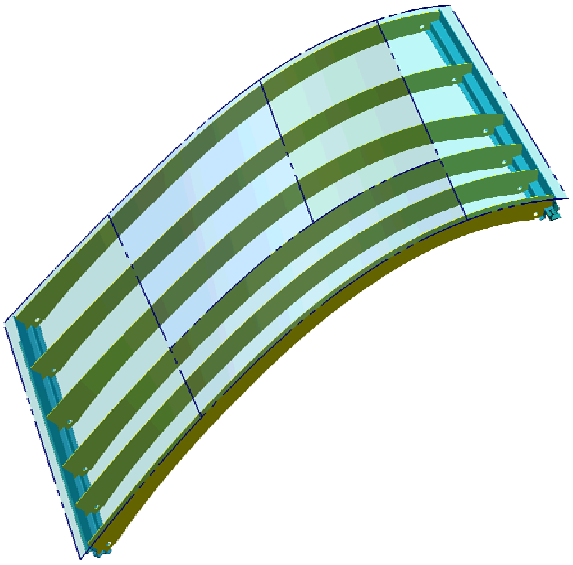

Figure VI-10: AZCO's panel system

The constrained gaussian curvature approach employs surface curvature metrics inherent to differential surface representations as a predictor of surface constructibility. The surface elements are represented by the software as Bézier and NURBS surfaces, discussed in Section V.D.3 above. Many available NURBS modeling packages provide utilities for visualizing and analyzing gaussian curvature on surfaces. During rationalizing activities, CAD

operators have simply to check the curvature readouts of the software against these established limits.

Unfortunately, the constraints and controls inherent to these surface representations do not map particularly well to those of paper surfaces. NURBS based formalisms have been developed to support a much larger class of continuously smooth surfaces. The available controls for positioning and shaping NURBS surfaces provide little guidance for efforts to develop constrained curvature configurations. The operator must address the gaussian curvature constraint “manually”, by manipulating the surface form until the desired surface curvature has been achieved. Ironically, the class of NURBS surfaces is built on a geometric representation that is less constrained than desirable, or not constrained appropriately for the task. In the next section, alternative surface representations will be described where these constraints are more directly imposed by the surface representation.

B. DEVELOPABLE SURFACES

1. Introduction

The previous discussion presented the concept of surface (gaussian) curvature as a useful metric for assessing the constructibility of surfaces. Its limitations as a true predictor of the behavior of sheet material and system behaviors were discussed. An essential limitation of the technique is that we can not truly expect sheet metal or other sheet material surfaces to adopt any measurable gaussian curvature in their configuration, without some substantial degree of in plane deformation of the surface occurring.

There exists a special class of d*evelopable* surfaces, which guarantee zero gaussian curvature, despite the existence of substantial and variable normal (out of plane) curvature. Consequently, developable surfaces can be unrolled into a flat plane configuration with no deformation “in the plane” of the surface. The potential applications of such surface constructs in fabrication are readily apparent, for this is the behavior that we expect of a sheet of fabricated surface material: the ability to fold and unfold into the shape of the surface without stretching. Developable surfaces are thus an important element of the arsenal of techniques used by the firm for constructibility modeling.

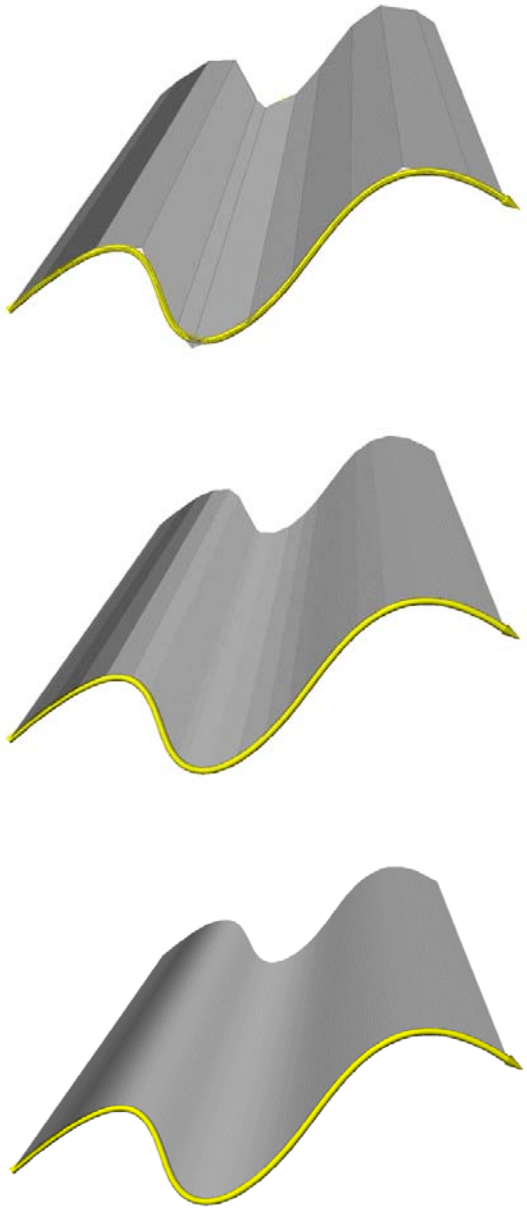

Figure VI-11: Developable surface as the limit of a family of planes

Developable surfaces map *isometrically* and *conformally*[22] to a planar surface, in that arc lengths of curves and angles between curves on the developable surface and its unfolded configuration are equal. The notion of a plane, continually folded in space up to the configuration of a developable surface should be kept firmly in mind, for the definition of developable surfaces will indeed result in configuration of planes "rolled" into space.

One important consequence of this rolled plane configuration is the existence of straight lines of ruling on the surface, where the surface normals at any two points on a given line of ruling are parallel. Spatially, we can envision these lines of ruling as infinitesimally spaced hinges along which the surface can unfold without otherwise changing in shape (Figure VI-11). This existence of a straight line of ruling with invariant surface normal is the basis for a differential definition of developable surfaces, below. The following represent equivalent definitions of conditions on developable surfaces:

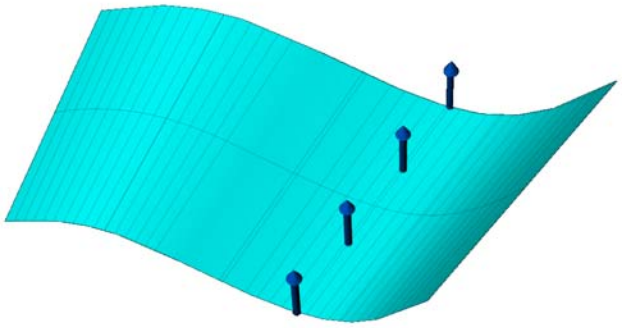

Figure VI-12: Parallel normal vectors on a developable surface

- The mapping of a developable surface onto a plane is isometric and conformal
- A surface whose gaussian curvature is zero
- A straight line of ruling exists on each point of the surface; a principal direction with 0 curvature is aligned with this line of ruling.
- The surface normals along a line of ruling are parallel.

In previous sections, the focus of discussion was the establishment of localized differential properties of surfaces as a specific point of consideration. In moving forward with a presentation of the definition of developable surfaces, we will again begin by considering the localized conditions of developable surfaces at a point. However, in addition, this localized consideration will be extended to the properties of surfaces "in large", and the means by which developable properties of surfaces can be guaranteed over the extent of the surface.

The definition of gaussian curvature, established in (V.53), was:

$$\kappa_{GAUSS} = \kappa_{N_{max}} \kappa_{N_{min}}$$

In order for κ_{GAUSS} to be equal to zero, necessarily at least one of the principal curvatures must be of 0 magnitude. The geometric interpretation of a curve with 0 curvature is of course a straight line. However, the existence of a localized straight line condition at points on the surface will not be a sufficient condition to guarantee developability. The previous discussion of surface curvature disclosed that a local straight line on the surface existed at every point of negative curvature. We consider initially the class of surface forms generated as a family of straight line isoparametric curves in one of their directions, and then subsequently consider the conditions required to guarantee that a principal direction "lines up" with this isoparametric curve on the surface at large. Elements of this general formulation are drawn from Kreysig[47] and Chalfant[19].

2. Ruled Surfaces

We begin by defining the class of surfaces generated by a straight line in one of its parametric directions. The class of *ruled surfaces* is defined as a surface with at least a one parameter family of straight lines as the isoparametric curves that generate the surface. We might initially revisit our discussion of parametric surfaces to consider where this requirement will be defined. The Euclidean nature of the $\mathbf{R}^2$ parametric (u,v) space is unaltered by this requirement. The impact of this condition is felt in the qualities of the resulting, embedded surface in $\mathbf{R}^3$. However, the locus of this constraint is in the embedding $\mathbf{R}^2 \rightarrow \mathbf{R}^3$ function itself. Our definition of ruled surface must thus define constraints on the mapping function that results in this straight line condition observable on the embedded surface in $\mathbf{R}^3$.

By convention, for the purposes of consistency in this discussion, we will consider the parameter v to be the parameter that traces a line in $\mathbf{R}^3$ as its value is traversed. Geometrically, we may envision a ruled surface as the surface described by the path of a straight line as it is travels through space. The resulting straight lines embedded in space are termed the *generatrices* of the ruled surface. In turn, the path taken by the line as it travels through space may be envisioned as a curve in space, termed the *directrix* of the surface[48].

We may thus reformulate the parametric surface mapping function solely in terms of the directrix curve $\alpha(u)$ and the distance along unit vector $\beta(u)$, whose direction in space is a function of the distance along the directrix curve (Figure VI-13):

$$\sigma(u,v) = \alpha(u) + v\beta(u) \qquad \text{(VI.1)}$$

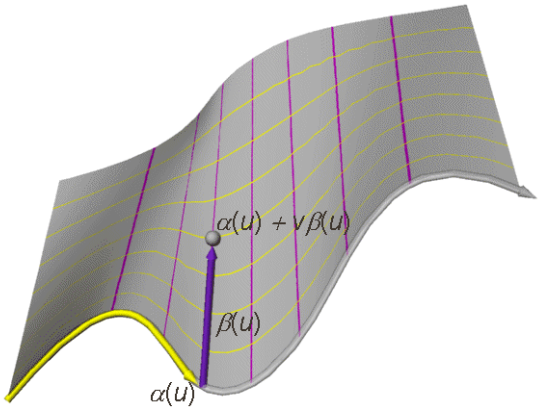

Figure VI-13: Basic ruled surface definition

The vector β may be pictured as a vector field whose direction in space is a function of *u*, while $\alpha(u)$ may be viewed as a curve in space to which this vector space is applied (Figure VI-14). Given this parameterization, we may consider the shape of the surface by considering the variation of the vectors $\alpha(u)$ – the directrix curve and its derivatives the tangent and normal vectors, and the variations of the generator vector $\beta(u)$. We consider these vectors in a coordinate system whose origin is at a point on the surface, $\sigma(u,v)$. Differentiating σ in (VI.1) with respect to *u* and *v* yields:

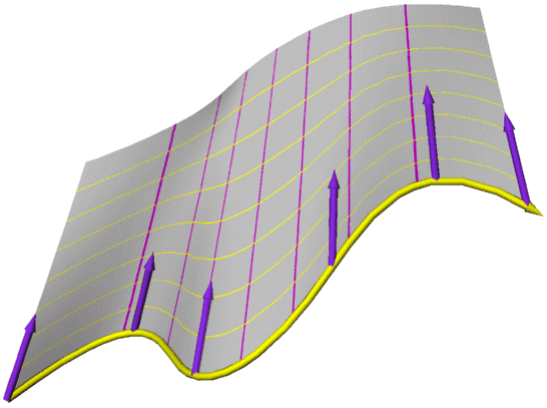

Figure VI-14: Ruled surface as a vector field

$$\begin{aligned}
&\sigma_u(u,v) = \dot{\alpha}(u) + v\dot{\beta}(u)\\
&\sigma_v(u,v) = \beta(u)\\
&\sigma_{uu}(u,v) = \ddot{\alpha}(u) + v\ddot{\beta}(u)\\
&\sigma_{uv}(u,v) = \dot{\beta}(u)\\
&\sigma_{vv}(u,v) = 0
\end{aligned} \qquad \text{(VI.2)}$$

From the first fundamental form (V.39) $eg - f^2 = \left|(\sigma_u \times \sigma_v)\right|^2$ the surface normal is:

$$\begin{aligned}\mathbf{N} &= \frac{R_u \times R_v}{|R_u \times R_v|} \\ &= \frac{\left(\dot{\alpha}(u) + v\dot{\beta}(u)\right) \times \beta(u)}{\sqrt{eg - f^2}} \\ &= \frac{\dot{\alpha}(u) \times \beta(u) + v\left(\dot{\beta}(u) \times \beta(u)\right)}{\sqrt{eg - f^2}} \\ &= \frac{\dot{\alpha}(u) \times \beta(u)}{\sqrt{eg - f^2}}\end{aligned} \tag{VI.3}$$

for all ruled surfaces. Gaussian curvature was defined as (V.52)

$$\kappa_{GAUSS} = \frac{ln - m^2}{eg - f^2}$$

where (V.44):

$$l = \sigma_{uu} \cdot \mathbf{N}$$
$$m = \sigma_{uv} \cdot \mathbf{N}$$
$$n = \sigma_{vv} \cdot \mathbf{N}$$

For ruled surfaces of the form (VI.1) $n = \sigma_{vv} \cdot \mathbf{N} = 0$, since by definition the generators do not change direction along *v*. Curvature is thus reduced to the form

$$\begin{aligned}\kappa_{GAUSS} &= \frac{-m^2}{eg - f^2} \\ &= \frac{\left(\sigma_{uv} \cdot \mathbf{N}\right)^2}{eg - f^2} \\ &= \frac{\left(\dot{\beta}(u) \cdot \dot{\alpha}(u) \times \beta(u)\right)^2}{\left(eg - f^2\right)^2}\end{aligned} \tag{VI.4}$$

In this equation, the vector $\dot{\alpha}$ is the tangent vector to the directrix curve, $\beta(u)$ the vector along the ruling line or generatrix, $\dot{\beta}(u)$ the vector representing the change in the generatrix vector as traversal of the parametric variable *u* is undertaken.

Our previous discussion of surface curvature established gaussian curvature as an important metric of the “paperness” of surface forms. The existence of substantial gaussian curvature is the feature of surface forms that prohibits their assuming flattened shapes without in plane deformation. We now establish the conditions under which ruled surfaces guarantee the

absence of such bi-directional surface curvature. Equation (VI.4) provides the necessary conditions for zero gaussian curvature of ruled surfaces:

$$\sigma_{uv} \cdot \mathbf{N} = \dot{\beta}(u) \cdot \dot{\alpha}(u) \times \beta(u) = \left| \dot{\alpha} \ \beta \ \dot{\beta} \right| = 0 \qquad \text{(VI.5)}$$

Geometrically, we may state that if the mixed partial derivative σ_{uv} varies only in the plane of the surface (perpendicular to the surface normal), zero gaussian curvature and hence developability conditions are guaranteed. In turn, this condition is guaranteed if the three vectors $\dot{\alpha}, \beta,$ and $\dot{\beta}$ are co-planar.

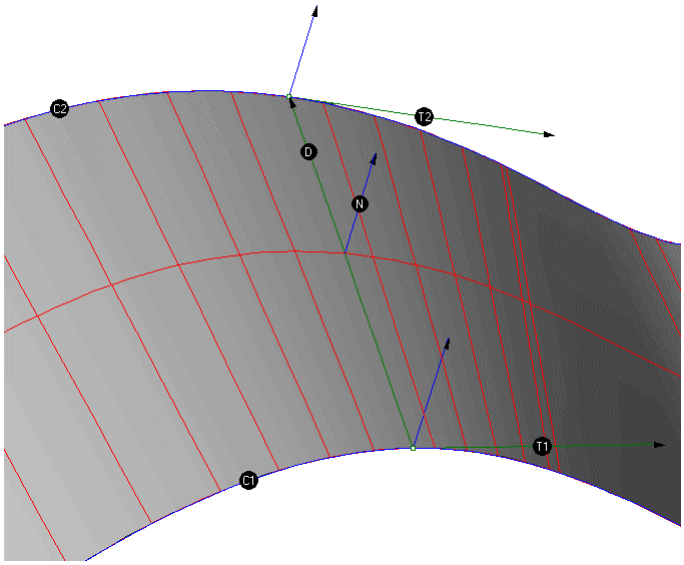

Figure VI-15: General developable surface condition on parametric surfaces

3. Canonic Forms

The conditions expressed in (VI.5) specify a constraint on the relative variations of the directrix curve and the generatrix vector necessary for developability. As such, this condition provides a "test" for parametric surfaces of ruled form. If the above stated condition follows from the specific parametric form of the ruled surface, then developability is assured. We now present the possible constraints on ruled surfaces that guarantee global conformance of the surface with the condition (VI.5).

We begin by reviewing the "normalized" arc-length curve form of the directrix curve α and the Frenet vector field coordinate field that this parameterization disclosed (Section V.D.1). We may take each of the frame vectors of the curve $\alpha(u)$ and reapply it as the vector $\beta(u)$ to describe a ruled surface uniquely determined by the shape of the curve and its variations in space. These canonical (tangent, normal and binormal) surfaces of α allow relations between the vector fields α and β to be globally defined for the ruled surface. We consider each of these surfaces to identify characteristics of the ruled surface guaranteeing developability conditions.

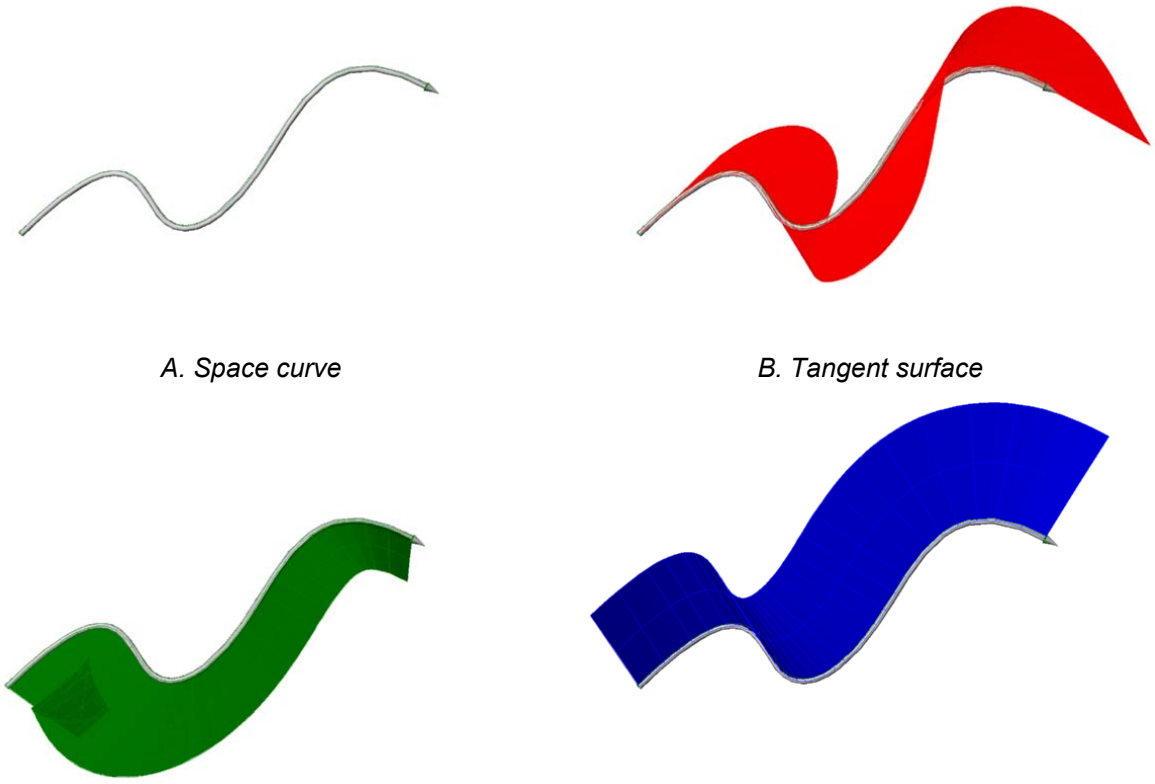

A. Space curve *B. Tangent surface*

C. Normal surface *D. Binormal surface*

Figure VI-16: Space curve and Frenet field surfaces

In the case of the tangent surface (Figure VI-16B), the generatrix vector β is the tangent **t** of the curve α, hence $\beta = \dot{\alpha}$. The determinant of the matrix $\left|\dot{\alpha}\ \beta\ \dot{\beta}\right| = \left|\dot{\alpha}\ \dot{\alpha}\ \dot{\beta}\right|$ is necessarily 0, since two of the columns are equal. Thus the tangent surface of any space curve is a developable surface. Tangent developable surfaces are an important class of developable surfaces for potential consideration in developable surface applications. These surfaces will be considered further below.

Next we apply the principal normal vector, and consider the conditions on the space curve required to guarantee developability of the resulting ruled surface (Figure VI-16C). From (VI.5) and (V.26):

$$\left|\dot{\alpha}\ \beta\ \dot{\beta}\right| = \left|\dot{\alpha}\ \mathbf{n}\ \dot{\mathbf{n}}\right| = \left|\dot{\alpha}\ \mathbf{n}\ \left(-\kappa\mathbf{t} + \tau\mathbf{b}\right)\right| = \left|\dot{\alpha}\ \mathbf{n}\ \tau\mathbf{b}\right| \qquad \text{(VI.6)}$$

The three vectors $\dot{\alpha}, \mathbf{n}, \textit{and } \tau\mathbf{b}$ are linearly independent, but the determinant of the matrix will equal 0 if the torsion τ of the space curve is everywhere zero, since the final column of the matrix will be 0 in this case. A space curve with torsion equal to zero everywhere lies in a plane; the normal vector **n** will universally lie in the plane as well, and the resulting surface is, trivially, a region of the plane inhabited by the curve $\alpha(u)$.

Finally, we consider the binormal vector of the curve, and note that in this case:

$$\left|\dot{\alpha}\ \beta\ \dot{\beta}\right| = \left|\dot{\alpha}\ \mathbf{b}\ \dot{\mathbf{b}}\right| = \left|\dot{\alpha}\ \mathbf{b} - \tau\mathbf{n}\right| \tag{VI.7}$$

Again, the determinant vanishes again in the case that the torsion of the space curve is 0 and the curve lies in a plane. Geometrically, the binormal vector is orthogonal to the plane of the curve, and we have the case of a generalized cylinder, extruded in the direction normal to the plane of the curve.

We note a final, canonical ruled surface whose developability is assured: a cone where all generatrix vectors pass through a common point in space. In this case, the generatrix is the vector from points on the space curve $\alpha(u)$ to a fixed point **c**. The normalized vector $\beta(u)$ is:

$$\begin{aligned} \beta &= \frac{\alpha - \mathbf{c}}{\left|\alpha - \mathbf{c}\right|} \\ \dot{\beta} &= \frac{\dot{\alpha}}{\left|\alpha - \mathbf{c}\right|} \end{aligned} \tag{VI.8}$$

and the matrix determinant is:

$$\left|\dot{\alpha}\ \beta\ \dot{\beta}\right| = \left|\dot{\alpha}\ \beta\ \frac{\dot{\alpha}}{\left|\alpha - \mathbf{c}\right|}\right| = 0 \tag{VI.9}$$

since $\dot{\alpha}$ and $\dot{\beta}$ are linearly dependent.

The previous discussion has identified four canonical developable surfaces forms, derived from ruled surfaces, upon which developability can be guaranteed:

1. Planar surfaces,
2. Cylindrical surfaces, where the generatrix is always parallel over the surface,
3. Conic surfaces, where the generatrix passes through a common point,
4. Tangent developable surfaces, described by the tangent vector of the space curve at each point.

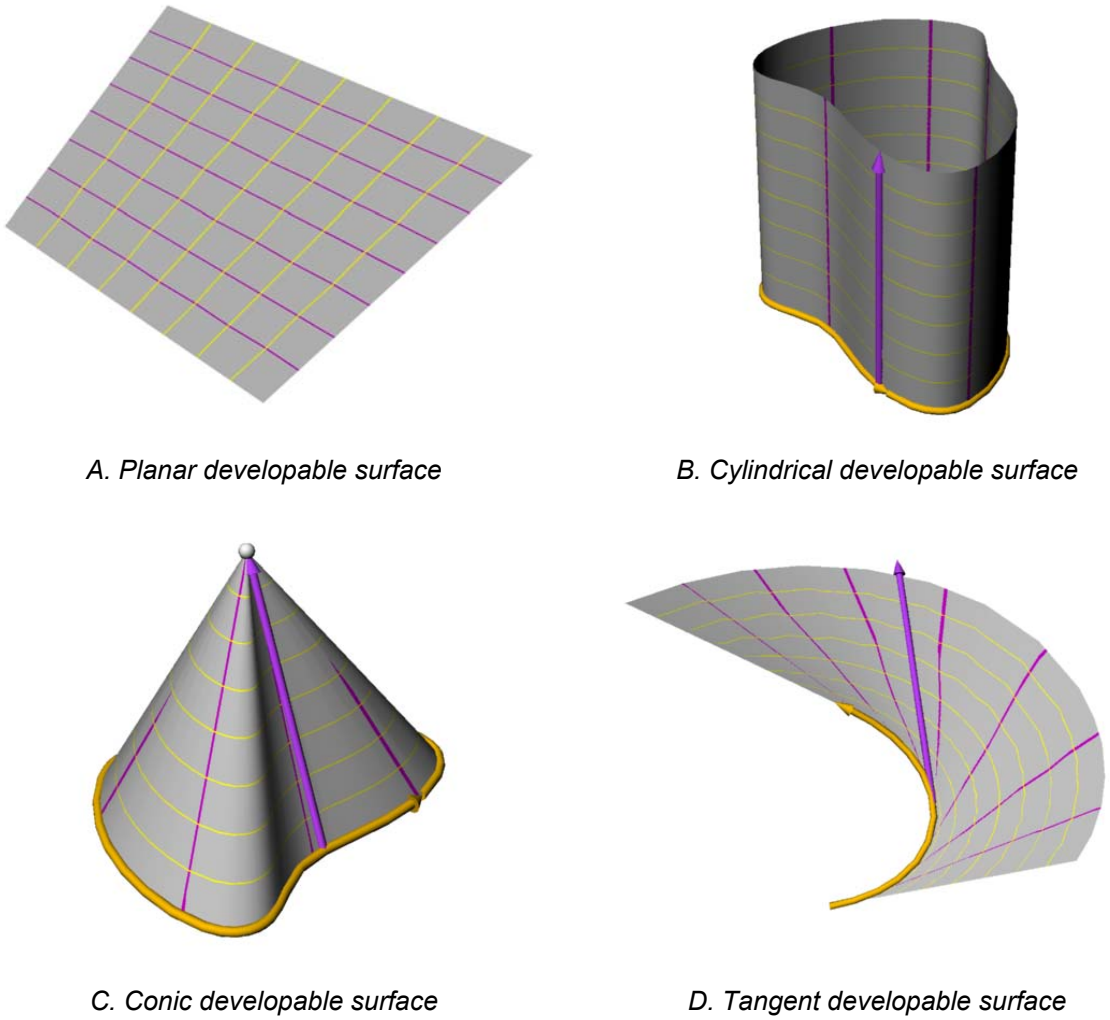

A. Planar developable surface *B. Cylindrical developable surface*

C. Conic developable surface *D. Tangent developable surface*

Figure VI-17: Canonical developable surface forms

Theoretically[49], any developable surface may be decomposed into surface sections from one of these four classes. Figure VI-18A presents such a composition, while Figure VI-18F shows the underlying cylinder, cones, plane and tangent developable patches generating the developable surface.

There are, however, some fairly stringent restrictions on the surfaces that can be constructed as compositions of these basic developable surface types, which make developable surfaces a difficult class of surfaces to model with. These restrictions are manifested as infeasible or degenerate conditions on the surfaces that are generated through one of the above canonical classes of developable surfaces.

As an example, consider what happens if we attempt to extend the tangent developable surface shown in Figure VI-18D to the left, beyond the directrix curve $\alpha(u)$. This will turn out to be impossible. Extending the generatix vector in the opposite direction (Figure VI-19) produces a second developable surface, not an extension of the first one. The directrix curve represents a location of degeneracy of the developable surface, and is termed the *edge of regression*. There is no other possible developable surface that can join our original surface in tangency at this edge. A similar such degenerate feature is found at the vertex of the conic developable surface (Figure VI-18B).

The edges of regression and similar infeasible conditions on developable surfaces frequently crop up, both in modeling activities and numerical solutions to the generation of these surfaces. The

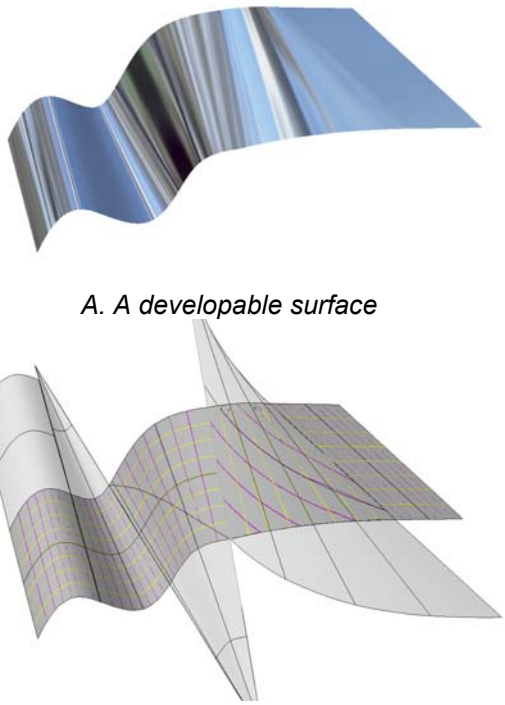

A. A developable surface

B. Its decomposition

Figure VI-18:developable surface and its decomposition into developable regions

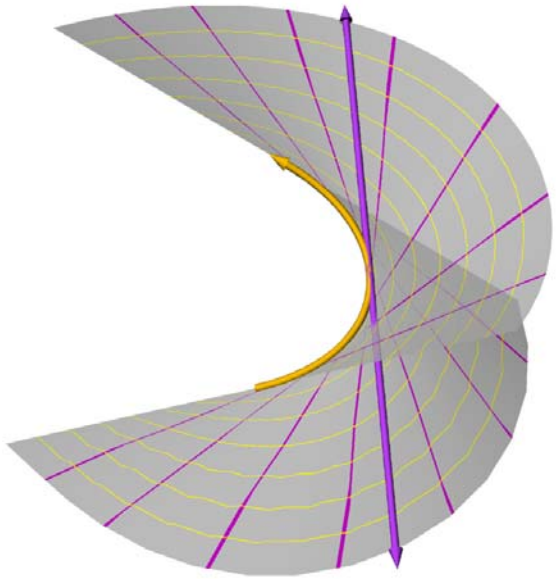

Figure VI-19: A tangent developable surface of two sheets.

locations of inflection points found in the composition shown in Figure VI-18F, between adjoining patches, are similar sources of discontinuities. These features are not found directly in other approaches to the modeling of paper surfaces such the constrained gaussian curvature approach, or modeling through physical means. However, other analogous constraints exist. In physical modeling, attempts to force a sheet of paper into an infeasible configuration will result in crinkling, buckling or tearing of the paper. In the developable surface approach, these "catastrophic" actions are manifested in infeasible conditions of the numerical approach, due to the stringent requirement of 0 gaussian curvature on the differential forms developed in (VI.1) and (VI.5).

4. Numerical Approaches

The question of providing useful CAD applications to produce developable surfaces has received substantial study 9,11,19,30,67,68. The general approach of approximating developable surfaces as sequences of constrained canonic forms has been described above. Other numerical solutions take a related approach, in generating developable surfaces as the limit case of these individual classes of developable patches.

We may describe a ruled surface as the family of lines that join two space curves. From Section V.D.1, we may reparameterize these two curves to be generated from a common parameter that varies along the lengths of the curves. If we define the two curves as $\alpha_1(u)$ and $\alpha_2(u)$, we may define a line that joins the two points on these curves at a given value of u. The distance along this straight line is simply a weighted "blending" of the points $\alpha_1(u)$ and $\alpha_2(u)$:

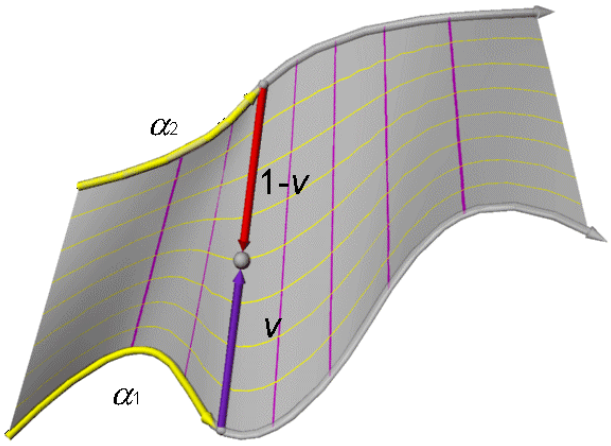

Figure VI-20: Ruled surface defined by edge curves

$$\sigma(u,v) = (1 - v)\ \alpha_1(u) + v\ \alpha_2(u) \qquad \text{(VI.10)}$$

This parameterization is equivalent to (VI.1) if we define:

$$\alpha(u) = \alpha_1(u)$$
$$\beta(u) = \frac{\alpha_2(u) - \alpha_1(u)}{\left|\alpha_2(u) - \alpha_1(u)\right|} \qquad \text{(VI.11)}$$

Several CAD applications support the generation of developable surfaces between input edge curves. Rather than develop the surface into explicitly defined conic, cylindrical and planar elements, this algorithm approximates a developable surface joining the edge curves as a ruled surface, and finds ruling directions on the edge curves such that (VI.5) is satisfied. The algorithm begins on one edge curve $\alpha_1(u_0)$, and "searches" for points on the opposing curve $\alpha_2(u_0')$ such that the tangent vectors $\dot{\alpha}_1(u_0)$ and $\dot{\alpha}_2(u_0')$, and the vector $\alpha_2(u_0')$ - $\alpha_1(u_0)$ all lie in a plane, and are thus linearly dependent. The algorithm repeats this search for all points on the two directrix curves, proceeding in a directed fashion along the two curves. The algorithm steps along the curves at sufficiently short intervals such that a ruled surface generated between successive ruling lines in the software's native (Bézier, NURB) surface formulation lies within some small tolerance of the input curves.

The edge curves of the physically modeled paper sheet are the most prominent features digitized as part of the digital reconstruction of paper surfaces. Many techniques for the creation of developable surfaces, including that utilized in the CATIA DEVELOP module, provide control of the developable surface by these edge curves. However, in the general case, it is impossible to construct a developable surface from two arbitrary curves in space. A simple example is presented in (Figure VI-21). There is no singe developable patch which can match these curves, nor are there a set of patches with tangency continuity which can. The curves may be joined by a series of tangent developable surfaces and cones, with a common line of ruling at their joint. However, these patches will in general have a discontinuity in surface tangency at their joint. Again, this problem has an analogue in the physical modeling realm. If we attempt to force a

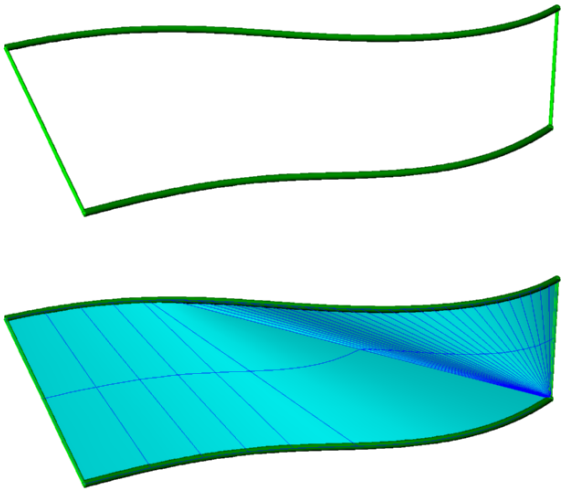

Figure VI-21: Input edge curves resulting in an infeasible developable surface condition

sheet of material over two curves in space, in general the material will not be able to comply without some wrinkling or buckling, or deviation from the desired input.

The use of guide curves derived from digitized physical paper surfaces provides a good point of departure for this approach, since these curves are often closely approximate developable surface directrix curves as a consequence of their materially guided behavior. However, even limited distortion of these guide curves – including that generated by digitizing tolerances or crinkling of the material paper – will produce infeasible conditions. The process of rationalizing digitized edge features into acceptably continuous developable surfaces is a time consuming process requiring skilled CAD operators. The CAD operators must "straighten out" one or both of the edge curves, to generate the planarity condition required by (VI.5) .

Additionally, the edge curve generation approach presumes a straight line along two of the surfaces' edges. In practice, this is almost never the case on physical material sheets, where all edges typically are curved. On inspection, it is evident that a single material sheet theoretically assumes a complex configuration of multiple developable patches, joined in tangency along their ruling lines (Figure VI-22). The reconstruction of this composition of patches for each sheet of physically modeled material places an additional burden on the CAD modeling effort.

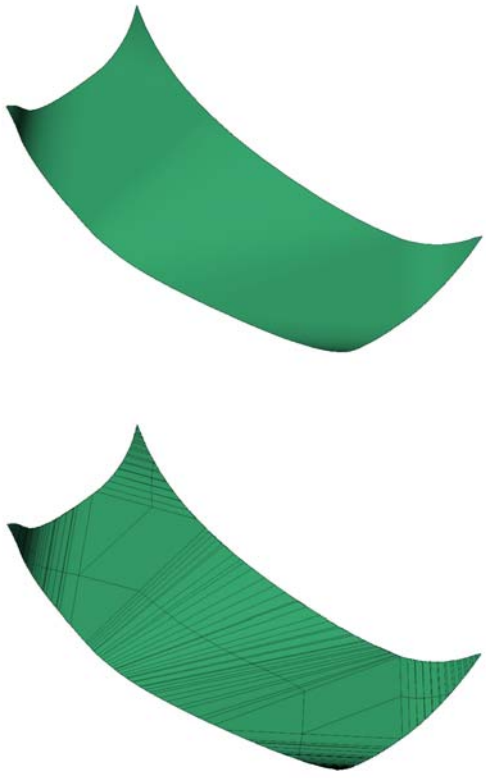

Figure VI-22: Paper sheet and developable regions

The pursuit of improved methods for modeling developable surfaces has been a focus of research efforts by the firm. The assessment of edge curve developable surface generation provided above discloses a key limitation of this approach: the input controls (the edge curves) are

ill suited to the solution, since these controls essentially guarantee infeasible conditions. Furthermore, when infeasible conditions are encountered, there is poor feedback to guide the operator toward improved conditions.

Often, the ruling lines on the physical surfaces are digitized in addition to the edge curves (Figure III-11A). These ruling lines provide a good indication of the "flow" of the developable surface, not apparent simply in the edge features. We can turn the problem around, and consider these ruling lines to be the primary input controls to developable surface algorithms.

The formulation of developable surfaces as constraints on ($1 \times n$) Bézier or NURBS surfaces has been pursued by several researchers[3,19,9,11,68,67]. Note that an order 1 curve in the u direction guarantees a ruled surface. The two sets of control vertices (0,0…n-1) and (1,0…n-1) describe the edge curves to the surface as in (VI.10) above. The problem now becomes one of identifying the relative positions of control points in space that guarantee invariance of surface normal along lines of ruling, and providing these constraints to the user in an intuitive and interactive way. Lang and Röschel[50] provide the key constraints on Bézier surfaces guaranteeing developable conditions:

$$\det\left(x(0,v), x(1,v), x_u(0,v), x_u(1,v)\right) = 0 \quad \forall v \in [0,1] \tag{VI.12}$$

and derive a set of five equations satisfying this condition for weighted Bézier surfaces of order (1,2):

$$\begin{aligned}
&\delta_{0101} = 0 \\
&\delta_{0102} + \delta_{0201} = 0 \\
&\delta_{0202} + \delta_{0112} + \delta_{01201} = 0 \\
&\delta_{0212} + \delta_{1202} = 0 \\
&\delta_{1212} = 0
\end{aligned} \tag{VI.13}$$

where δ_{ijkl} is the determinate of four control vertices' locations and weights:

$$\begin{aligned}
\delta_{ijkl} &= \mathbf{p}^w_{0i}\mathbf{p}^w_{0j}\mathbf{p}^w_{1k}\mathbf{p}^w_{1l}B_{ijkl} \\
B_{ijkl} &= \det\begin{bmatrix} 1 & 1 & 1 & 1 \\ \mathbf{p}^x_{0i} & \mathbf{p}^x_{0i} & \mathbf{p}^x_{1k} & \mathbf{p}^x_{1l} \\ \mathbf{p}^y_{0i} & \mathbf{p}^y_{0j} & \mathbf{p}^y_{1k} & \mathbf{p}^y_{1l} \\ \mathbf{p}^z_{0i} & \mathbf{p}^z_{0j} & \mathbf{p}^z_{1k} & \mathbf{p}^z_{1l} \end{bmatrix}
\end{aligned} \tag{VI.14}$$

This equation can be distilled down to two basic conditions on the weighted control points of quadratic Bézier.

1. Successive pairs of (4) control points form a “ladder” configuration, where the four control points describe a plane.
2. The weights of the six control points result in a proportional triple, $(\mathbf{p}_{00}^{w} : \mathbf{p}_{01}^{w} : \mathbf{p}_{02}^{w}) = (\mathbf{p}_{10}^{w} : \mathbf{p}_{11}^{w} : \mathbf{p}_{12}^{w})$. Given values for the weights $\mathbf{p}_{00}^{w}, \mathbf{p}_{02}^{w}, \text{and } \mathbf{p}_{10}^{w}$, and predefined *x,y,z* locations for all vertices, we can solve for the remaining weights to ensure developability of the surface. A quadratic equation determines the necessary weight on the intermediate vertex $\mathbf{p}_{01}^{w}$:

$$\left(\mathbf{p}_{01}^{w}\right)^{2} = \mathbf{p}_{00}^{w}\mathbf{p}_{01}^{w} \frac{B_{0201}B_{0202}B_{0212}}{B_{0201}B_{0112}B_{1202} + B_{1201}B_{0212}B_{0102}} \qquad \text{(VI.15)}$$

   The remaining weights $\mathbf{p}_{11}^{w}, \text{and } \mathbf{p}_{12}^{w}$ can now be determined from the proportional triple, above.

This formulation furthermore provides a test for the feasibility of constructing a developable surface based on the input vertices’ locations. If the quantity $\left(\mathbf{p}_{01}^{w}\right)^{2}$ defined in (VI.15) is less than zero, then the square root will not be a real number, and the vertex locations can not produce a developable surface.

On the basis of this approach, an approach to the interactive construction of developable surfaces has been created (Figure VI-23). In Figure VI-23A, the basic (1,2) developable surface patch is shown. We distinguish between the two pairs of edge vertices, shown in green, and the pair of intermediate vertices, shown in blue. Any of these vertices can be manipulated interactively. The solver dynamically adjusts the locations of the other five vertices to ensure a ladder configuration, and solves the quadratic equation (VI.15) to determine the required vertex weights. More elaborate developable surface configurations are supported as sequences of these basic developable patches. The patches are constructed by associating the end vertex pair of an original patch with the beginning pair of a subsequent patch (Figure VI-23B). A planarity condition is imposed on last four vertices of the previous patch and the first four vertices of the subsequent patch, to ensure tangency at the seam.

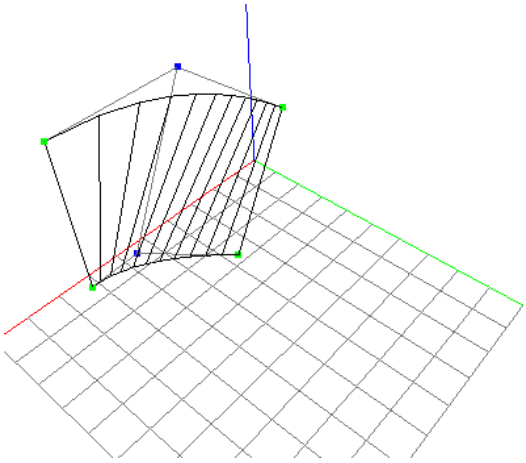

A. A single patch

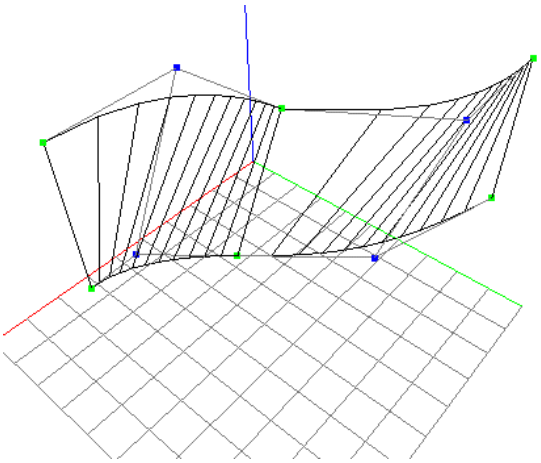

B. Two patches joined in tangency

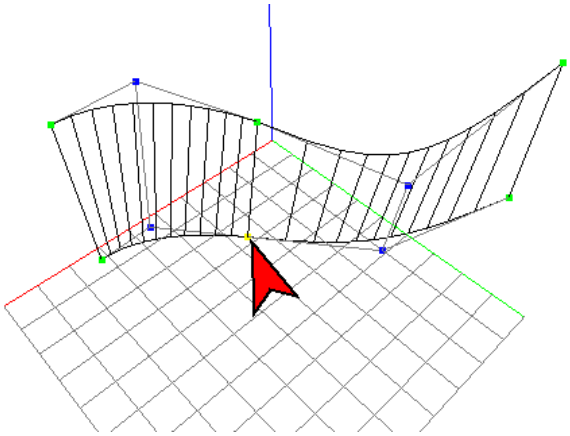

C. Modification by moving ruling line point

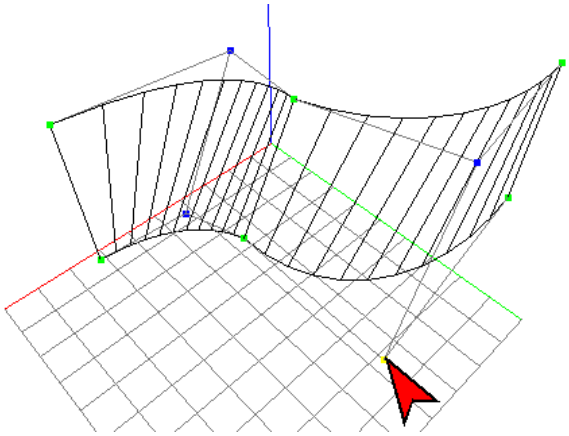

D. Modification by adjusting tangent plane

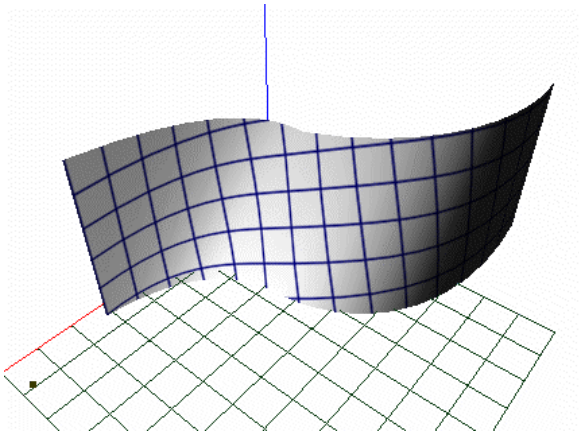

E. Mapping of 2D developed space

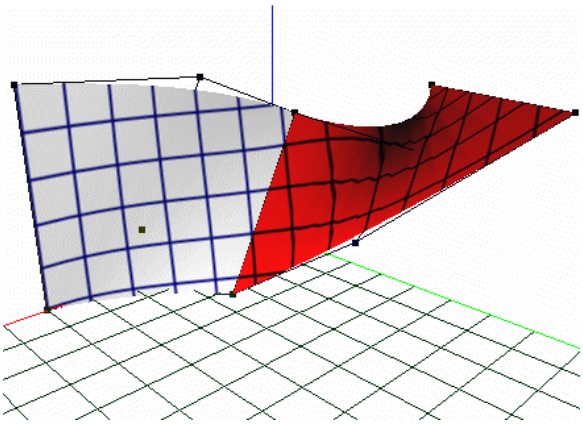

F. User generation of infeasible condition

Figure VI-23: Developable surface approach based on (1,2) weighted Bézier patches

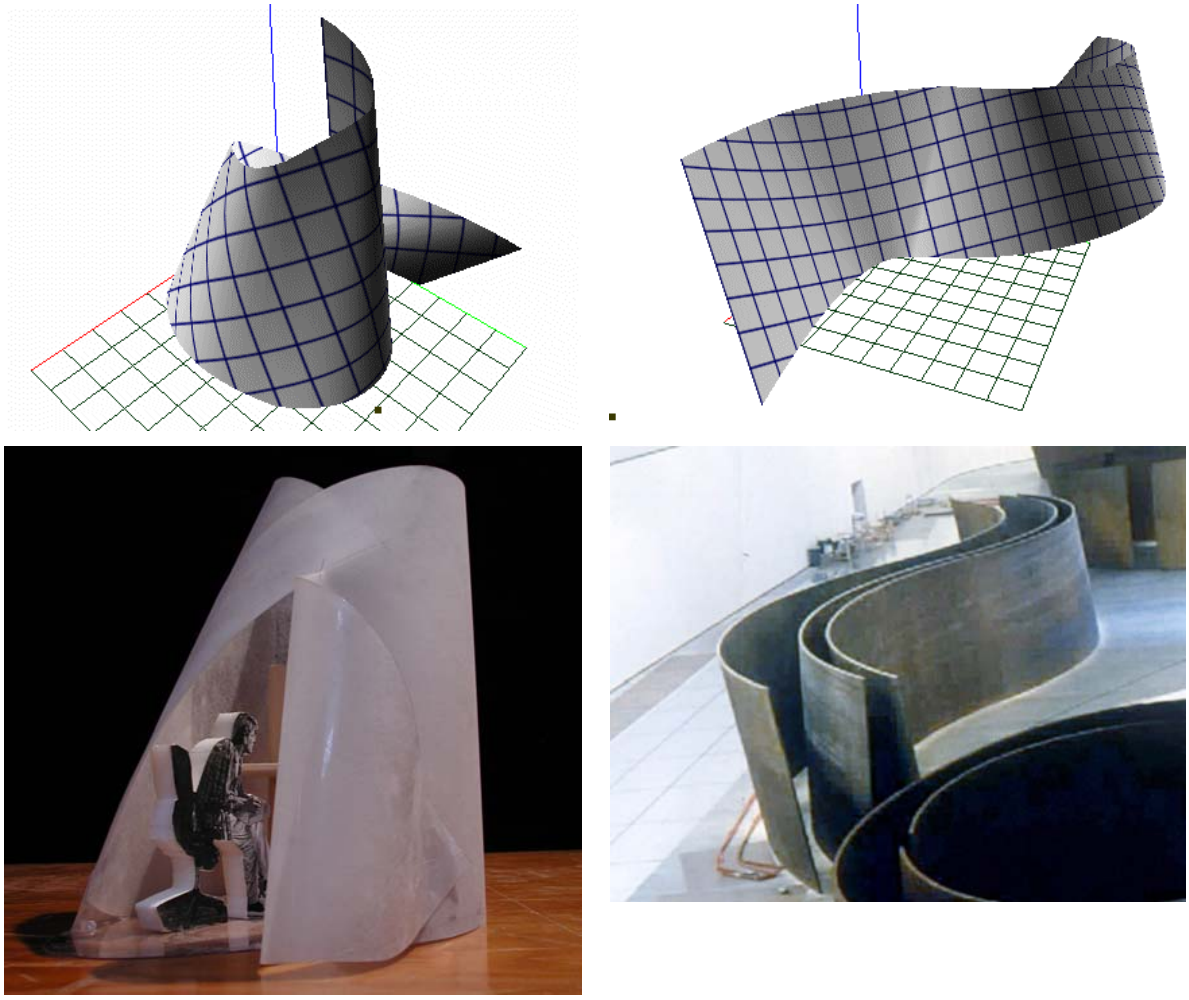

Figure VI-24: Results of the developable surface application

Modifying one of the edge vertices of this assembly results in a variation in the shape of the edge curve (Figure VI-23C) while moving an intermediate vertex adjusts the tangency of the surface at the neighboring edge vertices (Figure VI-23D).

The developed space of the configuration is also dynamically computed. Figure VI-23E shows a view of this unfolded space on the surface of the developable assembly.

Infeasible developable conditions can still be imposed in this interface. If the user moves a control point to a location resulting in an infeasible condition on one or more of the developable patches, the infeasible patches are highlighted to alert the user, and a simple ruled surface is constructed over the region (Figure VI-23F). The user receives dynamic feedback of this condition, and can reposition the vertex to remove the infeasible condition.

This application demonstrates the possibility of constructing developable surfaces by controlling the ruling lines, as opposed to the edge curves. These features have a more direct relationship to the developable surface conditions than edge curves. As a result, user interactions can usually produce quality developable surfaces. Figure VI-24 shows some developable surface constructions, and analogous designed surfaces.

5. Developable Surface Applications on the Construction of the Weatherhead Project

The Peter B. Lewis Building of the Weatherhead School of Management at Case Western Reserve University is perhaps the most ambitious example of developable surface based construction to date. Previous projects had employed developable surface as one means for generating constrained gaussian curvature forms during rationalization modeling. Weatherhead takes a radically different approach, using the straight lines of ruling found on developable surfaces as a principal element of system constructibility strategies.

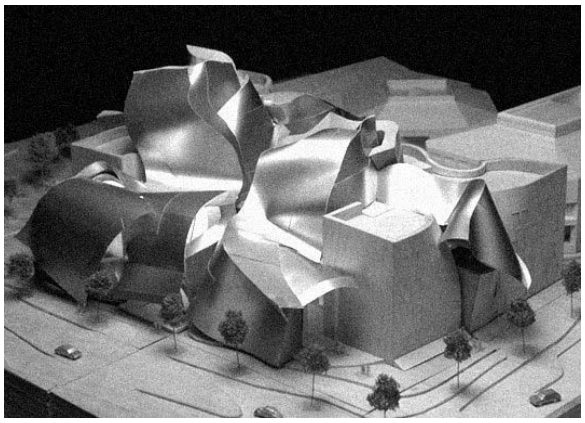

Figure VI-25: Weatherhead project design model

The project construction is comprised of three major systems[73]. A cast in place concrete slab and column system defines the primary structure of the project. The exterior walls of the project are similarly cast in place concrete, finished in brick, and define a fairly simple rectangular form with some areas of surface curvature at the top of the walls. The concrete structure forms a three sided enclosure around an atrium in the center of the project.

A structural steel system is supported on the concrete slab system, generating the external curved metal forms of the project. The steel enclosure system cascades over the concrete structure, and descends down to ground level on the open side of the atrium. Two towers of class rooms stand in the middle of the atrium. These “Buddha” towers, and other interior surfaces of the atrium, are finished with a lath and plaster system. All three of these systems

are generated from rationalized developable surface forms, and make some use of surface lines of ruling in different ways.

Efficiencies of construction had to be found to meet the academic institutional budget of the project. Two guiding intentions were employed in the development of project systems as a means for reducing the project cost while still achieving the ambitions for the project form.

One innovative cost saving measure was to remove a secondary system strategy that had been prevalently used on many prior projects. On projects including the Guggenheim Bilbao and the Experience Music Project, the primary steel system only approximated the design surface (Section III.F). The actual dimensional control system for these projects was achieved through an additional system between the primary structure and the finish surface enclosure. On the Guggenheim project, the dimensional control system is developed through a series of template curved tubes that are attached to the primary system. On the EMP project the finish form is achieved by a shaped panel system, attached to the primary structural steel rib system by adjustable connections.

The Weatherhead cladding system removes the need for a secondary steel system, drawing on the primary structural steel directly as both the support and dimensional control system for the surface cladding. This strategy reduced the material and labor costs associated with an additional system, but placed additional requirements on the tolerances and positioning of the primary structural system.

With this strategy for the structure and dimensional definition of the surface system, a second efficiency was enabled. The developable characteristics of the surface guaranteed that straight geometry occurred in at least one direction on the curved surface. This vast simplification of the form's construction allowed the final surface system to be constructed in the field, through low tech, manual construction methods performed directly on the building surface. To enable these efficiencies, strictly developable surfaces would be required for all project forms. The design surface model was rationalized in light of this requirement.

Rationalization of the project into purely developable forms proved to be an enormous challenge. The strict limitations on surface forms imposed by developable surface

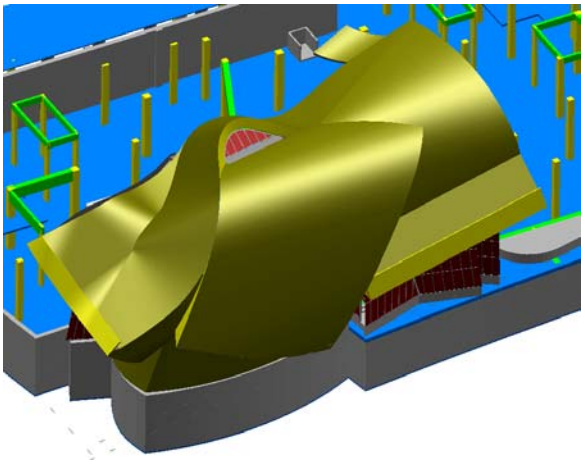

Surface model, based on developable surfaces

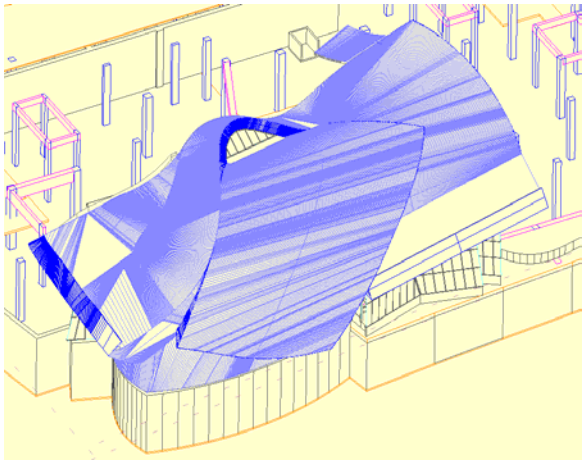

Developable surface elements and ruling lines

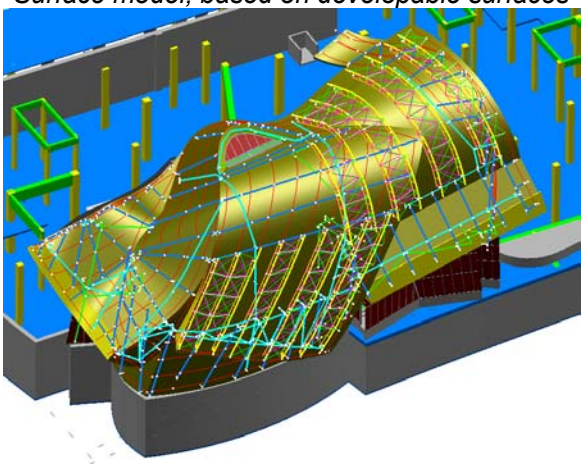

Primary & Secondary System wire frame

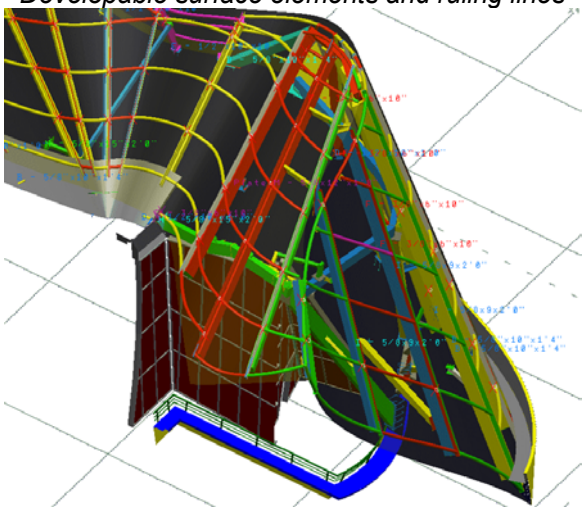

Structural shop drawing

Figure VI-26: Digital developable surface modeling (Weatherhead)

geometries were difficult and time consuming to reconcile with the project design. Often, the developable surface rationalization required re-interpretation of the design surface found unacceptable by the project designers. The surface was re-worked many times until a satisfactory form was achieved. Two “Class A” automotive styling surface modelers were contracted from the Detroit Michigan area to perform the work. These skilled surface modelers required approximately six person months just to perform the rationalization.

The exterior concrete walls, while predominately planar, were folded back into developable surface configurations at their top edges. This configuration allowed formwork to be developed using plywood sheet, bent into developable surface configurations. Two strategies for the development of this form work were used at different phases of the project. Initially, most of the curves concrete surfaces were constructed with plywood form work, supported by straight members that followed the lines of ruling established in the CATIA model (Figure

A. Developable surface formwork

B. Template cut formwork

Figure VI-27 Curved surface concrete formwork

VI-27A). As the project progressed, the process was modified to construct the concrete formwork from plywood sheathing on template cut forms (Figure VI-27B). In the case of the concrete system, the advantage of using straight, unformed materials for the formwork construction was apparently outweighed by the difficulty of positioning the linear members on site into the required configurations. The developable surface configurations of the curved concrete structure was still used to advantage. But on these surfaces, developable surface condition came to be relied on only as a guarantee that the plywood formwork would conform to the shape.

The structural steel and metal enclosure system had more a ambitious agenda for the use of developable surfaces its fabrication strategy. The lines of ruling were to be used both to gain efficiency in the primary structure, and in the construction of the final substrate of the finish surface.

The primary steel structure is developed through two quite distinct systems[23]. One system is

Figure VI-28: Stick and pipe structural system

employed where the lines or ruling course in a predominately vertical direction (Figure VI-28). Here, the primary direction of loading is in the direction of the ruling lines. Straight steel tubes sections between 8”x4” and 20”x12” are employed, depending on the local axial and bending loading determined by the engineering analysis. These tubes are supported by the concrete structure, and span between slab edges offset approximately 1’2” from the finish surface. Where slab edges do not occur at the required support points for the primary steel, the design of additional secondary steel assemblies were required.

The columns are connected by a series of custom curved steel pipes 4” in diameter. The pipe system is defined by a series of horizontal planar cuts with the finish surface, again offset inward to accommodate the dimensions of the cladding system. These cuts lines are spaced at 4’ vertical increments, to support a finish surface capable of spanning a maximum of 6’ along the direction of ruling. The pipe system additionally provides the lateral and racking stability of the structure.

The fabricator proposed that the pipe system be constructed as into a series of prefabricated frames, spanning from tube to tube. The assembly of structural tube systems and ladders were assembled off site, in the fabricators’ shop to guarantee conformance with the digital information in a controlled setting. These prefabricated elements were then disassembled, shipped and re-assembled on site.

Figure VI-29: Ladder truss system

A second system was designed for conditions where the lines of ruling coursed in an approximately horizontal direction. Here, the primary direction of loading is across the line of ruling. To address the primary loading, a curved, Vierendeel truss system was designed. The curved trusses as constructed from two curves, again defined as offsets of the design surfaces. These exterior and interior pipes were joined by a series of plates to complete the truss assembly (Figure VI-29). The trusses are typically spanned directly by the finish surface substrate.

Initially, it was envisioned that the interior pipe would correspond to the geometry of the project interior surfaces. However, this two sided control of the truss geometry was eventually deemed too complicated to design while simultaneously addressing the structural requirements of the elements. In retrospect, the interior chord of the trusses could have been more economically constructed using segmented, rather than curved, pipes.

In the Weatherhead system, the primary structural system is the focus of the most intensive engineering and fabrication efforts. This relative complexity paid off on the finish surface, which is vastly simplified relative to previous projects. The finish system is comprised of a series of hat channels, which attach directly to the curved pipes of the primary steel system. These hat channels are positioned on site along the lines of ruling established in the CATIA model. These panels are fixed directly onto the pipe system with steel nails, then are simply cut to size at the edges and seams between surface forms. A series of overlapping galvanized sheet metal panels complete the substrate of the finish surface. An ice and waterproofing membrane is attached to the galvanized back panel. Finally, the finish shingle system is applied on site, attached to clips that are

Figure VI-30: Back pan on hat channels

Figure VI-31: Finish surface layers

Figure VI-32: Shingled developable form

screwed through the self healing waterproofing membrane. The shingles are designed with a small metal gutter channel, to further assist in diverting water to the outside of the system. Insulation is provided on the interior side of the hat channels.

In cases where the finish surface slopes less than 25%, the cladding system is modified slightly to become a roofing system. Stainless steel sheet is used in place of the galvanized back panel to avoid corrosion. The stainless steel sheets welded together to form a continuous water barrier. The shingle clips are tack welded directly to this surface.

The question of system tolerances was a major concern during the development of these systems. As is many times the case on Gehry's projects, no exact precedent for any of these systems existed on prior projects by either the firm or any of the partnering construction organizations. The strategies of using the primary structural system as the dimensional control, and performing the rest of the fabrication on site, presented many opportunities for loss of dimensional control through deviation from the CATIA geometry. Additionally, the dimensional tolerances of the finish cladding system were not fully understood at the time, but were presumed to be quite stringent. One concern was that the attachment of the hat channels would be compromised if successive pipes did not result in perfectly straight lines of ruling. A second concern was that either the back panel system or the shingle system would fail, resulting in water leakage. An additional concern was that deviation of the pipe system from the nominal locations established in the CATIA model would read through to the finish as the surface substrate was forced over the pipes. To address these concerns, the specification for the pipe system required that these elements be no more than 1/16" from the CATIA geometry at any point.

None of these failure conditions have occurred in the construction. The surface assembly exhibited enough flexibility of all components to accommodate the construction variations from designed conditions. In retrospect, even the driving system requirement of purely developable surfaces has proven to be an unnecessarily stringent requirement. The Weatherhead system could be more appropriately represented as a ruled surface, with some as yet not established gaussian curvature limitations. This would have provided additional flexibility of the surface form to both the project designers and the CATIA modeling team. However, it must be recognized that the initial design development decision to rationalize the form into purely developable surfaces has resulted in a system with virtually no problems

during construction. This stringent requirement on the surfaces has translated into some space to maneuver in the field.

Experiences on the Weatherhead project show the substantial opportunities for construction efficiencies offered by developable surfaces. The presence of lines of ruling in the geometry of developable surfaces is a major, somewhat serendipitous benefit of this representation of paper surfaces. Additionally, the presence of an invariant surface normal facilitates connections to framing members without angular variation in the connection detail. The benefit of having at least one sub-system of the cladding strategy comprised of straight stick elements is obvious.

There is, however, one major and non-intuitive draw back to the construction of developable surface forms. The “flow” of the ruling lines on a developable surface is highly – and non-intuitively – governed by subtle variations the surface quality. Supporting structural systems are compelled to follow the spatial layouts of these ruling lines. This can result in a structural organization with many special conditions for supports and column locations. This rather complex organization stands in contrast to the relatively simple structural organizations of planar cut ribs in curvature constrained panel systems. While the efficiency of constructing curved surface forms from straight linear elements presents a potential cost efficiency over planar rib constructions, this efficiency can be offset by the lack of control in the locations of these members.

C. SUMMARY OF EXISTING PAPER SURFACE REPRESENTATIONS

In the historical progression of Gehry's body of work, it is possible to trace the progressive development of paper surface geometries and their associated techniques of description and modeling. This progression shows a continuing expansion of the class of admissible paper surface forms, as improved representation and fabrication techniques permit less constrained geometries to be feasibly supported in the building process. The planar forms of Gehry's early work, described in Section IV.A, represent the point of departure of this progression.

Cylindrical and conic forms begin to appear on relatively early projects, including the Winston Guest House, Edgemar Development, and the Chiat Day Building. These forms appear tentatively, sparing applied in an overall composition of planar forms. Prior to the introduction of computer modeling techniques in the firm's process, paper surfaces take Euclidean forms, true cones and cylinders. Their more general counterparts were formulated as developable surfaces in Section VI.B. This constraint is imposed on these early projects by limitations of traditional documentation. The complexity of determining geometric relationships between more complex, non-Euclidean conic forms was simply beyond the capabilities of traditional architectural delineation.

The exploration of a vocabulary of conic forms continues to be expanded on Gehry's projects until the introduction of computer modeling in 1990. The Weissman Museum (Figure VI-33) represents the culmination of this approach. Each face of the west façade is delineated through traditional geometric constructions. The difficulty of performing this construction though traditional architectural delineation is clearly evident in the construction documentation.

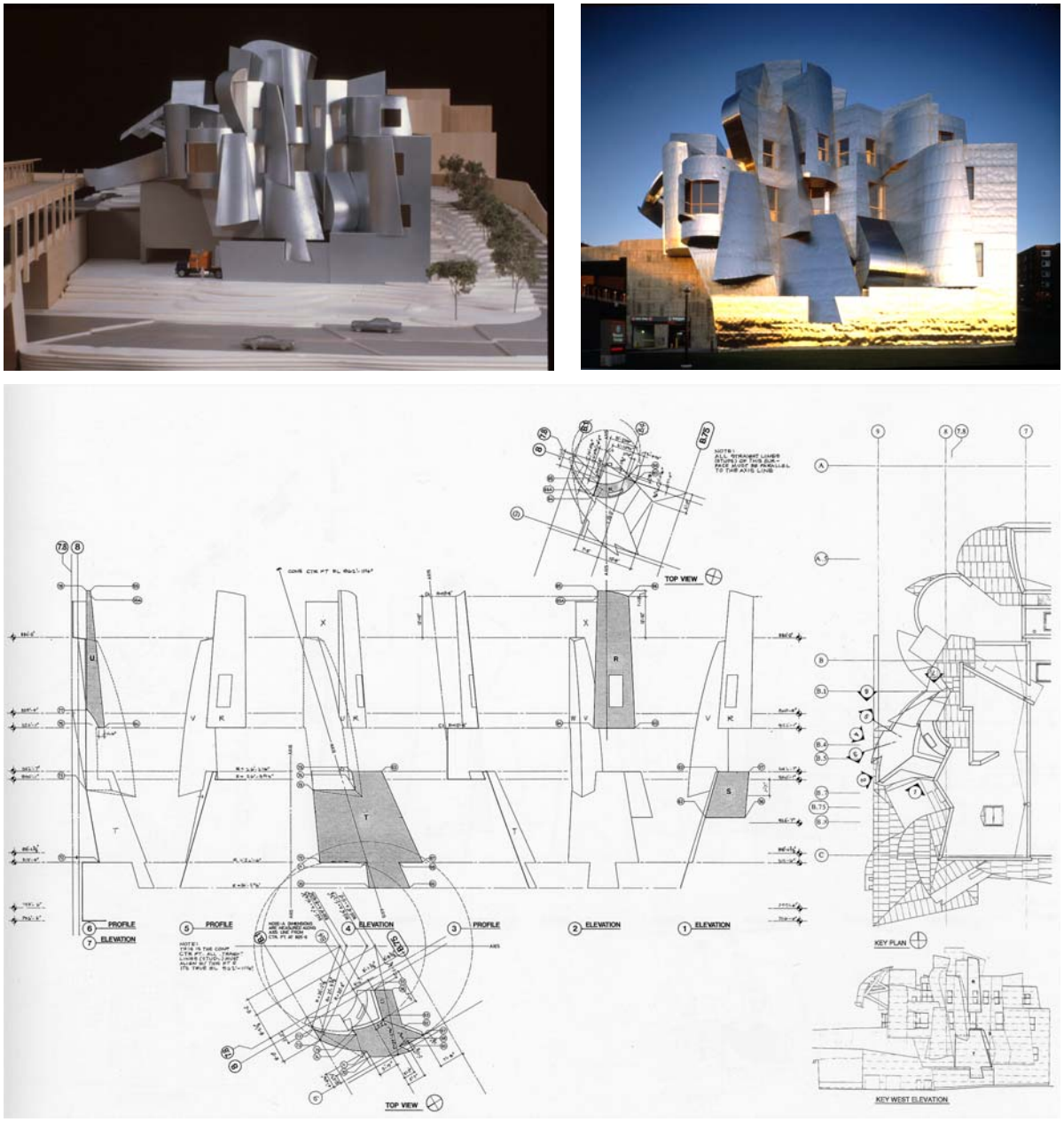

Figure VI-33: Conic form rationalization through traditional documentation (Weissman)

A. Physical design model

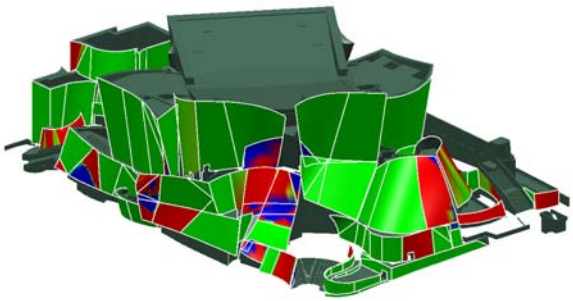

B. Decomposition of the geometric construction, gaussian curvature analysis

Figure VI-34: Conic form rationalization through digital documentation (DCH)

The early computer models of the Disney Concert Hall (Figure VI-34) document the extension of the firm's manual approach to developing complex geometries through a vocabulary of Euclidean surface elements. In the initial design of the DCH project, prior to 1998, the project was intended to be clad in CNC milled stone panels. The project geometry attempted to achieve some of the economic benefits of mass production by the use of the quadratic surfaces. Economic constraints on the project dictated that certain economies of scale were necessary. The design team responded to these constraints by developing cost projections for different complexities of surface qualities. Planar surfaces were naturally assumed to be of lower cost than curved areas. In curved surface areas, distinctions were made between the relatively simple geometries of conic forms and fully free form areas. It was determined that economies of scale could be taken advantage of on conic surfaces, due to the regularity of panel elements across the latitude of a section through the conic form. A budget limiting percentages of the project's surface area in these categories was developed prior to finalization of the concert hall's shape.

It is worth noting that the initial design development on this project was conducted in 1992, when numerically controlled milling technologies were available, but computing performance and information distribution mechanisms were at an earlier stage of development than today. Today, with improved efficiency of computational methods, the cost implications of CNC cutting are more directly tied to the machining time, and less to the computation and operator time necessary for generating the CNC tool paths for the cutting operations. Thus economic efficiencies of batch production of similar pieces, which must still be individually processed

by the CNC milling equipment, seem to be less significant than they must have seemed in 1989.

The project design was re-visited in 1998, when the decision was made to change the finish material from milled stone panels to stainless steel. The conic surfaces were re-interpreted as developable surfaces, involving a different strategy for the direction of sub-framing, but without altering the shapes of the surfaces. Significantly the same project forms admit two radically different approaches to efficiency of construction, one based on regularities of element shapes, the second on ruling lines and the unfolding of panel geometry.

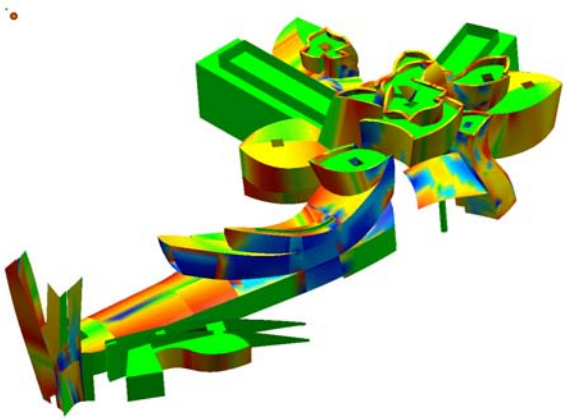

Figure VI-35: Gaussian Curvature mapping on Bilbao Project

The Guggenheim Bilbao project, represents a dramatic extension of the firm's approach to the representation of paper surface forms. While stone was initially selected for DCH, the surface of Bilbao is comprised of sheet metal surfaces. Thus economic constraints were presented to the design team in terms of limiting the surface forms to those that could be assumed by sheet materials. The physical design models on Bilbao were generated by folding large paper elements (relative to the overall scale of the project) into form. The strategy presumed that shapes which were constructed of large paper surfaces in the scale physical models could be fabricated from individual sheet materials in actual construction. During initial computer modeling exercises, the digitized data from the physical models were re-interpreted using developable surfaces. These initial results did not entirely satisfy the design team. The forms generated by developable surfaces were deemed too constrained relative to the initial physical design models. Additional CAD modeling operations were performed on the initial developable surfaces, where the surfaces were "puffed out" – deformed such that limited double curvature was introduced into the shapes. Heuristics were determined dictating the degree to which double curvature would be introduced into the surfaces. The utility of these heuristics was limited at the time. The fabricator determined that the surfaces up to a sixty foot sphere could be fabricated. CATIA allowed the curvature

at individual points on the surface to be sampled. The principal radii at these sampled points was limited to a minimum of sixty feet in either of the two principal directions.

The geometric qualities of the EMP project represent in some sense a culmination of the firm's paper surface modeling research and design explorations. On this project, the fully curved free form shapes of the original design were supported as a composition of gaussian curvature constrained paper surface forms. Admittedly, this support of fully free form shapes is approximate, as the forms are rationalized into shapes exhibiting curvature acceptable given constructibility constraints. These rationalization operations can be read in the final project (Figure VI-36).

In the period since the completion of EMP, developable surface and constrained gaussian curvature applications have developed in parallel. Although the gaussian curvature approach presents more generous constraints on project form, the economic efficiencies of straight lines of ruling presented by the developable surface approach are considerable. The tough constraints of developable surfaces on project forms seem to project the energy of the sheet material surfaces as they are formed in space better than the more relaxed qualities of the gaussian curvature approach. The Weatherhead project represents perhaps the most ambitious application of developable surface forms to date.

The two paper surface representations present remarkably different strategies for the representation of similar shapes. These differences are manifested in the substantially different approaches to construction suggested by each representation. However, both strategies require tight tolerances on the framing system required to achieve a form that will match the predicted shape. If the geometry of the framing system does not adequately provide a shape onto which sheet materials will form, then either substantial forming of the cladding material will need to be undertaken, or warping of the surface will occur. Failures of cladding or substrate materials may occur, or waterproofing requirements for the system may not be achieved, resulting in a roof or wall system that leaks. Certainly, the desired architectural quality of the surface will not be achieved, as the cladding buckles and ripples about fasteners and joints. For simple, canonical classes of paper surfaces such as planar, cylindrical or conical forms, the predictive capabilities required to assure developability of the surface are not particularly great. However, to achieve the freely flowing shapes allowed by the most general classes of paper surfaces, the predictive capabilities required to engineer

and fabricate cladding system elements while maintaining the accuracy required for system integrity are substantial.

A. Weatherhead: Developable system

B. EMP: constrained curvature

Figure VI-36:Rationalization comparison

The geometric constraints presented by the two approaches are sufficient to guarantee conformance of the system geometries with the behavior of sheet materials. However, these constraints come at a price. The control structures supported by the associated CAD techniques do not intuitively guide the user to feasible sheet material shapes. The NURBS surface representations – manipulated by control points – tend to produce shapes with localized variations in smoothness – exactly the opposite of the desired result. Similarly, manipulation of the edge curves that are used to generate developable surfaces will generally result in surfaces with triangle discontinuities. The actual operator activities required to produce paper surface forms using either of these techniques are not directly discernable from the input controls, and require substantial manipulation by experienced users to “tease out” surface imperfections.

Both techniques are developed as constraints on NURBS based parametric surface representations. The shapes produced by these techniques are largely irrespective of actual qualities of the materials used. For gaussian curvature controls, a wide range of material and fabrication phenomena are subsumed into a simple, and rather impoverished, metric. The developable surface technique predicts identical surface constraints irrespective of the actual materials employed.

If the geometric properties of NURBS based surfaces are under constrained for paper surface applications, then the properties of developable surface based representations and systems fall at the other extreme. Developable surface representations are highly constrained, often resulting failing to produce feasible configurations for digitized data from physical paper models. The constraints of zero gaussian curvature and purely linear directrices of developable surfaces are quite rigid constraints, which render these systems to be somewhat incompatible with the characteristics and digitized features from the more “lenient” paper prototypes.

On the other hand, the topological characteristics of parametric surface representations are well suited to paper surfaces. The notion of a Euclidean, parametric space that is topologically “sheet like” – and the extension of this representation to assemblies that are combinatorially constructed from topological sheets - maps well to the qualities of paper and other sheet like materials, and their organization in assemblies.

VII. PHYSICAL MODELING

A. INTRODUCTION

The approaches to digital modeling of paper surfaces described in the previous chapter have substantial limitations relative to the qualities of such simple modeling tools as physical paper materials. The common characteristics of both approaches – reliance on differential geometry heuristics and constructs – have limited capabilities for representing the behavior of physical materials and operations. The pursuit of digital representation techniques that provide a closer affinity to the materials and operations of physical modeling and full scale fabrication remains an active area of research by the firm's computing staff. This section presents research that more directly pursues representation of the properties of the sheet materials themselves: their qualities and modes of deformation, physical properties such as ability to stretch and bend, their response to forces, etc. A radically different alternative to the simulation of paper surfaces will be presented, one that relies on direct simulation of material properties and behaviors.

Materials simulation is far from a new topic. Vast research by the engineering community has been directed toward the representation of structural and mechanical behaviors of physical bodies. The materials and bodies pursued through these disciplines are as large as the class of all materials and forms of use in engineering applications. The representation of paper surface forms through physical simulation positions this work within this body of research.

Efforts to adopt a physical simulation approach to the modeling of paper surface forms are complicated by the broad scope and ambiguities inherent to this problem, presented in Section IV.C. In this effort, we seek to capture those formal and operational qualities that are common among a wide scope of building design and construction activities, from schematic design explorations in scale using physical modeling materials, through to the actual operations of fabricating craftsmen in the shop or field. The accuracy of representing any of these specific processes through a common representational strategy is likely to be qualitative at best. On the other hand, the analysis of the firm's existing techniques presented in Chapter VI disclosed similar limitations. Despite these limitations, the existing approaches have been able to successfully integrate representation of project formal qualities with fabrication constraints. We should expect a physical modeling approach to the representation

of paper surface forms to provide at least some improvement in serving the common ground between these disparate representational requirements.

The general class of problems concerning the motion and deformation of objects are encompassed by kinematics. Within kinematics, applications where the concern is to determine the ultimate rest state resulting from force effects on bodies are generally approached as statics problems, while solutions where the response of the object to these effects over time are considered through dynamics. While it may appear that the deformation of paper surfaces is appropriate for solution through statics, it will turn out that elements of the dynamic behavior of the sheets as they are deformed over time will be worthy of consideration as well.

One broad class of analysis potentially applicable to paper surface modeling is the theory of elasticity, wherein the geometric form of the sheet results from an initially un-deformed body – with certain parameterizable material properties – whose shape results as a response to externally applied forces by deformation of the body. Solution of such problems take the form of well known relationships between body stress (internal forces incurred by the body, usually as a result of externally applied forces) and the deformation or strain of the body. Solutions are developed through an analysis of infinitesimal elements of the body and the characteristics of these elements in response to stress forces of the loading scenario under consideration. The overall behavior of the body is solved by integrating the element level response over the totality of the body.

Until the advent of computer modeling, problems in these domains were largely limited to the inquiry of certain canonical shapes (e.g. square plates, cylindrical shells, etc.) for which the integration could be solved in closed form. The advent of high performance computing has allowed for element level analysis to be extrapolated to the global deformation of the shape by considering each element's behavior independently within the context of the assembly solution. These approaches consider elements, not of infinitesimal character, but rather as elements of small but finite size. The body is discretized into assemblies of elements whose individual shapes permit an explicit solution for deformation due to externally applied forces. Conditions of continuity and compatibility between adjoining elements are imposed, and the global behavior of the body is determined by considering the inter-related behavior of the individual elements.

One broad distinction that is made in terms of solution techniques for elastic problems is the question of linearity of the problem and its solution. Elasticity problems may introduce linearity or non-linearity in two ways: material linearity, and deformation linearity. The general stress – strain relationship defined by Hooke's law:

$$f = kd \tag{VII.1}$$

implies a linear relationship between stress and strain. Many materials exhibit effectively linear stress-strain relationships for small scale deformations, but this simple relationship becomes more complex as larger scale deformations introduce more complex responses.

Similarly, many solution techniques employ linearized approximations of geometric equations in their solutions, including small angle approximations, where trigonometric functions are approximated into simpler forms which hold approximately for small angles. For structural analysis problems, where one may reasonably anticipate the deformation of a building component will be small relative to its overall dimensions, linearized approximations of the geometry of motion are completely appropriate.

In considering sheet material solutions of the types appropriate for modeling paper surfaces, clearly the linear geometric approximations will be inappropriate, as the anticipated deformation of the body will be quite large. However, the notion of linear approximation of material properties seems to be plausible, at least at a qualitative level appropriate for schematic design requirements. One problem characteristic that will indicate whether the sheet material responds in a linear fashion would be whether plastic deformation occurs in the material; that is to say, given input forces that deform the material, would the material return to its original flattened shape if these forces were removed? In the simulation of paper surfaces, the answer to this question would be: partly. Certainly the shapes under consideration do not develop the large scale, ductile deformation associated with stretch forming of material. However, typically some residual deformation of the sheet will remain in sheet metal or plywood that has been substantially curved.

Analysis of sheet like bodies has taken a wide variety of forms, again dependent on the characteristics of the body and results to be solved for. These techniques have been developed for analysis of structural assemblies including concrete shells, and shear walls or

other structural elements whose behavior is principally two dimensional. These approaches have been incorporated into a wide variety of commercially available structural finite element solver programs. Most of the theory and application regarding the behavior of plates, shells, and membranes under loading presumes small deformation appropriate for structural bodies that are quite rigid, and are expected to experience small scale deformation relative to their overall dimensions. Again, most of the commercial applications for building structural engineering are concerned with the static behavior of these elements, although modal analyses – an essentially static solution that supports the analysis of the system's oscillatory behavior – are also supported. These techniques can provide highly accurate, detailed analysis of structural elements in reasonable solution times.

The theory and applications for the solution of fully deformable material bodies, including non-linear inelastic behavior, is also quite mature. Techniques and commercial applications in this category are varied, including solvers appropriate for the analysis of large scale plastic deformation and even catastrophic events such as explosions. These applications may utilize highly non-linear representations of strain behavior. Solution techniques may use non-linear representations of geometric deformation, or may discretize the behavior of the system into small, incremental motions over time. A potentially serious limitation of many of these approaches is the time to solution. Robust techniques may require the solution of coupled partial differential equations for the various modes of motion, and will require the iterative solution of these equations over many time steps in order to perform the simulation.

As a generalization of physical modeling problems, differing representations of the problem domain – involving differing approximations of the body's shape and behavior – can produce dramatically different accuracy of prediction, with related differences in computational expense. This relationship between the accuracy of representation of a bodies behavior and the computational expense to achieve the solution should be not surprising.

This question of desired accuracy of solution in the simulation of paper surfaces is an important one. In principle, the problem domain could be tackled as one of extraordinary complexity, involving plastic deformation of the sheet material under loading, friction resistances between sheets at their joints, and accurate solutions for fastener's structural behavior. However, it is not clear whether this high level of complexity of solution technique

would provide results that would merit the substantial penalties in terms of computational expense.

In developing a materials modeling based approach to paper surfaces for design applications, a primary consideration is to achieve tools whose speed of solution is sufficient for designers and drafters to model shapes interactively. A solution technique that accurately produces the most subtle details of behavior will not be useful if modification of surfaces to reflect changes in design requires hours of off-line computation. At a global level – where large scale surface shapes are under consideration, a solution technique that can qualitatively direct the shape to a feasible form may be sufficient, if interactive speeds can be achieved. At the level of verifying a specific sheet's shape to determine appropriate placement of framing members, solution techniques with potentially higher accuracy may be required.

The solution methods employed by the engineering communities have generally favored detailed computational models of physical behavior, resulting in highly accurate solutions, at the expense of potentially long solution times. This predilection is easy to understand in engineering applications where life and equipment safety are issues.

At perhaps the opposite end of the spectrum, new physical modeling approaches are appearing in computer animation applications. Substantial work has been undertaken in the simulation of deformable objects in general, and in the simulation of deformable surfaces in particular. These physical modeling applications provide reasonable, qualitative behavior of physical bodies for the purposes of computer animation. These approaches are generally concerned with the time variant behavior of the systems, with time varying effects such as collisions between objects, temporally modified constraints on the objects (e.g. the motion of a human character supporting a cloth object). Simulation for the purposes of computer animation has the demand of achieving a visual realism that produces a perceptual accuracy of physical behavior with substantial degrees of detail, but performs a certain trade off between accuracy of the simulation and computational speed. These simulations are typically rendered off line, so interactive speeds are not a requirement. The strongest demand on such simulations is the degree of detail required.

Great attention by the computer graphics community has been focused on the simulation of cloth, for the purpose of clothing characters in animations. Notable work in this domain has been research by Feynman[26], Terzopoulus[89], Provot[71], Baraff and Witkin[5], and many others. Ng[59] provides an overview and comparison of the various techniques employed by these authors.

B. DEFORMABLE BODY MOTION

This section outlines the basic framework of material body deformation, appropriate for application to paper surface simulation. The discussion follows closely the derivations of classical texts on the theory of elasticity, including Marsden and Hughes[53]. We will be considering the motion of a material body, and the relative motion of parts of this body, in response to external effects (typically represented as forces), over the progression of time. It is useful when considering this transformation of the body over time, to focus on a primary, invariant *reference configuration B* as the original, un-deformed state relative to which all future deformed configurations of the body will be considered. We consider the reference configuration *B* to have a coordinate system and "space" independent of the world space $\mathbf{R}^3$. This will allow variations in positions to be viewed from the perspective of the body, irrespective of deformation or positioning in space. It will be convenient when considering rates of deformation of the body appropriate for calculation of stresses experienced by the body to have this invariant coordinate system available to which changes in the body configuration may be compared.

When considering solid bodies, this body coordinate system will be of course 3-dimensional. For other types of objects, including the 2-D surface objects that will be used to represent paper surfaces, it will not be necessary to maintain an independent out-of plane axis for the body space, and in fact a two dimensional coordinate system and associated space will be preferable. Coordinates of the body in the 2D reference space will be denoted $\mathbf{u} \in B$, and are termed *material points*, while corresponding coordinates in world space will be denoted $\mathbf{x} = (\mathbf{x}^1, \mathbf{x}^2, \mathbf{x}^3) \in \mathbf{R}^3$, and are termed *spatial points*. A *configuration* of B is a mapping ϕ: $B \rightarrow \mathbf{R}^3$, which maps points in body space to locations in the world coordinate system. Over the course of time, the body will undergo motion, represented as a sequenced *family* of configurations: the deformed shapes of the body over time. The notion of the mapping function ϕ will thus be embellished to incorporate the notion that the function maps material points to spatial points, not simply as a function of the point's body space coordinates, but also as a function of a time parameter t. This function is notated:

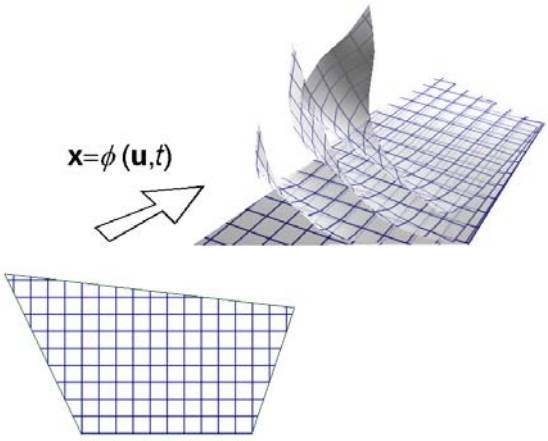

Figure VII-1: Deformable body mapping function

$$\mathbf{x} = \phi(\mathbf{u}, t) \qquad \text{(VII.2)}$$

The function ϕ may now be seen as an "engine" which takes in material point locations and as well as "points in time", and delivers locations in $\mathbf{R}^3$ space. Since the values returned by ϕ are actually a 3-tuple $\mathbf{x} = (\mathbf{x}^1, \mathbf{x}^2, \mathbf{x}^3)$, we can consider the function ϕ as being comprised of three component functions, $\phi = (\phi^1, \phi^2, \phi^3)$, each of which take the input variables $\mathbf{u} = (\mathbf{u}_1, \mathbf{u}_2) = (u, v)$ and t, and return one of the spatial coordinates

Note that the formulation of this material deformation problem is quite similar to the parametric surface representations explored in Part 2. We have simply introduced an extra dimension, time, to input of the manifold representation of surfaces $\mathbf{x} = \sigma(\mathbf{u})$ (V.29). In the same manner that we fix the parameter $\mathbf{u}_2$ in (V.29), setting it equal to some constant c, and view the result as a curve in space $\mathbf{x} = \sigma(\mathbf{u}_1, c)$, we can freeze the variable t in (VII.2) and

view the result as a simply as a surface in $\mathbf{R}^3$. Alternatively, we can fix the parameters $\mathbf{u}_1$ and $\mathbf{u}_2$ and view the function $\mathbf{x} = \phi((c_1, c_2), t)$ as a function that defines the path in space of a single parametric point (c_1, c_2) over time. This similarity between parametric surface and deformable body representations is far from coincident. Both are subsumed within the general construct of manifolds, presented in Section V.C. From a manifold perspective, there is no distinction between the time parameter t and the spatial parameters $\mathbf{u}_1$ or $\mathbf{u}_2$. The deformable body representation simply changes the degree of the problem from the form $\mathbf{R}^2 \rightarrow \mathbf{R}^3$ to the form $\mathbf{R}^3 \rightarrow \mathbf{R}^3$. The distinction between time and space parameters is found only in the internal definition of the function ϕ, i.e. what ϕ "does with" the parameters, not any special properties of the parameters themselves.

The notion of a global function representing the full history of a complicated shaped object and its state at all points over time may seem like an overwhelming construct to readers rusty in calculus. Indeed, this function is not one that can in general be described explicitly, except for fairly simple objects following fairly simple paths. In subsequent sections, when specific solution techniques are discussed, the presence of such a global function will be presumed as an organizing structure, but will never be directly solved for. Rather, we will determine localized characteristics of this function on the basis of the state of the body, and pursue numerical solutions designed to locally trace the path of the body in space and time along this function.

With the notion of the mapping function ϕ established, rates of change in the shape or location of the body may be determined by taking derivatives of the function with respect to either material coordinates or time. By holding the material coordinates $\mathbf{u}$ constant in the function $\mathbf{x} = \phi(\mathbf{u}, t)$, we achieve a function representing the path of a point on the body through space as time is varied. Taking the derivative of ϕ with respect to t will produce a function representing the velocity of points of the body, represented as a 3-dimensional space vector for each point $\mathbf{x}_i \in B$. This vector will be located in $\mathbf{R}^3$, pointing in the direction of the path in space of the point, with a length equal to the speed of the point. The components of this space vector will be the derivatives of the components functions, $\partial\phi/\partial t$. The acceleration of the body, unsurprisingly, takes the form of the second derivative of ϕ with respect to time, i.e. $\partial^2\phi/\partial t^2$.

Similarly, we can hold t fixed in the function $\phi(\mathbf{u}, t)$, and consider the shape of the body relative to that of the reference configuration by taking derivatives of ϕ with respect to **u**. The partial derivatives of ϕ^i with respect to the material coordinates $\mathbf{u}_j$ form a matrix $\mathbf{F}^i_j = \partial\phi^i/\partial\mathbf{u}_j$, called the *deformation gradient*. This matrix of derivatives embodies both a rotational component, forming the transformation of the material coordinates of the body into the spatial coordinates due to rigid rotation of the body, and a component representing the deformation of the body due to stretch or compression. The deformation gradient may be decomposed as:

$$\mathbf{F} = \mathbf{RU}$$

Where **R** is the rotation matrix and **U** is the *right stretch tensor*. The strain deformation of the body at a point may be determined directly from the stretch tensor, by determining the eigen values of this matrix. Higher degree derivatives of the mapping function ϕ with respect to **u** may of course be found.

For the general cases of arbitrary paper shapes and input constraints, representing the function ϕ explicitly is not possible, so we can not solve this equation directly. However, we can determine, for a given configuration of the body **x** at a time t, features of the function ϕ that will allow us to understand the impending rates of change in **x** as a function of t. Specifically, we can determine the strain function of ϕ by comparing the shape of **x** to that of the reference configuration **u**. We will then be able to work backwards to produce an understanding of the shape of the function ϕ in the "direction" of the parameter t. In order to attain this solution, we discretize the complex continuum of both the reference configuration B and the time domain t into an assembly of discrete, inter-related intervals. Discretization transforms the partial differential equation of motion into a system of linked ordinary differential equations, allowing the solution for each element of the body to be considered initially independently. This localized consideration of the problem can be adopted to produce approximations of the rates of change of ϕ at discrete points in time. These localized states of the problem (in space and time) can be integrated numerically by stepping through time, determining the current configuration of the body, determining the localized shape of the function ϕ from its approximated derivatives, and projecting the state of the simulation forward for some interval of time. The state of the body at this new point in time is then

checked relative to the reference configuration, and the process is repeated until the converged state of the body has been detected.

With the inclusion of a damping effect, which generates a incremental resistance to the direction of motion, we can anticipate that – presuming no influxes of energy into the system are introduced - the body will ultimately wind up converging to a rest state and deformation at some point in time. To paraphrase, for some value t_{rest} the magnitude of the velocity vector $\mathbf{v}(\mathbf{u}, t_{rest})$ will be within some neighborhood of 0 for all B. At that point, the desired shape and location of the body, representing the body's response to all applied external forces, will have been determined. The theoretical goal of the simulation is to determine the shape of the deformed body $\mathbf{x}_{rest} = \phi(\mathbf{u}, t_{rest})$ at this future time of convergence.

C. A SIMPLE EXAMPLE

As a point of departure, a simple representation of physical sheet materials is presented in this section. This simple model will be extended to a more robust formulation in subsequent sections of this chapter. The approach discussed in this section is derived from that proposed by Provot[71] and others. It draws on a simplified, linear representation of the localized differential equations of motion. The mathematics employed in solving these differential equations is at the level of high school physics, where acceleration, velocity and location are related through straight forward multiplications of the derivatives with time.

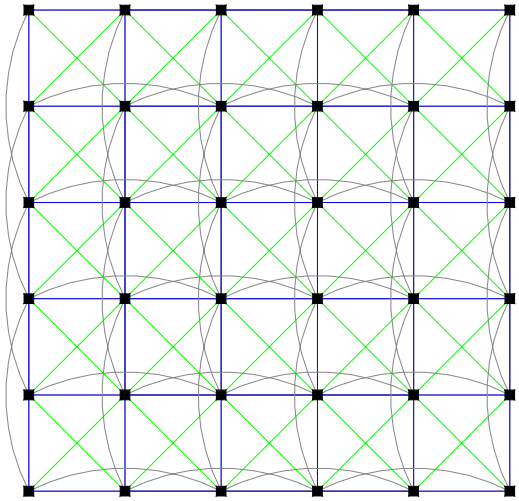

Figure VII-2: A simple mass-spring model of sheet materials

The surface is represented as an initially flat array of points organized in a grid. The material properties of the surface (mass, stiffness, etc.) are abstracted as a set of mass points at the nodes of the grid, and springs which join these nodes. The mass of a square of material is allocated to the node at its center. Springs join an individual node to its neighbors. The

relative location between two joined nodes determines the kind of stress to which the given spring responds .

1. Springs which join a node to its nearest horizontal / vertical neighbors govern the behavior of the node when subjected to internal axial forces.
2. Springs that join a node to its diagonal neighbors govern internal shear force response.
3. Springs which join a node to the horizontal / vertical neighbors located two units away govern the flexural behavior of the intermediate node.

As the surface deforms from its initial flat geometry, the relative lengthening or shortening of the springs exert an opposing force on the two nodes which join the spring. Figure VII-3 provides a graphical demonstration of the spring behavior. Each force is represented as a vector, with both direction in space and magnitude. A force on a particle $\mathbf{p}_0$ due to a spring of rest length l joining $\mathbf{p}_0$ to a particle $\mathbf{p}_1$ is simply:

$$\mathbf{f}_{spring} = K_{spring} \frac{|\mathbf{p}_1 - \mathbf{p}_0| - l}{l} \frac{\mathbf{p}_1 - \mathbf{p}_0}{|\mathbf{p}_1 - \mathbf{p}_0|} \qquad \text{(VII.3)}$$

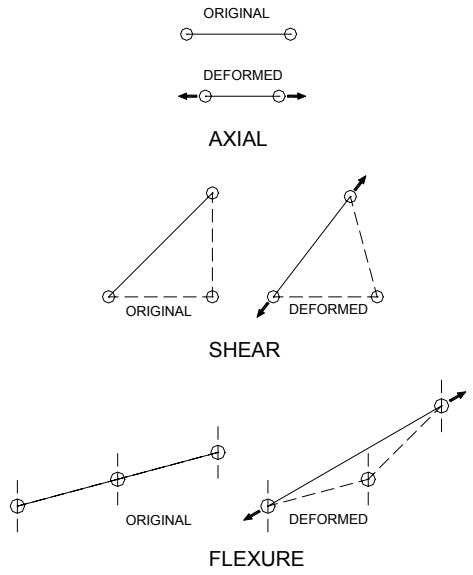

Figure VII-3: Deformation modes of the idealized spring assembly

where $\frac{\mathbf{p}_1 - \mathbf{p}_0}{|\mathbf{p}_1 - \mathbf{p}_0|}$ is simply a unit vector in the direction $\mathbf{p}_0 \rightarrow \mathbf{p}_1$, and K_{spring} is a constant that dictates the stiffness or force associated with the spring. Differing stiffness constants may be allocated to the spring types (1 - 3). Variations in these relative spring constants affect the qualitative behavior of the surface material. Approximate values for these spring constants could be determined from the material properties of the material, thickness of the material and distance between the nodes.

In addition to the internal forces of the material stiffness, the surface may be subjected to external forces, including:

- gravity

- positioning during fabrication
- framing and fastening constraints.

These external actions on the surface can be formulated in a variety of ways, depending on the type of behavior of interest. The actions manifest themselves as force vectors – possibly varying over time – acting on the mass nodes. As a simple example, the action of gravity is formulated as the vector:

$$\mathbf{f}_{\text{gravity}} = \begin{bmatrix} 0 \\ 0 \\ -ma_g \end{bmatrix} \tag{VII.4}$$

where a_g is the acceleration of gravity and m the mass of the node. This force is applied constantly on each node in the surface representation.

An additional damping force is added to each node, based on the velocity of the node at a give point in time:

$$\mathbf{f}_{damp} = -K_{damp}\mathbf{v}_0 \tag{VII.5}$$

The damping component tacked on to each particle as a function of its velocity, ensures that a rest state will ultimately occur. If this damping factor were not figured in, the surface could oscillate indefinitely.

To solve for the deformed surface under loading, all of the force vectors acting on an individual node at a particular point in time t_0 are summed, producing a force vector **f** acting on the node. The surface state is then considered at an incremental time step $t_0 + h$. The algorithm uses a simple linear method for approximating the changes in surface state over this time step:

We consider the system for a specific time step (t_0, $t_0 + h$), with a known position of all particles $\mathbf{x}_0$ and known velocity $\mathbf{v} = \dot{\mathbf{x}}$, the system is solved for a new position vector $\mathbf{x}_{0+h}$, and a new velocity vector $\mathbf{v}_{0+h}$. The differential equations representing the system are:

$$\frac{d}{dt}\begin{pmatrix}\mathbf{x}\\ \dot{\mathbf{x}}\end{pmatrix} = \frac{d}{dt}\begin{pmatrix}\mathbf{x}\\ \mathbf{v}\end{pmatrix} = \begin{pmatrix}\mathbf{v}\\ \mathbf{M}^{-1}\mathbf{f}(\mathbf{x},\mathbf{v})\end{pmatrix} \tag{VII.6}$$

Discretizing the equations, we define

$$\Delta\mathbf{v} = \mathbf{v}(t_0 + h) - \mathbf{v}(t_0)$$
$$\Delta\mathbf{x} = \mathbf{x}(t_0 + h) - \mathbf{x}(t_0) \quad \text{(VII.7)}$$

The solution to the differential equation in (VII.6) approximates $\Delta\mathbf{x}$ and $\Delta\mathbf{v}$ as

$$\begin{pmatrix} \Delta\mathbf{x} \\ \Delta\mathbf{v} \end{pmatrix} = h \begin{pmatrix} \mathbf{v}_0 \\ \mathbf{M}^{-1}\mathbf{f}_0 \end{pmatrix} \quad \text{(VII.8)}$$

These equations are simply:

$$\Delta\mathbf{v} = h\frac{\mathbf{f}(\mathbf{x},\mathbf{v})}{\mathbf{m}} \quad \text{(VII.9)}$$

$$\Delta\mathbf{x} = \mathbf{v} = \mathbf{v}_0 + h\Delta\mathbf{v} \quad \text{(VII.10)}$$

$$\mathbf{x} = \mathbf{x}_0 + h\Delta\mathbf{x} \quad \text{(VII.11)}$$

In this simple formulation, these three equations may be solved independently (for each particle) and sequentially, once the force vector **f**(**x**,**v**) has been determined. First, $\Delta\mathbf{v}$ is solved for by multiplying the time step size by force, and dividing by the mass of the particle. Adding the change in velocity $\Delta\mathbf{v}$ to the previous velocity produces the new particle velocity. The change in location $\Delta\mathbf{x}$ is similarly solved for (VII.10), by multiplying the new velocity by the time step. The change in particle location is added to the current location to produce the particle location at the end of the time step.

Note that a particle's location and velocity are each represented by three values, representing respectively, the location and velocity's 3 spatial components. A total of 6 values must be stored for each particle during the simulation. Each component is approximated as a *linear* function over the time step, and represents an independent function that may be independently solved for.

The acceleration of the node is equal to the force on the node divided by the node's mass:

$$\mathbf{a}(t_0) = \mathbf{f}(t_0) / \mathbf{m} \quad \text{(VII.12)}$$

The velocity of the node is equal to the old velocity plus the new acceleration multiplied by the time step.

$$\mathbf{v}(t_0) = \mathbf{v}(t_0) + h\,\mathbf{a}(t_0) \quad \text{(VII.13)}$$

The new node location is equal to the old location plus the new velocity multiplied by the time step.

$$\mathbf{x}(t_0 + h) = \mathbf{x}(t_0) + h\,\mathbf{v}(t_0) \quad \text{(VII.14)}$$

As a result of solving these three equations, we have new node locations, velocities and accelerations. On the basis of the new point locations and their distances from each other, the new spring forces can be computed. Viewed in its entirety, the simulation presents the object shape and path in space over the lifetime of the simulation. The algorithm is repeated until point locations stabilize, and the velocity of each point falls below a specified minimum value.

The approach taken offers compelling initial results for modeling sheet based materials with a range of material properties (Figure VII-4). Despite the visually compelling results produced by this formalization, there are some critical limitations of the approach. The current material model only qualitatively represents the physical forces in the material. It is unlikely that the spring constants and their organization in this formulation would be sufficient to predict true materials' behavior accurately enough for fabrication applications.

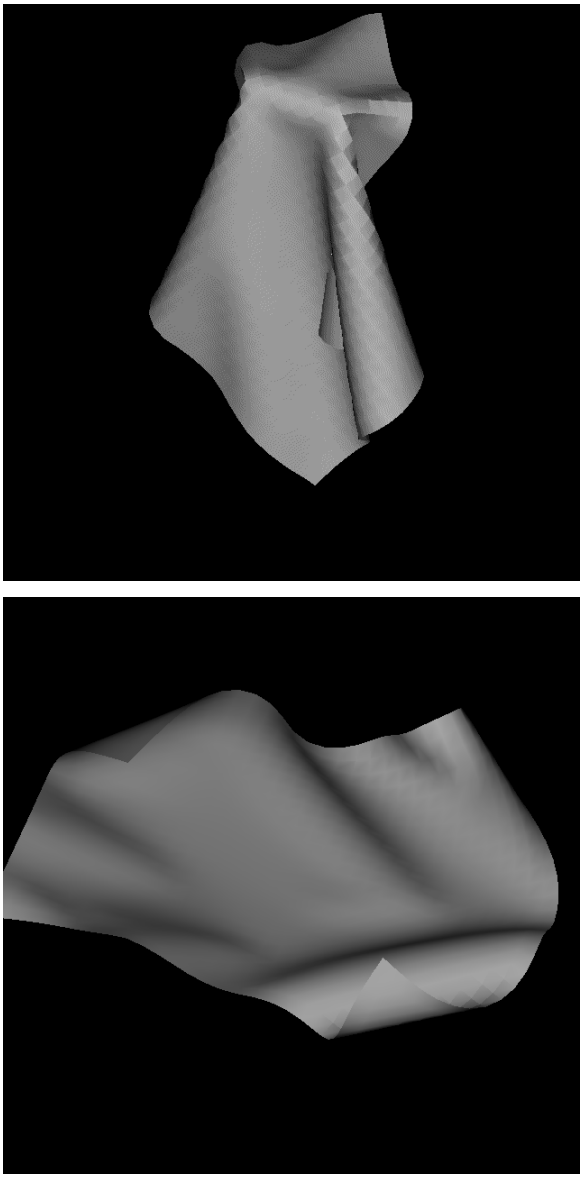

Figure VII-4:Results of materials simulation based on a simple spring model

The flexure formulation is particularly weak. The representation of bending force is related to changes in the distance between alternating nodes. This approximation makes the assumption that the material stiffness due to stretching and shearing is high enough relative to the bending stiffness that changes in the distances between directly neighboring nodes is negligible. While this is typically true for thin, flexible materials, many potential materials such as cloth will allow non-trivial axial deformation. This deformation will impact the forces derived due to bending. Additionally, the concept of using spring length as a parameter results in a bending force that varies with the small angle approximation for the cosine of the bending. Bending forces will not begin to kick in until the angle is large, and variations in the angle at small angles will produce little change in the bending force. A preferred formulation of the bending force would be related to the sine of the angle for small angles, where small variations in the angle from flat would produce proportional changes in opposing force. However, modifications to the representations of forces on the system – in particular stress strain relationships within the simulation could be augmented to improve the accuracy of this representation (albeit with potentially substantial computation costs).

There is a more critical limitation of the above approach to solving the differential equations of motion, in terms of the stability of the solution. This is a well known limitation of the forward Euler method solution (VII.8) to the differential equation of motion. The above described method limits it understanding of the path of a particle in space by considering only velocity - the first derivative of the particles' location. The form of the solution – and that of the paths taken by the particles – is linear. At each step in the simulation, the trajectory of each particle is determined; the particle is then sent down this trajectory in a straight line for the period determined by the time step *h*. For small time steps this approach closely approximates the "true" motion of the original, pre-discretized body *B*. As the time step is increased, the collective locations of particles at a given time map less and less well to this true shape. At each time step the spring forces attempt to draw the discretized body back to the true shape of the deformed body. For time steps greater than a certain duration, the discrepancy is large enough that the spring forces will actually force the particles to diverge, as each step causes the particles to overshoot their correct locations by greater and greater distances. At that point, the simulation will be considered to have achieved instability, and the surface form in the simulation will appear to have exploded.

The time step size required for instability to occur depends on a number of factors[4], including the number of particles in the simulation, the proportion between time step and spring constants, and the variation in spring constants in the simulation. The time step decreases at least as a factor of the number of particles *n*. Since the number of computations during an iteration is again proportional to *n*, the growth in time required for solution is at least n^2. This drastically limits the number of particles, and the level of detail, that can be supported by this simple numerical solution. If the time step exceeds a value roughly constrained by the speed at which forces propagate through the spring matrix, the solution becomes unstable. The prototype of the application described above (written in AutoCAD r14 C++) takes approximately 5 minutes to converge for a 30 x 30 node mesh – obviously too slow for interactive applications.

D. IMPLICIT INTEGRATION APPROACH

A more robust alternative is to adopt a solution method that takes into account higher derivatives of the differential equations of motion $\mathbf{x} = \phi(\mathbf{u}, t)$. This section takes an approach closely related to that proposed by Baraf and Witken[5] for the simulation of cloth materials – one directly applicable to the simulation of paper surfaces as well.

In order to address the instability issues of the example, a formulation of the motions of mass particles is adopted that is quadratic in time, as opposed to the linear example above. We will thus be drawing on higher, second order derivatives of the equations of motion. The inclusion of these higher order derivatives in the linked solution of the particle assembly introduces additional computational requirements. The Taylor series expansion for the integration of the position vector **x** at time $t_1 = t_0 + h$ is:

$$\mathbf{x}(t_0 + h) = \mathbf{x}(t_0) + h\dot{\mathbf{x}}(t_0) + \frac{h^2}{2!}\ddot{\mathbf{x}}(t_0) + \frac{h^3}{3!}\ddot{\mathbf{x}}(t_0) + \frac{h^n}{n!}\frac{\partial \mathbf{x}^n}{\partial t^n} + \ldots \qquad \text{(VII.15)}$$

In the example above, the solution technique approximates this function only to the first derivative, resulting in $O(h^2)$ error:

$$\mathbf{x}(t_0 + h) = \mathbf{x}(t_0) + h\dot{\mathbf{x}}(t_0) + O(h^2) \qquad \text{(VII.16)}$$

The current approach will introduce an additional, second order term:

$$\mathbf{x}(t_0 + h) = \mathbf{x}(t_0) + h\dot{\mathbf{x}}(t_0) + \frac{h^2}{2!}\ddot{\mathbf{x}}(t_0) + O(h^3) \quad \text{(VII.17)}$$

The solution technique is generally concerned with solving the ordinary differential equation:

$$\ddot{\mathbf{x}} = \mathbf{M}^{-1}(-\frac{\partial E}{\partial \mathbf{x}} + \mathbf{f}) \quad \text{(VII.18)}$$

where E is a scalar energy function representing the internal state of the material, while **f** is a function of **x** representing external forces acting on the body. The vector **x** is the geometric state of the material – an ordered 3n vector composed of the x,y, and z coordinates of the spatial points of the material. The matrix **M** represents the mass distribution of the body over the spatial points.

The first step in this solution is to formulate the internal and external forces such that the first and second derivative terms in (VII.17) may be computed. The solution technique begins by introducing a *behavior function*, which models the various phenomena in the simulation as localized equations in terms of the states of one or more of the particles. For example, the behavior function for a spring between two particles is simply:

$$C(\mathbf{p}, \mathbf{q}) = |\ \mathbf{p} - \mathbf{q}\ | - l_0 \quad \text{(VII.19)}$$

i.e., the value is the difference of the distance between the two particles' locations and some ideal spring length l_0. From the perspective of this single spring, the state of the particle configuration is optimal when $C(x_1,x_2) = 0$, or the distance between the two points is equal to the spring's ideal length. Forces generated on particles by the behavior functions will be in the direction of this optimal state. The force formulation is produced by first defining a scalar energy function

$$E = \frac{k_s}{2} C \cdot C \quad \text{(VII.20)}$$

where k_s is a stiffness constant. The force due to this scalar potential is the negative of the energy gradient, so the force on a particle represented in the function $C(\mathbf{x}_1, \ldots, \mathbf{x}_n)$ is:

$$\mathbf{f}_i = -\frac{\partial E}{\partial \mathbf{x}_i} = -k_s C \frac{\partial C}{\partial \mathbf{x}_i} \tag{VII.21}$$

Thus, we are able to determine on the basis of a general behavior function the direction and magnitude of forces on the individual particles that minimize the non-optimality expressed by the behavior functions.

E. BACKWARDS EULER METHOD

While in the simple example described in Section VII.C is solved using only a knowledge of the state of the system at the beginning of a time step t_0, the *backwards Euler* solution requires knowledge of the state of the equations of motion at the terminus of the step $t = t_0 + h$:

$$\begin{pmatrix} \Delta\mathbf{x} \\ \Delta\mathbf{v} \end{pmatrix} = h \begin{pmatrix} \mathbf{v}_0 + \Delta\mathbf{v} \\ \mathbf{M}^{-1}\mathbf{f}(\mathbf{x}_0 + \Delta\mathbf{x}, \mathbf{v}_0 + \Delta\mathbf{v}) \end{pmatrix} \tag{VII.22}$$

It is in the new formulation for the force function $\mathbf{f}(\mathbf{x}_0 + \Delta\mathbf{x}, \mathbf{v}_0 + \Delta\mathbf{v})$ that the higher order terms that produce additional stability in the solution must be provided. This function is rendered to first order approximation as:

$$\mathbf{f}(\mathbf{x}_0 + \Delta\mathbf{x}, \mathbf{v}_0 + \Delta\mathbf{v}) = \mathbf{f}_0 + \frac{\partial \mathbf{f}}{\partial \mathbf{x}}\Delta\mathbf{x} + \frac{\partial \mathbf{f}}{\partial \mathbf{v}}\Delta\mathbf{v} \tag{VII.23}$$

Substitution into (VII.22) yields:

$$(\mathbf{I} - h\mathbf{M}^{-1}\frac{\partial \mathbf{f}}{\partial \mathbf{v}} - h^2\mathbf{M}^{-1}\frac{\partial \mathbf{f}}{\partial \mathbf{x}})\Delta\mathbf{v} = h\mathbf{M}^{-1}(\mathbf{f}_0 + h\frac{\partial \mathbf{f}}{\partial \mathbf{x}}\mathbf{v}_0) \tag{VII.24}$$

Left multiplying the equation by the mass matrix M results in:

$$(\mathbf{M} - h\frac{\partial \mathbf{f}}{\partial \mathbf{v}} - h^2\frac{\partial \mathbf{f}}{\partial \mathbf{x}})\Delta\mathbf{v} = h(\mathbf{f}_0 + h\frac{\partial \mathbf{f}}{\partial \mathbf{x}}\mathbf{v}_0) \tag{VII.25}$$

This is the equation that will be solved in matrix form to produce the values for the vector $\triangle\mathbf{v}$. With the values of $\triangle\mathbf{v}$ determined, solution for the updated particle locations can be determined by "plugging in" the values for $\triangle\mathbf{v}$ in the upper part of (VII.22).

Equation (VII.25) has the following components:

- **M**, the mass matrix.
- The force vector $\mathbf{f}_0$ determined from the energy function as per (VII.21).
- The $\partial\mathbf{f}/\partial\mathbf{x}$ term, which appears twice, once on the left side of the equation multiplied by h^2 and $\triangle\mathbf{v}$, and again on the right side of the equation multiplied by h and $\mathbf{v}_0$. This is the first derivative of the force function by **x**, i.e. the *second* derivative of the energy function. Consequently (VII.25) requires a second derivative of the behavior function C. Taking the derivative (VII.21) with respect to **x** yields:

$$\frac{\partial \mathbf{f}_i}{\partial \mathbf{x}_j} = -k_s \left(\frac{\partial C(\mathbf{x})}{\partial \mathbf{x}_i} \frac{\partial C(\mathbf{x})^T}{\partial \mathbf{x}_j} + \frac{\partial^2 C(\mathbf{x})}{\partial \mathbf{x}_i \partial \mathbf{x}_j} C(\mathbf{x}) \right)$$

- $h\frac{\partial \mathbf{f}}{\partial \mathbf{v}}$, where h is the time step and $\partial\mathbf{f}/\partial\mathbf{v}$ the derivative of the force function with respect to velocity.

F. MATERIAL FORMULATION

In this section, details of the formulation of the energy functions, corresponding to specific modes of deformation for paper surfaces are presented. The modes of behavior of the system that the solution will be concerned with are *internal forces* acting between mass particles as a function of the deformation of the surface, and *external forces* such as springs, cables, viscous damping and gravity. The internal behavior of the material are rendered into three distinct deformation modes with corresponding force formulations:

1. Axial deformation, representing stretching or compression of the material. Of these, stretch will be the most common behavior, since compressive actions will typically result in buckling and bending of the material.

2. Shear deformation, representing in-plane skewing of the material. The treatment of this action will be the main characteristic distinguishing the modeling of paper surfaces from similar cloth simulations in the literature.

3. Bending deformation, represented as an angular deviation from flat at edges within the body of the material.

In constructing the formulations of the internal material forces, the deformed body principles of Section VII.B above will be revisited. It will be also beneficial to keep in mind the terminology and representation of parametric surfaces presented in Section V.D.

1. Derivatives of the Mapping Function ϕ

Consider a set of *i* particles with unchanging material coordinates (u_i,v_i) in a 2D planar space, and simultaneous spatial $\mathbf{x}_i$ coordinates in $\mathbf{R}^3$. The function:

$$\phi(u,v) = \mathbf{x} \tag{VII.26}$$

maps 2D material coordinates to spatial coordinates in $\mathbf{R}^3$. The stretch deformation is represented by the derivatives of this function with respect to *u* and *v*:

$$\phi_u = \partial\phi/\partial u \tag{VII.27}$$
$$\phi_v = \partial\phi/\partial v$$

These functions describe vectors in $\mathbf{R}^3$, analogous to the tangent vectors to the parametric curves describes in Chapter V. The magnitudes of these vectors for a given point represent the stretch (or compression) in the material directions of (u,v).

We can approximate these functions locally, by considering the deformation of a triangular region of the material in $\mathbf{R}^3$, and comparing the deformed shape of the triangle relative to its shape in parametric space. On this basis, we approximate a mapping function $\mathbf{x}= \omega(u,v)$ between parametric and world space that is applied over the region of an individual triangle. We consider the triangle with labeled nodes *i*, *j*, *k.* and define the $\mathbf{R}^3$ vectors representing the differences between the vertices' spatial coordinates:

$$\triangle x_1 = \mathbf{x}_j - \mathbf{x}_i \tag{VII.28}$$
$$\triangle x_2 = \mathbf{x}_k - \mathbf{x}_i$$

And similar differences in the (u,v) planar, parametric space of the material coordinates:

$$\triangle u_1 = u_j - u_i \,,\ \triangle v_1 = v_j - v_i \tag{VII.29}$$
$$\triangle u_2 = u_k - u_i \,,\ \triangle v_2 = v_k - v_i$$

Making the assumption that ω_u and ω_v are constant over the region defined by the triangle, we may state:

$$\Delta\mathbf{x}_1 = \omega_u \Delta u_1 + \omega_v \Delta v_1 \qquad \text{(VII.30)}$$
$$\Delta\mathbf{x}_2 = \omega_u \Delta u_2 + \omega_v \Delta v_2$$

which in turn allows the solution for ω_u and ω_v, the derivates of ω with respect to u and v:

$$\begin{aligned}(\omega_u \;\; \omega_v) &= (\Delta\mathbf{x}_1 \;\; \Delta\mathbf{x}_2)\begin{pmatrix}\Delta u_1 & \Delta u_2 \\ \Delta v_1 & \Delta v_2\end{pmatrix}^{-1} \\ &= \frac{1}{\Delta u_1 \Delta v_2 - \Delta u_2 \Delta v_1}\,(\Delta\mathbf{x}_1 \;\; \Delta\mathbf{x}_2)\begin{pmatrix}\Delta v_2 & -\Delta u_2 \\ -\Delta v_1 & \Delta u_1\end{pmatrix} \\ &= \begin{pmatrix}\dfrac{\Delta\mathbf{x}_1 \Delta v_2 - \Delta\mathbf{x}_2 \Delta v_1}{\Delta u_1 \Delta v_2 - \Delta u_2 \Delta v_1} & \dfrac{-\Delta\mathbf{x}_1 \Delta u_2 + \Delta\mathbf{x}_2 \Delta u_1}{\Delta u_1 \Delta v_2 - \Delta u_2 \Delta v_1}\end{pmatrix}\end{aligned} \qquad \text{(VII.31)}$$

2. Stretch Formulation

With the differential functions for ω_u and ω_v defined, we defined energy functions associated with stretch in the u and v directions as:

$$C_{stretch\_u}(\mathbf{x}) = a\, K_{stretch\_u}\,(\,|\omega_u| - 1) \qquad \text{(VII.32)}$$
$$C_{stretch\_v}(\mathbf{x}) = a\, K_{stretch\_v}\,(\,|\omega_v| - 1)$$

Where a is the area of the triangle (in constant, material space) and $K_{stretch\_u}$, $K_{stretch\_v}$ are constants indicating the relative stiffness of the material in stretch. While for many of materials these two constants may be equal, there are many types of materials where we may want to selectively vary the stiffness in the two directions (for example, corrugated materials, plywood, chain link meshes, etc.)

$$\begin{aligned}\frac{\partial \|\omega_u\|}{\partial \mathbf{x}_i} &= \frac{\partial \omega_u}{\partial \mathbf{x}_i}\frac{\omega_u}{\|\omega_u\|} \\ \frac{\partial \omega_u}{\partial \mathbf{x}_i} &= \begin{bmatrix}\dfrac{\partial \omega_u^1}{\partial \mathbf{x}_i^1} & \dfrac{\partial \omega_u^1}{\partial \mathbf{x}_i^2} & \dfrac{\partial \omega_u^1}{\partial \mathbf{x}_i^3} \\ \dfrac{\partial \omega_u^2}{\partial \mathbf{x}_i^1} & \dfrac{\partial \omega_u^2}{\partial \mathbf{x}_i^2} & \dfrac{\partial \omega_u^2}{\partial \mathbf{x}_i^3} \\ \dfrac{\partial \omega_u^3}{\partial \mathbf{x}_i^1} & \dfrac{\partial \omega_u^3}{\partial \mathbf{x}_i^2} & \dfrac{\partial \omega_u^3}{\partial \mathbf{x}_i^3}\end{bmatrix}\end{aligned} \qquad \text{(VII.33)}$$

If k $\neq$ l $\frac{\partial \omega_u^k}{\partial \mathbf{x}_i^l} = 0$, the derivative of ω with respect to a component of **x** is independent of any other component of **x**, and we may say:

$$\frac{\partial \omega_u}{\partial \mathbf{x}_i} = \begin{bmatrix} \frac{\partial \omega_u^1}{\partial \mathbf{x}_i^1} & 0 & 0 \\ 0 & \frac{\partial \omega_u^2}{\partial \mathbf{x}_i^2} & 0 \\ 0 & 0 & \frac{\partial \omega_u^3}{\partial \mathbf{x}_i^3} \end{bmatrix} = \frac{-\Delta v_2 + \Delta v_1}{\Delta u_1 \Delta v_2 - \Delta u_2 \Delta v} \mathbf{I}_3 \qquad \text{(VII.34)}$$

$$\mathbf{I}_3 = \begin{bmatrix} 1 & 0 & 0 \\ 0 & 1 & 0 \\ 0 & 0 & 1 \end{bmatrix}$$

Similarly,

$$\frac{\partial \omega_u}{\partial \mathbf{x}_i} = \frac{-\Delta v_2 + \Delta v_1}{\Delta u_1 \Delta v_2 - \Delta u_2 \Delta v} \mathbf{I}_3$$

$$\frac{\partial \omega_v}{\partial \mathbf{x}_i} = \frac{\Delta u_2 - \Delta u_1}{\Delta u_1 \Delta v_2 - \Delta u_2 \Delta v} \mathbf{I}_3$$

$$\frac{\partial \omega_u}{\partial \mathbf{x}_j} = \frac{\Delta v_2}{\Delta u_1 \Delta v_2 - \Delta u_2 \Delta v} \mathbf{I}_3$$

$$\frac{\partial \omega_v}{\partial \mathbf{x}_j} = \frac{-\Delta u_2}{\Delta u_1 \Delta v_2 - \Delta u_2 \Delta v} \mathbf{I}_3$$

3. Shear Function Formulation

The shear energy is approximated as by the angle of deformation in the plane of the material, for each triangle. By small angle approximation, we can presume this angle is approximately equal to its cosine for small angle deformations, and hence is formulated as the inner product of the variations in the derivatives of the mapping function:

$$\begin{aligned} C_{shear}(\mathbf{x}) &= a \omega_u{}^T \omega_v \\ &= a \begin{bmatrix} \omega_u^1 & \omega_u^2 & \omega_u^3 \end{bmatrix} \begin{bmatrix} \omega_v^1 \\ \omega_v^2 \\ \omega_v^3 \end{bmatrix} \qquad \text{(VII.35)} \\ &= \frac{a \sum_{n=1..3} \left(\left(\mathbf{x}_j^n - \mathbf{x}_i^n \right) \Delta v_2 - \left(\mathbf{x}_k^n - \mathbf{x}_i^n \right) \Delta v_1 \right) \left(- \left(\mathbf{x}_j^n - \mathbf{x}_i^n \right) \Delta u_2 + \left(\mathbf{x}_k^n - \mathbf{x}_i^n \right) \Delta u_1 \right)}{(\Delta u_1 \Delta v_2 - \Delta v_1 \Delta u_2)^2} \end{aligned}$$

$$\frac{\partial C_{shear}(\mathbf{x})}{\partial \mathbf{x}_i} = \frac{a\begin{bmatrix}\left(-\Delta v_2 + \Delta v_1\right)\left(-\left(\mathbf{x}_j^n - \mathbf{x}_i^n\right)\Delta u_2 + \left(\mathbf{x}_k^n - \mathbf{x}_i^n\right)\Delta u_1\right) + \\ \left(\Delta u_2 - \Delta u_1\right)\left(\left(\mathbf{x}_j^n - \mathbf{x}_i^n\right)\Delta v_2 - \left(\mathbf{x}_k^n - \mathbf{x}_i^n\right)\Delta v_1\right)\end{bmatrix}_{n=1..3}}{\left(\Delta u_1 \Delta v_2 - \Delta v_1 \Delta u_2\right)^2}$$

$$\frac{\partial C_{shear}(\mathbf{x})}{\partial \mathbf{x}_j} = \frac{a\begin{bmatrix}\Delta v_2\left(-\left(\mathbf{x}_j^n - \mathbf{x}_i^n\right)\Delta u_2 + \left(\mathbf{x}_k^n - \mathbf{x}_i^n\right)\Delta u_1\right) \\ -\Delta u_2\left(\left(\mathbf{x}_j^n - \mathbf{x}_i^n\right)\Delta v_2 - \left(\mathbf{x}_k^n - \mathbf{x}_i^n\right)\Delta v_1\right)\end{bmatrix}_{n=1..3}}{\left(\Delta u_1 \Delta v_2 - \Delta v_1 \Delta u_2\right)^2} \qquad \text{(VII.36)}$$

$$\frac{\partial^2 C_{shear}(\mathbf{x})}{\partial \mathbf{x}_i \partial \mathbf{x}_j} = \left[\frac{\partial^2 C(\mathbf{x})}{\partial \mathbf{x}_i^k \partial \mathbf{x}_j^l}\right]_{k,l} \in \mathbf{R}^3 \times \mathbf{R}^3$$

$$\frac{\partial^2 C_{shear}(\mathbf{x})}{\partial \mathbf{x}_i^k \partial \mathbf{x}_j^l} = \delta_{kl} a\left[\frac{\partial \omega_u}{\partial x_i^k}\frac{\partial \omega_v}{\partial x_j^l} + \frac{\partial \omega_u}{\partial x_j^l}\frac{\partial \omega_v}{\partial x_i^k}\right]$$

where δ_{kl} is the kroneker delta, equal to 1 if $k = l$, 0 otherwise. Therefore:

$$\frac{\partial^2 C_{shear}(\mathbf{x})}{\partial \mathbf{x}_i \partial \mathbf{x}_j} = a\left(\frac{\partial \omega_u}{\partial x_i}\frac{\partial \omega_v}{\partial x_j} + \frac{\partial \omega_u}{\partial x_j}\frac{\partial \omega_v}{\partial x_i}\right) \qquad \text{(VII.37)}$$

4. Bend Function Formulation

In contrast to the stretch and shear formulations, where these functions are considered relative to the deformation of a single triangle, the bending of a triangulated mesh will be considered by changes in the angle between two triangles, at the adjoining edge. If we presume that the reference configuration is initially flat, initial angle at each edge is 0 and the energy associated with bending deformation will be proportional to the angle θ formed at the edge:

$C_{bend}(\mathbf{x}) = K_{bend}\theta$ (VII.38)

This angle is equivalent to the angle between the normals of the two triangles $\mathbf{n}_1$ and $\mathbf{n}_2$. Letting **e** be the unit vector parallel to the edge, the trigonometric relations for the angle are:

$\sin(\theta) = (\mathbf{n}_1 \times \mathbf{n}_2) \bullet \mathbf{e}$ (VII.39)

$\cos(\theta) = \mathbf{n}_1 \bullet \mathbf{n}_2$

$$\mathbf{n} = \frac{\overrightarrow{\mathbf{x}_i\mathbf{x}_j}}{\left\|\overrightarrow{\mathbf{x}_i\mathbf{x}_j}\right\|} \times \frac{\overrightarrow{\mathbf{x}_i\mathbf{x}_k}}{\left\|\overrightarrow{\mathbf{x}_i\mathbf{x}_k}\right\|} = \frac{1}{\left\|\overrightarrow{\mathbf{x}_i\mathbf{x}_j}\right\|\left\|\overrightarrow{\mathbf{x}_i\mathbf{x}_k}\right\|} \begin{bmatrix} \Delta\mathbf{x}_1^1\Delta\mathbf{x}_2^2 - \Delta\mathbf{x}_1^2\Delta\mathbf{x}_2^1 \\ \Delta\mathbf{x}_1^2\Delta\mathbf{x}_2^0 - \Delta\mathbf{x}_1^0\Delta\mathbf{x}_2^2 \\ \Delta\mathbf{x}_1^0\Delta\mathbf{x}_2^1 - \Delta\mathbf{x}_1^1\Delta\mathbf{x}_2^0 \end{bmatrix} \tag{VII.40}$$

$$\mathbf{e} = \frac{\overrightarrow{\mathbf{x}_j\mathbf{x}_i}}{\left\|\overrightarrow{\mathbf{x}_j\mathbf{x}_i}\right\|} \tag{VII.41}$$

If we presume that **e** varies little as a function of **x**, then

$$\frac{\partial \mathbf{n}}{\partial \mathbf{x}_i} = \frac{1}{\left\|\overrightarrow{\mathbf{x}_i\mathbf{x}_j}\right\|\left\|\overrightarrow{\mathbf{x}_i\mathbf{x}_k}\right\|} \begin{bmatrix} 0 & -\Delta\mathbf{x}_2^2 + \Delta\mathbf{x}_1^2 & -\Delta\mathbf{x}_1^1 + \Delta\mathbf{x}_2^1 \\ -\Delta\mathbf{x}_1^2 + \Delta\mathbf{x}_2^2 & 0 & -\Delta\mathbf{x}_2^0 + \Delta\mathbf{x}_1^0 \\ -\Delta\mathbf{x}_2^1 + \Delta\mathbf{x}_1^1 & -\Delta\mathbf{x}_1^0 + \Delta\mathbf{x}_2^0 & 0 \end{bmatrix} \tag{VII.42}$$

$$\frac{\partial \mathbf{n}}{\partial \mathbf{x}_j} = \frac{1}{\left\|\overrightarrow{\mathbf{x}_i\mathbf{x}_j}\right\|\left\|\overrightarrow{\mathbf{x}_i\mathbf{x}_k}\right\|} \begin{bmatrix} 0 & \Delta\mathbf{x}_2^2 & -\Delta\mathbf{x}_2^1 \\ -\Delta\mathbf{x}_2^2 & 0 & \Delta\mathbf{x}_2^0 \\ \Delta\mathbf{x}_2^1 & -\Delta\mathbf{x}_2^0 & 0 \end{bmatrix}$$

$$\frac{\partial \mathbf{n}}{\partial \mathbf{x}_k} = \frac{1}{\left\|\overrightarrow{\mathbf{x}_i\mathbf{x}_j}\right\|\left\|\overrightarrow{\mathbf{x}_i\mathbf{x}_k}\right\|} \begin{bmatrix} 0 & -\Delta\mathbf{x}_1^2 & \Delta\mathbf{x}_1^1 \\ \Delta\mathbf{x}_1^2 & 0 & -\Delta\mathbf{x}_1^0 \\ -\Delta\mathbf{x}_1^1 & \Delta\mathbf{x}_1^0 & 0 \end{bmatrix}$$

$$\begin{aligned} \frac{\partial C_{bend}(\mathbf{x})}{\partial \mathbf{x}_i} &= \frac{\partial \theta}{\partial \mathbf{x}_i} \\ &= -\frac{1}{\sin(\theta)} \frac{\partial \cos(\theta)}{\partial \mathbf{x}_i} \\ &= \frac{1}{\cos(\theta)} \frac{\partial \sin(\theta)}{\partial \mathbf{x}_i} \end{aligned} \tag{VII.43}$$

where

$$\begin{aligned} \frac{\partial \cos(\theta)}{\partial \mathbf{x}_i} &= -\sin(\theta)\frac{\partial \theta}{\partial \mathbf{x}_i} \\ \frac{\partial \sin(\theta)}{\partial \mathbf{x}_i} &= \cos(\theta)\frac{\partial \theta}{\partial \mathbf{x}_i} \end{aligned} \tag{VII.44}$$

$$\begin{aligned}\frac{\partial^2 C_{bend}(\mathbf{x})}{\partial \mathbf{x}_i \partial \mathbf{x}_j} &= \frac{\partial^2 \theta}{\partial \mathbf{x}_i \partial \mathbf{x}_j} \\ &= -\frac{1}{\sin(\theta)} \frac{\partial^2 \cos(\theta)}{\partial \mathbf{x}_i \partial \mathbf{x}_j} + \frac{1}{\sin(\theta)^2} \frac{\partial \sin(\theta)}{\partial \mathbf{x}_i} \frac{\partial \cos(\theta)}{\partial \mathbf{x}_j} \\ &= \frac{1}{\cos(\theta)} \frac{\partial^2 \sin(\theta)}{\partial \mathbf{x}_i \partial \mathbf{x}_j} - \frac{1}{\cos(\theta)^2} \frac{\partial \sin(\theta)}{\partial \mathbf{x}_i} \frac{\partial \cos(\theta)}{\partial \mathbf{x}_j} \\ &= -\frac{1}{\sin(\theta)} \frac{\partial^2 \cos(\theta)}{\partial \mathbf{x}_i \partial \mathbf{x}_j} + \frac{\cos(\theta)}{\sin(\theta)} \frac{\partial \theta}{\partial \mathbf{x}_i} \frac{\partial \theta}{\partial \mathbf{x}_j}\end{aligned} \tag{VII.45}$$

where:

$$\begin{aligned}\frac{\partial^2 \cos(\theta)}{\partial \mathbf{x}_i \partial \mathbf{x}_j} &= -\cos(\theta) \frac{\partial \theta}{\partial \mathbf{x}_i} \frac{\partial \theta}{\partial \mathbf{x}_j} - \sin(\theta) \frac{\partial^2 \theta}{\partial \mathbf{x}_i \partial \mathbf{x}_j} \\ &= \frac{1}{\sin(\theta)} \frac{\partial \sin(\theta)}{\partial \mathbf{x}_i} \frac{\partial \cos(\theta)}{\partial \mathbf{x}_j} - \sin(\theta) \frac{\partial^2 \theta}{\partial \mathbf{x}_i \partial \mathbf{x}_j} \\ \frac{\partial^2 \sin(\theta)}{\partial \mathbf{x}_i \partial \mathbf{x}_j} &= -\sin(\theta) \frac{\partial \theta}{\partial \mathbf{x}_i} \frac{\partial \theta}{\partial \mathbf{x}_j} + \cos(\theta) \frac{\partial^2 \theta}{\partial \mathbf{x}_i \partial \mathbf{x}_j} \\ &= \frac{1}{\cos(\theta)} \frac{\partial \sin(\theta)}{\partial \mathbf{x}_i} \frac{\partial \cos(\theta)}{\partial \mathbf{x}_j} + \cos(\theta) \frac{\partial^2 \theta}{\partial \mathbf{x}_i \partial \mathbf{x}_j}\end{aligned} \tag{VII.46}$$

Figure VII-5 provides an initial view of the sheet material simulation, with a corresponding graph of the internal strain deformation associated with the shape.

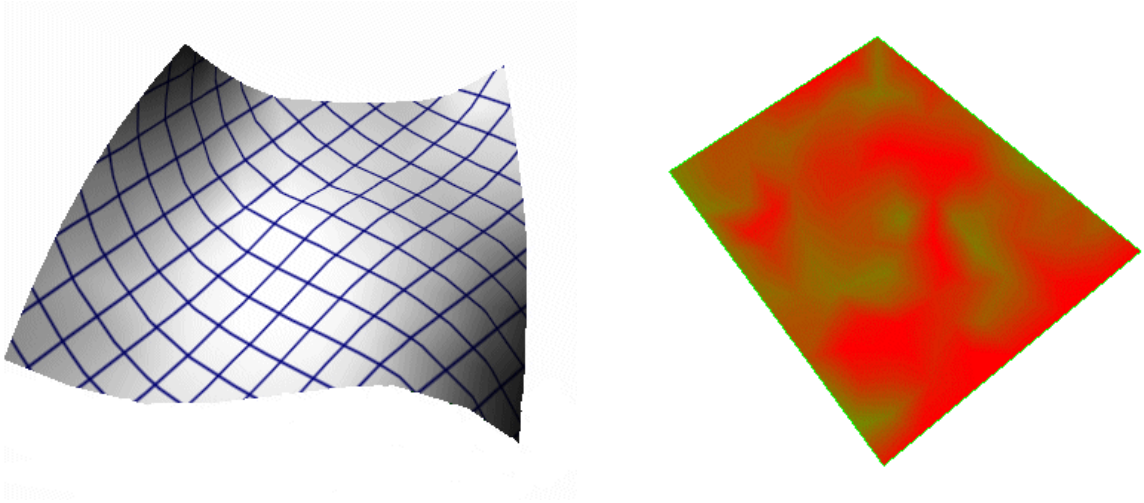

Deformed shape in R^3, with R^2 coordinate mapping on surface

Corresponding strain map in R^2

Figure VII-5: Sheet configuration and internal strain map

5. Damping

The definition of an appropriate damping function is critical to the simulation. Although the formulation represents the behavior of the paper material as a dynamic, time based simulation, the primary concern in this application is the ultimate, static behavior of the materials once they have "settled down" to a minimal energy configuration state, and the velocities and accelerations of the particles have fallen to within some threshold of 0. A "springy" system without the presence of damping will oscillate about the rest state, and never settle down. Thus damping serves the important function of driving the simulation to the rest state, by dissipating the kinetic energy in the system. At the same time, damping competes with the action of forces, and their associated accelerations and velocities, in driving the system toward the minimal energy rest state. Thus, tuning the damping to allow efficient translation of the mass particles toward the rest state, while minimizing over-shooting and oscillation, is an important component in efficiently moving the simulation toward solution.

Damping serves a second important function in the stability of the simulation. By damping out residual forces resulting from the second order approximation of the differential equations of motion, a damping component allows larger time steps to be achieved while still allowing stability of the simulation.

A straight forward formulation of damping effects on a particle is viscous damping, where the force on the particle is inversely proportional to the particle's velocity:

$$\mathbf{f}_{damp} = - K_{damp}\,\mathbf{v}(\mathrm{x}) \qquad \text{(VII.47)}$$

which approximates the behavior as if it were immersed in some motion resistant medium such as air, water, or "jelly" – depending on the value of K_{damp}. Barraf and Witkin's formulation draws on the second term of (VII.24), $h\mathbf{M}^{-1}\frac{\partial \mathbf{f}}{\partial \mathbf{v}}$, as the means for formulating damping associated with a given deformation mode. The damping acts on the component of system velocity in the $\partial C/\partial x$ direction, and provides damping associated with a energy function condition C as:

$$\mathbf{f}_{damp} = -K_{damp}\frac{\partial C}{\partial \mathbf{x}_i}\dot{C}(\mathbf{x}) \qquad \text{(VII.48)}$$

While this formulation results in more believable time based simulations of motion, it results in additional computational overhead in computing the additional energy function derivatives. Since our paper simulator application is concerned principally with accurately representing the rest state of the body, this additional overhead required to provide a more realistic simulation of the body's behavior over time does not seem necessary, and the more straight forward viscous damping formulation has been used in the simulator.

6. Springs

In the paper modeler, a spring is typically an object – and associated energy condition - that attempts to bring a mass particle within a specified distance of either a location in space or another mass particle. The desired distance may be 0, or some desired rest length of the spring. The general formulation of spring energy functions is :

$$C_{spring}(\mathbf{x}_1, \mathbf{x}_2) = K_{spring}\,(|\,\mathbf{x}_1 - \mathbf{x}_2\,| - l\,) \qquad \text{(VII.49)}$$

where l is the rest length of the spring. Note that we may select varying values of K_{spring} for different springs in the system, resulting in differing types of behavior for individual springs.

There are a variety of useful applications of spring objects in the modeler:

- As a means for fixing the material in space. Individual mass particles can have springs affixed to specific spatial locations. These springs will guide the simulation to a solution where the particles remain spatially located near these determined points in space.

- As a means for user manipulation of the materials. Mass particles may be attached to space points indicated by the user. These locations may be interactively manipulated by mouse motion. The material particles will attempt to follow the motions of the mouse as the simulation progresses. The location indicated by the user may be dynamically updated between solution steps.

- As a means for joining mass particles together. Springs may be attached between two mass particles, in which case the solver will attempt to bring these two particles within

some relative distance of each other. Again, this distance may be 0, or some other desired length.

There are a number of issues in the use of spring elements to achieve these goals using an energy based solution. If we are interested in the particle being actually located at a target point in space, thus the rest length of the spring $l = 0$. The spring element will compete with the rest of the objects in the simulation in trying to achieve this goal. Thus if other forces are pulling on the mass particle to which the spring is affixed, the particle will be only relatively near the ideal location. The relative strength of the attracting force is dictated by the magnitude of K_{spring}. Setting the value of K_{spring} large relative to the other K values in the simulation will reduce the distance between the node and the goal locations, but will never bring the distance to exactly zero. Additionally, making the value of K_{spring} excessively large will introduce stiffness into the solution, resulting in a decrease in the stable time step.

An alternative is to simply force the location of the mass particle to a position in space. The solution of the simulation will provide a displacement of the particle on the basis of the energy function, but we can presume an additional effect, not included in the solution formulation, that drives the particle back to the pre-determined location. The result is that changes in the particle's location are ignored. This approach works well when the particle is already at the desired position. But moving the particle instantaneously to a new location will introduce large deformations in simulation objects related to the particle, which can lead to instability. Constraining a mass particle to follow exactly a motion specified by mouse movement will jerk the particle around in space, resulting in idiosyncratic motion of the particle and associated influxes of kinetic energy into the system if springs are attached to the particle.

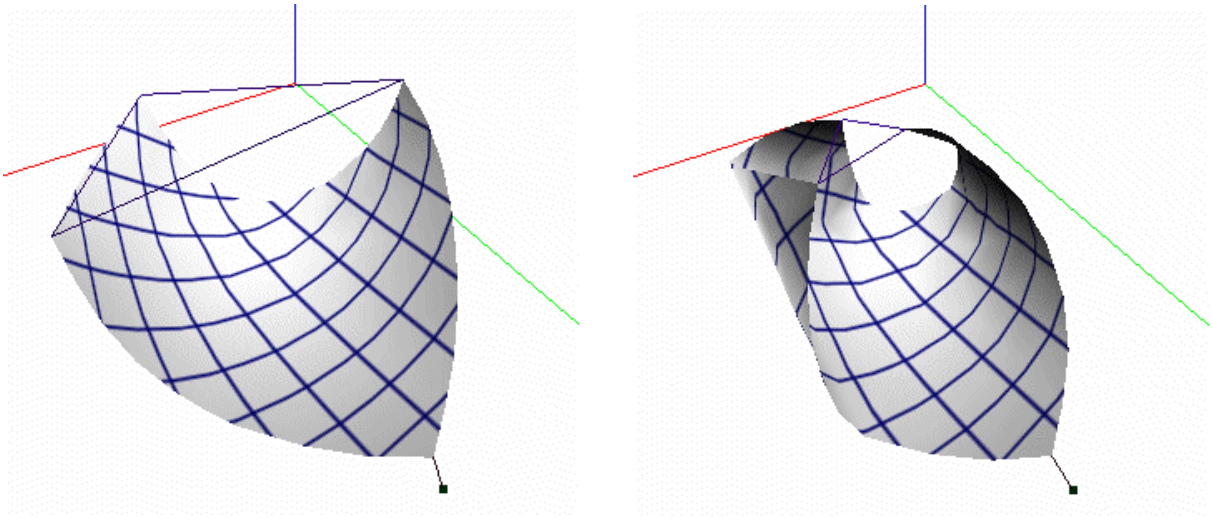

Figure VII-6: Spring assembly with variations of spring force coefficient

7. Gravity and Attraction

A variety of phenomena may be represented by forces acting in a direction in space. A simple example is the force of gravity acting on the body. This is represented simply as:

$$\mathbf{f}_{\text{gravity}} = m\, a_g\, [0\ 0\ -1]^T \qquad \text{(VII.50)}$$

where m is the mass of particle, and a_g the gravitational acceleration.

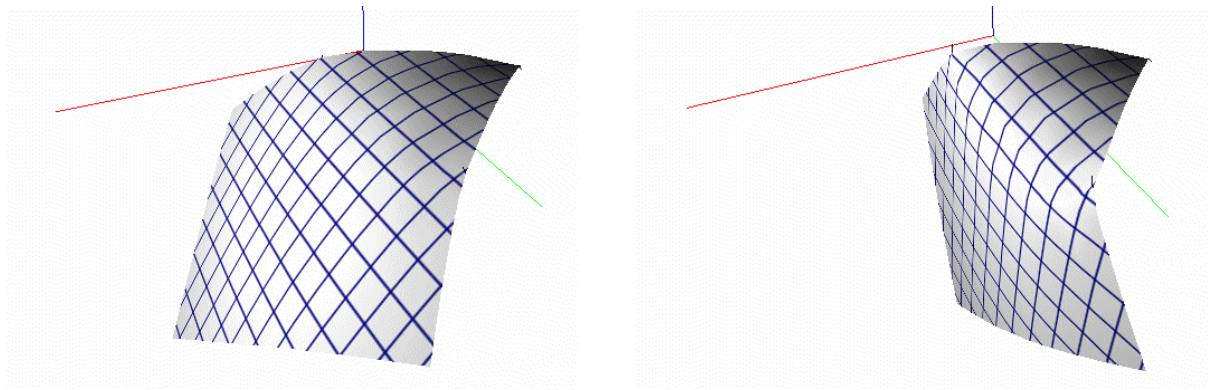

Figure VII-7: Varying the gravitational constant

Other forces may be similarly formulated. An important example is notion of an attractor force, which exerts a force toward some shape. This may be viewed as a sort of vacuum or, at closer range, fastening phenomenon, that attempts to draw the material toward an ideal shape.

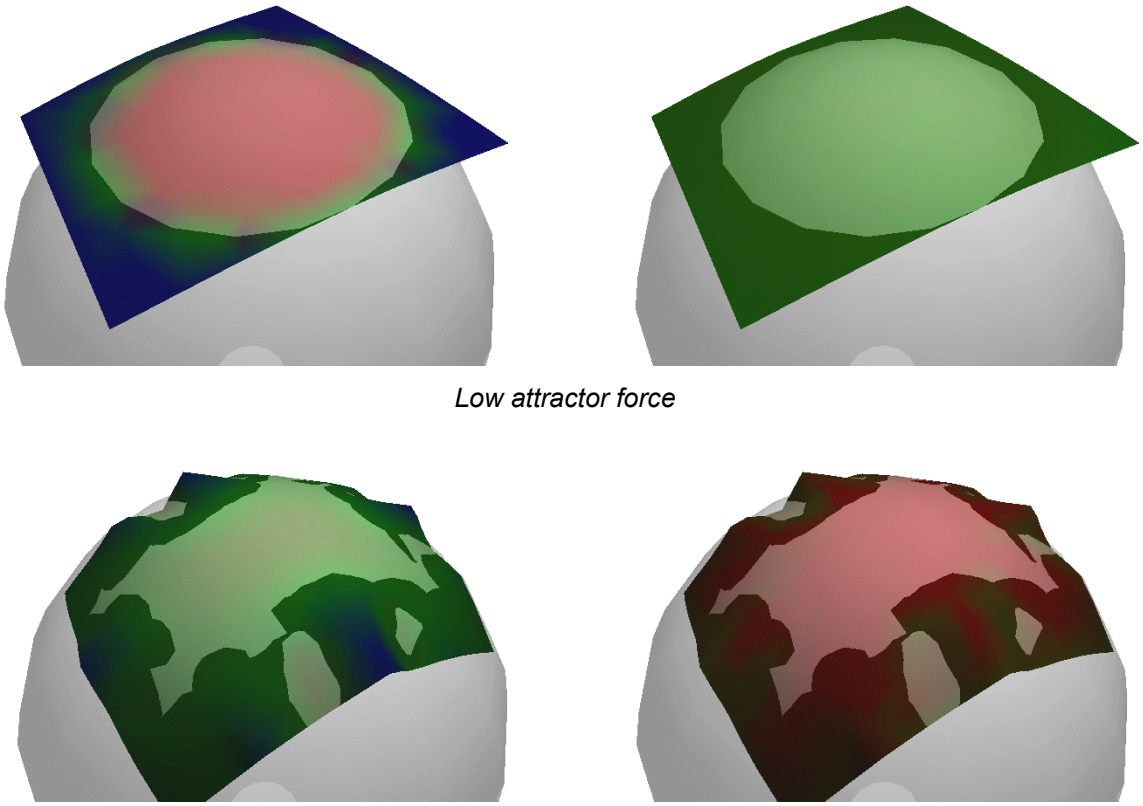

Low attractor force

High attractor force

Distance function mapping *Strain function mapping*

Figure VII-8: Variation of attractor force coefficient

An example is shown in Figure VII-8, where the paper material is drawn toward a set of spheres by fastening forces of varying intensities. In the case of a sphere

$$\mathbf{f}_{sphere} = \boldsymbol{m}\, K_{sphere}\, (|\mathbf{x} - \mathbf{c}| - r) \bullet (\mathbf{x} - \mathbf{c})/(|\mathbf{x} - \mathbf{c}|) \qquad \text{(VII.51)}$$

Where **c** is the location of the center of the sphere, r is the sphere's radius, and $(\mathbf{x} - \mathbf{c})/(|\mathbf{x} - \mathbf{c}|)$ is the unit vector from the particle's location to the center. Other shapes may present more complicated geometric formulations of gravitation towards the shape, generally directed along the normal vector to the closest point on the object.

G. SOLUTION METHOD

So far a number of physical phenomena of interest in the simulation of paper surface behavior have been described. This section picks up from Section VII.E, presenting the construction of the global matrices and vectors of Equation (VII.24), and discusses an

efficient method for the solution of this equation, based on the conjugate gradient solution method.

1. Matrix Construction

Constraints in the system are formulated using the general equation from (VII.25):

$$(\mathbf{M} - h\frac{\partial \mathbf{f}}{\partial \mathbf{v}} - h^2\frac{\partial \mathbf{f}}{\partial \mathbf{x}})\Delta\mathbf{v} = h(\mathbf{f}_0 + h\frac{\partial \mathbf{f}}{\partial \mathbf{x}}\mathbf{v}_0)$$

The formulations discussed in Section VII.VII.F expand on this function by providing the internal and external constraint functions and their derivatives. If we ignore the velocity based components of this function and expand, we have:

$$(\mathbf{M} - h^2\frac{\partial \mathbf{f}}{\partial \mathbf{x}})\Delta\mathbf{v} = h\mathbf{f}_0 + h^2\frac{\partial \mathbf{f}}{\partial \mathbf{x}}\mathbf{v}_0 \qquad \text{(VII.52)}$$

where the force in the direction *i* is:

$$\mathbf{f}_i = -k_s C(\mathbf{x})\frac{\partial C(\mathbf{x})}{\partial \mathbf{x}_i} \qquad \text{(VII.53)}$$

and the force derivative in the direction of with respect to the direction *j* is:

$$\frac{\partial \mathbf{f}_i}{\partial \mathbf{x}_j} = -k_s\left(\frac{\partial C(\mathbf{x})}{\partial \mathbf{x}_i}\frac{\partial C(\mathbf{x})^T}{\partial \mathbf{x}_j} + \frac{\partial^2 C(\mathbf{x})}{\partial \mathbf{x}_i \partial \mathbf{x}_j}C(\mathbf{x})\right) \qquad \text{(VII.54)}$$

Equation (VII.25) may be formulated as a matrix solution of the form **Ax=b.** The right hand side of the equation takes the form of a 3*n* block vector, where the forces acting on the i^{th} particle are entered in the i^{th} block of the vector. Similarly, the left hand side of the equation, representing the force derivatives, may be organized as a 3*n*x3*n* block matrix, where the (3 X 3) block element (i, j) contain the derivative of the energy function $\frac{\partial \mathbf{f}_i}{\partial \mathbf{x}_j}$.

	x_0	y_0	z_0	x_1	y_1	z_1	x_2	y_2	z_2	x_3	y_3	z_3			
x_0	$\frac{1}{m_0}$			$\frac{\delta fx0}{\delta x1}$	$\frac{\delta fx0}{\delta y1}$	$\frac{\delta fx0}{\delta z1}$	$\frac{\delta fx0}{\delta x2}$	$\frac{\delta fx0}{\delta y2}$	$\frac{\delta fx0}{\delta z2}$	$\frac{\delta fx0}{\delta x3}$	$\frac{\delta fx0}{\delta y3}$	$\frac{\delta fx0}{\delta z3}$	$\Delta\mathbf{v}_{x0}$		$\mathbf{f}_{x0}$
y_0		$\frac{1}{m_0}$		$\frac{\delta fy0}{\delta x1}$	$\frac{\delta fy0}{\delta y1}$	$\frac{\delta fyo}{\delta z1}$	$\frac{\delta fy0}{\delta x2}$	$\frac{\delta fy0}{\delta y2}$	$\frac{\delta fyo}{\delta z2}$	$\frac{\delta fy0}{\delta x3}$	$\frac{\delta fy0}{\delta y3}$	$\frac{\delta fyo}{\delta z3}$	$\Delta\mathbf{v}_{y0}$		$\mathbf{f}_{y0}$
z_0			$\frac{1}{m_0}$	$\frac{\delta fz0}{\delta x1}$	$\frac{\delta fz0}{\delta y1}$	$\frac{\delta fz0}{\delta z1}$	$\frac{\delta fz0}{\delta x2}$	$\frac{\delta fz0}{\delta y2}$	$\frac{\delta fz0}{\delta z2}$	$\frac{\delta fz0}{\delta x3}$	$\frac{\delta fz0}{\delta y3}$	$\frac{\delta fz0}{\delta z3}$	$\Delta\mathbf{v}_{z0}$		$\mathbf{f}_{y0}$
x_1	$\frac{\delta fx1}{\delta x0}$	$\frac{\delta fx1}{\delta y0}$	$\frac{\delta fx1}{\delta z0}$	$\frac{1}{m_1}$			$\frac{\delta fx1}{\delta x2}$	$\frac{\delta fx1}{\delta y2}$	$\frac{\delta fx1}{\delta z2}$	$\frac{\delta fx1}{\delta x3}$	$\frac{\delta fx1}{\delta y3}$	$\frac{\delta fx1}{\delta z3}$	$\Delta\mathbf{v}_{x1}$		$\mathbf{f}_{x1}$
y_1	$\frac{\delta fy1}{\delta x0}$	$\frac{\delta fy1}{\delta y0}$	$\frac{\delta fy1}{\delta z0}$		$\frac{1}{m_1}$		$\frac{\delta fy1}{\delta x2}$	$\frac{\delta fy1}{\delta y2}$	$\frac{\delta fy1}{\delta z2}$	$\frac{\delta fy1}{\delta x3}$	$\frac{\delta fy1}{\delta y3}$	$\frac{\delta fy1}{\delta z3}$	$\Delta\mathbf{v}_{y1}$		$\mathbf{f}_{y1}$
z_1	$\frac{\delta fz1}{\delta x0}$	$\frac{\delta fz1}{\delta y0}$	$\frac{\delta fz1}{\delta z0}$			$\frac{1}{m_1}$	$\frac{\delta fz1}{\delta x2}$	$\frac{\delta fz1}{\delta y2}$	$\frac{\delta fz1}{\delta z2}$	$\frac{\delta fz1}{\delta x3}$	$\frac{\delta fz1}{\delta y3}$	$\frac{\delta fz1}{\delta z3}$	$\Delta\mathbf{v}_{z1}$	=	$\mathbf{f}_{y1}$
x_2	$\frac{\delta fx2}{\delta x0}$	$\frac{\delta fx2}{\delta y0}$	$\frac{\delta fx2}{\delta z0}$	$\frac{\delta fx2}{\delta x1}$	$\frac{\delta fx2}{\delta y1}$	$\frac{\delta fx2}{\delta z1}$	$\frac{1}{m_2}$			$\frac{\delta fx2}{\delta x3}$	$\frac{\delta fx2}{\delta y3}$	$\frac{\delta fx2}{\delta z3}$	$\Delta\mathbf{v}_{x2}$		$\mathbf{f}_{x2}$
y_2	$\frac{\delta fy2}{\delta x0}$	$\frac{\delta fy2}{\delta y0}$	$\frac{\delta fy2}{\delta z0}$	$\frac{\delta fy2}{\delta x1}$	$\frac{\delta fy2}{\delta y1}$	$\frac{\delta fy2}{\delta z1}$		$\frac{1}{m_2}$		$\frac{\delta fy2}{\delta x3}$	$\frac{\delta fy2}{\delta y3}$	$\frac{\delta fy2}{\delta z3}$	$\Delta\mathbf{v}_{y2}$		$\mathbf{f}_{y2}$
z_2	$\frac{\delta fz2}{\delta x0}$	$\frac{\delta fz2}{\delta y0}$	$\frac{\delta fz2}{\delta z0}$	$\frac{\delta fz2}{\delta x1}$	$\frac{\delta fz2}{\delta y1}$	$\frac{\delta fz2}{\delta z1}$			$\frac{1}{m_2}$	$\frac{\delta fz2}{\delta x3}$	$\frac{\delta fz2}{\delta y3}$	$\frac{\delta fz2}{\delta z3}$	$\Delta\mathbf{v}_{z2}$		$\mathbf{f}_{y2}$
x_3	$\frac{\delta fx3}{\delta x0}$	$\frac{\delta fx3}{\delta y0}$	$\frac{\delta fx3}{\delta z0}$	$\frac{\delta fx3}{\delta x1}$	$\frac{\delta fx3}{\delta y1}$	$\frac{\delta fx3}{\delta z1}$	$\frac{\delta fx3}{\delta x2}$	$\frac{\delta fx3}{\delta y2}$	$\frac{\delta fx3}{\delta z2}$	$\frac{1}{m_3}$			$\Delta\mathbf{v}_{x3}$		$\mathbf{f}_{x3}$
y_3	$\frac{\delta fy3}{\delta x0}$	$\frac{\delta fy3}{\delta y0}$	$\frac{\delta fy3}{\delta z0}$	$\frac{\delta fy3}{\delta x1}$	$\frac{\delta fy3}{\delta y1}$	$\frac{\delta fy3}{\delta z1}$	$\frac{\delta fy3}{\delta x2}$	$\frac{\delta fy3}{\delta y2}$	$\frac{\delta fy3}{\delta z2}$		$\frac{1}{m_3}$		$\Delta\mathbf{v}_{y3}$		$\mathbf{f}_{y3}$
z_3	$\frac{\delta fz3}{\delta x0}$	$\frac{\delta fz3}{\delta y0}$	$\frac{\delta fz3}{\delta z0}$	$\frac{\delta fz3}{\delta x1}$	$\frac{\delta fz3}{\delta y1}$	$\frac{\delta fz3}{\delta z1}$	$\frac{\delta fz3}{\delta x2}$	$\frac{\delta fz3}{\delta y2}$	$\frac{\delta fz3}{\delta z2}$			$\frac{1}{m_3}$	$\Delta\mathbf{v}_{z3}$		$\mathbf{f}_{y3}$

Figure VII-9: Matrix organization

2. Numerical Solution

The behavior of a specific constraint in the system affects only a small number of material particles in the system – specifically:

- (3) particles of a given triangle over which stretch and shear forces are considered
- (4) particles comprising the two triangles joined at an edge undergoing bending
- (2) particles joined by a spring
- a single particle connected by a spring to a point in space

The block matrix and block vector entries will be non-zero only for the particles inter-related by a constraint. The rest of the entries into these constructs will be zero. The linear independence of the constraints allow constraint entries to be summed.

Each particle in the system is represented as an object with a state, comprised of its:

- mass, $m_i \in \mathbf{R}$
- current position in space, $\mathbf{x}_i \in \mathbf{R}^3$
- current velocity, $\mathbf{v}_i \in \mathbf{R}^3$
- index into the global stiffness matrix and force vectors

At the beginning of each time step, the global derivative matrix **A** is initialized to be equal to the inverse of the mass matrix 1/**M**, while the force vector global force vector **b** is set to 0. A time step *h* is considered as input to the solution – the means for determining this time step is presented in VI.H.3 below.

Each constraint is considered in turn, and for each constraint the related pairs of particles are considered independently. The energy function *C* – a scalar - is computed for each constraint. The derivatives of the constraint's energy function $\partial C(\mathbf{x})/\partial \mathbf{x}_i$ are determined for each particle associated with the constraint. The second derivatives $\partial^2 C(\mathbf{x})\partial \mathbf{x}_i \partial \mathbf{x}_j$ are then computed for each particle pair.

The force on each particle $\mathbf{f}_i$ is computed in a straightforward fashion using (VII.53), multiplied by the time step, and the result added to the global force vector in the particle's associated block – the i^{th} block of the force vector $\mathbf{b}_i$. Similarly, the second derivative component $h^2 \frac{\partial \mathbf{f}}{\partial \mathbf{x}} \mathbf{v}_0$ is computed from the force derivative of the particle, the time step squared, and the velocity of the particle at the beginning of the time step.

The derivative of the force on particle *i* with respect to the variation in each of the constraint's associated particles *j* is next computed from the general form (VII.54), and added into the global force derivative matrix at the block $\mathbf{A}_{i,j}$. The change in velocity of the particles is determined by solving the linear equation:

$$\triangle \mathbf{v} = \mathbf{A}^{-1}\mathbf{b} \qquad \text{(VII.55)}$$

From this result, the new velocities of the particles are computed in a straight forward fashion by summing the particles' velocities $\mathbf{v}_0$ with $\triangle \mathbf{v}$. The new particle positions are then computed

by adding the multiplying this new velocity by the time step and adding to the original particle position.

The solution of (VII.55) requires that the inverse of the matrix **A** be computed. Under the most general circumstances, this inversion is of order $O(n^3)$ complexity – a potentially heavy penalty in the performance of the backwards Euler simulation approach. However, characteristics of the matrix can be taken advantage of to reduce the computational complexity of this inversion. This linear system is sparse, since block matrix elements are non zero only for those entries corresponding to particles inter-related by constraints: the neighboring particles in the mesh, or particles joined by springs. The sparisty pattern for a simple system is illustrate in Figure VII-10 below.

Additionally, since $\partial \mathbf{f}_i / \partial \mathbf{x}_j = \partial \mathbf{f}_j / \partial \mathbf{x}_i$ the matrix is symmetric. Furthermore the matrix **A** is positive definite, since the energy in the system is never less than zero. These conditions are sufficient to allow the matrix inversion to be conducted numerically, using a conjugate gradient method[70,76]. This approach reduces the computational complexity of the matrix inversion to approximately $O(n \log_n)$, well justified on the basis of the larger time steps afforded relative to the forward Euler solution method.

	x_0	y_0	z_0	x_1	y_1	z_1	x_2	y_2	z_2	x_3	y_3	z_3			
x_0	$\frac{1}{m_0}$			-1	0	0							ΔV_{x0}		f_{x0}
y_0		$\frac{1}{m_0}$		0	0	0							ΔV_{y0}		f_{y0}
z_0			$\frac{1}{m_0}$	0	0	0							ΔV_{z0}		f_{y0}
x_1	1	0	0	$\frac{1}{m_1}$									ΔV_{x1}		f_{x1}
y_1	0	0	0		$\frac{1}{m_1}$								ΔV_{y1}		f_{y1}
z_1	0	0	0			$\frac{1}{m_1}$							ΔV_{z1}	=	f_{y1}
x_2							$\frac{1}{m_2}$						ΔV_{x2}		
y_2								$\frac{1}{m_2}$					ΔV_{y2}		
z_2									$\frac{1}{m_2}$				ΔV_{z2}		
x_3										$\frac{1}{m_3}$			ΔV_{x3}		
y_3											$\frac{1}{m_3}$		ΔV_{y3}		
z_3												$\frac{1}{m_3}$	ΔV_{z3}		

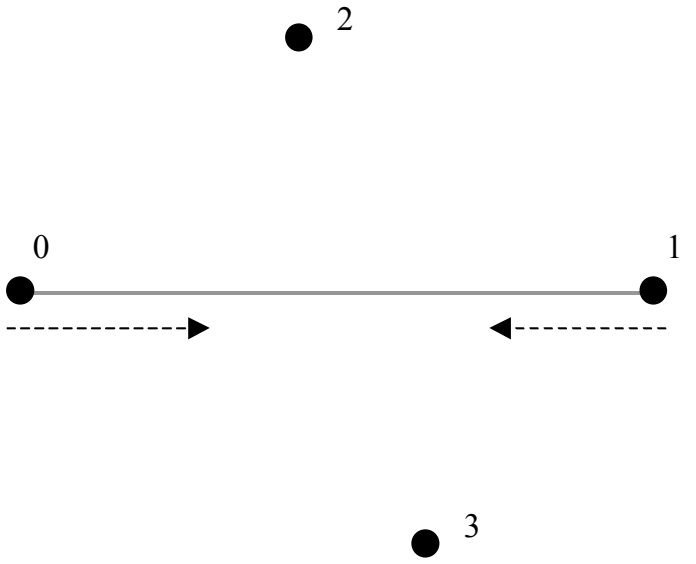

Figure VII-10: Sparsity pattern of a simple-mass spring system

H. THE INTERACTIVE FRAMEWORK

1. Introduction

On the basis of the solution method presented above, a prototype interface has been developed to demonstrate the functionality and user interactions supporting physical modeling of paper surfaces. Among the goals for the prototype:

- Support modeling of a variety of materials, including paper-like materials and cloth- or mesh-like materials,
- Provide intuitive tools for manipulating sheet elements,
- Support the simulation of physical phenomena affecting material placement, including cables and fasteners, and features found in real material assemblies such as rips, creases, cuts and dodges,
- Allow manipulations in interactive time,
- Provide mechanisms supporting the rationalization of ideal shapes, by guiding material assemblies toward these shapes,
- Provide a framework for the automation of rationalization operations, to be discussed in Part 3.

The prototype is organized around the dual notions of space presented in Part 2:

- A *global*, Euclidean $\mathbf{R}^3$ space, containing material sheets, lights, and other objects which interact with sheet entities,
- One or more *local*, $\mathbf{R}^2$ material or parametric spaces of the individual sheet entities, where interaction with features of the sheets may be manipulated.

Sheet entities thus have a dual representation in the simulator, the 3D potentially deformed representation in the global space, and a representation of the flattened, “paper space” of the material itself.

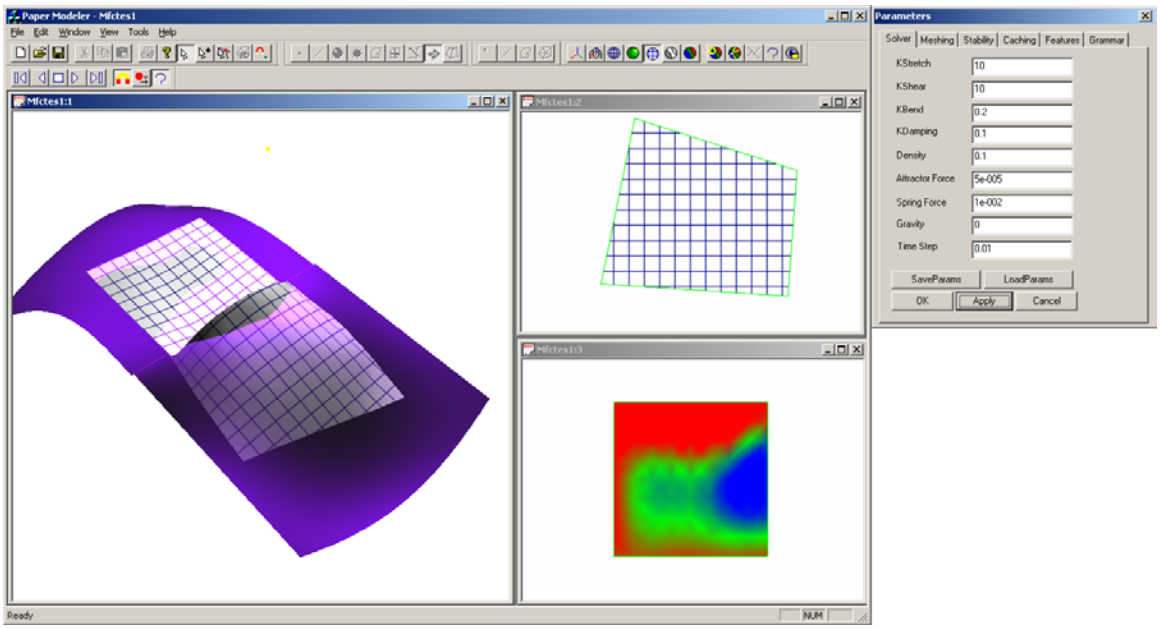

Figure VII-11: Paper simulator interface

Figure VII-11 shows an overview of the simulator space. A view port into the global 3D space is on the left, displaying two material sheets positioned in space, and a Bézier surface attractor object. In the middle are two view ports into the separate 2D spaces corresponding to the two material sheets. The top view simply displays a grid representing the material space coordinates of the sheet, while the bottom view displays a graph showing the distance between the sheet and the attractor. Multiple 2D view ports on individual spaces are supported. Mouse based interactions support rotation, translation and zooming of the space view, and mechanisms for positioning and deforming objects in space. Similar capabilities are supported in the material views, although all such interactions are limited by the two dimensional nature of the space. At right, a dialog allows editing of the solution parameters.

A variety of geometric object types are supported by the interface; most have potential implications for the behavior and deformation of material sheets. Geometrics support individual coloring and, where appropriate, transparency. Examples of 3D spatial objects supported by the interface include:

- The material sheet objects themselves

- Various surface based “attractor” objects, suitable for representing design surfaces, to be discussed below. Currently supported types include spheres, planar polylines, and Bézier surface patches.
- Point lights, affecting the visual appearance of the simulation.

The focus of the simulator is of course concentrated on the representation of the material sheets themselves. There are several modes by which these sheets may be selectively represented (Figure VII-12), again in spatial (3D) or material (2D) views:

- Materials and other objects may be viewed in wireframe mode, showing the boundaries and meshes of objects (Figure VII-12A).
- The simulation may be viewed in a simple Phong shaded view (Figure VII-12B),
- The material meshes may be viewed in a grid paper mode – where a texture map is applied to the material sheets, applying the (u,v) material coordinates of the sheets (Figure VII-12C), This allows a visualization of the material coordinates, and their deformation into space.
- Environment mapping (Figure VII-12D) provides a “mirrored finish” representation of the sheets. This technique is often used in product manufacturing applications, since it provides a sense of the localized deformations and other qualities of the surfaces.

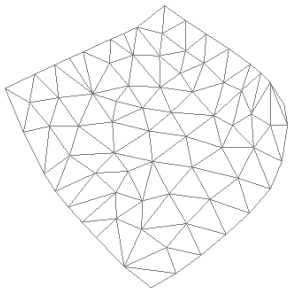

A. Mash view

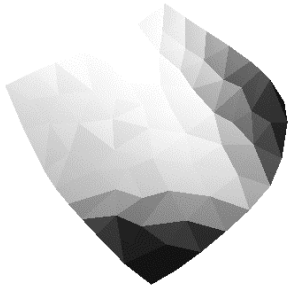

B. Shaded view

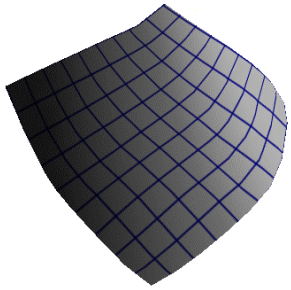

C. Grid paper view

Figure VII-12: Sheet views

- Finally a variety of heuristics about the behavior of the material such as in plane deformation, curvature, and distance from some target object in space may be mapped onto the sheet surface and visualized (Figure VII-12E).

2. Meshing

A variety of mechanisms have been developed to support the modification of sheet elements. The dual nature of material sheets of having a behavior as a flat sheet, and as a three dimensional object deformed in space are observed.

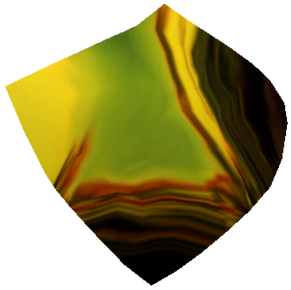

D. Environment Map

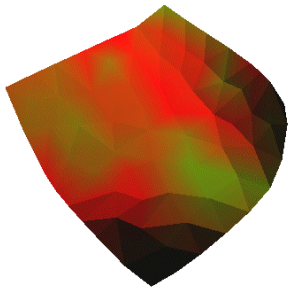

E. Metric graph

Figure VII-12, ctd.

Modification of material sheets in 2D form occurs through a dedicated 2D, Euclidean material world, presented to the user through one or more 2D view ports. The undeformed shape of the sheet is constructed by insertion of boundaries and other features into the sheet's material space. Supported features include:

- Sheet boundaries, represented by closed polylines. Users may dynamically modify the polylines boundary descriptions, by moving the boundaries in 2D space, and by moving, inserting or deleting individual vertices of the polylines. Boundaries may self intersect, and more than one individual sheet boundary may be included, supporting sheets which are not necessarily contiguous. Internal boundaries, representing holes in the sheets are also supported. This behavior is analogous to the physical operation of cutting out the shape of a sheet from a physical sheet of material.

- A variety of additional features – instantiating special, localized behavior of the sheets - are supported by the interface. These include cut locations, where a physical discontinuity is inserted into the material, and "creases" – locations where tangency discontinuity may be allowed by the material simulation. These features are generated by the user by insertion of linear elements into the sheet's material space. The user selects the behavior of the feature by selecting the desired behavior from the linear element's object modification dialog box. The mechanics of feature insertion are discussed in Part 3, below.
- Point objects in material space similarly represent a number of features. Points may represent the location of specific nodes in the material mesh, discussed below. They are also used to represent areas to be removed from the material, when internal boundaries

are created. Special point nodes may be inserted to generate the location of spring constraints, whose behavior is further modified in world space.

The figure below shows a view of a material sheet generated from a number of the features described above, including interior and exterior boundaries, a “cut” feature, a region indicated for material removal, and two spring constraints.

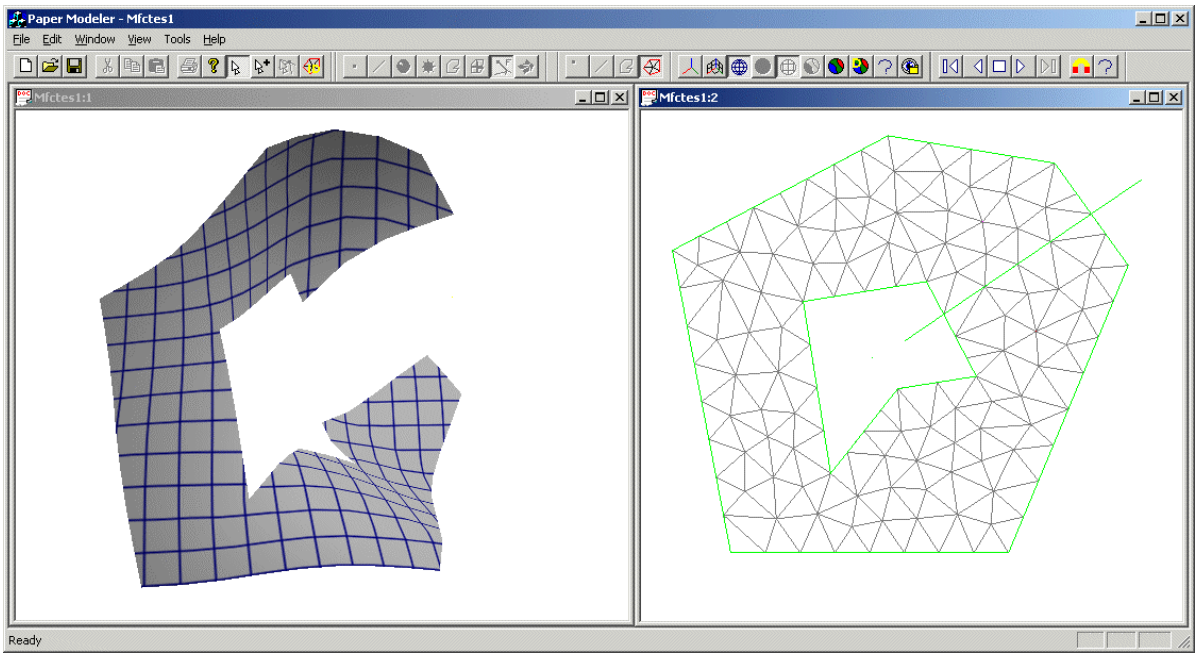

Figure VII-13: Sheet modifications

Generation of a mesh from these sheet features is a core capability of the simulator. The material formulation developed in Section VII.F presumes a material modeled as an assembly of triangles, joined at edges. The speed of the simulation, in terms of the amount of computation of an individual time step, and the size of the feasible time step, are directly related to the number of triangles being solved for. Thus, control of the mesh is a critical component of achieving interactive simulator behavior. Meshing is achieved by a Delaunay triangulation algorithm, through a publicly available library provided by Schewchuk[77]. When a change of state is indicated by one of the sheet features, the sheet initiates a re-meshing procedure. Boundaries, segments and vertices are collected into the triangulation structure. Mesh input node locations are specified in terms of the 2D material space coordinates; the 3D deformation of the mesh has no direct implication on the meshing procedure itself.

The new mesh must be re-bound to the existing 3D shape of the old mesh, in order to allow the simulation to proceed continuously after re-meshing has taken place. The existing 2D topology of the previous mesh provides the basis for a linearized representation of the function ϕ, which maps 2D coordinates to 3D coordinates. For each 2D region corresponding to an individual triangle, the 3D space plane associated with the triangle allows a 3D location to be determined for any vertex whose 2D coordinates lie in the interior of the triangle in material coordinates. Changes in features may result in a new mesh with vertices that lie outside the existing mesh boundaries. For these vertices, approximate locations may be determined by considering the plane normal to the closest boundary vertex of the existing mesh (Figure VII-14). For either interior or exterior vertices, the resulting location will be only a linearized approximation of the true spatial coordinates of the material. The re-meshing technique relies on additional solution steps to re-position mesh vertices, resolving variations in the mesh internal state introduced by the linearized approximation of vertex positions.

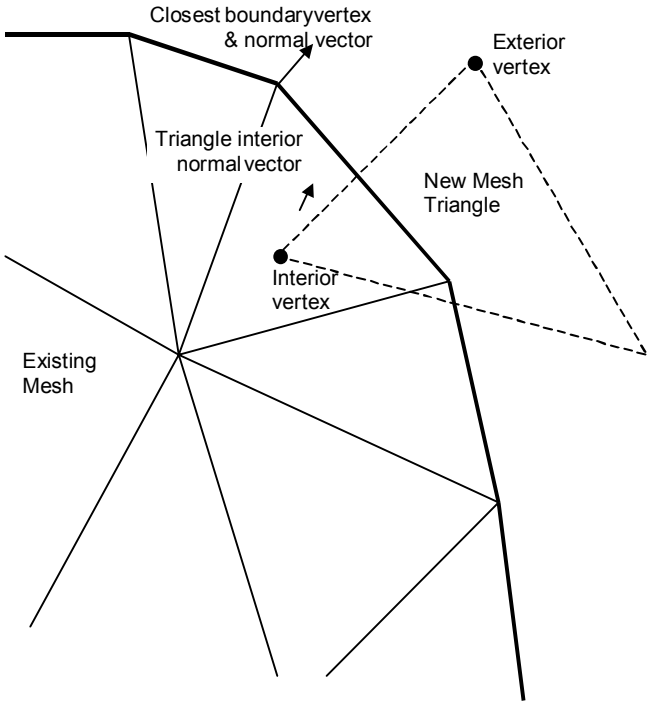

Figure VII-14: Remeshing

The remainder of the sheet modifications occur through manipulation of the sheet in 3D spatial views. While the material space modifications affect the envelope of the sheet, and the inclusion of features, the spatial modification affect the deformation of the sheet and its response to other objects in the simulation.

The principal means by which sheets are deformed in space occurs by attaching spring elements to the sheet at user defined locations. These springs may be attached as permanent fixtures in the simulation, binding a fixed (u,v) location on the surface to a fixed spatial point. The spatial point may be interactively controlled, by selecting the point and

dragging it to a different location. Nodes may also be interactively joined together with springs, and existing springs may be interactively deleted.

The material may also be positioned interactively, through a command mode that allows dynamic, temporary attachment of positioning springs. In this mode, the user grabs the material by holding down a mouse button while the cursor is over one of the material's mesh points. A spring is temporarily generated between the material point and the spatial point under the cursor. Holding down the mouse button, the user may drag the temporary spring's spatial point through space. Releasing the mouse button removes the temporary spring. This interaction feels very similar to physically grabbing the material at a point, and moving it in space. The user may also

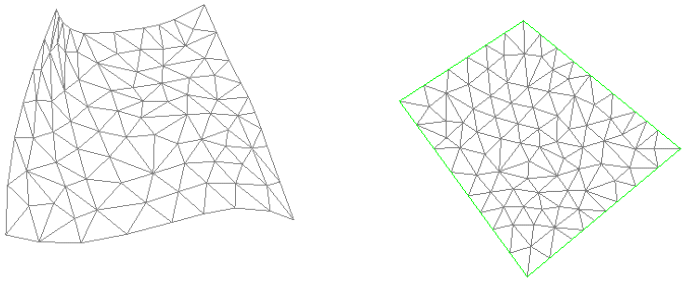

Base Mesh in $\boldsymbol{R}^3$ *Base Mesh in $\boldsymbol{R}^2$*

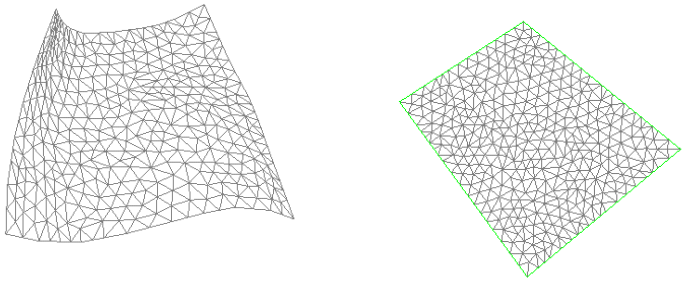

Mesh Refinement

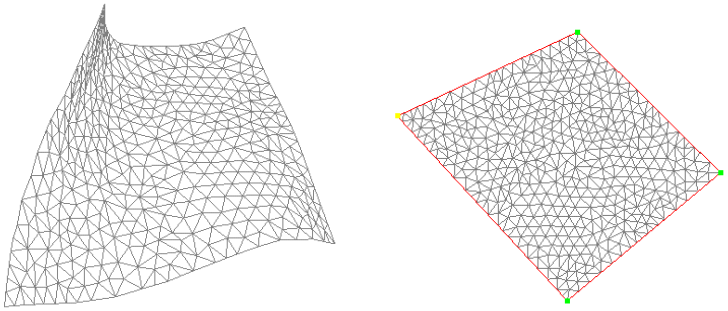

Extrapolation of mesh beyond solution boundaries

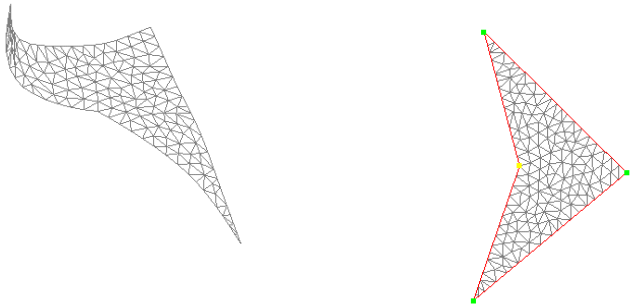

Trim back of mesh boundary

Figure VII-15: Mesh operations

elect to make the spring permanent – fixing the material point permanently to the desired location.

3. Attractor Objects

The simulator is not simply intended to allow interactive manipulation of sheet materials. A second important application is to allow the rationalization of ideal surface shapes. This use is addressed by allowing the selective application of an attractive force between the material sheets and other shapes in the simulation. A variety of spatial objects support this attractive force, including sphere objects and smoothly continuous surface objects based on Bézier surface patches.

The attractor force is represented as a force between each of the material points in the sheet, and the closest point of the closest attracting object in the simulation. For each object in the simulation comprised of a smoothly continuous surface, the closest point to a given material point will be point on the object whose surface normal passes through the material points location in $\mathbf{R}^3$. For spheres this is an easy computation, since this normal will be aligned with the line between the material point and the sphere's center point. For Bézier surfaces, a algorithm is used that finds this point on the surface[65]. For each of the sheet's mesh vertices, these closest point algorithms are run for each attractor object in the simulation, and the closest of these points is selected as the actual attractor object. A force in the direction of the vector between the mesh point and the surface normal point of the attractor is enacted on the mesh point. The strength of this attractive force is controlled by a parameter set globally for the simulation.

The effect is to draw the sheet materials to objects in the simulation. At the same time, the material's internal constraints counteract the tendency of the attractor objects to deform the sheet into a potentially infeasible shape. The magnitude of this force must of course be limited, so that the attractive force does not overwhelm the internal material constraints.

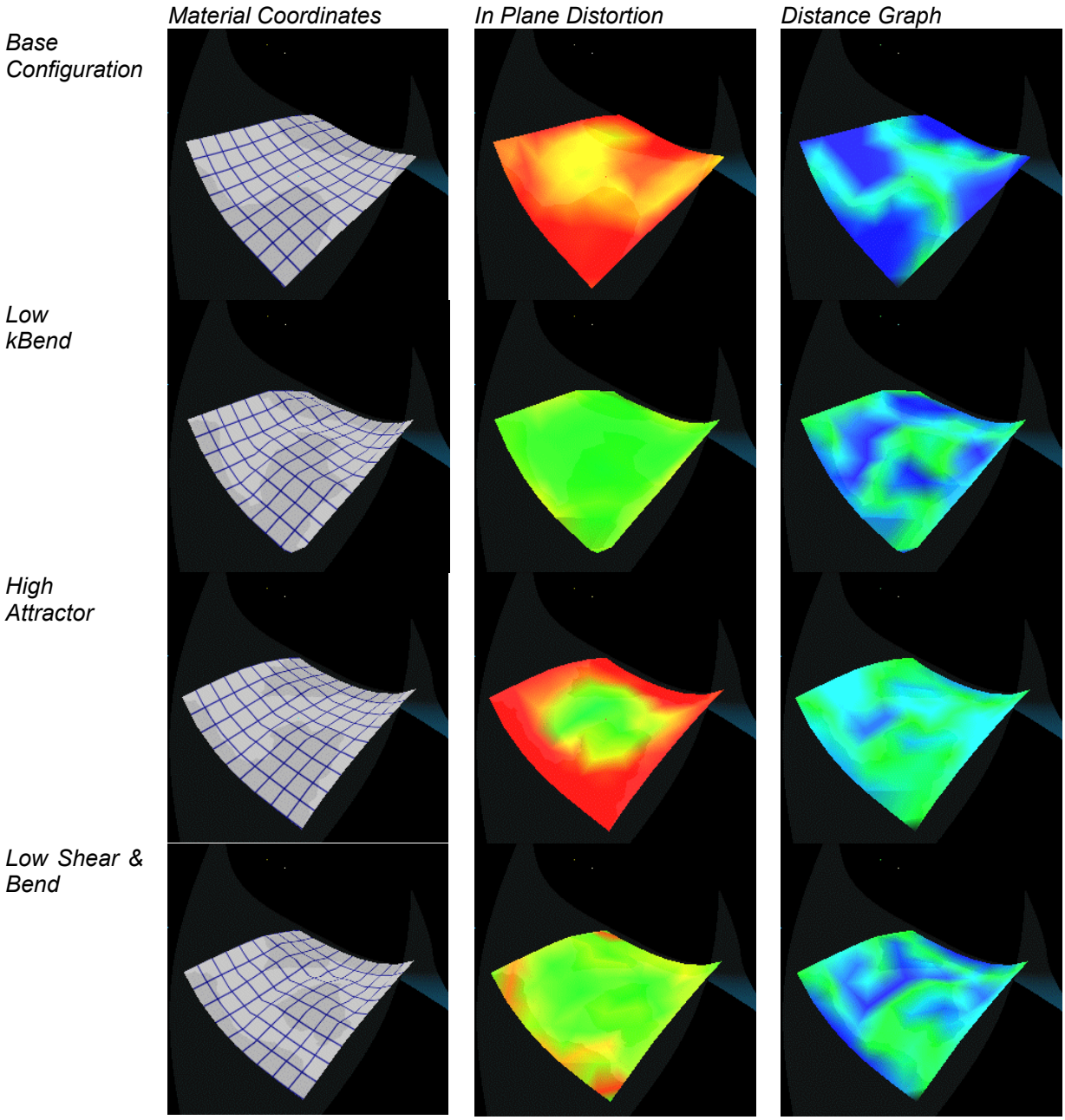

Figure VII-16: Variation of simulation parameters

4. Solution

The material formulation is solved in an independent processor thread from the graphics display and user interactions, to support additional speed on multiprocessing machines. Initially a candidate time step *h* is provided based on the previous solution history. The solver traverses all entities exhibiting constraint behavior, determines the necessary derivatives, and populates the solution matrix and vector with the appropriate numerical values for the constraint. The block matrices for each particle pair and block vectors for each particle are cumulatively summed for all the constraints in the simulation.

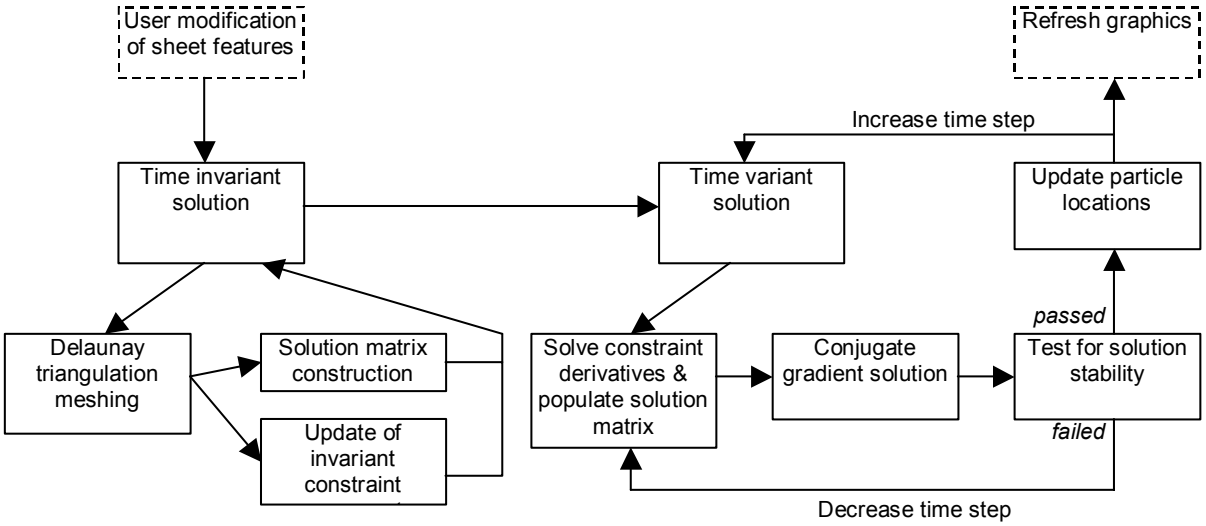

Figure VII-17: Elements of the simulation algorithm

Once the solution matrix and vector have been determined, these objects are passed to a conjugate gradient solution subsystem, which inverts the solution matrix. The velocities and new particle positions are then computed. The results are then tested for behavior suggesting that the simulation has achieved instability. If such conditions are found, the simulation is rolled back to the previous state, the time step is reduced and the materials solution is repeated. If the solution is found to be stable, the state of the mass particles is updated to reflect the solution, and the solution process is re-started at the new time state. The solution process solves continuously until halted by the user, or until the solution has converged to within specified velocity / acceleration tolerances.

In order to maximize solution efficiency, it is important to make distinctions among components of the solution that vary at each time step and components which are invariant

as long as the 2D mesh remains the same. Different user or simulation events may trigger refreshing of either or both of these sets of components. Changes in sheet features requiring a change of the mesh will require a refresh of time invariant components. Changes requiring a refresh of time invariant components will require re-generation of the time dependent components as well.

Components of the solution which are invariant over time steps include:

- The mesh topology, including vertex / edge / triangle structure and adjacencies
- Vertex material coordinates, and components of the solution determined solely from material coordinates, including the triangle derivates $\triangle u_1, \triangle u_2, \triangle v_1, \triangle v_2$, and the inverse of the material gradient $\begin{pmatrix} \Delta u_1 & \Delta u_2 \\ \Delta v_1 & \Delta v_2 \end{pmatrix}^{-1}$ from Section VII.B,
- The size and sparsity structures of the solution matrix **A** and vector **b** from Section VII.G.1.
- The mass matrix **M**, and a pre-conditioning matrix for the conjugate gradient solver $\mathbf{M}^{-1}$.

Components of the solution that are time variant, and must be re-generated at each step include:

- The spatial coordinates of end locations for fixed springs – if modified by users,
- Changes in material or constraint constants, including stretch, shear, bending, and spring forces.
- Spatial coordinates, velocity and $\triangle \mathbf{v}$ vectors for all mass particles,
- The energy function derivates
- The numerical valuation of the solution matrix and vector **A** and **b**,

5. Time step selection and instability detection

The initial time step for the solution is provided by a default, or provided by the user through a dialog box. In order to achieve computational efficiency of the solution, the time step should be as large as possible without resulting in instability. Unfortunately, there is no determinate way to compute either the appropriate time step or to detect for instability. Additionally, the size of a stable time step varies over the course of the simulation. For example, a flat mesh with no acceleration or constraints can be solved for an indeterminately large time step

(although the results aren't particularly interesting!). Heuristics are employed to search for an appropriately large time step, and to check the solution to determine whether instability has occurred.

If the previous solution was achieved in a stable manner, the current time step may be increased slightly. We multiply the existing time step by a small factor, which may be set by the user. A default multiplier of 110% is used for increasing the time step between subsequent stable solutions. If the solution is determined to be unstable, a more drastic reduction multiplier (default 70%) is used to get the solution quickly back on track, with the knowledge that subsequent stable solutions will soon get the solution moving forward again quickly.

There are a number of heuristics that can be employed to check for stability. The most obvious and direct is to check for what seem like dangerous changes in velocity – the $\triangle\mathbf{v}$ resulting from the solution of the matrix equation. An excessive deformation of any triangle edge relative to its undeformed configuration may also signal impending instability.

I. ISOMETRIES

The materials modeling formulation presented in this chapter offers some substantial improvements over the existing paper surface representations currently employed in the firm's digital process. The principal benefits of the materials simulation representation are the result of a more sophisticated representation of the actual constraints imposed by the surface materials on project forms. The material formulation provides the solution of paper surface configurations internally, allowing the user to interact with the surfaces in a manner similar to that provided by physical sheet materials. Certain features of physical sheet forms are quite difficult to reconstruct using constrained gaussian curvature approaches, and are prohibited by developable surface representations.

At the same time, the material simulation representation has much in common with these representations, by virtue of their shared topological basis as $<\mathbf{R}^2 \times \mathbf{R}^3>$ manifolds. This shared topological basis suggests some additional comparisons of these representations, and allows the possibility for either integrating these representations into a common framework.

In describing the parametric representation of these surfaces a occurring in a proper Euclidean space, we have taken on certain structures of this space that deserve further inquiry. Specifically, our parametric space representation assumes the character of a metric space, with length and distance metrics defined on the coordinate descriptions of elements within the space. This distance metric forms the basis for establishing continuity and proximity of points within a region of parametric space associated with the sheet. We might inquire what other implications the structuring of a parametric space distance metric has on our problem description.

The topology of neighborhoods is preserved under transformation between parametric and world space representations. Whether or not distances are preserved is dependent on the nature of the mapping function $F : D \rightarrow R$. In general, little affinity between the distance, curvature or other shape qualities is preserved under parametric $\leftrightarrow$ world space mappings. As an example, isometric curves of the form $u = u_C$ ($v = v_C$) are represented as straight vertical (horizontal) lines in parametric space. Their shape characteristics in world space are dictated by the form of the mapping function σ. In the case of Bézier formulation, this function takes on the form of the Bézier basis function to the tensor product surface σ:

$$\sigma(u,v) = \sum_{i=0}^{n}\sum_{j=0}^{m} B_{i,n}(u)\, B_{j,m}(v)\, \mathbf{P}_{i,j}$$
$$B_{i,n}(u) = \frac{n!}{i!(n-i)!} u^i (1-u)^{n-i} \qquad \text{(VII.56)}$$

The shape of the isoparametric curves in $\mathbf{R}^3$ is defined by this shape function, and specified through the placement of the control points $\mathbf{P}_{i,j}$ in R^3. In general, there is little we can say about the shape of an isoparametric curve in R^3 from its properties in $\mathbf{R}^2$ beyond such topological properties as connectedness and continuity. For this reason, isoparametric curves on surfaces, while readily available in most CAD surface applications, are of little use in constructibility applications. In general, shape functions such as length and curvature are not preserved across parametric surface mappings, so the parametric space representation of surfaces are of little interest in design applications.

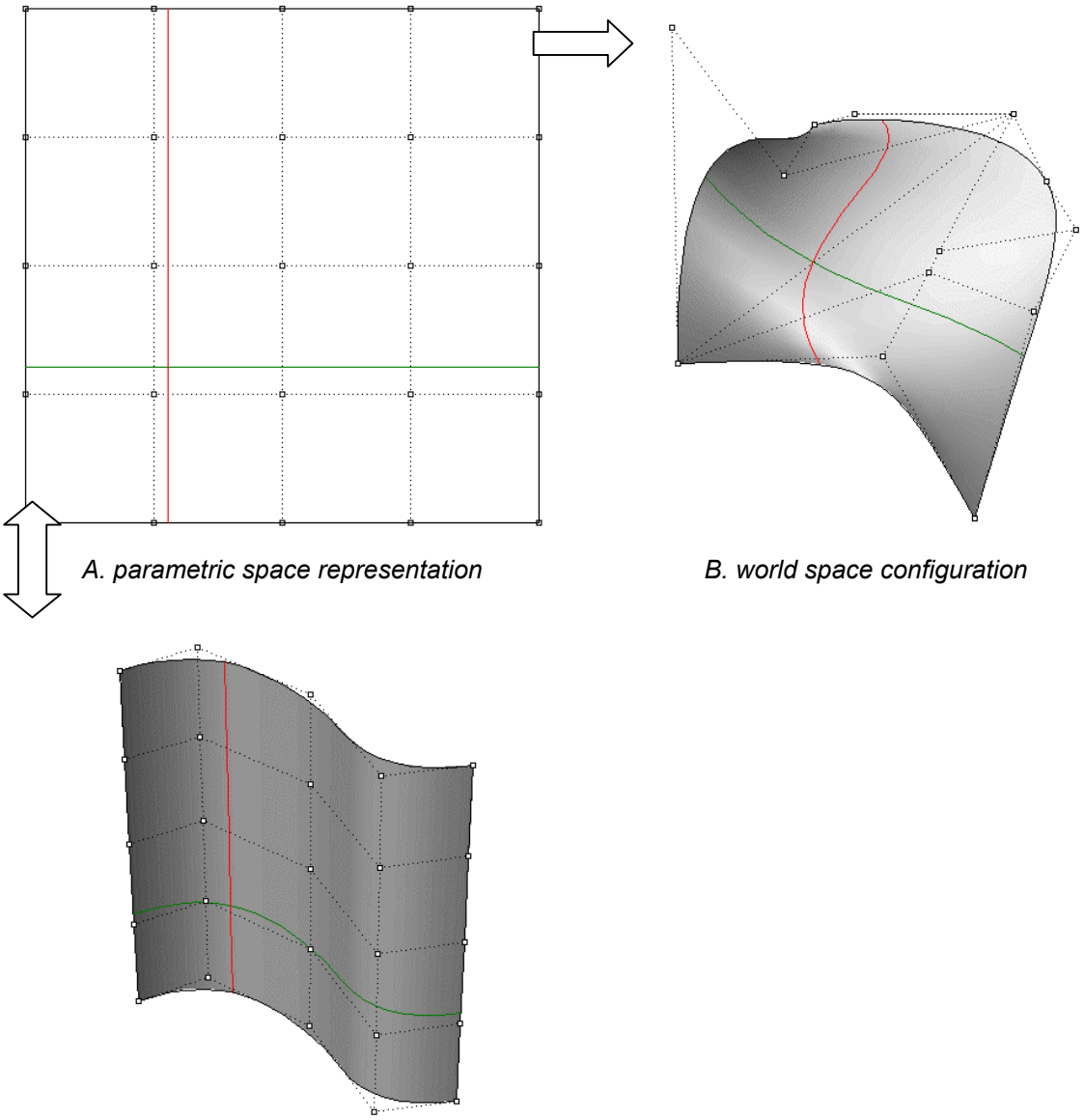

A. parametric space representation

B. world space configuration

C. A special case

Figure VII-18: Isometries of parametric mapping on Bézier surfaces

Figure VII-18C represents a notable exception, where the configuration of surface control points results in a cylindrical developable surface. If scaling or other affine transformations are controlled, the parametric surface mapping will be an isometry: length and gaussian curvature are bi-directionally preserved.

There are classes of surfaces on which important shape metrics may be preserved across parametric mappings. These surfaces are of great importance to paper surface modeling. Developable surfaces present admit a two dimensional representation of interest in design. As with other parametric surfaces, the mapping between parametric and world space

configurations do not preserve shape functions. However, developable surfaces may be isometrically *developed*, unfolded into an alternative Euclidean 2-space configuration. Length, distance, geodesic curvature, and other shape functions are bi-directionally preserved across this transformation. Note that the developed 2-space and parametric space representations are distinct. Topological properties are retained across both transformations.

Developability plays a critical role in Gehry's process. Developing of surfaces allows surface panels to be unfolded into patterns that can be cut from flat sheet. Other component geometry such as fastener locations, panel breaks, and intersections with other construction systems may be mapped between the developed and world space configurations. Note, however, that this developed surface space is not to be confused with the parametric space representation that structures the initial coordinization of the surface.

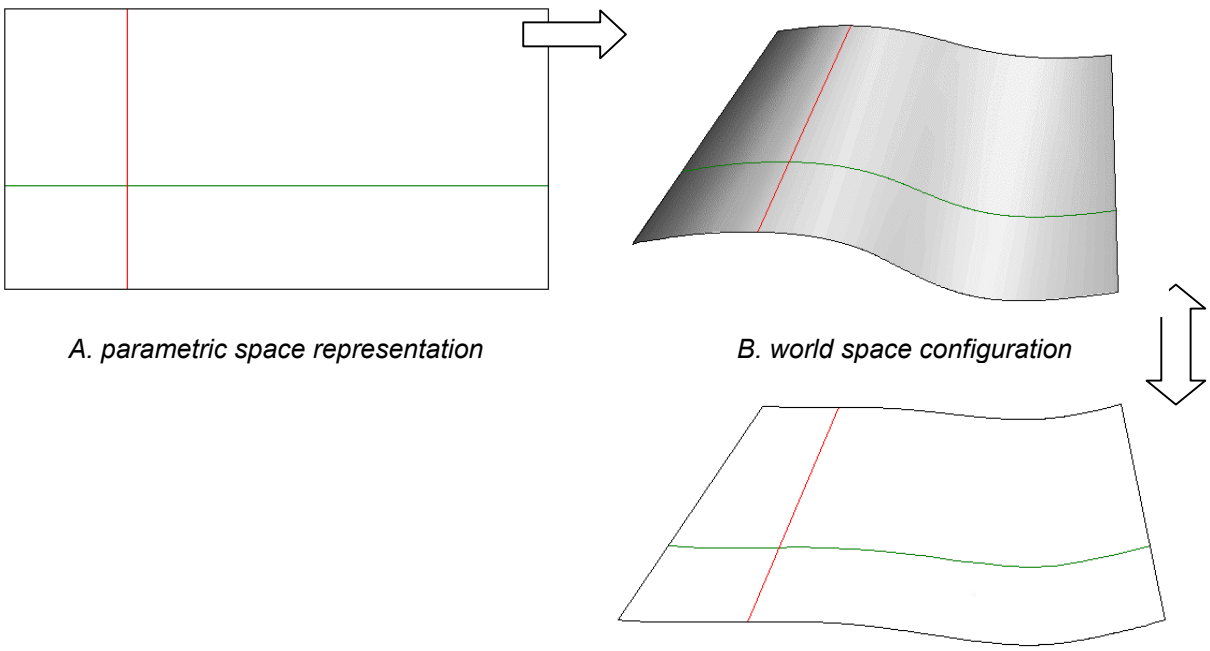

A. parametric space representation

B. world space configuration

C. flattened developable surface

Figure VII-19: Isometries of developable surfaces

We may now make an important observation on the materials modeling surface representation. The materials modeling representation is predicated on a tight correspondence between the shape of a sheet's undeformed configuration as a region of

material space, and its deformed configuration in $\mathbf{R}^3$. The energy functions presented in Section VII.F are described by stretch and shear deformation, computed from the derivatives of the mapping function.

In applying the physical modeling approach to paper surfaces, we are principally concerned with materials where the in plane stretch and shear siffness is quite high compared to bending and other force phenomena. We can achieve large scale deformations of the sheet's configuration in world space while incurring insubstantial deformation in the sheet.

If we presume small in-plane deformation of the surface in its $\mathbf{R}^3$ configuration, the mapping between parametric and world spaces will be approximately isometric. Qualitatively, we can observe this fact in the material simulations presented in Chapter VII and below. Lengths, angles and geodesic curvatures are preserved between geometric features in parametric space and their transformed counterparts on the surface in $\mathbf{R}^3$.

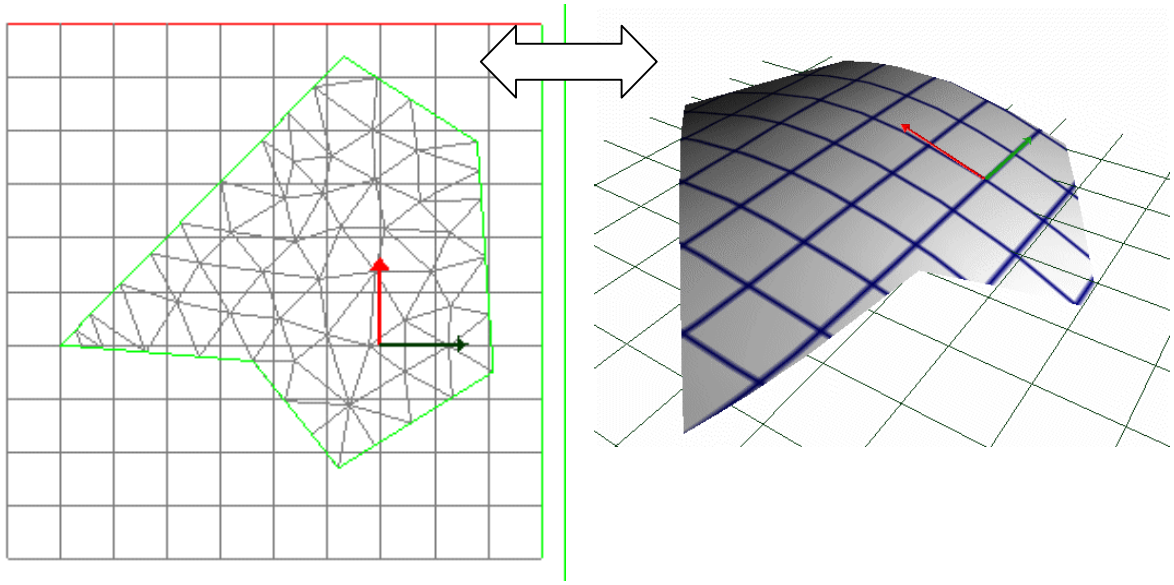

Material space configuration *"world" space configuration*

Figure VII-20: Isometries of the materials based formulation

The material space representation thus has an important spatial and design quality. It is the originating, two dimensional paper space of the surface in its flat, pre-configured state. Designed objects draw important shape qualities from their occupancy of this space. Cuts and other operations performed by designers on the materials are appropriately represented by shape features in material space. The impacts of these features' shapes on the feasible

configurations of the sheet in $\mathbf{R}^3$ are also represented. In particular, linear elements in material space are mapped to geodesic curves in the world space configuration. The material modeling approach thus supports two critical designers' views on the elements that are being operated on: the paper space of the sheet and operations in the plane of the surface, and the subsequent deformation of these sheets into spatial configurations.

The common manifold framework underlying these representations suggests the opportunity for performing mapping operations between these surface constructs. In particular, the developable surface representation offers the feature of straight lines of ruling, which were shown to be of interest in fabrication. It is of interest to be able to map between developable surface and materials surface representations, drawing on developable surface constraints on project applications where the associated constructibility opportunities are warranted, and switching over to a more generous paper surface representation on other areas of the project.

The mapping from a developable surface representation to one based on materials simulation is can be performed in a fairly straight forward manner. Developable surfaces provide the unfolded, 2-space representation of its developed configuration. This representation of the surface can be directly converted to the triangulated region of $\mathbf{R}^2$ space associated with the materials simulation approach. The coordinates of the surface in $\mathbf{R}^3$ can similarly be provided to the equivalent materials based spatial representation. Figure VII-21 shows this mapping, a capability provided by the material simulation prototype.

The reverse mapping, unfortunately, is not as straight forward. The physical modeling representation is a super set of developable surfaces. While all developable surface forms can be represented by the physical modeling approach to arbitrary accuracy, the representation of physically modeled forms as developable surfaces requires a rationalization strategy, and is likely to encounter conditions of infeasibility.

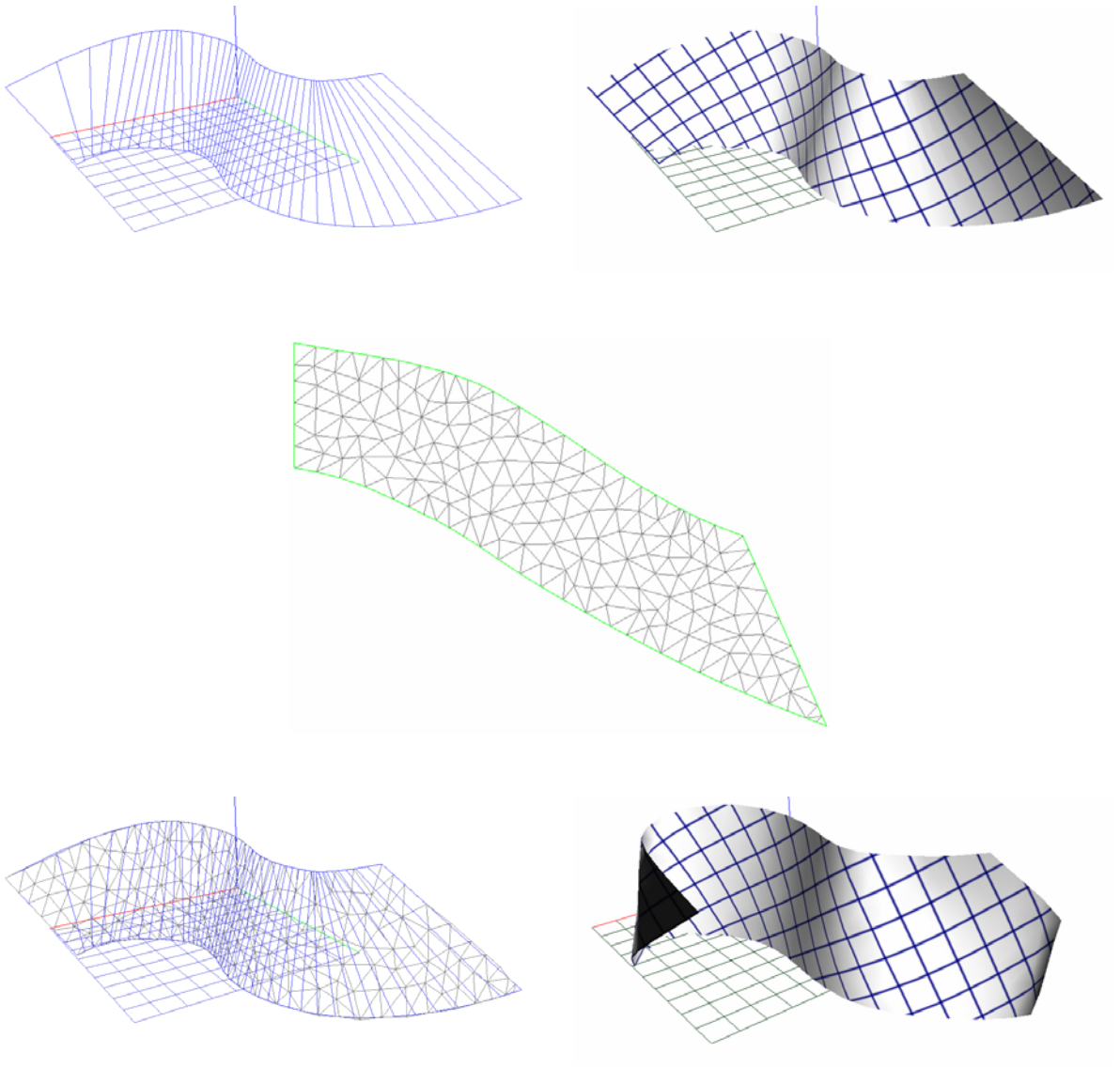

Figure VII-21: Translation between developable and material representations

J. MATERIALS MODELING APPLICATION: GUGGENHEIM INSTALLATION

The first application of the materials modeling prototype on a Gehry project occurred in June, 2001, on a sculptural installation in the Gehry Retrospective show, installed in the rotunda of the New York Guggenheim museum. The sculpture called for the installation of 10 steel mesh curtains, to be hung from the concrete radial structural members supporting the skylight of Wright's design. The curtain assembly was to be constructed out a wire mesh material, comprised of interwoven spirals of steel wire oriented approximately horizontally. The curtains were built up out of three layers of the material, separated approximately 6" by wire spacers. The curtains were to be positioned by a series of cables attached from the curtains to points on the ceilings of the galleries neighboring the rotunda.

An initial design for the installation was developed during approximately three months prior to the opening of the exhibit. Each of the curtains was designed to be suspended the full height of the rotunda, from an attachment mechanism on the skylight structural members to a height of approximately 10' above the rotunda floor, for an approximate vertical dimension of 80'.

The cables would be connected to two parallel steel rods, attached to the mesh face, and located approximately ¼ of the distance from the edges of each panel. These steel rods would provide additional stiffness of the material in the vertical direction, and locally stiffen the material, to minimize distortion of the material at the points of connection to the cables. From its initial position oriented radially aligned with the skylight structural members, each curtain would describe an S-shaped curve, sweeping downward and clockwise in a similar sense to the organization of the rotunda parapet and galleries, until it eventually aligned roughly with the surface of the rotunda parapet.

Each of the curtain assemblies was to be tied back from both sides of the curtain at each level of the rotunda. The Guggenheim required that no attachments be made into the surfaces facing the rotunda itself. Additional structural requirements of the galleries dictated that attachments for tension cables be placed in a ring approximately 12' outward from the parapet edge into the ceiling of the galleries.

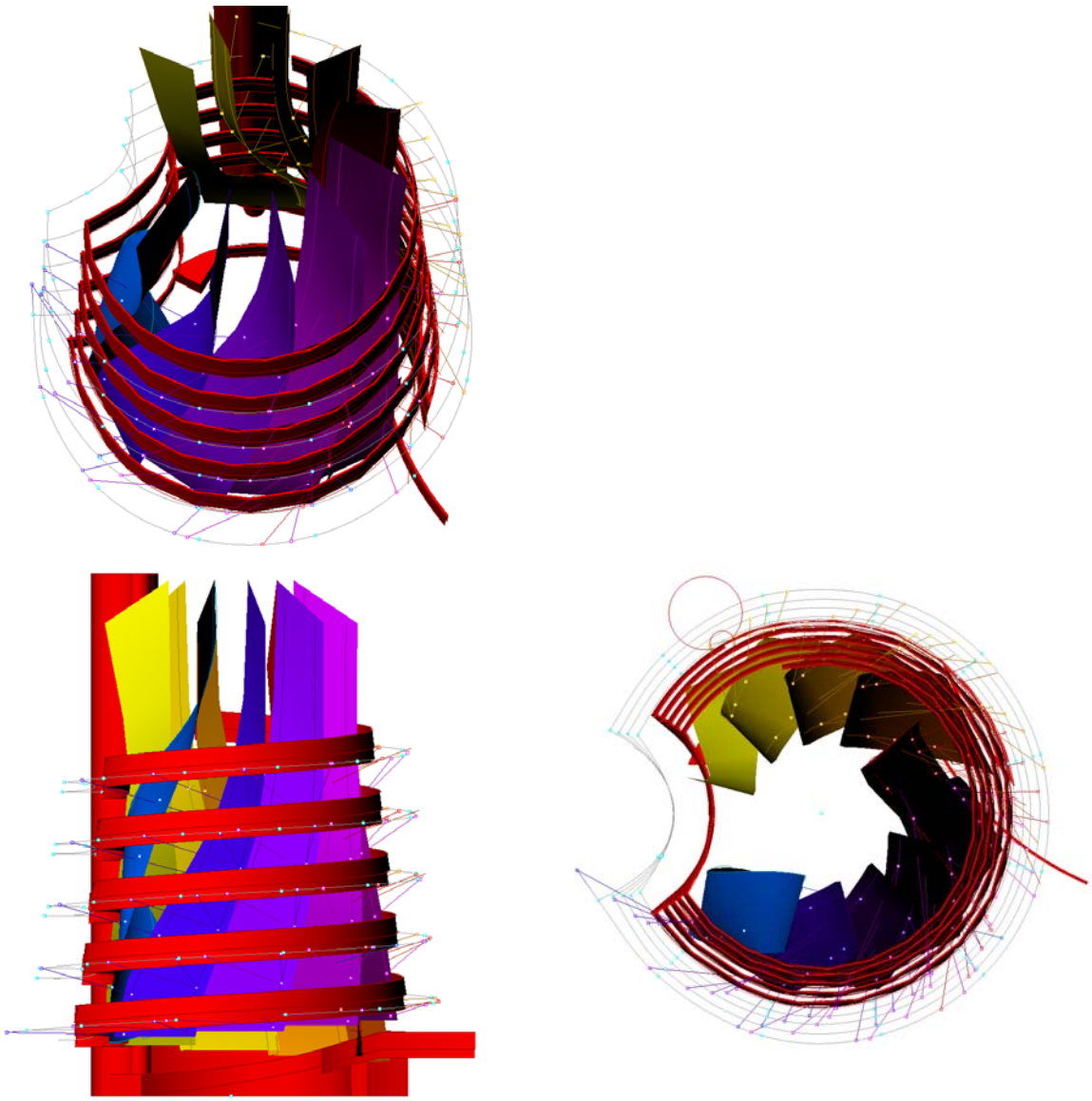

Figure VII-22: Original developable surface scheme (Guggenheim mesh installation)

An initial computer model of the assembly was made prior to installation (Figure VII-22). The curtains were represented as developable surfaces, as an initial approximation of the behavior the sheet material of the mesh would assume. It was assumed that the strength of the wire mesh in the horizontal direction, coupled with the rigidity of the vertical bars, would generate a material behavior that was approximately equivalent to that presented by developable surfaces. The cables would be attached at a sufficient number of locations to allow the surface form to be guided into position during site installation. In this scheme, the intention was to allow cables to pierce neighboring curtains as necessary to generate the desired shape. The developable surface models of the curtains were flattened to produce

patterns for material cut-out. Two weeks before the opening of the exhibition, the cut out sheets were sent to the museum for on site installation by the project designers and museum installation staff.

On-site installation of the sculpture was problematic. The large size of the sheets, combined with the spatial confines of the rotunda space, and museum staff's concern for the integrity of the rotunda's structure and finish, all impeded interactive adjustment of the sheet's fastening strategy. The strategy of piercing neighboring sheets with tie back cables proved problematic, since it was difficult to know exactly where the cable should feed through. Most importantly, the sheets did not behave like the paper surfaces presented by the developable surface based geometry model. The material proved to be far more flexible than initially understood, and the effects of gravity on the material caused it to sag substantially between fastening points. The opening of the display occurred with only half of the sheets installed, most in temporary, pinned back locations.

After the opening of the exhibition, it was decided to attempt another study of the sheet sculpture, and a second round of installation. The study was conducted through the use of the materials modeling application. Two weeks were allocated for the study.

The design assumptions and conditions during this phase of the sculpture's design were substantially fixed by decisions made in the initial design phase. The sizes and shapes of the sheets were already defined and had already been fabricated. On the basis of these conditions, and with the initial design intent serving as a point of departure, the simulator was used to develop a strategy for establishing cable configurations that generated a form acceptable to the project designers.

Additional design guidelines were established. Configurations involving cables punching through neighboring panels were avoided, due to the difficulty of controlling locations of cable punch throughs with sufficient precision. A maximum of four attachment points per sheet was established.

The existing fabricated profiles of the curtains proved to be a major constraint on the configurations that could be achieved. The bottom dimension of the panels was larger than the distance along the rotunda edge. This created problems for configurations where cables were to be attached to both sides of a panel, since these cables would invariable intersect the neighboring panels.

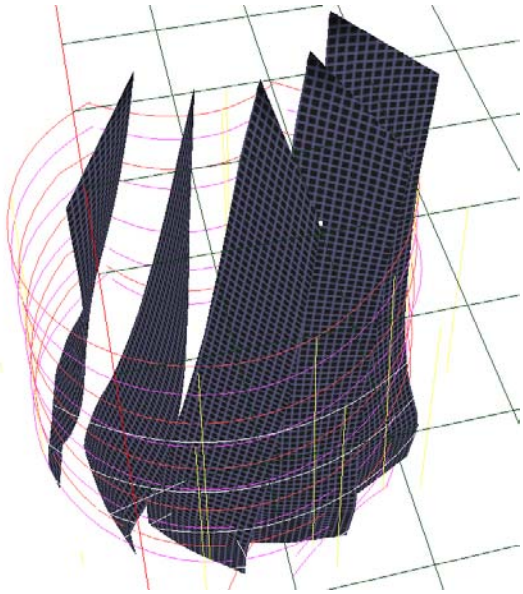

Figure VII-23: Initial design proposal based on materials simulation.

The simulator program was modified to include the effects of gravity on the materials. Capabilities for importing sheet boundaries from existing CAD packages were added, along with capabilities for importing the geometry of the rotunda. The meshing program was modified to allow nodes along the top edge of the panel at the skylight structure to be fixed in space.

An initial strategy was proposed, where the panels would be attached at three points at the lowest level of the rotunda: one point on the outer edge (from the rotunda center), and two points on the inner edge, a third of the horizontal dimension from the edge (Figure VII-23). This layout would allow both edges to be controlled, while preventing the cables from intersecting the neighboring panels. Additionally, the strategy would produce an “S” curve in the panel, both vertically and across the bottom edge of the panel. When the design had been established, information delineating the strategy was sent to the museum, including precise locations for cable attachments on the panels, locations for attachment to the gallery structure, and individual cable lengths (Figure VI-24).

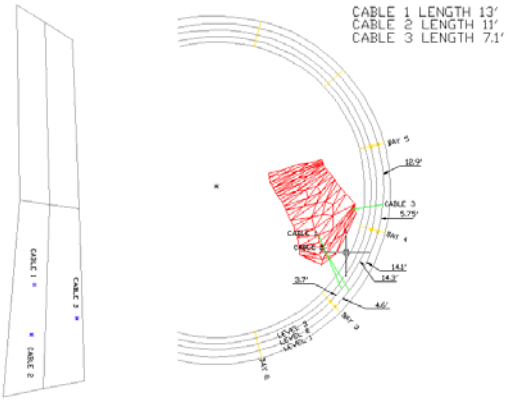

Figure VII-24: Dimensional data from simulator for sheet placement on site

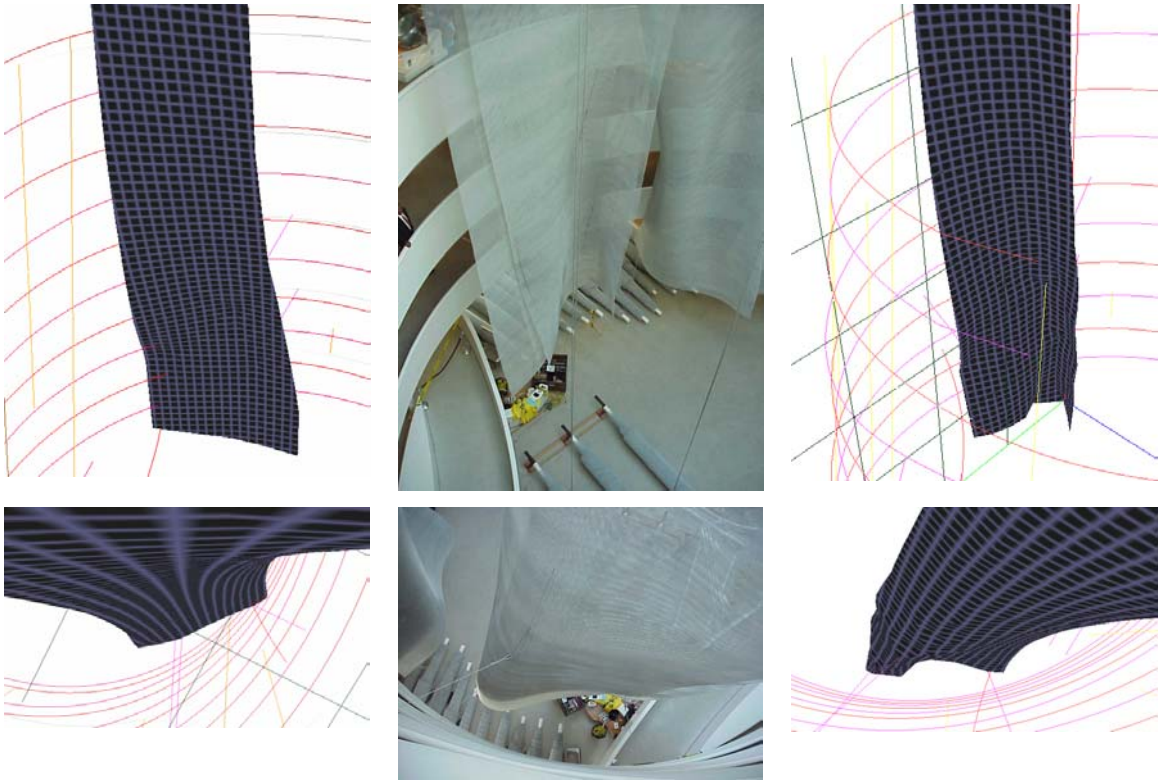

Original prediction *Results in field* *Recalibration results*

Figure VII-25: Recalibration of material properties based on initial installation results

This second round of installation produced additional surprises for the design and modeling team. The material proved to be even more flexible than assumed during the material simulation, causing the panel to collapse under the effects of gravity. This resulted in a severe S-curve in the bottom edge of the panel, a result found undesirable by the project designers (Figure VII-25). On the basis of the mockup result, the strategy of attachment on the panel interiors was found to not be workable and was abandoned.

The material parameters were modified to correspond with the results from the mockup study, and a new set of configurations were attempted in the simulator. The driving concern at this point in the design was to produce a strategy that could accommodate the flexibility of the panel, while allowing cables to pass outside of adjoining panels. A special feature was developed in the simulator graphics that would allow multiple copies of a single sheet to be visualized, rotated around the rotunda. This allowed the relative positioning of the sheets and cables to be assessed as the sheet was interactively moved. Figure VII-26 shows some of the intermediate schemes produced through design iterations with the materials simulator.

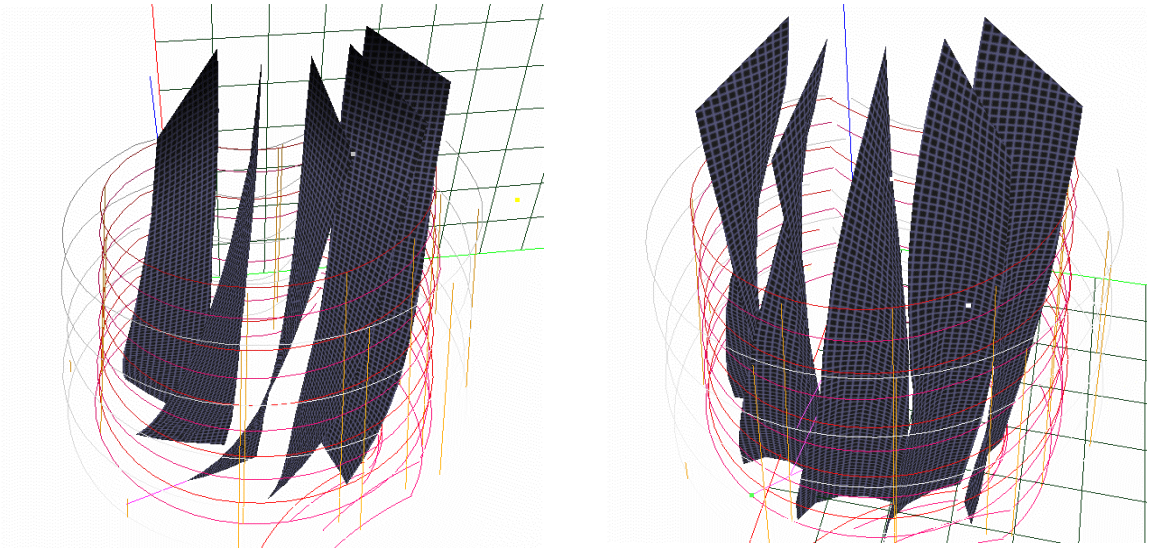

Interim layout strategy *Final layout strategy*

Figure VII-26: Materials simulation design iterations of mesh curtain installation

The design team finally settled on a strategy where each panel would curve “above and over” its neighbor, prior to being attached at the outside edge only. This strategy required attachments higher up on the panels. The distances between the panels would be tight at this the point of passing over, so the prediction of the materials modeler would have to be substantially correct. On the basis of this scheme, data was again sent to the museum for on site mock up.

This time, the results of the mock up confirmed the assumptions of the simulator, and the feasibility of the strategy. Dimensions for cable placement on the flat patterns of the individual sheets, cable lengths, and locations for cable attachment points in the rotunda were established for each panel. These dimensions were again provided to team as per Figure VII-24 above.

Figure VII-27 below shows relationships between the materials modeling simulation and the final mesh curtain installation in the exhibit.

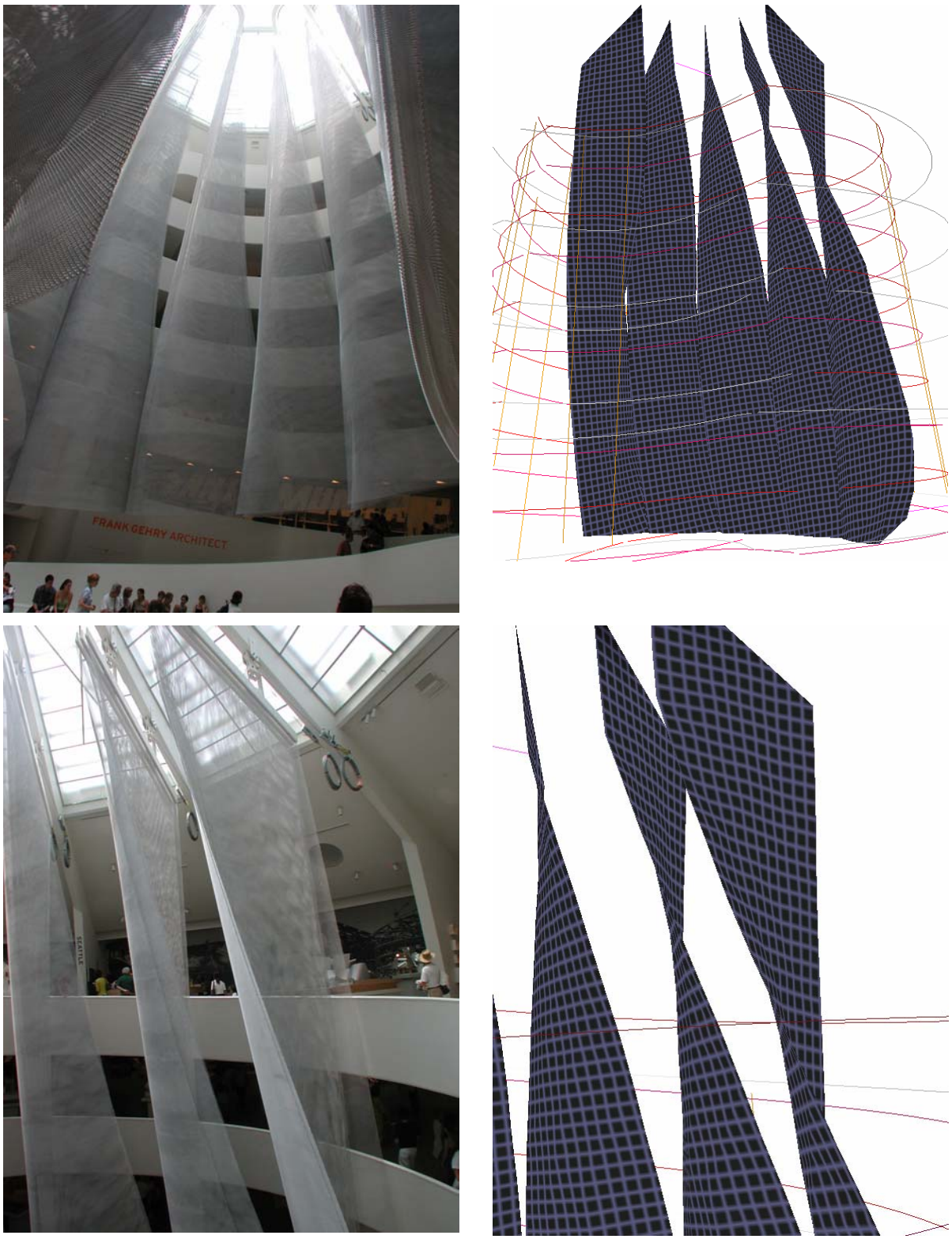

Figure VII-27: Final installation and simulation

PART 3: THE GENERATION OF SURFACE ASSEMBLIES

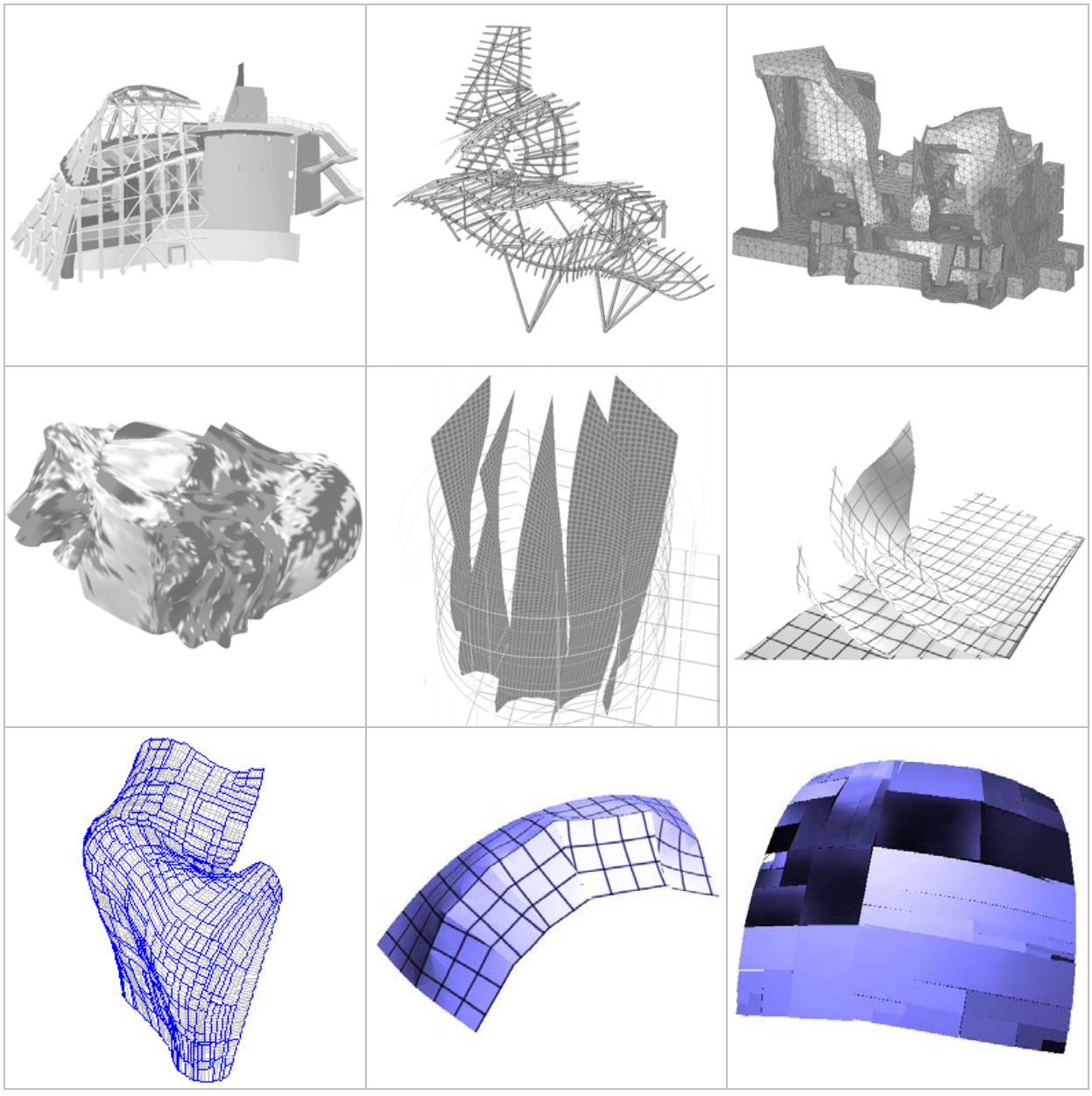

VIII. GENERATING ASSEMBLIES

In Part 1 of this thesis, a set of issues were identified in the rationalization, documentation and constructibility of Gehry's surface forms. The notion was presented of materially guided intentions and systems in the physical modeling, digital modeling and fabrication of these forms. The class of "paper surfaces" were introduced in Part 2, shapes whose qualities are defined by a set of specific material behaviors and constructibility requirements. Issues in the computational modeling of these materially guided surfaces and systems were presented.

This section extends these geometric constructs – initially developed toward simulating the geometric behavior of individual material surfaces - to consider the behavior of surface elements as they combine to form larger organizations. The motivation for this work will be to direct the mathematical constructs developed in Part 2 toward solutions of constructibility issues on larger scale compositions of sheet assemblies. This effort will specifically target rationalization activities, developing approaches to the generation of surface element assemblies whose organizations are guided by rules of constructibility and other project performance requirements.

In order to apply the formalisms developed previously in this work to the rationalization of surface assemblies, we must extend the previously defined geometric models of paper surfaces in two fundamental ways:

1. **Extension of the topological model**. The constructs developed in Part 2 focused on the notion of an $\mathbf{R}^2$ manifold embedded in Euclidean 3-space. The Euclidean structuring of the parametric space representation provided certain regularity to the descriptions of the sheet elements, regularity unavailable from a perspective based purely on the sheets' description in the containing 3-space. Certain topological properties such as connectedness of the shape's region and its relationship to its boundary were identified on the basis of the sheets' parametric space descriptions.

Extending this approach to inspect assemblies of elements will require extending the topological model of surfaces as manifolds to consider the ways in which these spatial representations combine. Well established theory of such combinatoric topologies exists[2,38]. In applying these topological combinatorics to the construction of sheet assemblies, we will

principally be concerned with operations performed on the boundaries of sheet elements as they are “stitched together” to form larger organizations. This inquiry will provide a mathematical basis to support operations on organizations of surface manifolds.

2. **Generative operations on surface assemblies.** With a formal structure in place to structure the description of surface element assemblies, the inquiry will turn toward ways in which operations on these assemblies may be performed. Rationalization operations will be re-formulated as transformation operations on assemblies, directed toward goals of satisfying performance metrics on these assemblies. The topological structuring of sheet assemblies may be drawn on to support contemporary approaches to the development of *generative systems*.

With these structures in place, we will have a basis for formally defining *shape families* or *classes,* on the basis of sets of assumptions regarding element geometric representation, organizations of elements and operations on these elements. A shape class may be defined by a description of the type of geometric element used, and the allowable organizations of these elements. Alternatively, we can view the shape class as the set of all shapes generated from a specification of elements and transformations. Both aspects of this description provide constraints on the feasible set of “valid” shapes. A shape is a member of a shape class if it can be generated using only the assumptions valid in the definition of the class. If the organizational rules have been developed in response to constructibility requirements then, by definition, satisfactory inclusion of candidate shapes into an appropriately defined shape class will guarantee satisfaction of these constructibility requirements, and any shape which is a member of the class will satisfy these requirements. Specific surface fabrication and construction systems will be closely associated with a specific shape class.

An example paper surface composition from Gehry's schematic design phase modeling is shown in Figure VIII-1at right. Intuitively, there is a language of forms apparent in this construction. We recognize elements of this language: the sheets of paper and felt. In turn, these elements are assembled with a more or less consistent set of operations on these base elements. The shape is constructed by cutting sheets of material, folding these sheets in space, and joining these elements together at their boundaries. Frequently, adjustments to the boundary of an element are made on the model, trimming the boundaries of joined elements to a closed configuration.

Figure VIII-1:Physical sketch model, showing two shape classes (Ohr Museum)

The boundaries of sheets and their joining to neighbors are clearly important characteristics contributing to the overall shape. It will be beneficial to have available the description of a sheet by its boundary configuration in an unfolded or "flattened" state, as this representation is an invariant characteristic of the sheet's shape, independent of its manipulations in 3D space. The relationship between these perspectives was developed in the materials modeling approach in Chapter VII. There are additional, higher level features which merit consideration. "Dodges" and "inserts " are evident – sheets that have been split and either the edges closed or additional material added. Sheets may also overlap, providing an alternative construct generating continuity of the surface assembly.

A. GENERATIVE SYSTEMS AND SHAPE GRAMMARS

The notion of elements and transformational operations on these elements is at the heart of work in shape grammar theory and method. This theory provides an algebraic basis to describe shapes through topologies of shape – part relations.

The basic algebraic components of shape grammars are often presented in the literature[80] as:

$A \rightarrow B$ (VIII.1)

$C \geq \tau(A)$ (VIII.2)

$C \rightarrow C - \tau(A) + \tau(B)$ (VIII.3)

Equation (VIII.1) establishes the transformation rule to be considered for application. Shape *A*, identified in some field of consideration is replaced with a separate shape *B*. Typically, the field of consideration in which this identification will occur is a design - an existing shape *C*.

Equation (VIII.2) defines the identification operation by which the transformation rule is applied to a design *C*. Some transformation of A is identified as being a part of the design shape *C*. In the existing literature, this transformation is presumed to be one of the Euclidean transformations.

Finally, Equation (VIII.3) presents the production operations on the base shape *C*, given the defined transformation, and the identification circumstances identified in (VIII.2).

Often, grammar applications to design applications presume multiple transformation rules, operating sequentially on a progressively developed design shape. A grammar is defined in (Stiny, Gips[84, 81]) as a 4-tuple of the form:

$S = < V_T, V_M, R, I>$ (VIII.4)

where:

- V_T is a finite a set of *terminal shapes*, a spatially organized set of (maximal) Euclidean elements
- V_M is a finite a set of *marker shapes*, a spatially organized set of (maximal) Euclidean elements
- *R* is a finite set of transformation rules, of the form $u \rightarrow v$, where *u* and *v* are shapes composed of shapes from V_T and V_M .

- I is an initial shape on which transformation R are applied.

Marker shapes serve to uniquely direct the application of rules to specific shapes in the composition, and to drive the application of rules in a deterministic fashion. The grammar terminates when there are no marker shapes left in the composition.

The possibility of such operations is founded on a topology of shapes and parts of shapes. Initial literature[76] presents the basis for an algebra of shapes, using examples of Euclidean elements (points, lines, planar regions, volumes) and transformations of these elements (translation, rotation, scaling, mirroring). Shapes are sets of elements. Shape *A* is part of another shape *B* (*A* < *B*) in such case that every element of shape *A* is contained in some element of *B.* This allows a topology of shapes to be developed on the partial ordering of shape – subshape relationships. A Boolean algebra may then be defined on shapes, their sums, products, and complements, on the basis of this topology of shapes.

This topological structuring of shapes bears some similarity to earlier results of point set topology[43]. In point set topology, a shape is defined simply as a set of points. The structuring of Euclidean and other metric spaces[7] supports the development of neighborhoods as a means for determining connectedness and compactness of point sets. In this formalism, shape – subshape relations and algebras on shapes are replaced with a topology of point sets. The point set (shape) *A* is a part (subshape) of *B* (read *a* < *b*) iff every point in *A* is also in *B*.

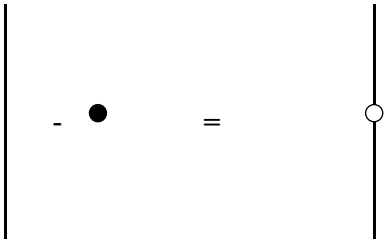

Subtraction operation on different element types in point set topology

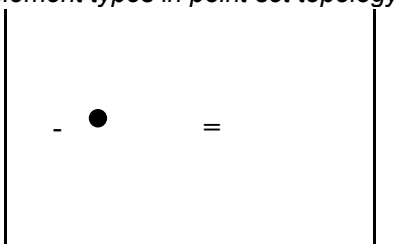

Corresponding shape grammar operation, preserving shape types

Figure VIII-2: Point set versus shape grammar subtraction

Shape grammar literature diverges from point set theory in that point set operations do not preserve the type or identity of shapes[25]. In point set topology, the subtraction of a point interior to a line from the line results in two lines, or a line with a single point missing (Figure VIII-2). Shape grammars admit Boolean operations only on elements of like types, so the above example has no effect on the line element.

In much of the original literature by Stiny[83], the shape grammar formalism is described through examples of Euclidean elements (lines, points, and higher dimensional shapes described by boundaries comprised of these elements) and Euclidean transformations. Stiny has shown that Euclidean shape grammars are closed under transformation. The regularities of such well defined objects, operated on in Euclidean space, lend a simplicity and elegance to the structuring of computations on these objects.

The introduction of non-Euclidean spatial structures into shape grammar theory requires us to re-consider the structure of shape grammars, distinguishing between elements of the formalism that are topological or algebraic in nature, and which are assumptions based on Euclidean characteristics of the space in which elements are described and transformed. Specifically, we wish to re-cast previous work on Euclidean space grammars into a form which can represent - and support operations on - more general manifolds.

Earl[24] develops further the topological structuring of shapes and their subshapes, and develops a treatment of shapes and their boundaries. This argument assumes connectedness and continuity of the space in which operations occur. These characteristics require that the space in which operations occur adopt the characteristics of a metric space (Section V.A), but do not require this metric space to be necessarily Euclidean. As such, Earle's formulation of shape – boundary relations are potentially applicable to the non-Euclidean realm of surface manifolds without modification.

The elements (lines and points) on which grammars operate are considered to be elemental, in a manner similar to Euclid[38] – constructs whose definition is implicit, and shared between author and reader. In computational applications, explicit descriptions of these elements must be formulated[45,46]. This explicit definition of shapes through numerical evaluations is sometimes perceived as an effort in mechanics, whose relationship to the algebraic formalisms of grammars is ill defined.

B. MANIFOLD GRAMMARS

1. Introduction

In Part 2 of this thesis, the description of surface shapes was developed through the structuring of manifolds. This section considers the formalisms necessary to adopt shape grammar theory to such shapes.

The structures of manifold theory provide the basic structures necessary and sufficient to establish algebras of shapes as presented above:

- The notion of Cartesian product spaces, including spaces of real numbers $\mathbf{R}^n$ and vector product spaces. The existence of metric functions on these spaces, necessary to define closure, continuity and neighborhoods or bounded regions, is presumed.
- Transformations or mapping functions between these spatial constructs.

It can be shown that these structures are sufficient to support the constructs associated with shape grammar theory:

- The notions of shapes, and spaces in which these shapes occur,
- Topologies of shape – part relationships, sufficient to allow the definition of Boolean algebras,
- Transformations on shapes.

In the conventional formalism of shape grammars, shapes are seen as entities occurring in, and distinct from, the spaces they inhabit. Manifold theory makes no such distinction between space and shape. Instead, a shape is perceived as a mapping or contract between two distinct spatial constructs, one intrinsic to the shape and presumed to be locally Euclidean, the other extrinsic, into which the shape is embedded or resides. The notion of a shape in analogously viewed in manifold theory as a transformational function that binds together, or translates between, spatial views of the object. This definition of shape-as-function is the basis for the shape's identity[79], and provides the basis for this identity to be preserved through transformations on the shape. Closure operators[83] may be defined on these functions. The structuring of shape-as-function furthermore consolidates the definition of the shape with a functional definition necessary to perform numerical computations.

Shapes described as mapping functions take on the topological characteristics of an $M \times N$ product space define by their relationship on these spaces. This product space not necessarily Euclidean nature, even if the spaces *M* are *N*. Rather, the manifold takes on spatial qualities determined by the mapping function. For differentiable maps, metric functions analogous to that Euclidean distance can be determined. Topologies of neighborhoods are typically preserved across this mapping.

As point of departure, we may consider trivial example of a line segment in $\mathbf{R}^2$, defined as an $\mathbf{R}^1 \times \mathbf{R}^2$ manifold. A might may be defined is a function of two $\mathbf{R}^2$ vectors:

$$\lambda : t \to \mathbf{p} + t\mathbf{q} \,|\, t \in (0,1) \qquad \text{(VIII.5)}$$

although certainly other equivalent definitions of the line function might be used. The boundaries of λ are the 0-dimensional points **p** and **p** + **q**.

The line λ may be viewed equivalently from three distinct spatial perspectives:

- as a closed region of the real line *t*,
- as a line element embedded in Euclidean 2-space,
- as a function or constraint defined in the <$\mathbf{R} \times \mathbf{R}^2$ > product space.

This last perspective is perhaps the least obvious, but most important perspective on the nature of this element. In the case of the above stated line definition (VIII.5), the line forms a constraint on the three variables of the product space (*t,* $\mathbf{u}^1$, $\mathbf{u}^2$):

$$\left(t, \mathbf{p}^1 + t\mathbf{q}^1, \mathbf{p}^1 + t\mathbf{q}^1\right) \qquad \text{(VIII.6)}$$

We often state as a condition for further extensions of the manifold structuring that the mapping function is invertible. In the case of the line, we can define an inverse function $\lambda^{-1} : \mathbf{u}^i \to t$, which maps from Euclidean 2-space parameters back to locations on the scalar number line *t*. A point on this line with $\mathbf{R}^2$ coordinates $\mathbf{u}^i$ maps to a point in line *t* by the vector dot product:

$$t = (\mathbf{u} - \mathbf{p}) \cdot \frac{\mathbf{q}}{|\mathbf{q}|} \qquad \text{(VIII.7)}$$

This inverse mapping is obviously only valid for regions $\mathbf{R}^2$ that are in the image of the original mapping function λ.

With this invertible function in hand, we may establish a topology of parts between similarly defined elements. Given two line segments l_2 and l_1 :

$$\begin{aligned}&\lambda_1 : t_1 \to \mathbf{p}_1 + t_1\mathbf{q}_1 \mid t_1 \in (0,1),\\ &\lambda_2 : t_2 \to \mathbf{p}_2 + t_2\mathbf{q}_2 \mid t_2 \in (0,1)\end{aligned} \tag{VIII.8}$$

with inverse functions:

$$\lambda_1^{-1} : \mathbf{u}_1 \to t_1$$
$$\lambda_2^{-1} : \mathbf{u}_2 \to t_2$$

We can determine product functions that map between the parametric space descriptions of these lines:

$$\begin{aligned}&\lambda_{1\to 2} : t_1 \to t_2, \quad t_2 = \lambda_2^{-1} \circ \lambda_1(t_1)\\ &\lambda_{2\to 1} : t_2 \to t_1, \quad t_1 = \lambda_1^{-1} \circ \lambda_2(t_2)\end{aligned} \tag{VIII.9}$$

A topology of part relations can be defined on these functions and their embeddings into a common space. A line segment λ_2 is a part of λ_1 ($\lambda_1 \geq \lambda_2$) in such case that the function $\lambda_{2\to 1}$ maps t_2 into t_1 on the range $t_1 = \lambda_{2\to 1}(t_2) \in (0,1)$. Production rules for determination of maximal elements may similarly be established. If $t_1(\mathbf{p}_1) < \lambda_{2\to 1}(\mathbf{p}_2) < t_1(\mathbf{p}_1 + \mathbf{q}_1) < \lambda_{2\to 1}(\mathbf{p}_2 + \mathbf{q}_2)$ then the maximal line $\lambda_1 + \lambda_2$ may be defined as the function:

$$\lambda_{1+2} : t \to \mathbf{p}_1 + t\left(\lambda_{2\to 1}(\mathbf{p}_2 + \mathbf{q}_2) - \mathbf{p}_1\right) \mid t \in (0,1) \tag{VIII.10}$$

Coordinates on λ_2 may be mapped into this new parameterization. Operations of complement (-) and product (.) are similarly established.

This approach to grammars on manifolds may be extended directly to higher order manifolds of arbitrary dimensions $<\mathbf{R}^m \times \mathbf{R}^n>$. In this thesis, our focus is on surface elements, embedded in $\mathbf{R}^3$. The structuring of manifolds is naturally extended to the descriptions and transformations of surfaces and their combinatorics.

Part relations can be determined on parametric surfaces embedded into a common Euclidean 3-space. Figure VIII-3 demonstrates this relationship for 2-manifolds embedded in $\mathbf{R}^3$. Two surfaces:

$\sigma_1 : U \in (\mathbf{u}_1) \rightarrow \mathbf{R}^3$

$\sigma_2 : V \in (\mathbf{u}_2) \rightarrow \mathbf{R}^3$

map bounded regions U and V of distinct parametric spaces into a common 3-dimensional space. Inverse functions σ_1^{-1} and σ_2^{-1} can be determined. σ_1 and σ_2 are C^∞ related by $\sigma_1 \circ \sigma_2^{-1}$ and $\sigma_1^{-1} \circ \sigma_2$, if $U \cap (\sigma_1^{-1} \circ \sigma_2)V \neq \varnothing$. If $(\sigma_1^{-1} \circ \sigma_2)V \leq U$, then σ_2 is a part of σ_1.

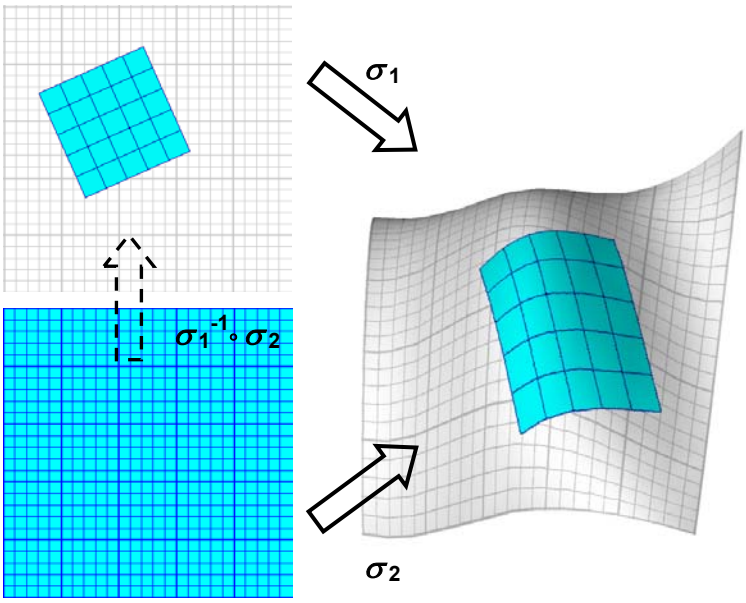

Figure VIII-3: Mapping of Euclidean space shape transformations

Transformations on manifolds are similarly described. The Euclidean transformations of conventional shape grammars are mappings of the form τ: $\mathbf{R}^n \rightarrow \mathbf{R}^n$ where Euclidean space elements of dimension n are transformed by the mapping function, then re-embedded back into the containing Euclidean n-space. For example, rotation about the origin in $\mathbf{R}^2$ may be defined as the 2×2 mapping function[28]:

$$\tau(u,v) = \begin{bmatrix} \cos\theta & -\sin\theta \\ \sin\theta & \cos\theta \end{bmatrix} \begin{bmatrix} u \\ v \end{bmatrix} \quad \text{(VIII.11)}$$

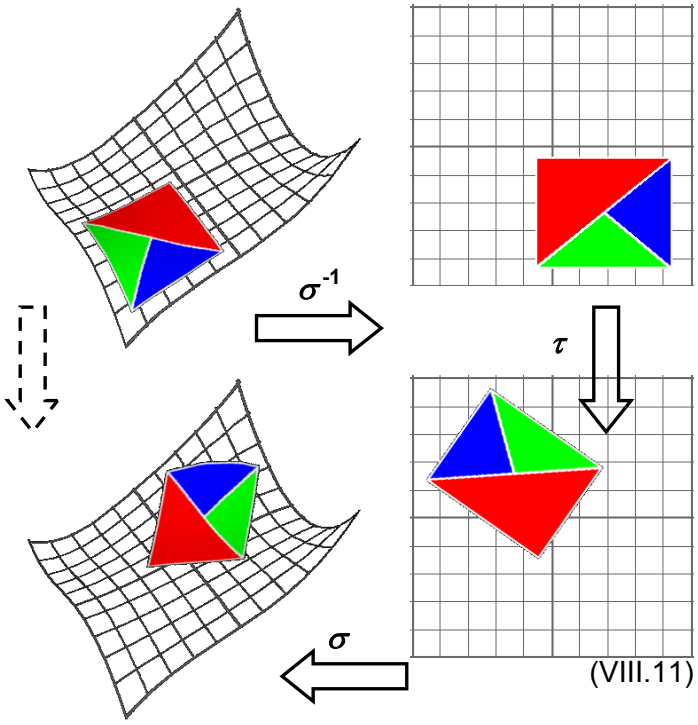

Figure VIII-4: Mapping of shape transformations

Transformations of this sort may readily be extended to manifold grammars. As an example, a transformation of a surface region in $\mathbf{R}^3$, $N \in \sigma(\mathbf{u})$, may be conducted as a transformation in the parametric space of the surface. The transformation of this embedded region is constructed as the contract between the parametric space rotational transformation and the mapping functions (Figure VIII-4):

$$\tau(N): \mathbf{R}^3 \rightarrow \mathbf{R}^3 \\ = \sigma \circ \tau \circ \sigma^{-1}(N) \qquad \text{(VIII.12)}$$

These examples illustrate an important aspect of the structuring of manifolds. Manifolds contract together to form more complex constructions. The "output" of one mapping serves as the "input" of a second mapping. The resulting object may be viewed from the perspective of its initial occupancy of the initial space, its final spatial configuration, or any of the intermediate spatial organizations.

This structuring was drawn on in the definition of curves on surfaces in Section V.D.2. The curve may be equivalently viewed from the perspective of:

- the real number line *t*,
- as a curve embedded in some $\mathbf{R}^2$ parametric space $\mathbf{u} = \alpha(t)$,
- as its ultimate configuration in $\mathbf{R}^3$ through the composite manifold structure $\mathbf{x} = \sigma \circ \alpha(t)$,
- or, if se so choose, even in composite $<\mathbf{R}^1 \times \mathbf{R}^2 \times \mathbf{R}^3>$ that results as a product of the mapping.

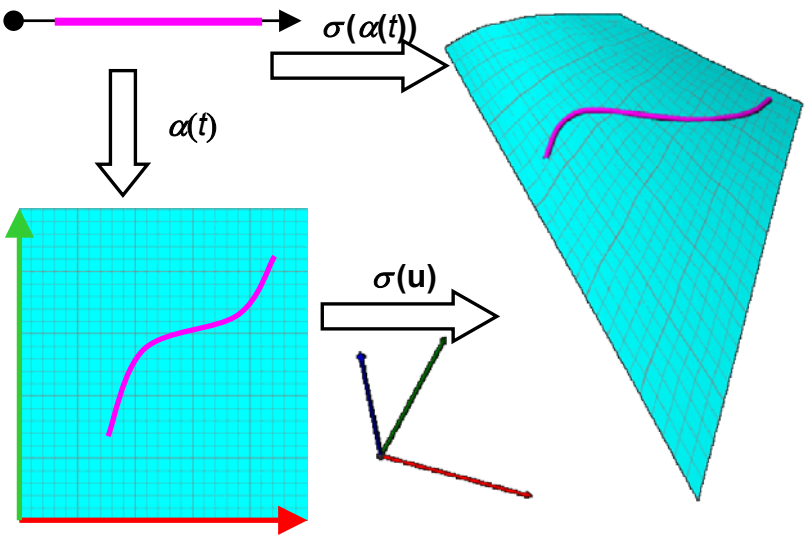

Figure VIII-5: Composition of a curve on surface as manifold

Although we posit that these representations are "equivalent", there is obviously additional complexity to viewing this object in higher order spaces as a consequence of the additional structuring imposed by the composite mapping. As we move toward developing grammars

on manifold objects, it will be beneficial to have any and all of these spatial views available in which we may choose at our discretion to define elements of the grammar. The mapping functions allow us to "know" a great deal about an object's higher order behavior, while still performing computations in reduced spatial representations to take advantage of problem simplifications afforded in these spaces.

2. Other Topological Spaces

So far, this discussion has focused on manifolds defined in real number Cartesian product spaces $\mathbf{R}^n$, to provide the basis for establishing differentiable mapping functions between spatial views on these objects. In many shape grammar applications, such real valued geometric descriptions alone are insufficient to capture the semantic requirements of the problem.

Labels and Weights

In Stiny's shape grammar formulation, labels and weights[82] present examples of such not-necessarily real valued or geometric shape attributes. Labels are, roughly, tokenized information, which may be bound to shapes in a design. As an example, lines on an architectural plan may represent materials; the set of material tokens may include {WOOD, CONCRETE, SHEET_ROCK, etc.}. Elements of different labellings do not combine in the Stiny's. Production rules employing multiple labeled elements may be considered to be grammars operating as parallel grammars, operating in the distinct spaces associated with each label. Weights may be considered to be values associated with design elements. These values may combine according to production rules. The product of a line of color RED and one colored YELLOW may be defined in a production rule to result in a line of color ORANGE.

The structure of manifold grammars naturally extends to include such additional, non-spatial parameters. In manifold theory, there is no distinction between variables that are spatial and those that are not. The inclusion of additional, real valued parameters on a manifold simply requires the extension of the problem formulation into a higher order space. For example, a colored line could be formulated as a 4-Dimensional object of the form $< t \times R \times G \times B >$, where R, G and B are the red, green and blue intensity values associated with the line. Such a "weighted" line may be mapped to the domain other line segments through the

transformations described above; if a line l_1 shares a common range with l_2 through some mapping, the product of these lines is the line:

$$l_1 \times l_2 = \left\langle \left(t_1 \times \lambda_{2\to 1}(t_2)\right), \quad \frac{R_1 + R_2}{2}, \quad \frac{G_1 + G_2}{2}, \quad \frac{B_1 + B_2}{2} \right\rangle \qquad \text{(VIII.13)}$$

The notion of weights or "extra spatial" parameters provides a mechanism for representing complex spatial metrics in simplified form. Consider the case of representing a point on a plane p_0 of distance d from a NURBS surface $\sigma(u,v)$. (Figure VIII-6). The product of points in a grammar with distance to some desired shape will be of interest in Chapter IX. The functional description of the product $<p \times d(\sigma)>$ is a difficult in practice, defined as:

$$d(p) = \underset{u,v}{Min}\left(\left|S(u,v) - p\right|\right) \qquad \text{(VIII.14)}$$

This function typically cannot be solved in closed form[64]. However, in developing grammars in the space of the plane, we may not need to know the complex derivation of this distance functions, and can map result back into the space of our grammar simply as an "extra" variable. We might draw on this variable as a "labelling field": on points defined on the plane. Points on the plane will assume the real-valued labelling associated with the distance parameter of the point.

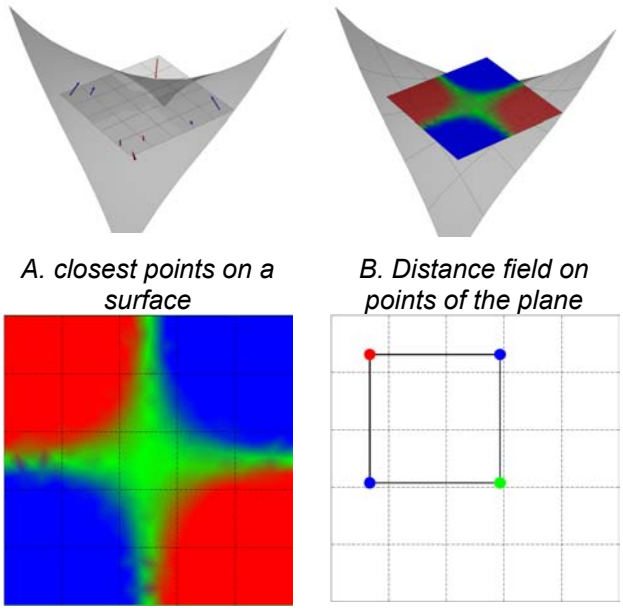

A. closest points on a surface *B. Distance field on points of the plane*

C. Point distance viewed as a "labelling field" *D. A labelling on points*

Figure VIII-6: Surface metrics as a parametric space labelling field

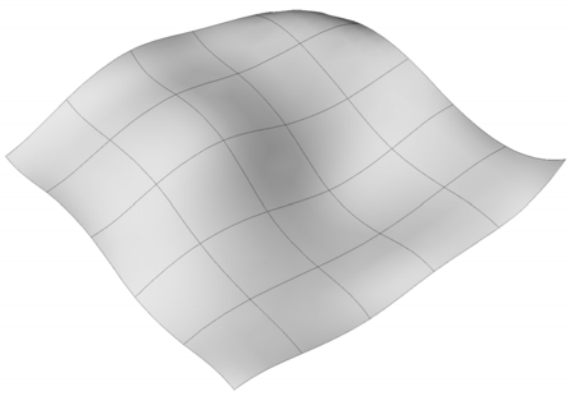

Surface in $\mathbf{R}^3$

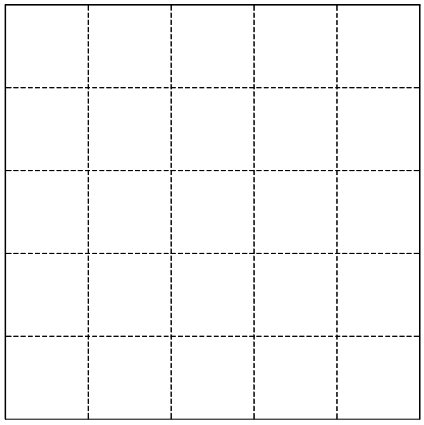

$\mathbf{R}^2$ parametric space

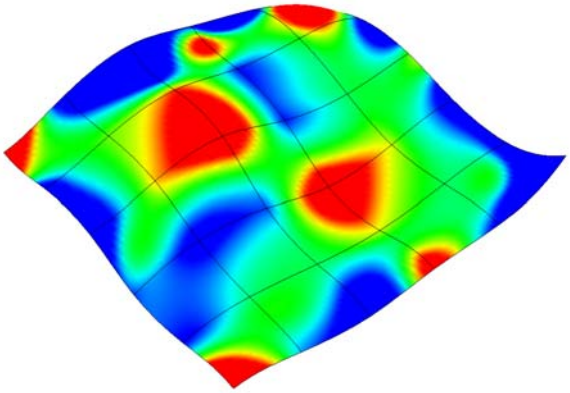

Surface gaussian curvature

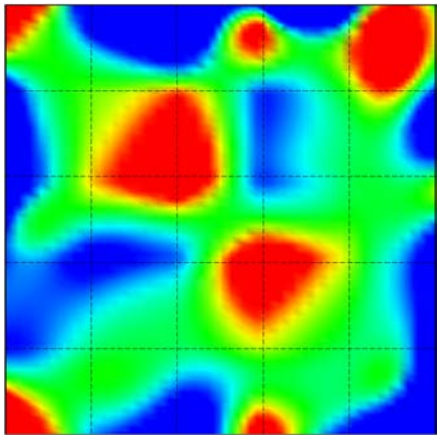

<$\mathbf{R}^2 \times \mathbf{R}$> parametric gaussian map

Figure VIII-7: Gaussian curvature mapping into parametric space

Other important geometric characteristics may be similarly addressed in grammatical constructs. The gaussian curvature of a surface represents a similar real-valued function on the (u,v) parametric space of the surface (Figure VIII-7).

Even higher order, vector based metrics may be addressed in similar fashion. The principal directions associated with surface curvature may be of interest in grammatical applications. The principal directions are $\mathbf{R}^3$ vector functions of the surface function S at the point $S(u_p, v_p)$ (Section V.D.2). Since these vectors are in the tangent plane of S at p, they may be mapped into the parametric space of S, by projecting these vectors into the dual space of the partial derivate vector space $(dS/d\mathbf{u})^*$. The magnitudes of these projections define two $\mathbf{R}^2$ Cartesian product spaces associated with the parametric representation of S. With this inverse mapping in place, we may consider establishing grammars in parametric space, drawing on associated the $\mathbf{R}^2$ mapped principal direction vectors as elements of the

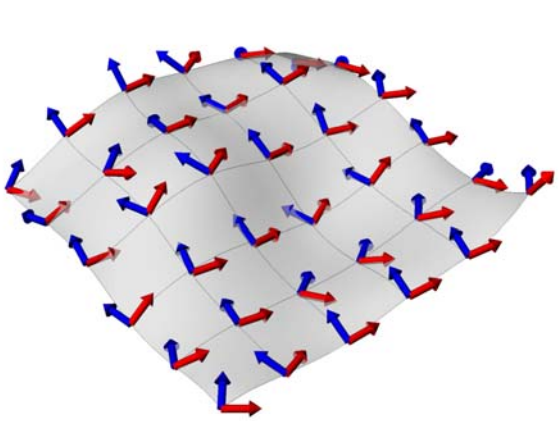

Principal directions on surface – vector field

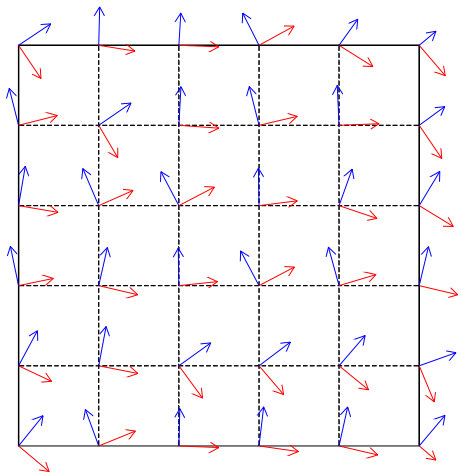

*<**R**^{2} × **R**^{2} × **R**^{2}> principal direction vector field*

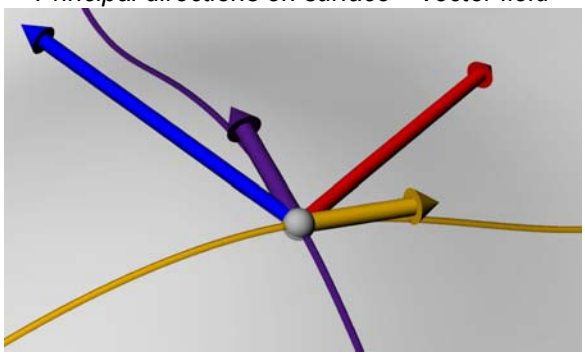

Principal direction vectors and parametric vectors dS/d***u***

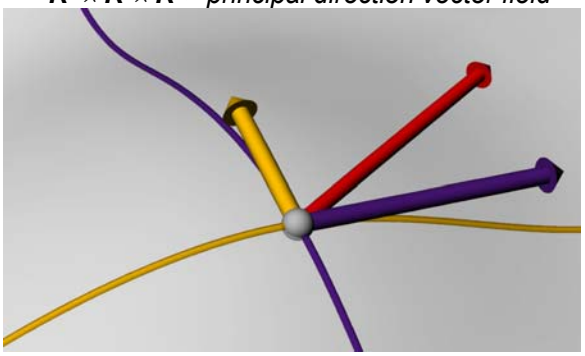

*Expansion of principal direction vector into tangent space of S , by projection onto the vectors (*dS/d***u***)**

Figure VIII-8: Mapping of surface differential properties to a vector field

grammar, directing transformational operations on shapes defined in the parametric space of the surface (Figure VIII-8).

Discrete Topologies

While weights are naturally supported by manifold grammars, the adoption of labellings is not so straight forward. Labellings present constructs in the discrete topology **Z**, a topological structure quite different from the real valued spaces on which manifolds are normally defined. Discrete topologies admit no notions of neighborhoods or boundaries, and all sets of discrete elements are open sets. There is, for example, no notion of nearness between the qualities of WOOD and STEEL. Thus we can not establish the differentiability among elements with differing discrete values. We can, however, choose to establish some gradation on these attributed objects, by establishing a product topology of the form **<Z** × **R>** and mapping between discrete values and some real valued attribute. In our architectural labeling

example, we can establish a material parameter stiffness, and map WOOD, STEEL, and other attributed elements to this parameter accordingly. Alternatively, we can adopt the approach proposed by Stiny, and treat the discrete value "axis" as defining disjoint sets of shapes.

Closely related are topologies on natural numbers $\mathbf{N} \in \{0, 1, 2, 3, \ldots\}$ and integers $\mathbf{I} \in \{\ldots, -3, -2, -1, 0, 1, 2, 3, \ldots\}$. The elements of these sets are likewise discrete. However, notions of nearness, neighborhoods and boundaries may be established on these topologies. The metric functions of distance may be defined similarly to that of real numbers: the distance between the integers 2 and 5 is of course $|5-2| = \sqrt{(5-2)^2} = 3$. Other less intuitive distance metrics can be defined on these elements. The "Manhattan geometry[91]", is a topology on horizontal and vertical lines in an integer space $<\mathbf{I} \times \mathbf{I}>$. We can define a distance metric a point $a = (a_1, a_2)$ to $b = (b_1, b_2)$ as $d(a,b): \mathbf{I} \times \mathbf{I} \rightarrow \mathbf{R} = |a_1 - b_1| + |a_2 - b_2|$, corresponding to the path taken by traversing between a and b exclusively along the streets of a grid, without cutting corners. This distance metric satisfies the axioms for valid distance functions: positivity, nondegeneracy, symmetry and triangle inequality[7]. Again, we can embed such integer based topologies into corresponding real valued topologies through fairly obvious mappings, although again differentiability can not be presumed.

Discrete topologies – and product topologies of real and discrete elements – have great utility to generative systems. The production systems developed in computer science and computational linguistics can be characterized as grammars on discrete symbols. Stiny and Gips provide "a uniform characterization"[84] of such systems.

Graphs

Graphs are one important such construct. A graph is a 2-tuple $<N, E>$ of a set of discrete elements or nodes (equivalently, vertices) $N = \{n_1, n_2, n_3, \ldots\}$ and a set of edges $E = \{ \{n_{i1}, n_{j1}\}, \{n_{i2}, n_{j2}\}, \{n_{i3}, n_{j3}\}, \ldots\}$, which associate pairs of vertices. Edges map $N \rightarrow N$ although this mapping is neither necessarily 1-1 nor onto, since a node may be joined by to more than one other node by multiple edges. Again, it may be of use to embed a graph into some Euclidean or other real valued space, by associating a node with a point space, resulting in a graph that takes the form $<(N \times \mathbf{R}^n) \times E>$. Graph edges, in turn, assume the form of curves joining the embeddings of nodes as functions on $\mathbf{R}^n$ of the form (VIII.5). Indeed graph theory establishes

the special class of *planar graphs*[90] isomorphic to a graph embedded into a plane without edges that cross in space.

Grammars on graphs may be developed that perform transformation operations on node and edge elements. Figure VIII-9 shows an example of a graph grammar, which generates subdivisions of triangles. The graph on the left hand side of the production rule is described by the set of nodes and edges:

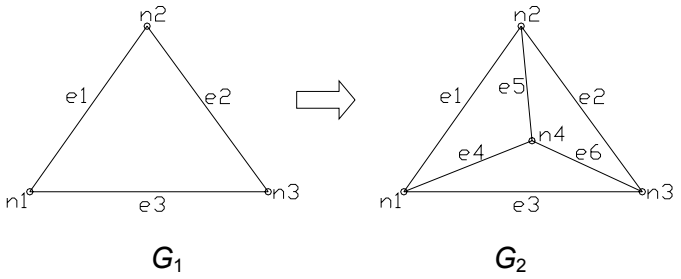

Figure VIII-9: Graph grammar resulting i n the subdivision of triangles

$G_1 = \{\{n_1,n_2,n_3\} , \{ \{n_1,n_2\}, \{n_2,n_3\}, \{n_3,n_1\} \} \}$

while the graph on the right side is represented by the graph:

$G_2 = \{\{n_1,n_2,n_3,n_4\} , \{ \{n_1,n_2\}, \{n_2,n_3\}, \{n_3,n_1\} , \{n_1,n_4\} , \{n_2,n_4\} , \{n_3,n_4\} \} \}$

The production rule $G_1 \rightarrow G_2$ results in the insertion of 1 additional node and 3 additional edges into a graph *G.* Parametric grammars may be considered to be graph grammars embedding into Euclidean or other space.

3. Complexes

Graphs and graph grammars have direct application to grammars on surface assemblies, in forming the basis for topologies of complexes. A complex is a topological space constructed of vertices, edges, and polygons[33]. Complexes are assemblies of *n*-simplexes, basic bounded, connected topological elements of dimension *n*. A simplex of dimension *n* is bounded by a set of simplexes of dimension *n*-1. Two *n*-simplexes join by topological identification of pairs shared boundary elements. Surface (polygon) elements combine by joining edges. Edges are joined together to form boundaries of polygons by topological identification of their boundary vertices. Vertices (respectively edges) may be identified with those of other equivalently dimensioned elements.

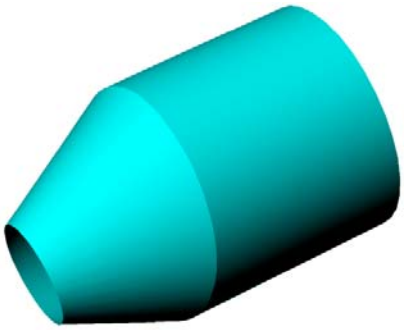

A. A surface complex

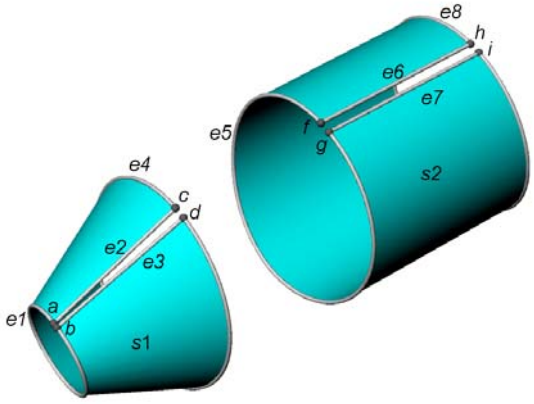

B. Its constituent simplexes and identifications

This description of spatial elements as complexes does not describe the specifics of a spatial object's inhabitance of space. Rather, it describes the connectedness of a spatial object in terms of the connectedness of its constituent elements. Complexes are a formulation of spatial objects as discrete topologies of constituent components.

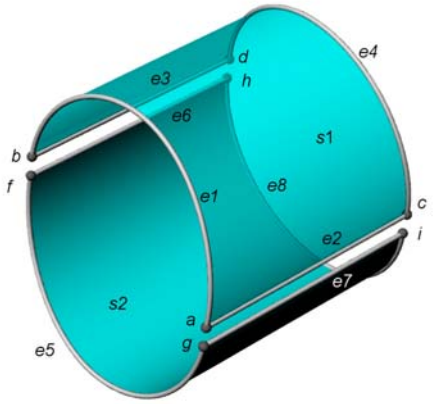

C. Transformation by re-identification

Figure VIII-10: A complex as adjacency graph

In these terms, a surface assembly may be considered a 5-tuple of the form <*F*, *E*, *V*, I_E , I_V > where *F* is a set of faces or polygons, *E* a set of edges, *V* a set of vertices, and I_E and I_V are, respectively, identifications of edges and vertices. Figure VIII-10A shows an example of a simple surface complex, comprised of two sub-surfaces. The elements of this complex are:

$F = \{s_1 , s_2 \}$

$E = \{e_1, e_2, e_3, e_4, e_5, e_6, e_7 \}$

$V = \{a, b, c, d, f, g, h, i \}$

$I_E = \{e_2, e_3\}, \{e_4, e_5\}, \{e_6, e_7\}$

$I_V = \{a, b\}, \{c, d , f, g \}, \{h, i\}$

Transformation operations on spatial objects may be developed as graph grammars in the topological space of these elements and their identifications, independent of their spatial descriptions. Figure VIII-10C postulates such a transformation on the complex, where substitutions occur in the identifications of the elements, of the form:

$I_E \rightarrow I_{E'}$: $\{e_2, e_3\}, \{e_4, e_5\}, \{e_6, e_7\} \rightarrow \{e_2, e_7\}, \{e_3, e_6\}$

$I_V \rightarrow I_{V'}$: $\{a, b\}, \{c, d , f, g \}, \{h, i\} \rightarrow \{a, g\}, \{b, f\}, \{c, i\}, \{d, h\}$

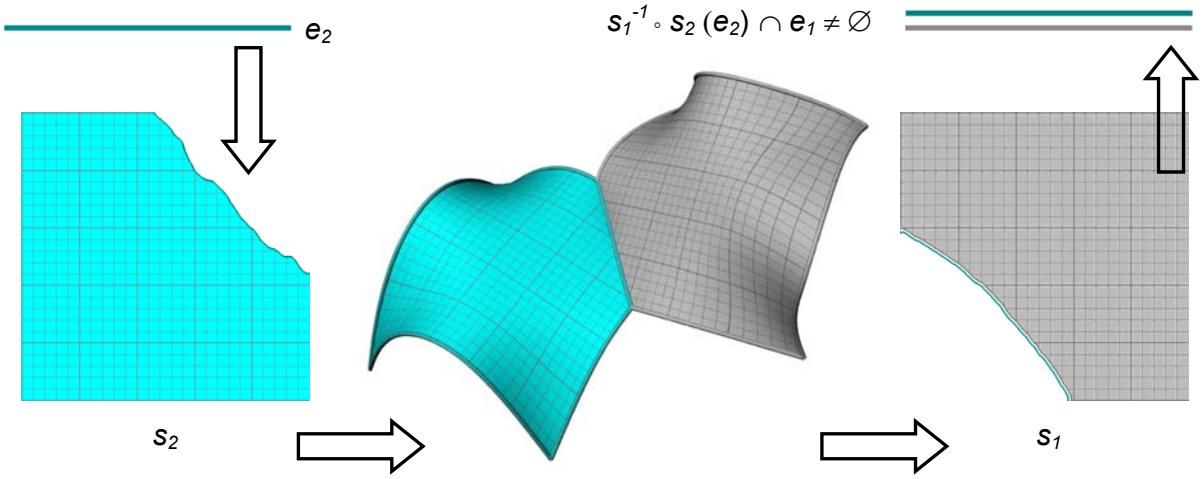

Figure VIII-11: Mapping of shared boundaries

This representation of surface assemblies as complexes is compatible with their organizations as manifolds. The graph representation of a complex may be mapped into the organization of manifolds and their subspace boundaries. The identification of sub-elements takes the form of embeddings. An edge e_1 of surface element s_1: $U \rightarrow$ $\mathbf{R}^3$ may be identified with an edge e_2 of s_2:$V \rightarrow$ $\mathbf{R}^3$ if the mapping $s_1^{-1} \circ s_2$ is at least C^0 continuous and $s_1^{-1} \circ s_2 (e_2) \cap e_1 \neq \varnothing$. The complex is C^k continuous at the edge between s_1 and s_2 if their charts are C^k related at this shared boundary (Figure VIII-11). This geometric continuity[28] describes the differential order of shape continuity across element to element connections. Surfaces may

simply be touching or closed (order G^0), tangent (G^1) or curvature continuous (G^2). Higher order differential continuities are possible. In practical paper surface applications, gradations of these qualities exist. Open seam conditions exist where edges are associated but do not exactly touch. An edge may be only close to joining, connected but with large gaps, tape or loosely fastened rivets or screws. An overlapping edge may partially constrain tangency or curvature continuity, but allow a certain degree of deviation from true G^1 or G^2 connectivity. Geometric continuity may be represented in the incidence graph as labellings on edge identifications.

The connectedness of a complex may be represented in the discrete space of graphs whose elements are these incidence coefficients[33]. We can draw on this simplified representation to perform transformations on surface assemblies. The triangle subdivision grammar shown in Figure VIII-9 presents one such example. This representation of this operation on the complex graph presents a vast simplification of the problem space. Of course, this representation hides all detail of how the transformation affects the actual embedding of the triangle assembly in space. If, as is likely, this knowledge is important to decision making by the grammar, we will again need to map spatial metrics back into the graph space, or conduct our grammar in the product space of the embedded graph with other spatial representations of the complex's constituent elements.

C. SUMMARY

This chapter has established a formal basis for the development of shape grammars of surface assemblies. This structuring views shapes as real, differentiable functions operating in Cartesian product spaces of the form $<\mathbf{R}^n \times \mathbf{R}^m>$. Shape boundaries are similarly described as sub-manifolds of the form $<\mathbf{R}^{n-1} \times \mathbf{R}^n>$, embedded in the parametric space of the shape. The important algebraic foundations of the shape grammar formalism, including notions of shape – part relations, Boolean algebras on shapes, and shape labellings and weights, were developed through this manifold representation.

The structuring of manifolds provides the potential for grammar operations on complicated spatial objects, such as our paper surface assemblies, to be conducted in spaces representing alternative, simplified, representations of these objects, while allowing the full richness of the objects' spatial behaviors to be referenced by the grammar.

IX. GENERATIVE RATIONALIZATION

This chapter presents several examples of grammars that have been applied on Gehry projects or are currently under development. In general, these applications are directed toward rationalization of the surface forms to address specific constructibility requirements. The strategies taken in this chapter differ depending on the application and the specific requirements of the surface fabrication strategy. However, some general characterizations of these approaches may be made.

- A pre-rationalized "ideal surface form" – perhaps the product of digitized physical models- is admitted as the input shape for rationalization operations.

- Surface elements and their boundary forms serve as the elements of the grammar. These surface elements are formally described as parametric mapping functions in $<\mathbf{R}^2 \times \mathbf{R}^3>$ space. The characteristics of this differentiable mapping function are specific to the constructibility problem under consideration. Examples include the constrained curvature, developable and materials based surface representations presented in Chapters VI and VII.

- The surface manifold is considered both a "micro" representation of the surface elements and a "macro" scale perspective of the assembly's organization as a whole. To simplify operations, grammars are typically conducted at least partially in the parametric space of the surface elements, drawing on Euclidean characteristics of this space, and the corresponding reduction of the space's dimensional order. Macro level operations are often conducted on the graph of boundary element identifications.

- Shape metrics and other heuristics from the 3-dimensional configuration are mapped onto these representations as labellings on grammar elements. These metrics provide the grammar with heuristics to assess the constructibility of assembly.

- The grammars perform substitution operations on sheet boundaries and other features in parametric space, and operations such as splitting or insertion of faces in the graph of the

surface complex. Substitution operations are performed toward the goal of satisfying constructibility conditions of the assembly.

A. GENERATIVE APPLICATIONS ON THE EXPERIENCE MUSIC PROJECT

The genesis of these applications was a series of rationalization studies conducted during design development on the Experience Music Project. Section VI.2 described the macro scale constrained gaussian curvature approach taken to rationalizing EMP's form. Additional rationalization operations were conducted both at a global scale as well as on the localized configuration of sheets during shop drawing generation. Automation efforts were conducted in parallel with the manual operations.

1. Design Development Applications

Initial design development rationalization studies were pursued over the period between March and May of 1997. The approach described in this section is based on an assumption that surface forms of any curvature can be constructed from flat sheets, deformed within some limited range, presuming that the dimensions of the surface sheets are varied in response to the surface curvature. Breaks in tangency between sheets accommodate some degree of curvature in the macro scale surface form. Decreasing the size of panels should increase the number of these tangency breaks, allowing greater degrees of curvature to be accommodated.

The design surface (Figure IX-1A) was initially approximated as a fine grained, rectangular grating[33] (Figure IX-1B). This regularized, integer space parameterization provided an efficient spatial construct on which to perform the grammar operations. The goal of the grammar was to determine a configuration of surface regions whose deviation from a plane was within a predetermined tolerance.

A. Input surface

B. m × n Tessellated mesh

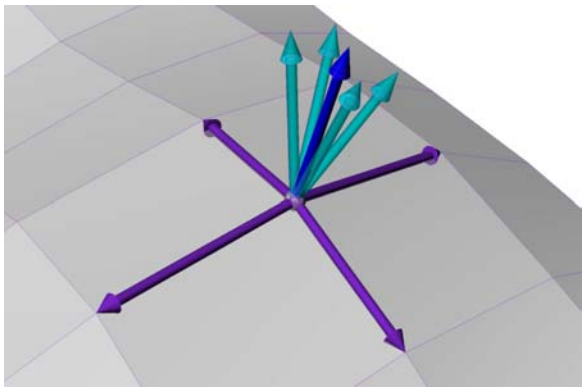

C. Construction of mesh normal at a point

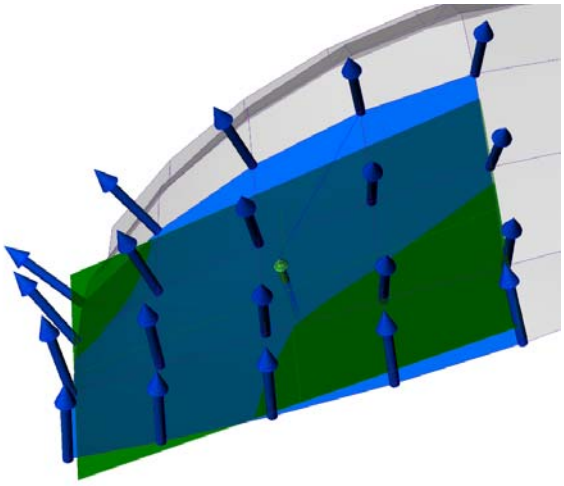

D. Determination of best fit plane on a region

Figure IX-1: Subdivision grammar metrics (EMP)

The algorithms begin by determining a best fit plane to the surface in a given rectangular region. Surface normals approximated for each facet neighboring a vertex are summed and normalized to provide a localized approximation of the surface normal at the vertex (Figure IX-1C). These localized surface normals are in turn summed over the rectangular region to determine an average surface normal for the region. The vertices in the region are then projected onto this vector. The span of these projected points provides a measure of the planarity of the surface region. If this deviation from the average plane on the surface region is within a specified tolerance, the region is considered to be acceptably planar. If not, a recursive subdivision is conducted on the region.

`

Subdivision strategies for surface approximation have significant attention in the computer science community. Analogues are found in shape grammar literature. The point of departure for these grammars is provided by the Mughul garden grammar[86]. The basic production rule of the Mughul grammar subdivides a square into 4 smaller squares. This operation may be recursively re-applied to generate localized, arbitrarily small square regions of the space.

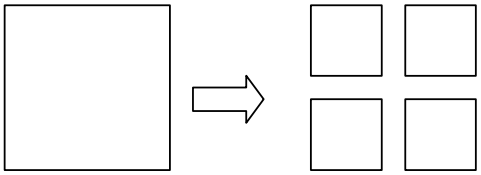

Figure IX-2: Base Mughul grammar production rule

This production rule can be tailored to perform subdivisions directed towards satisfying localized conformity conditions. Hokoda adopts this approach in image tiling applications[58]. His approach (Figure IX-4) performs a histogram on pixel brightness across a region of an image. The operation is performed in the $\mathbf{I}^2$ integer pixel space of an image of size 2^i. If the values vary by greater than some threshold, a bi-directional subdivision of the image region according to the rule in Figure IX-2 is performed. The subdivision is repeated recursively until a specified histogram threshold is encountered. The recursion is guaranteed to terminate, since the limit of recursion is one pixel, whose internal variation is guaranteed to be zero. This recursion will be guaranteed to terminate if the threshold functions tends toward zero as region size decreases. However, this is true for many interesting spatial metrics.

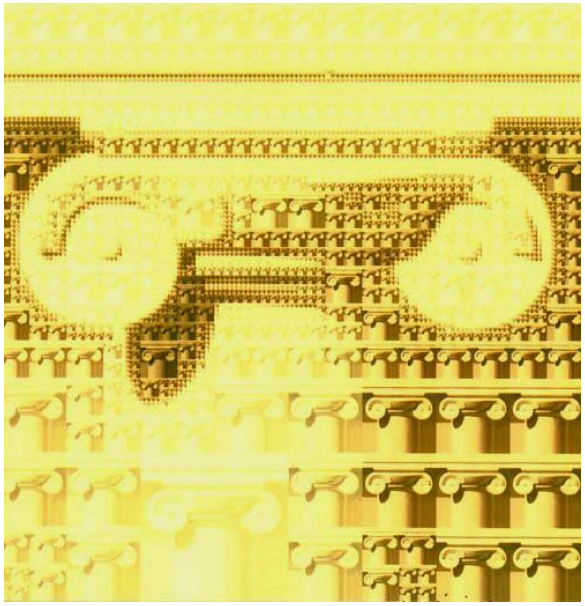

Figure IX-3: Image subdivision using a histogram metric

This subdivision strategy can be applied to any two dimensional rectangular grating $\mathbf{R}^2$ or $\mathbf{I}^2$ that admits a scalar metric field. An initial application of this approach to curved surface rationalization is shown in Figure IX-4A. This example correctly identifies flat regions of varying size, depending on the local surface curvature. However, there are limitations to this initial result. The layout is inefficient, producing more subdivisions than necessary. If a region under consideration only one small part out of plane, the algorithm will subdivide the region

into four sub-regions, where a subdivision into two might be sufficient. The algorithm also produces a relatively predictable pattern of equal sized regions with a very visible pattern of tessellation.

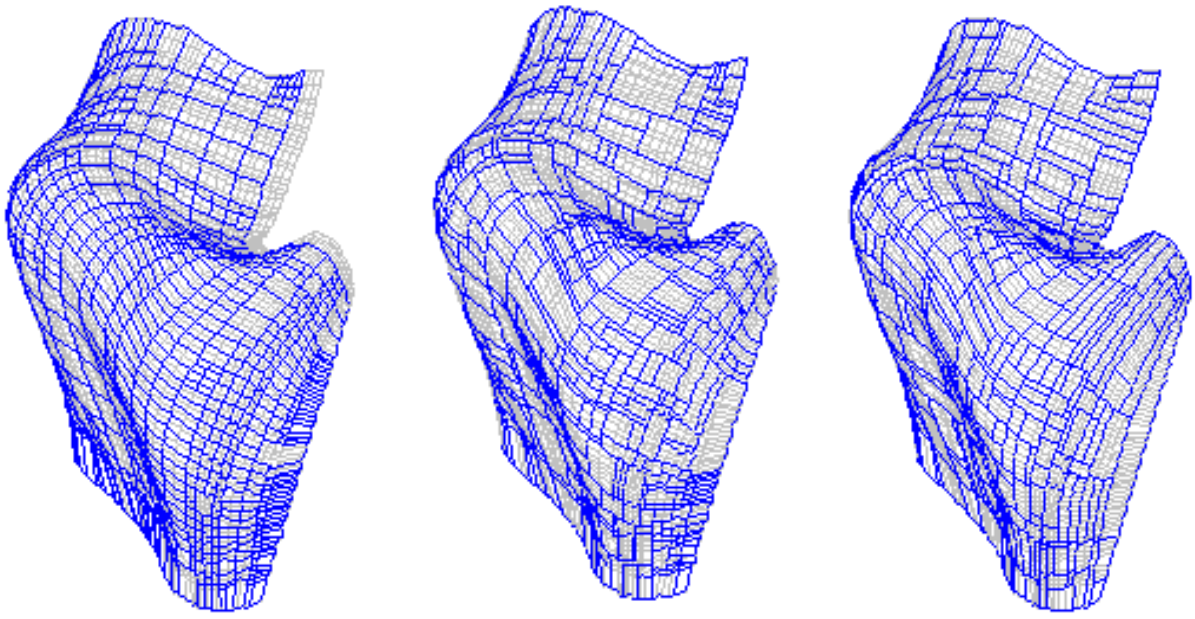

A *B* *C*

Figure IX-4: Subdivision grammar results

This simple subdivision algorithm can be improved on in a variety of ways. The most obvious means for improving the efficiency of the subdivision is to search for some best flat subregion, rather than simply splitting the region in the middle. The grammar shown in Figure IX-4B and Figure IX-5B divides the regions in half instead of quarters. At each step in the recursion, the grammar steps across the region in both horizontal and vertical directions, attempting to find a largest region with acceptable metrics. If such a region is found, the algorithm terminates on this valid subregion and recurses on the remainder of the initial region. A third approach is shown in Figure IX-4C and Figure IX-5C shows an additional modification, where the subdivision is not limited to two regions, but also allows a subdivision into 3 parts if an interior region is the largest acceptable region. This result provides the most optimal layout of regions in the series, and additionally generated random patterning qualities that were of interest to the project designers. These studies demonstrated the potential of subdivision grammars to addressing certain constructibility issues on surfaces, and additionally showed that the approach could be tailored to respond to qualities of design.

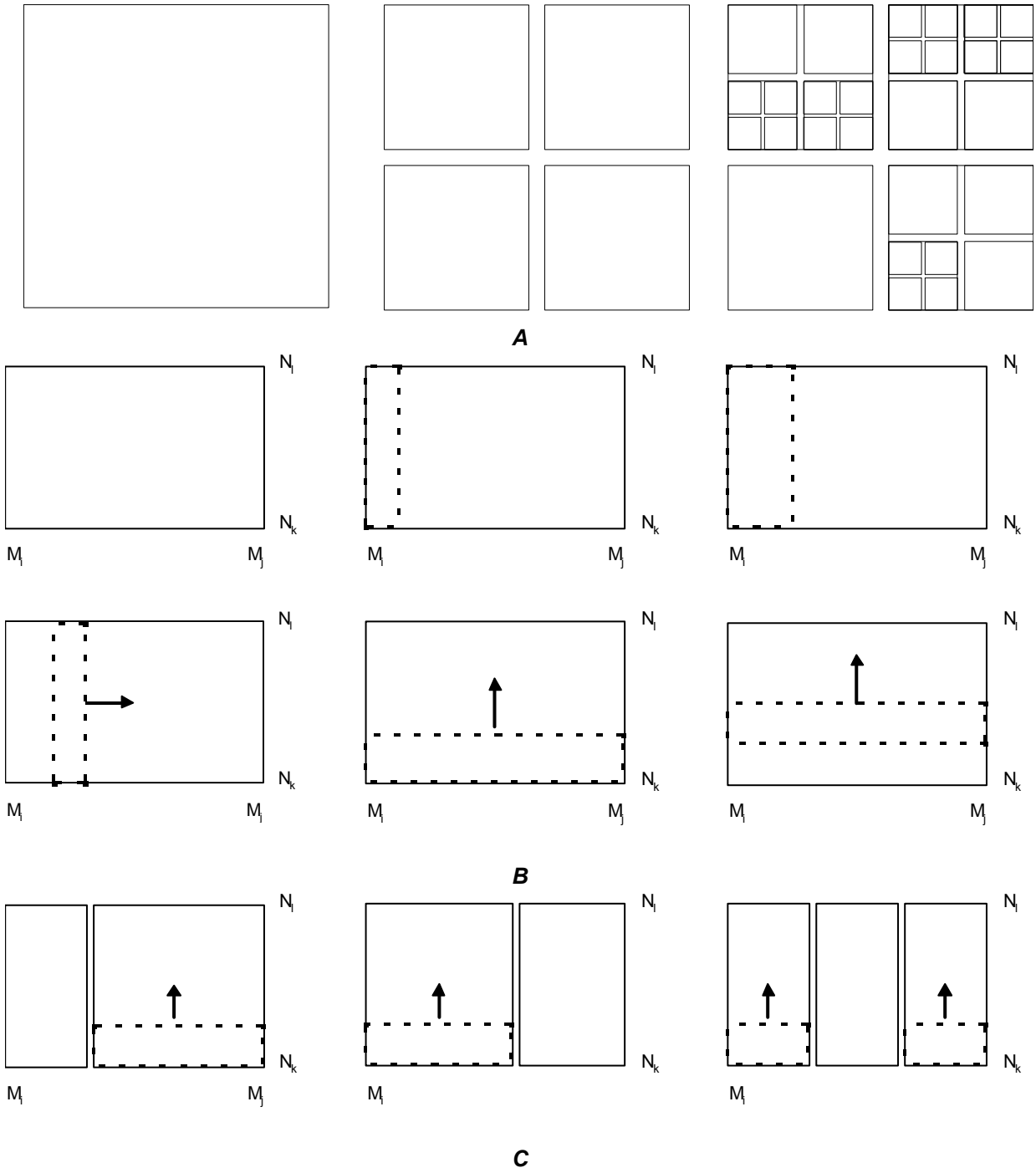

Figure IX-5: Rules of the subdivision grammar

During contract document preparation, the subdivision approach was modified to remove the necessity for a polygonized grating, and operated directly in the parametric space of the Bézier patch surface representation. Surface regions were defined on the basis of parametric coordinates along an isoparametric curve. However, planar cuts were required by

the fabricator, so a best fit normal plane was defined between the edge vertices of an isoparametric curve, and an intersection was created between this plane and the surface. The fabricator imposed additional constraints, limiting the size of a panel and face sheet to maximum dimensions of 10’ x 15’ and maximum square area of 100 square feet for panels, and a maximum 48” x 96” for face sheets based on available material sizes. The subdivision terminates at acceptable panel size, then is re-run on the resulting panels to define the face sheets. Figure IX-7 shows the results as they appeared on the design development package of the project.

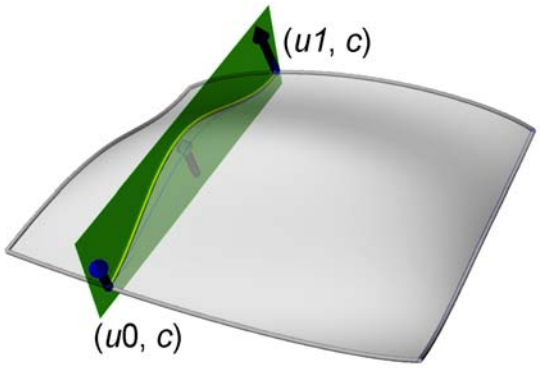

Figure IX-6: Basic parametric subdivision grammar

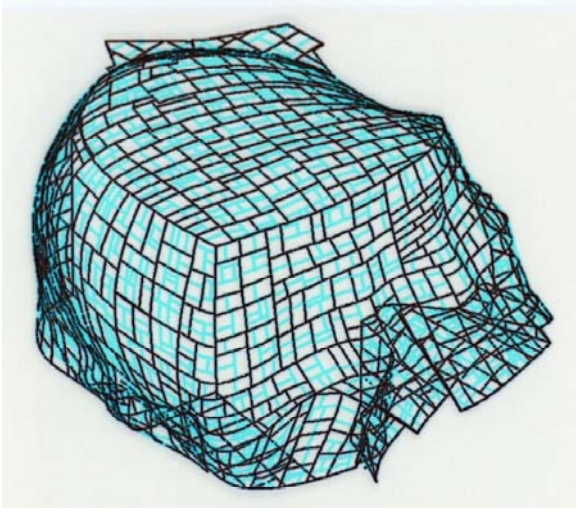

Figure IX-7: subdivision grammar applied to EMP design development models

Additional generative studies were conducted at the face sheet level. These studies attempted to optimize the layout of face sheets on an individual panel, on the basis of available material sizes. The production rules generating the face sheet configurations shown in Figure IX-8 represent a slight modification of those in Figure IX-5. In these examples, the subdivision grammar splits the panel along a line parallel to one of the panel edges, offset at a distance defined by the width of the available surface material. If the length of the resulting edge piece is greater than the length of the available material, the edge piece is further split into pieces of appropriate length. The algorithm is then recursively applied to the remainder of the panel. The algorithm terminates when the remaining region is smaller than the dimensions of the surface material. Each of the four region edges are successively offset at each level of the recursion. The result is a full traversal of the set of all possible face sheet configurations for the given panel dimensions and material sheet size.

Figure IX-8A Grammar for face sheet layout on panels
Test panel sides: 12'7", 10'4", 9', 8'3"
48"x96" material – all 29 permutations

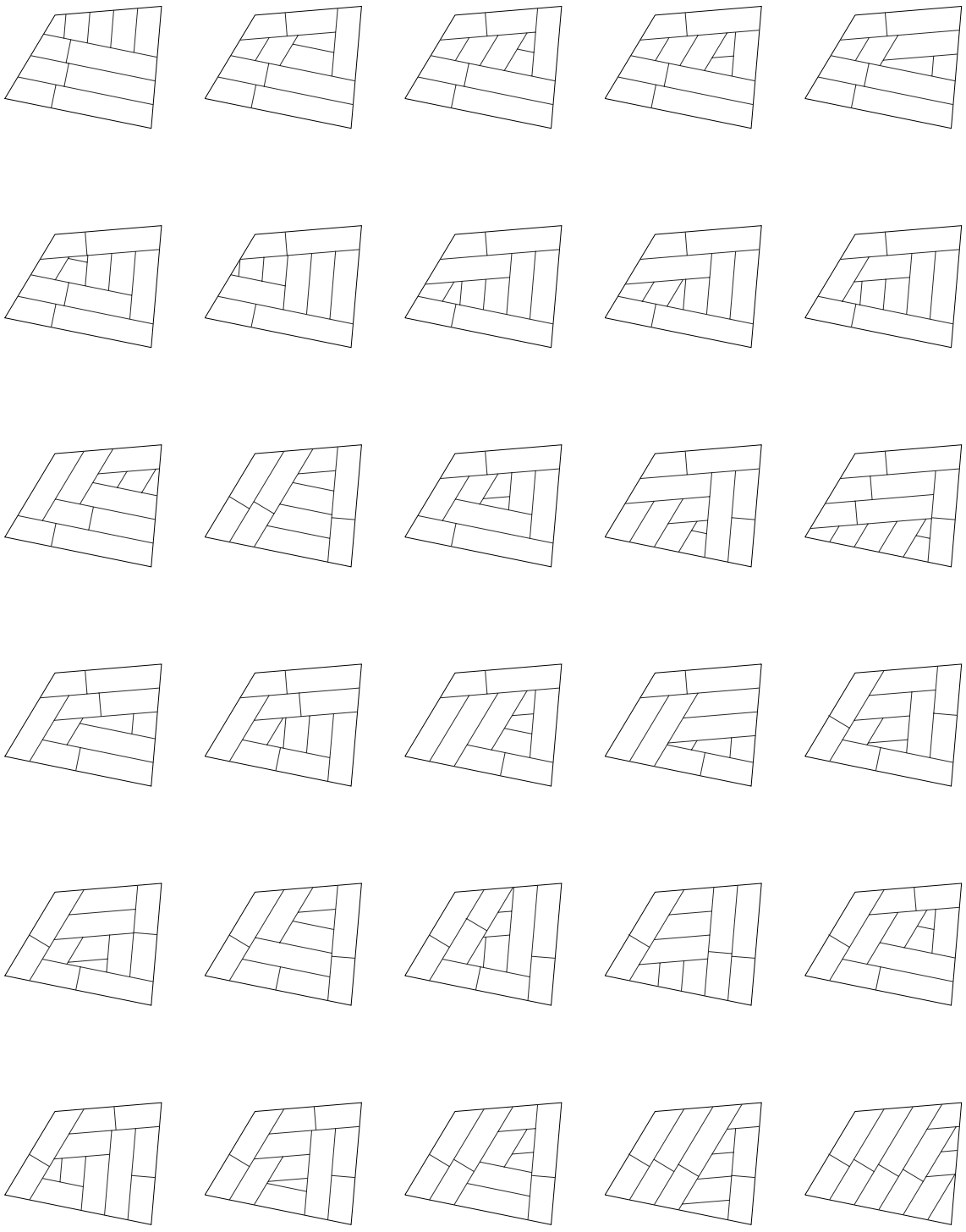

Figure IX-8B
24”x96” material – 30 of 11941 permutations

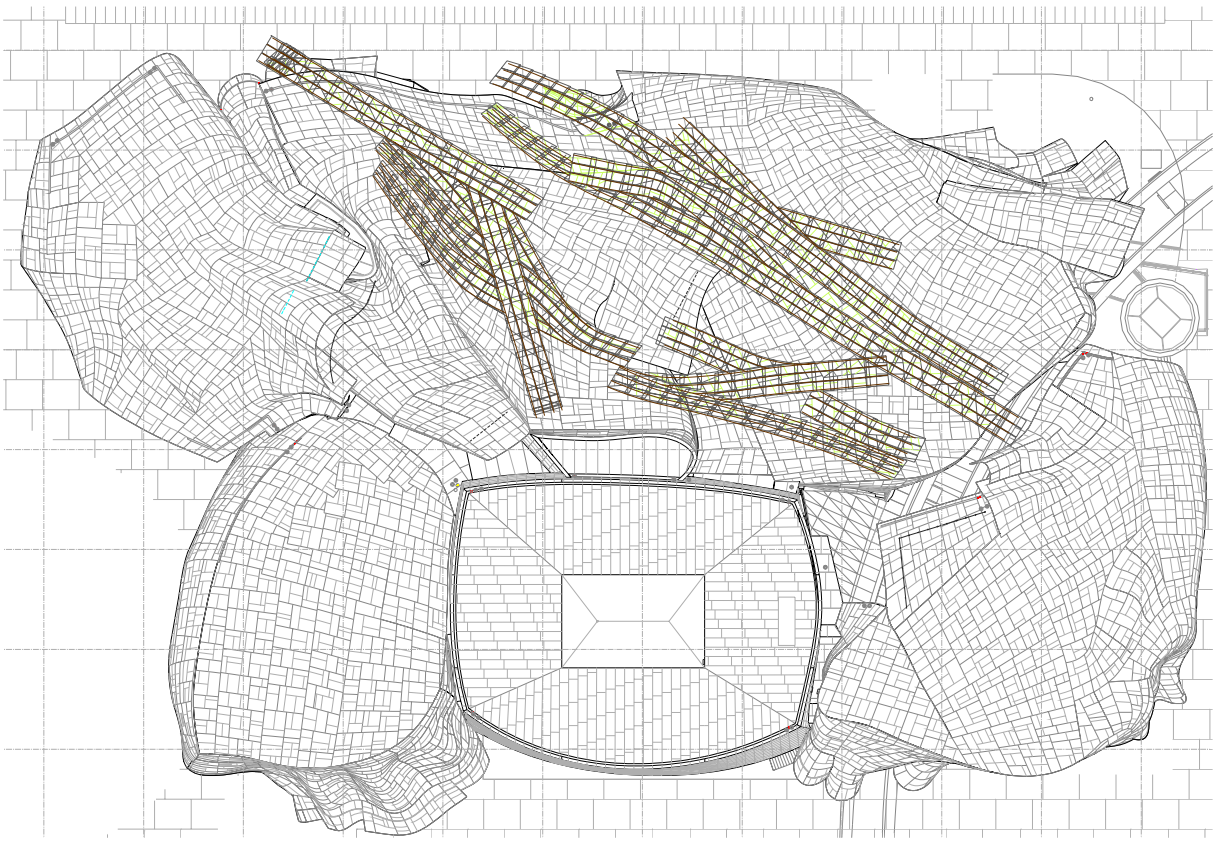

Figure IX-9: Subdivision grammar applied on EMP contract documents

2. Construction Documentation and Shop Drawing Phase Applications

The applications of rationalizing grammars described above provided substantial saving of effort for the CAD modeling team during contract document preparations. However, during constriction document and shop drawing phases, the set of rules imposed by the fabricator on the paneling system organization was substantially extended. These additional constraints resulted in requirements that could not be addressed by a completely automated approach.

The geometric complexity of the final cladding system are largely a product of the project's fast track schedule. The design of the rib and concrete shell structural system was finalized before details of the cladding system were known. Once the cladding system was designed, its organization had to be integrated with the already designed structural system organization. At the same time, design considerations regarding the pattern of panels on the

surface had to be addressed. The complexity of the cladding system organization is directly related to its response to these design and performance requirements.

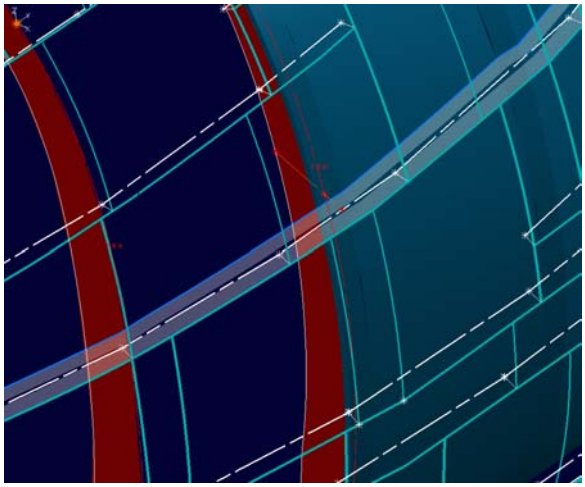

Figure IX-10: Pipe routing through interstitial space

The fabricator designed the cladding system using conventional pre-fabricated cladding system detailing, radically modified to support the curved project geometry. The decision was made to pre-fabricate the surface as panelized system, rather than construct the surface in the field. The panels are formed as a box configuration of planar, CNC cut fins that respond to the curvature of the CATIA surface model. Face sheets of the finish metal were fastened to the tops of these fins.

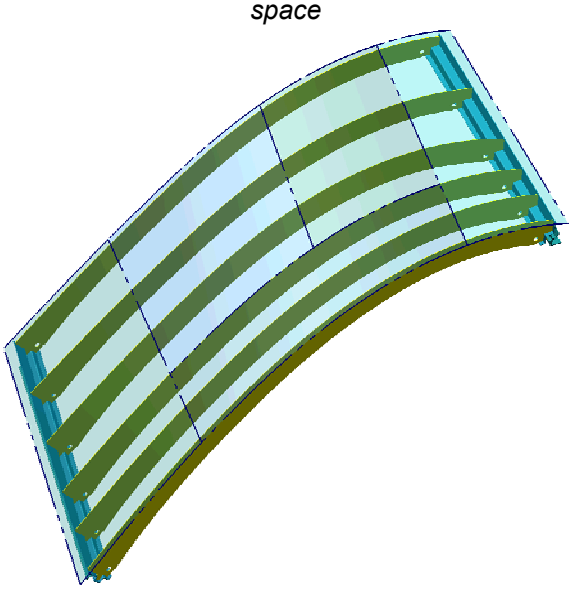

Figure IX-11: Panel framing

The strategy for fastening these panels to the structural frame relied on a modified detail from conventional cladding systems, called the “rock & roll” connection. A slot in the fins at the bottom edge of each panel is inserted into a ball connector on a metal extrusion. The panel is lowered onto the ball connector, then rotated about the connector until the top edge of the panel can be seated into the lower edge of the next extrusion above. The panel is then fastened to the top connector along its top edge. This strategy requires fasteners only at the top, free edge of the panel, removing the necessity for fasteners to be added at the lower edge, where the previously installed lower panel would prohibit access.

This connection requires a straight, linear extrusion along the bottom edge of each panel. On EMP, this extrusion is supported by a system of segmented tubes, which span between the ribs of the structural system. The major design challenge of the system became fitting the system of tubes into the small interstitial space between the design surface and the already

existing geometry of the structural rib and concrete shell. Each tube is initially viewed as a planar intersection with the surface, offset a pre-determined distance inward from the surface. The tube curve is then segmented into straight runs that “bounce” between pre-determined offsets from the finish surface and the concrete shell (Figure IX-10). Structural requirements imposed numerous additional geometric rules on the layout of the tube system. At the same time, the tube layout had substantial implications on the surface pattern, since the panel connection detail required a vertical panel break at each kink in the tube.

The fabricator provided an extensive set of rules in writing to the design team, which specified the geometric requirements of each panel system element. On the basis of these rules, a procedure for the layout of tubes and panel edge locations was established. These geometric rules can be considered a grammar on the organization of the elements:

1. First, a set of planar curves representing the tube locations and corresponding horizontal panel breaks are constructed on the surface.
2. Next, geometric operations are performed to bounce the tube center line between the offsets defining the interstitial space.
3. The kink locations are projected back on to the surface, to define the vertical panel breaks at the panel jambs. This defines regions on the surface, spanning vertically from tube to tube, and horizontally between tube kinks.
4. Additional horizontal panel breaks are added if the horizontal distance of the region is longer than can be accommodated by a single panel.
5. Finally, face sheets are laid out on each panel, through rules on face sheets similar to those presented in the previous section.

Figure IX-17 provides a listing of the geometric rules provided by the fabricator to the design team. The elements of the grammar are shown schematically in Figure IX-12, while Figure IX-13 through Figure IX-16 show the organization of the resulting system elements on Element 7 of the project.

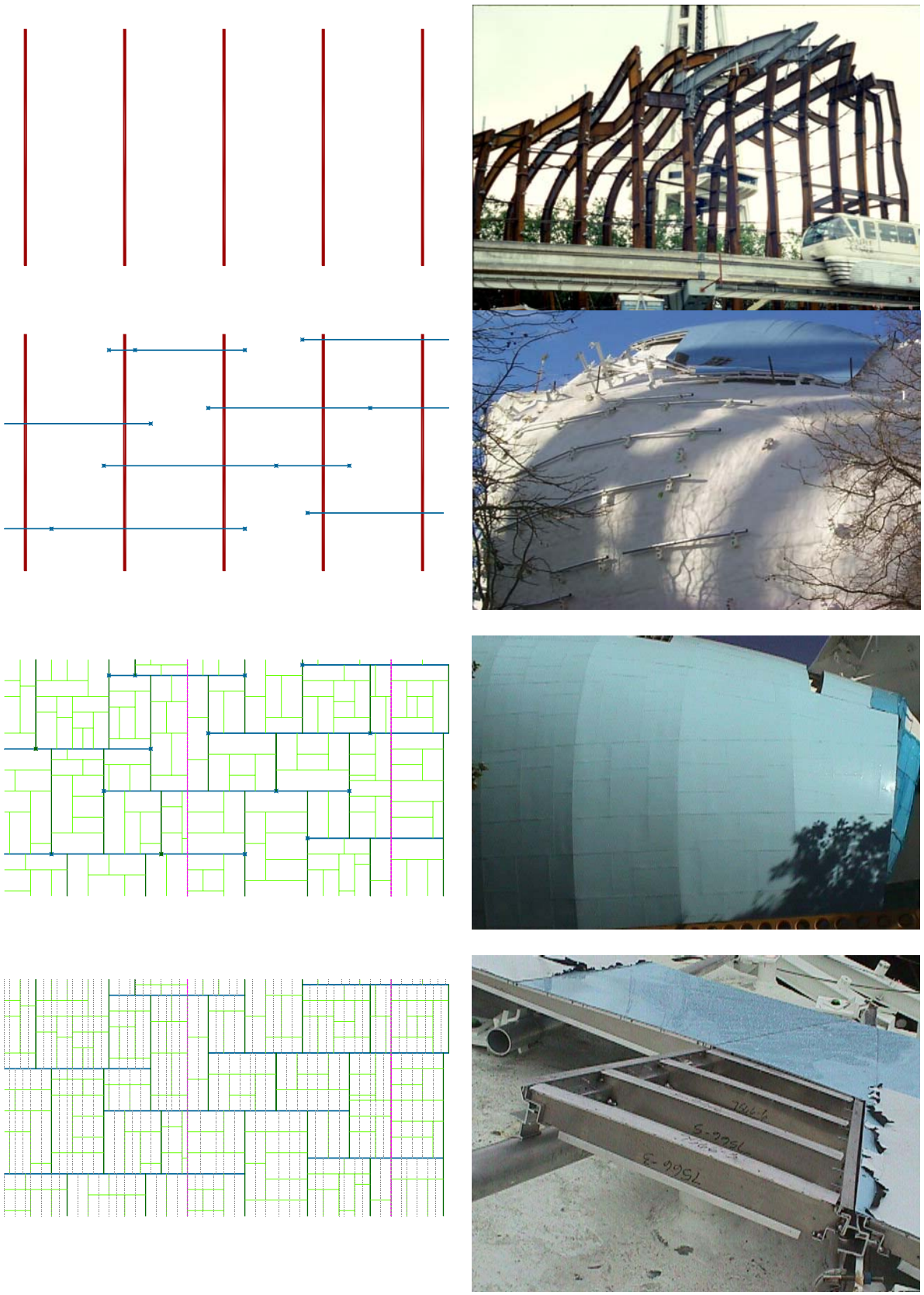

Figure IX-12: Elements of the EMP surface fabrication grammar

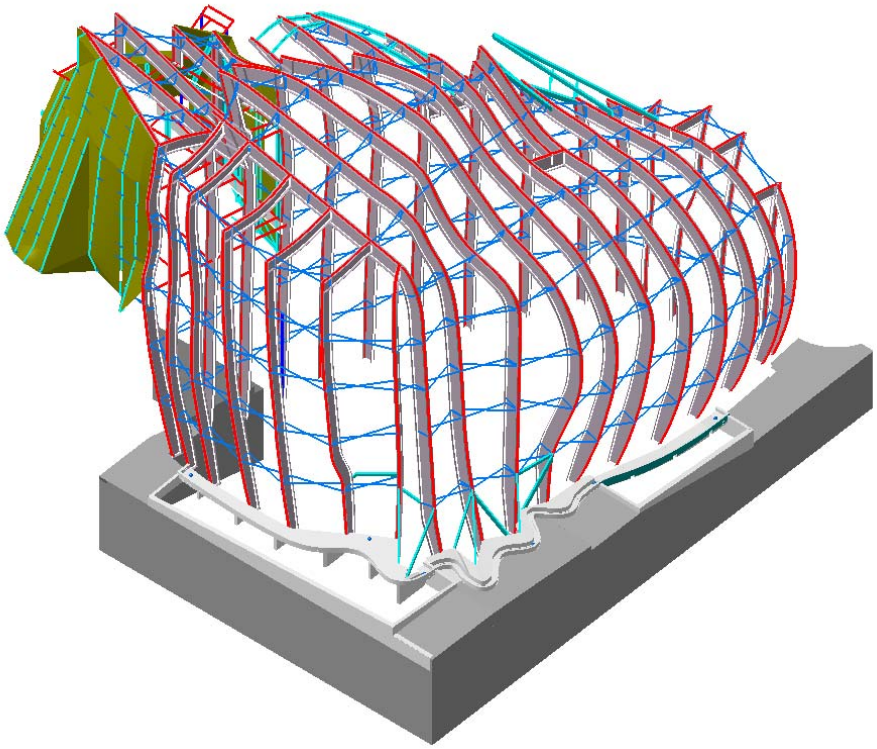

Figure IX-13: Structural rib system

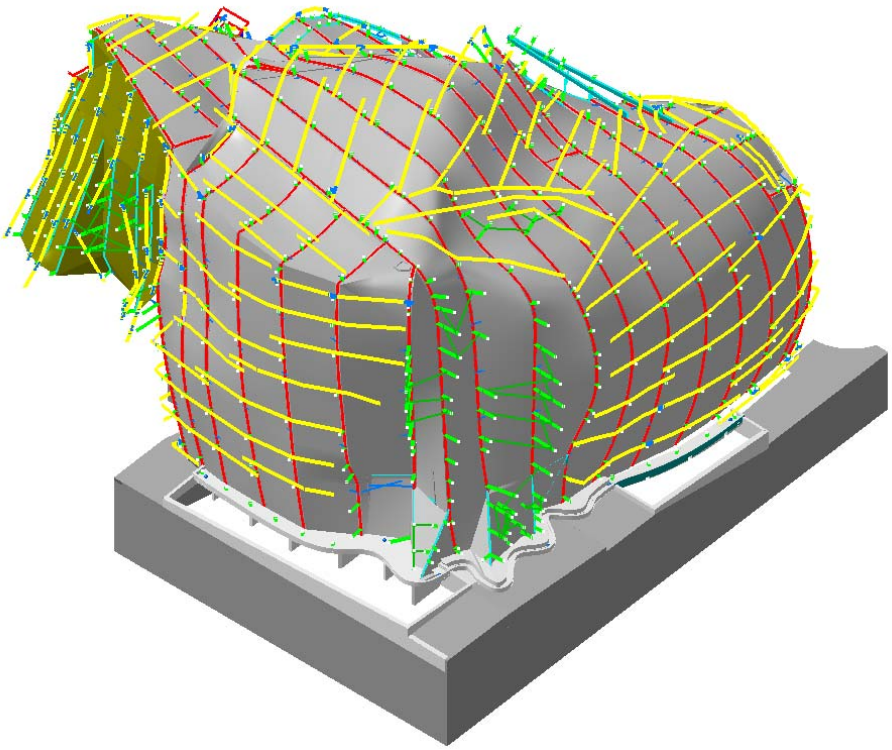

Figure IX-14: Tube and pedestal layout

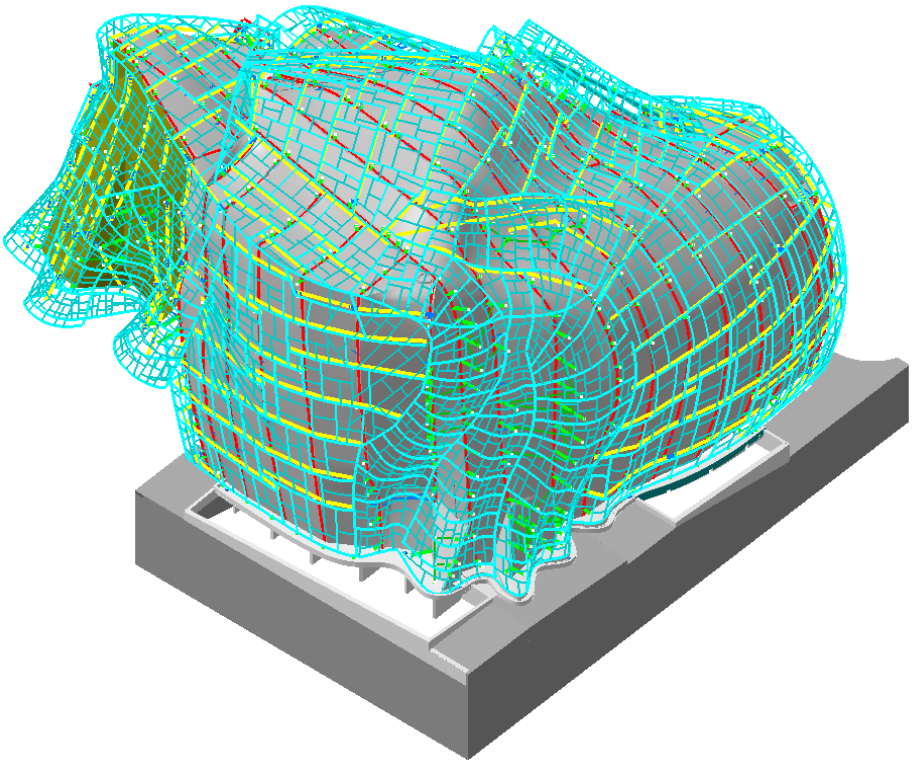

Figure IX-15: Panel and face sheet edges

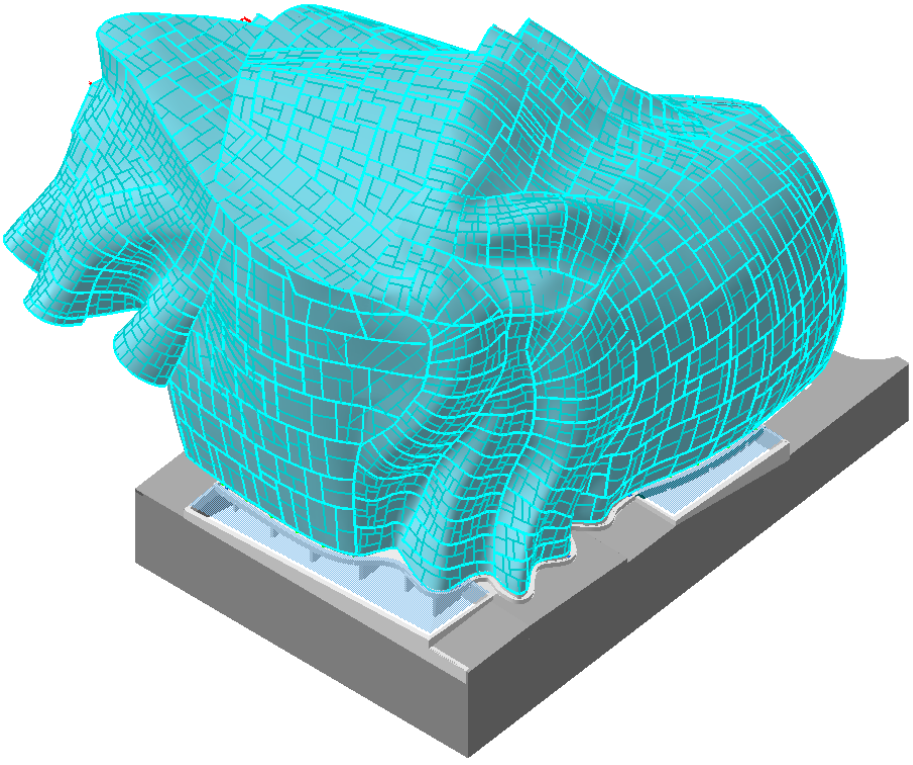

Figure IX-16: Finish surface

PANELS AND SHEETS

1. Panel may not exceed 192” in width
2. Sheets may not exceed 48” in width
3. If sheet is more than 45.5” in width, height must be limited to 45.5” (one sheet dimension must be < 45.5”)
4. There may not be more than 3 internal vertical sheet boundaries
5. Curves created to form the panel must have start points at the bottom or left.
6. The panel is limited to 120” for one dimension. If the panel is wider than 10’ it must be shorter than 120”. If the panel is taller than 210” the width must be less than 120”.
7. Maximum 1 kink in top tube per panel
8. Maximum 0 kinks in bottom tube per panel.
9. Must have minimum of one vertical internal curve (sheet break)
10. Tube must be no closer than 8.65” to the surface
11. Plane of vertical curves “relatively normal to surface
12. Kinks must be copied as individual linear elements.
13. No kinks (tangency breaks) in panel curves. Copy as individual curves.

PEDESTAL LOCATIONS

A. Construction of a typical pedestal
   1. Pedestal is 12.625” off the tube CL.
   2. Pedestal is ideally normal to the top of rib and on rib flange CL.
   3. Pedestal is 90° to long axis of the tube.
   4. Pedestal length is 1” shorter than plane cut the tube axis.
   5. Pedestal length is minimum 10.5”.

B. Miscellaneous pedestal rules
   1. Pedestal elbows ok if each leg of the elbow is at least 8” long.
   2. Pedestals must be located 12” min. from rib-rib intersections.
   3. Pedestals must be located 12” min. from rib splices.
   4. Avoid pedestals longer than 5’-6”.
   5. Keep pedestals min, 4” from rib corners.
   6. Avoid skewed pedestals of the side of the top ridge flange.
   7. Pedestal can be mounted to the web of a rib.

C. Quality control checks on pedestal placement
   1. The pedestals should have surfaces applied for interference checking.
   2. Run interference checks against floor slabs and shotcrete
   3. Check web mounted pedestals for x-bracing conflicts
   4. Check pedestal min and max lengths

TUBE LOCATIONS

A. Tube locations
   1. Tubes must be straights.
   2. Tubes must follow panel head and sill pattern.
   3. Tubes must be max length of 14’1 ¾” Rib to Rib if the tube is a twin span, 8’ if a single span.
   4. No more than 10’ tributary width applied to any one tube.
   5. Tube CL to shotcrete face is 6.5” minimum
   6. Tube CL to surface 8.65” minimum
   7. Ideal tube CL to top of rib is 15”
   8. Tube lengths must be planar between splice locations.
   9. Kinks in tubes cannot be closer than 36(Tan A/2 + Tan B / 2) where A= angle of 1st kink and B= angle of 2nd kink.
   10. Tube cantilever is max. 1/5 of anchor – anchor span.
   11. Minimum cantilever is 6” past CL of anchor.
   12. Tube single span can not be more than 10’.

B. Quality control checks on tube placement
   1. Run interference checks to ensure rules are maintained.
   2. If tube interferes with shotcrete or skin move tube within its plane to clear
   3. If tube can’t be re-located alter the surface geometry.
   4. Re-run interference checks after surface is moved.
   5. Review panel boundaries to comply with framing rules
   6. Run interference checks on floor slab and shotcrete models

PANEL FRAMING

A. Patterning & Fabrication
   1. Panel head and sill in plane with tubes
   2. Panel jambs must break at sill tube kinks or ends.
   3. Panel size is max 192 sf.
   4. Face sheets are ideally rectangular
   5. Face sheet area is inversely proportional to curvature
   6. Face sheet length is in direction of curvature
   7. Face sheet maximum size is 48” x 96”

Figure IX-17: Fabricators rules for panel placement

Much of the instantiation of these rules on the final project documentation was performed through manual operations, due to the geometric complexity of the problem and the limitations of geometric programming tools available at the time. However, elements of the problem were addressed through automation. The instantiation of face sheets described in rule 5 was conducted on some elements of the building using the subdivision strategy shown in Figure IX-8. Additional automation of the pedestal geometry was achieved.

Zahner's shop was able to substantially automate the fabrication of panel components. Zahner's automated panel layout program (ZAPLA), written in the parametric modeler PRO-ENGINEER, generated panel component geometry from the surface model and panel and face sheet boundaries provided by the architectural team. Shop tickets were generated for all components of the panel (Figure IX-18). Flattened profiles for each CNC cut element were also generated by the program.

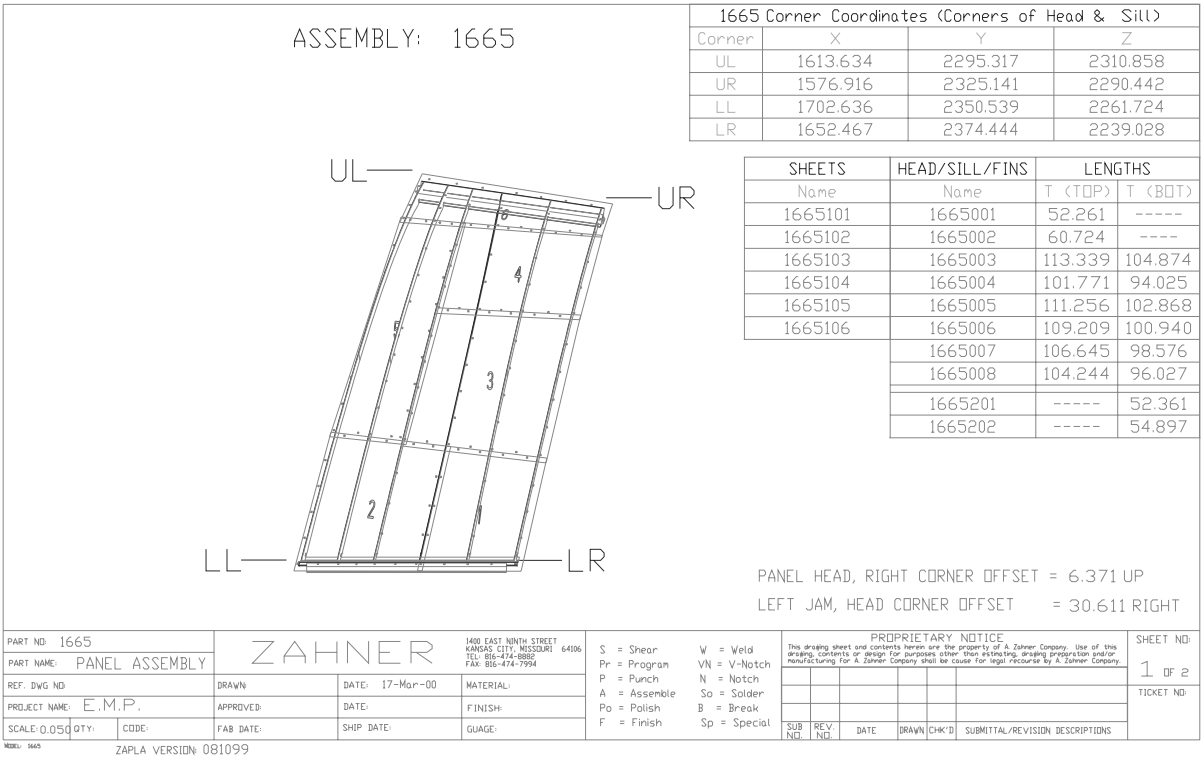

Figure IX-18: AZCO's Automatically generated shop drawings

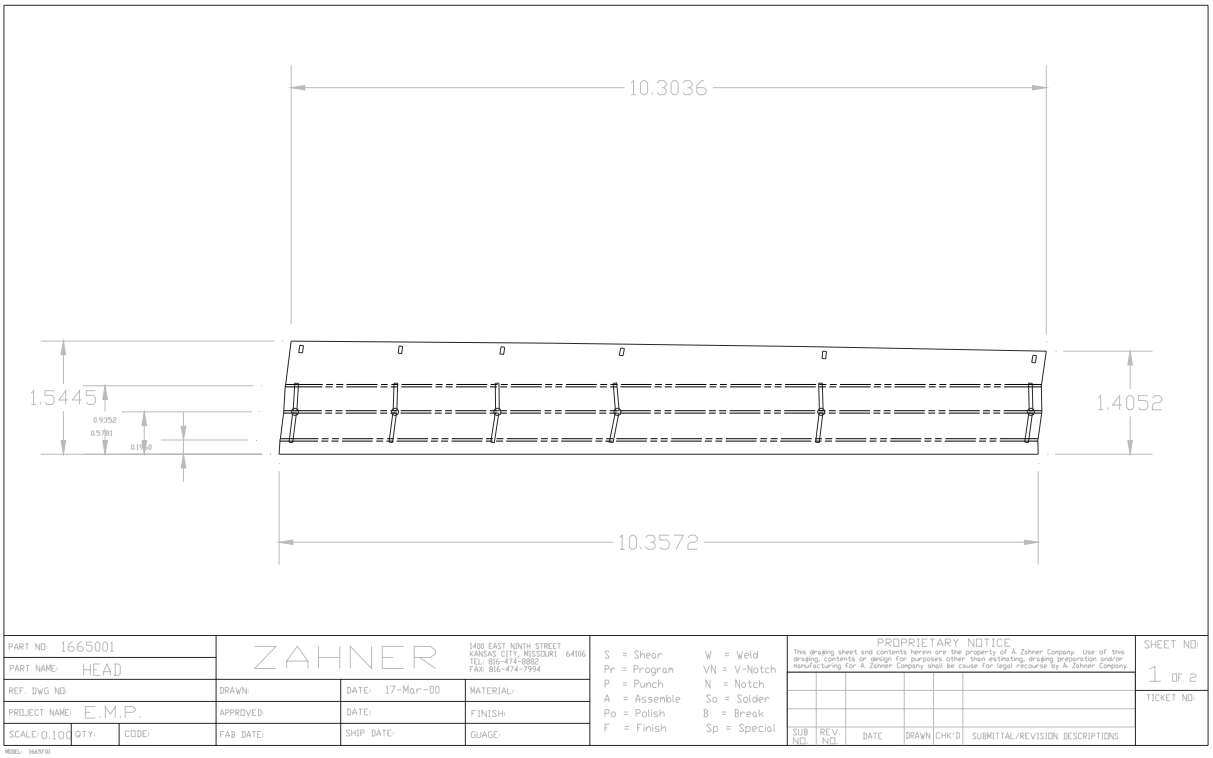

1665103					
Edge	# Holes	Hole Spacing	End Spacing	Edge Offset	Hole Offset
Top	***	***	***	1.250	235.541
Bottom	***	***	***	237.064	0.000
Left	4	7.3796	7.3796	0.000	0.500
Right	4	7.8621	7.8621	78.061	1.250

Sheet Edge Lengths	
Top	222.765
Bottom	223.669
Left	77.528
Right	77.571
Cross 1	237.064
Cross 2	235.541
Blank Sheet Size	
Stock value	0.250
Width	224.517
Height	78.061

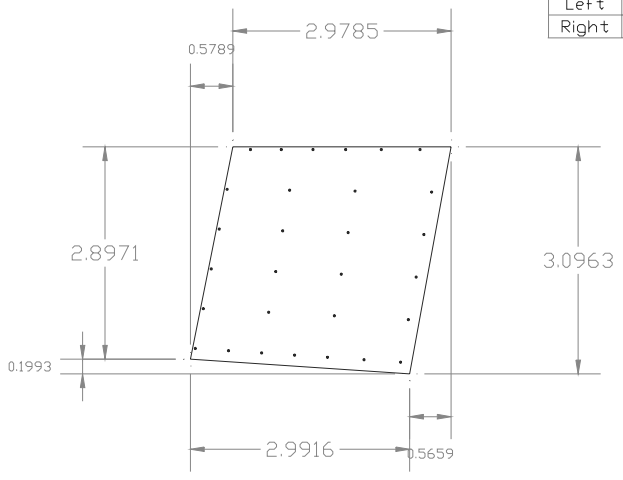

Figure IX-18, ctd.

B. MATERIALS BASED RATIONALIZATION

In this final section, discussion turns to the development of grammars on the basis of the materials simulation constructs developed in Chapter VII. In this section, the constructs developed to support materials based modeling of sheet materials will be re-directed toward applications of surface rationalization.

The materials modeling approach is well suited to applications of grammars on manifolds developed in Chapter VIII.B. We direct this application to problems where a desired surface form – provided by digitizing of schematic design physical models – is rationalized into constructible by assemblies of material sheets. Such a generative strategy will require the definition of the following components:

1. A notion of the space in which shapes, elements and transformation are defined,
2. A set of elements, with a topology of element-part relationships defined on these elements,
3. A set of possible transformations on these elements, and shapes developed as compositions of elements.

To this set of conditions, we will add the following to direct the definition of grammars toward the rationalization activities:

4. A goal toward the satisfaction of which shape transformations are directed,
5. A set of heuristics measuring of the fitness of produced shapes toward satisfaction of the goal.

1. Spaces and Elements

In Euclidean grammars, the notion of a space in which elements are defined and transformations occur is often assumed with little discussion. This space provides the "playing field" on which grammars occur, and contributes implicitly to the specification of valid elements of the grammar. The set of elements in Euclidean space grammars are the valid Euclidean elements of the space: points, lines, and bounded planar regions in Euclidean 2-space, with the inclusion of bounded volumes in $\mathbf{R}^3$.

In the formalism of grammars on manifolds developed in the previous chapter, the structuring of a pre-defined space of operation is no longer presumed, and the distinction between this presumed space and the elements inhabiting this space is no longer clearly defined. An element is defined as a function, mapping coordinates (and functions on these coordinates) between and intrinsic, parametric space and an extrinsic, containing space. The space of an element is determined by the partly by the structuring the intrinsic and extrinsic spaces, and through the mapping function defined by the element occurring in the product space of the intrinsic and extrinsic spaces. In turn, this structuring provides the basis space for the definition of boundary and other elements, defined in the parametric space of the containing element.

Several such interrelated manifold structures were presented in the development of the materials modeling formulation; all of these - individually and in combination - are candidates for grammatical constructions:

- Features of the surface were defined as 1-dimensional elements within the $\mathbf{R}^2$ parametric space of the surface. The boundary descriptions of the sheet – described as a closed set of edges connected at their boundary vertices – were the most important such features (Figure IX-19A). As this discussion of materials based grammars progresses, additional features defined in the parametric space of the surface will be presented.

- An edge graph is constructed on the basis of these sheet features. This edge graph resulted from a processing of the sheet features, to identify intersections of features, define the interior and exterior regions of the sheet, and characterize parts of features in terms of their relations to the sheet's interior and exterior (Figure IX-19B). The graph was defined through 0-dimensional vertices and 1-dimensional edges. The organization of sheet features resulted directly in the construction of the edge graph.

- The edge graph as discretized triangulations of a region of $\mathbf{R}^2$ parametric space. These surfaces are embedded in $\mathbf{R}^3$ world space through the $<\mathbf{R}^2 \times \mathbf{R}^3>$ mapping function $\phi_t : \mathbf{u} \rightarrow \mathbf{x}$ (Figure IX-19D).

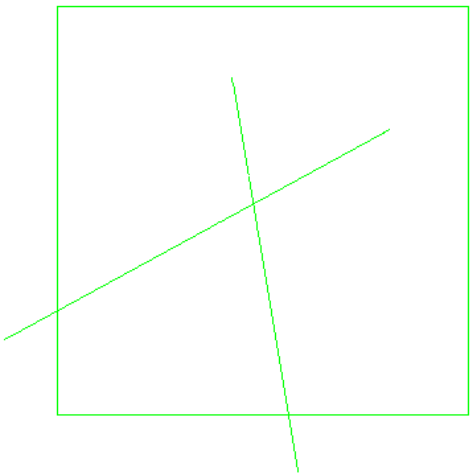

A. Sheet Features – boundary edges and vertices

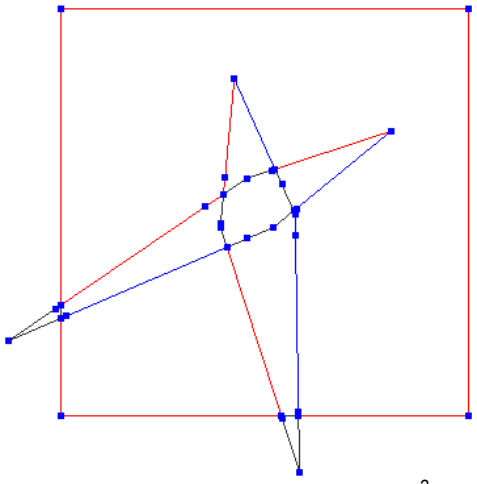

B. Edge graph, embedded in $\boldsymbol{R}^2$

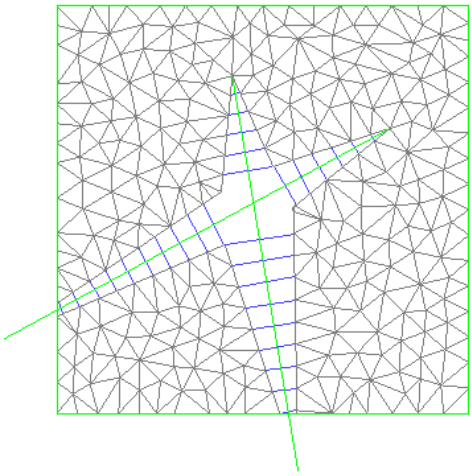

C. $\boldsymbol{R}^2$ *Triangulation*

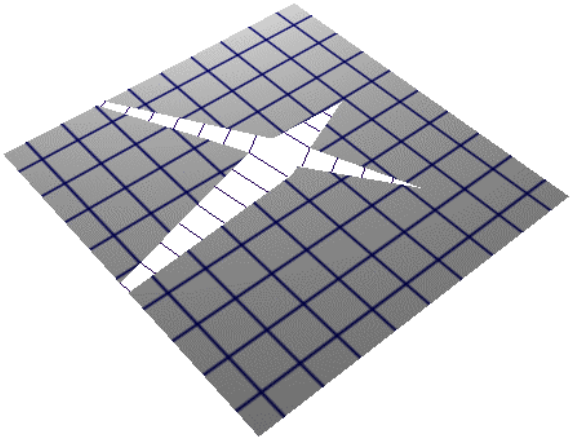

C. Undeformed shape in $\boldsymbol{R}^3$

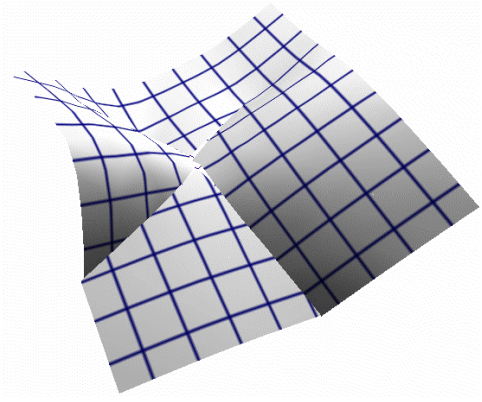

D. Shape after convergence

Figure IX-19: Manifold elements of the paper surface grammar

The materials modeling formalism developed in Chapter VII considered the construction and behavior of shapes formed from single sheets. As we move toward constructs supporting assemblies of such elements, representations of surface complexes developed in Section

VIII.B.3 will be developed on top of the representation of sheets. The structuring of sheet complexes – including identifications of boundary edges and vertices – will provide an additional framework on which transformational operations may be defined. Operations on the complex of sheets embedded in $\mathbf{R}^3$ will be undertaken in the graph representation of the complex. Examples of such operations might include splitting sheets – replacing sheet elements with 2 or more elements, and inserting of deleting of sheets. Similarly, we can modify the assembly by altering identifications between sheets boundary elements, introducing or removing continuity between sheet elements.

These elements of the formulation do not necessarily represent shapes themselves, but structures by which shapes may be defined. As defined in the grammar formalism, shapes are entities composed of elements. Shape types may be defined as pre-determined configurations of elements. For example, we are free to define a class of rectangles (Figure IX-20, and Section IX.B.6 below), and define grammars, operations and assemblies constructed on this class of elements, founded on the constructs defined above.

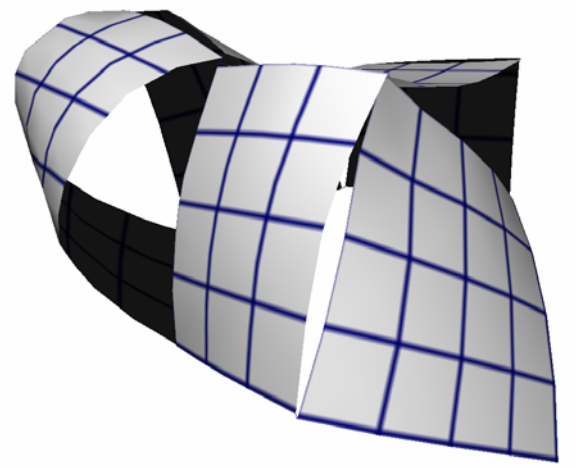

Figure IX-20: A construction of rectangular sheets and springs

2. Sheet Features

In the context of this discussion, a feature is a shape, constructed in the parametric space of a sheet, with implications on the sheet's topology or behavior. Features represent potential elements in a vocabulary of sheet based grammars. So far, discussions of features have focused on boundary elements of the sheet, specifically linear edges joined at their boundary vertices.

Obviously, the configuration of a sheet's boundary elements has implications on the flattened, parametric space shape of the sheet. The effects of a sheet's boundary on the potential configurations of a sheet in space are perhaps more subtle. Obviously, a change in the flattened shape of a sheet will necessarily change its configuration in space. However, it is worth noting that adding material to (removing material from) a sheet at its boundary will

increase (decrease) the local stiffness of the sheet, resulting in changes to the flexibility to which the sheet can assume certain configurations.

There is a potentially large variation of sheet configurations purely on the basis of boundary elements. Figure IX-21 shows some of these potential variations. Sheets can have internal boundaries, producing holes in the sheet, as in Figure IX-21A. A sheet's boundary elements can potentially result in self-intersections (Figure IX-21B). The arrangement of boundary elements can result in non-connected regions of parametric space, technically violating the precise definition of a manifold (Figure IX-21C). Multiple boundaries may partially intersect, resulting in configurations such as in (Figure IX-21D).

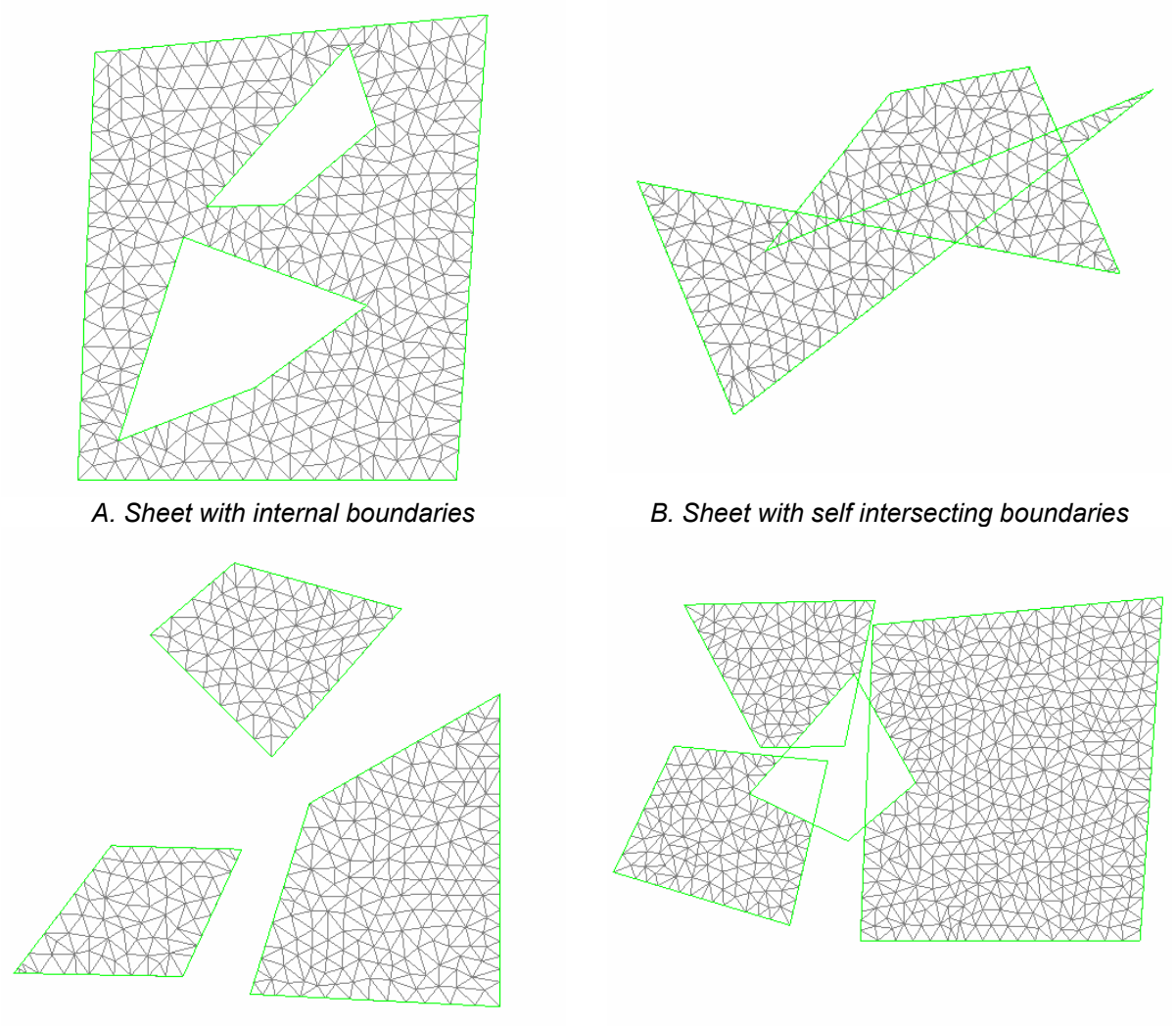

A. Sheet with internal boundaries

B. Sheet with self intersecting boundaries

C. Non-connected sheet

D. Sheet with multiple intersecting boundaries

Figure IX-21: Boundary and resulting mesh configurations

A subtle consideration is found in these various examples: rules must be established to define the ways in which multiple closed or intersecting boundaries interact. The region of parametric space defined by multiple boundaries may be defined as the union of their regions as individuals (as in Figure IX-21B), as their difference (Figure IX-21A), or through some other scheme (Figure IX-21D). These rule definitions may be considered potential elements of a grammar of sheets.

Other features are evident in the firm's paper schematic design models, which have implications on the behavior of sheets' configurations in space. Cuts, tears, creases and folds are all potential manipulations of the sheets configurations, that are manifested in the flattened, parametric space of the sheets. The dodges and inserts described in textile design are also possible design elements. This section discusses their resolution in the sheet material modeling approach, and in generative applications based on this approach.

A cut in the flattened representation of a sheet is has an interesting behavior, in that it results in a discontinuity of the sheet without actually affecting the sheet's 2-dimensional shape. We can represent this feature as a simple line in the feature representation of the surface. By itself, this feature insertion has little impact on the triangulation of the sheet's region, since it does not directly impact the boundary of the shape. In order for the feature to act as a cut, it is in fact the connectedness of the 2-dimensional complex of the triangulation that is altered. The identification of edges and vertices along the line of the feature in 2-space must be disrupted. In the modeling

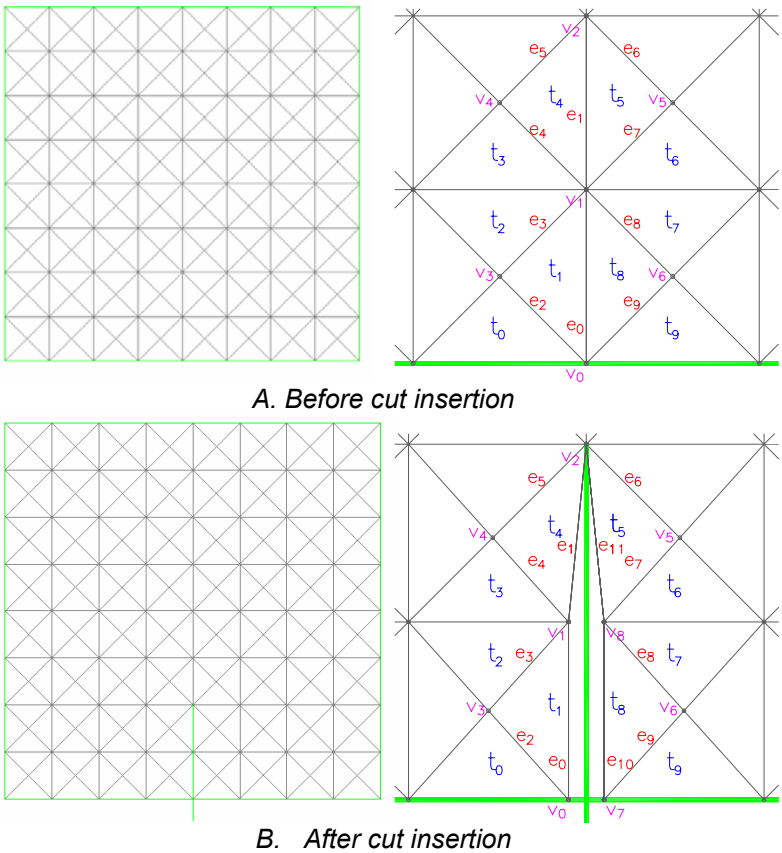

A. Before cut insertion

B. After cut insertion

Figure IX-22: Cut features and resolution in the triangulation

application, this is undertaken by associating edges and vertices produced along the cut with the feature, then “unzipping” the triangulation of these edges and vertices, inserting duplicate edges and vertices, and repairing the relationships between edges, vertices and triangular polygons to produce the necessary additional free edges and vertices while maintaining the integrity of the mesh.

Topologically, the cut is a so-called “non-manifold” feature, whose behavior as an edge, embedded in a region of $\mathbf{R}^2$ space, violates the simple structuring of 1-dimensional elements bounding 2-dimensional regions. A full non-manifold representation of design spaces is beyond the scope of this work, but the behavior can be accommodated by heuristic operations on the triangulation as described above, and shown in Figure IX-22. Again, we draw on the simplifications provided by different representations of the problem: from the perspective of a grammar, we may consider this non-manifold behavior of the edge as simply a CUT labelling in the feature space of the problem, and delegate the impact of this feature on the sheet’s topology to the triangulation complex.

Dodges are areas where material is cut from the sheet, and the edges of the cut are fastened together. This has the effect of locally shrinking the material in the region of the dodge. Inserts are locations where a cut is made, and material is inserted into the cut., locally stretching the sheet. Both of these actions have implications on the topology of the sheet, and on the complex of the triangulation.

Figure IX-23 shows the operations of dodge insertion. A new behavior on linear parametric features is developed, where the line feature defines a symmetric split line. The split line feature traces two pairs of edge elements, each pair connected by a symmetrically placed point off the line (Figure IX-23B).
One of the modes of behavior of this feature is simply to split the mesh open (Figure IX-23C). This splitting functionality must guarantee that edge generation is symmetric across the edge, so that distortion of triangles is not introduced. Figure IX-23C shows the mesh generation across the split feature. Pairings of mesh vertices are indicated with in dashed cyan line. Note that the edge graph must translate intersections of the split feature boundaries to its opposite edge, to again insure compatibility of edge identification without triangle distortion. Figure IX-23E shows the results of the dodge insertion on the 3-D sheet.

The dodge feature must next adjust the mesh to weld the edges of the feature together. This is accomplished by edge and vertex identification (Section VIII.B.3) Opposing edges and vertices of the mesh are joined together. This translation results in distortion of the associated triangles (Figure IX-23C), and of the embedded sheet in $\mathbf{R}^3$. Note that this distortion is enacted only on the $\mathbf{R}^3$ configuration only, since we wish to preserve the original triangle shapes in the materials simulation. Thus, the locations of vertices in $\mathbf{R}^2$ is unaltered and remains that shown in Figure IX-23C, while their locations in $\mathbf{R}^3$ are moved to join the opposing vertices (Figure IX-23D and F). This necessarily induces stress on the affected triangles, whose shapes in the time based simulation are stretched relative to their reference configurations in $\mathbf{R}^2$. This distortion is resolved over the course of

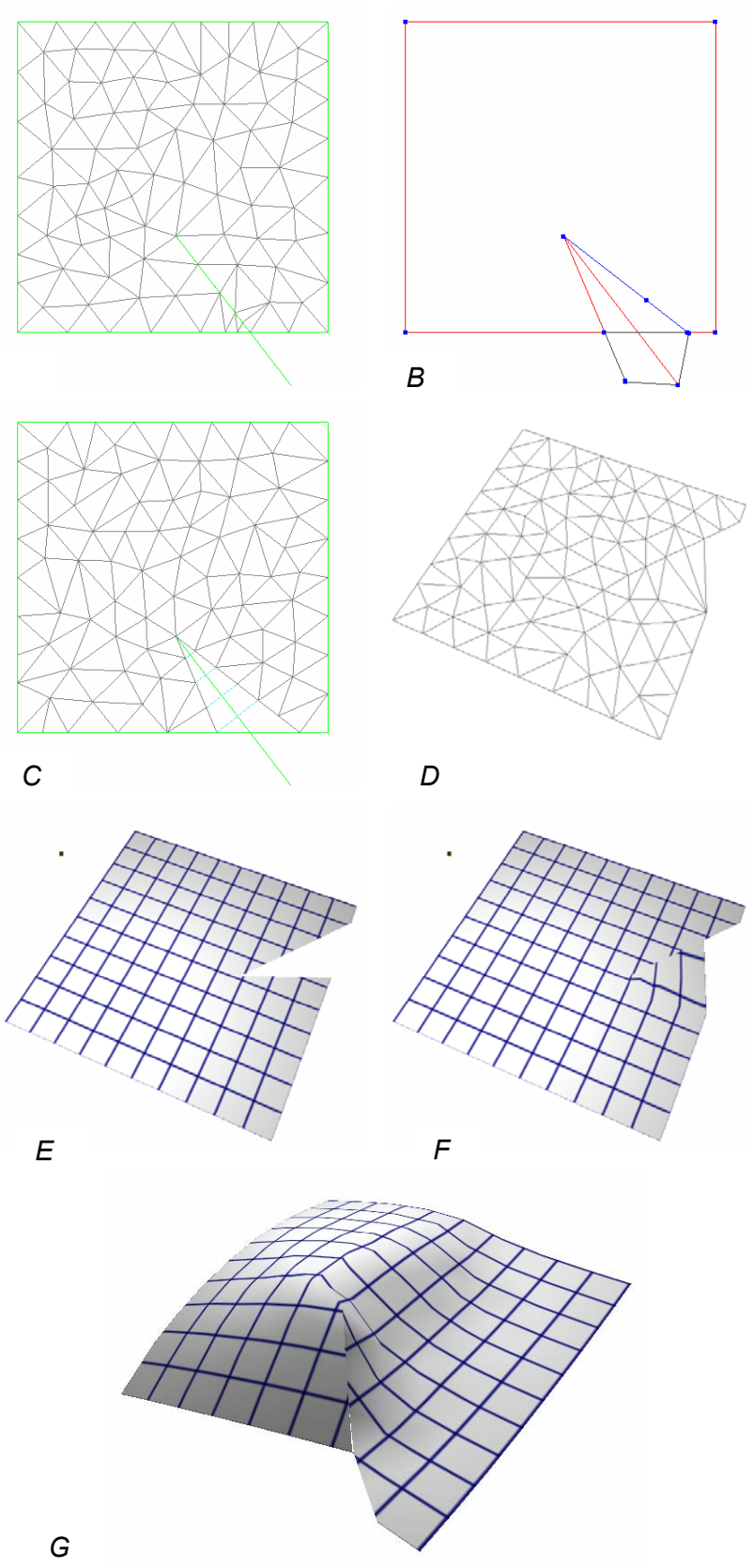

Figure IX-23: Dodge insertion

the simulation; the resolution results in principally out of plane deformation of the entire mesh. Figure IX-23G shows the resolution of the forces induced by the dodge insertion, as the simulation is run toward stability. Note that the dodge insertion approach must address conditions where one leg of the dodge is longer than another, and a free portion remains after the edge identification occurs.

Insert features (Figure IX-24) are conceptually similar. However, instead of material being removed symmetrically from the mesh, symmetric additions of material must occur along the feature edges (Figure IX-24B). In practice, this is more difficult than material removal, since the insertion would require overlapping of material in the flat space of the sheet, violating the topology of the sheet as a single, bounded region of Euclidean 2-space, and is difficult for the meshing algorithm to resolve. This problem can be resolved by treating the additions as separate sheets in their with their own parametric spaces, which are welded onto the

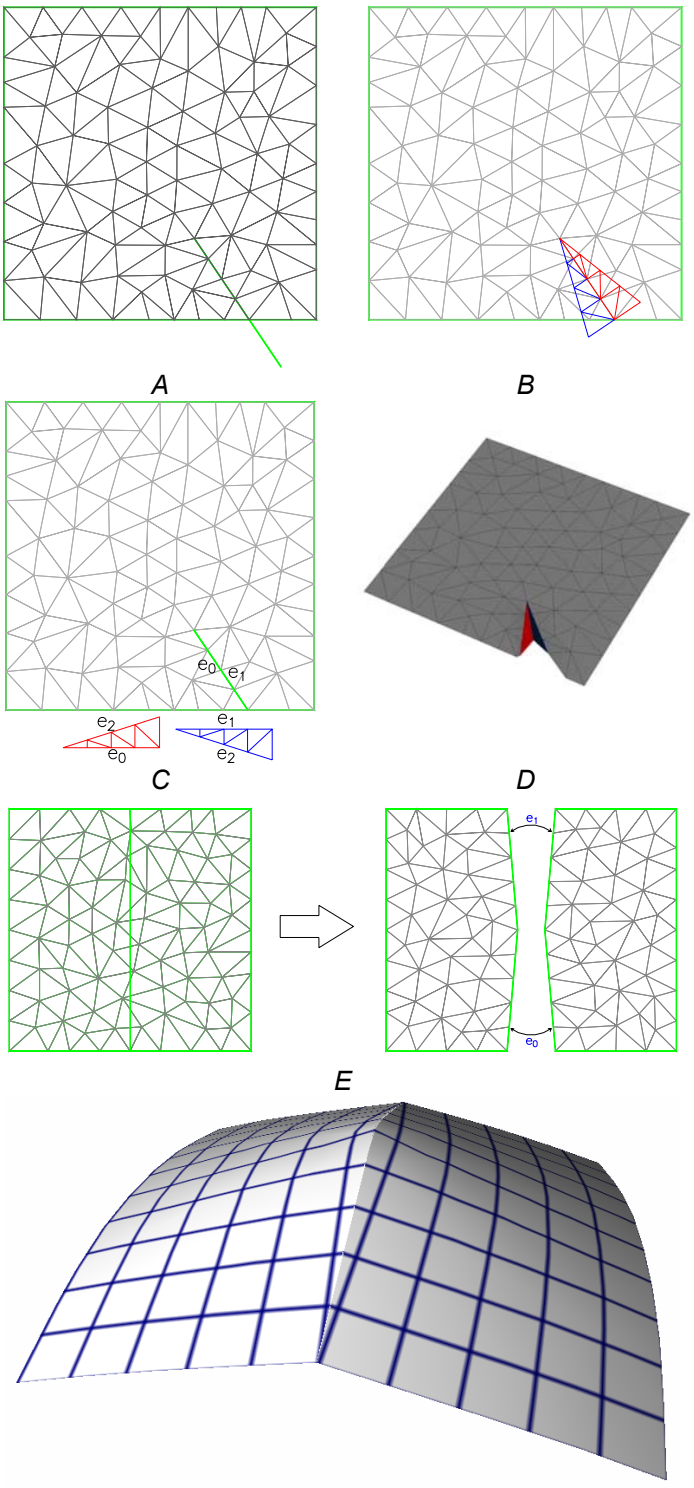

Figure IX-24: Insert creation

edges of the sheet feature (Figure IX-24C-D). This can introduce additional complexities, since the geometry of the insert will tend to product thin triangles, which create numerical problems for the material solver.
In practice, insert creation has been addressed by constraining inserts to occur only across boundaries between separate sheets. Insert placement is achieved by splitting the sheet into two separate sheets, and identifying edges of the sheets in space. This limits insert creation to configurations which completely traverse the sheet boundaries.

Two examples of feature behavior have been described so far: features which split the surface complex, generating a surface discontinuity between pairs of edges across the feature, and features which “weld” the edges generated by the feature. We can identify a few additional behaviors of interest. The feature can create a “hinge” configuration between edges across the feature. In the case of the simple, linear feature, this is simply achieved, by disabling the bending force on edges of the triangulation associated with the feature. This allows the simulation to proceed without imposing energy penalties on out of plane configurations between neighboring triangles across the feature.

Similarly, we will be interested in features that join neighboring regions of material, preserving tangency of the associated material regions across the feature. In the case of the linear feature, this is the trivial case: the feature has no behavior other than to create a line in the triangulation at the feature. In the case of dodges and inserts, we simply enable the bending energy formulation across the newly identified edges of the triangulation.

It is also advantageous to have a feature behavior that binds neighboring mesh regions in “proximal” continuity, where the edges are attracted to one another but are not necessarily constrained to meet exactly. This can be achieved in the material simulation by joining identified vertices across the feature with a spring of some selected stiffness. This is practically advantageous, since introducing continuity instantaneously between neighboring triangles can introduce large scale distortions of triangle configurations and the underlying energy function, resulting in instability of the material solution. The attractor behavior allows us to slowly increase the continuity of the mesh, to the point where full continuity can be numerically achieved.

These different feature types correspond roughly to the *order of geometric continuity*[28] of the surface at the feature, and the order of differentiability of the manifold charts across the feature. We may categorize these features as follows:

- Discontinuous – the surface is split across the feature
- Proximally continuous – attractor forces are introduced between identified vertices
- G^0 continuity – vertex and edge identification occurs across the feature
- G^1 continuity – bending forces are observed on neighboring triangles across the feature

A couple of caveats are appropriate regarding this categorization. First, the notion of G^1 tangency of the manifold is only approximate, since the mesh solution is linearized by the discretization of the surface manifold into triangles. In actuality, the triangles are of course not tangent at all, but rather guided toward tangency as the limit of the energy formulation. As triangle size is reduced, the energy function converges in fact toward G^2 geometric continuity where the surface curvature varies smoothly over the manifold. Second, we note in passing that the notion of proximally continuous conditions introduced by the attractor forces represent a smooth continuum between completely discontinuous – where the spring stiffness is 0 – to G^0 continuity, where the spring stiffness is infinite.

Two examples of feature shape – linear and split line - have been described and implemented in the solver. The symmetry of these shapes guarantee that the length along the edges of both sides of the feature are guaranteed, and that the impact of intersections with other features can be easily transferred to opposing edges. These characteristics are critical to guarantee edge identification without introducing undesirable deformations of the mesh, and simplify the process of creating opposing triangle edges of equal length.

These examples are of course only examples of a larger set of desirable shapes and associated geometric constructs which exhibit these characteristics (Figure IX-25). In particular, the spit edge configuration, while providing the useful ability to curve the edge shape in parametric space – and thereby introduce controlled deformations of the resulting configuration in $\mathbf{R}^3$ – creates this curvature only at its vertices. This results in a curvature discontinuity of the feature at these points. Smoother shapes such as arc and curves (Figure IX-25 C&D) would provide a smoother curvature variation, resulting in smoother variations of the surface complex as it is pulled into shape in $\mathbf{R}^3$. The potential exists for other shapes

whose length equivalencies are guaranteed by other means, including rotational symmetry (Figure IX-25 E).

The categorizations of A) edge identification and continuity and B) the resulting embedded shape of the feature may be viewed as independent labellings on linear features. Figure IX-26 shows elements of this matrix of feature behavior and shape type, and their implications on the resulting surface form in $\mathbf{R}^3$. Figure IX-27 shows a few of the possible shapes generated by the introduction of sheet features.

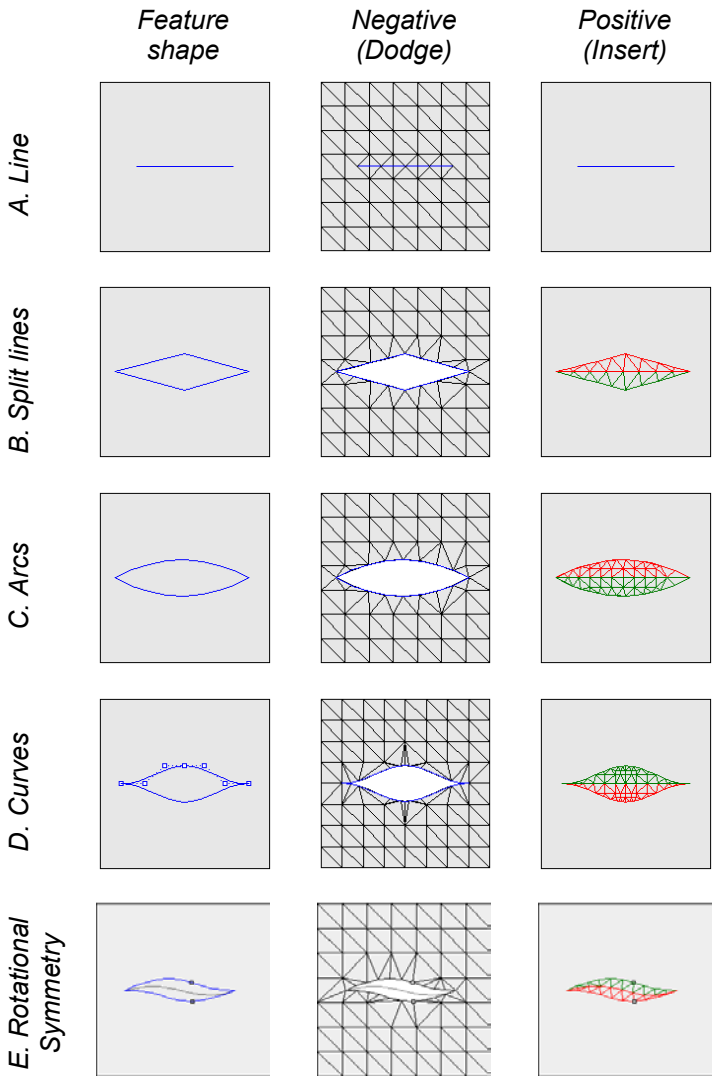

Figure IX-25: Possible 2D feature shapes

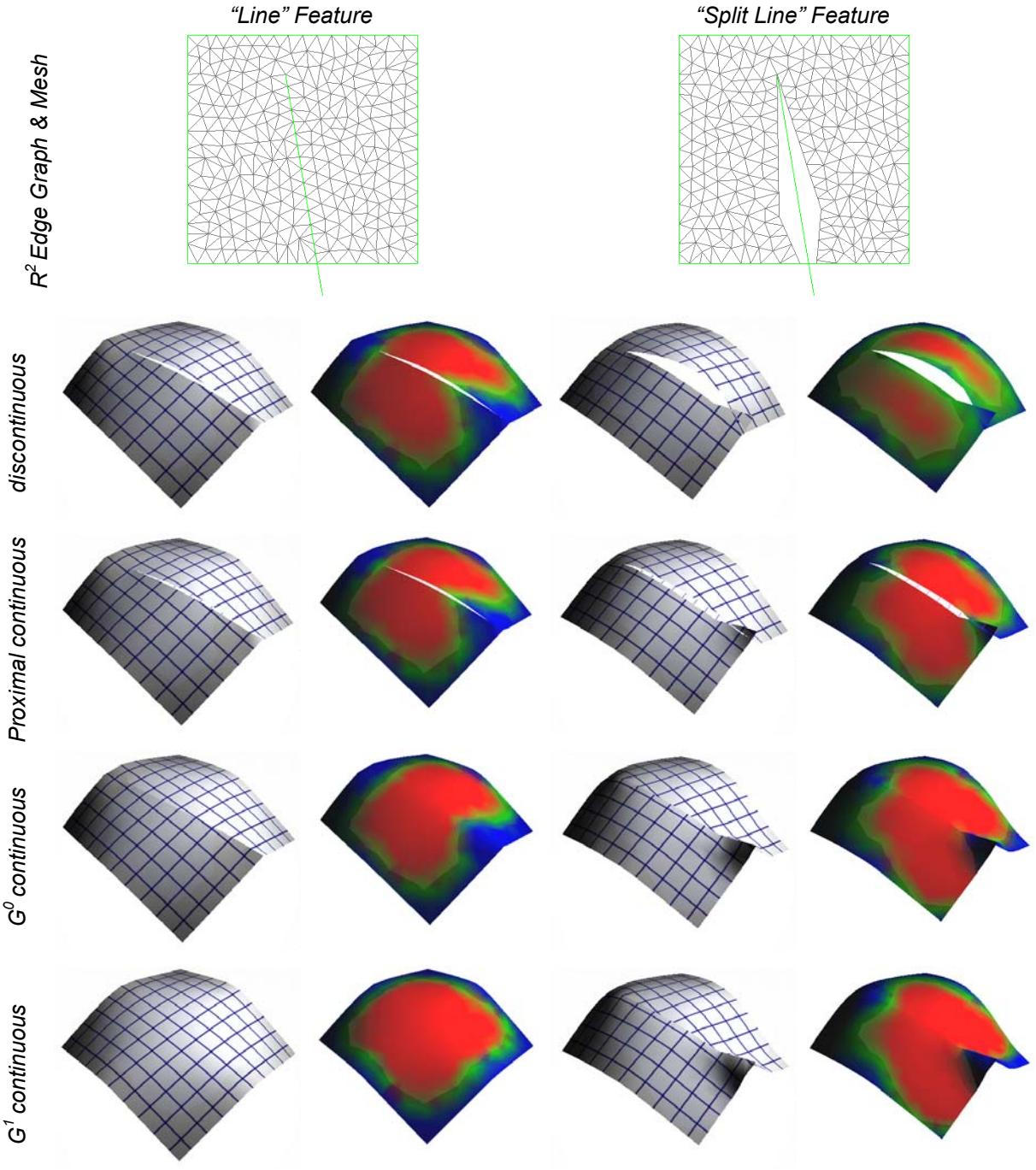

Figure IX-26: Matrix of feature behaviors and shapes

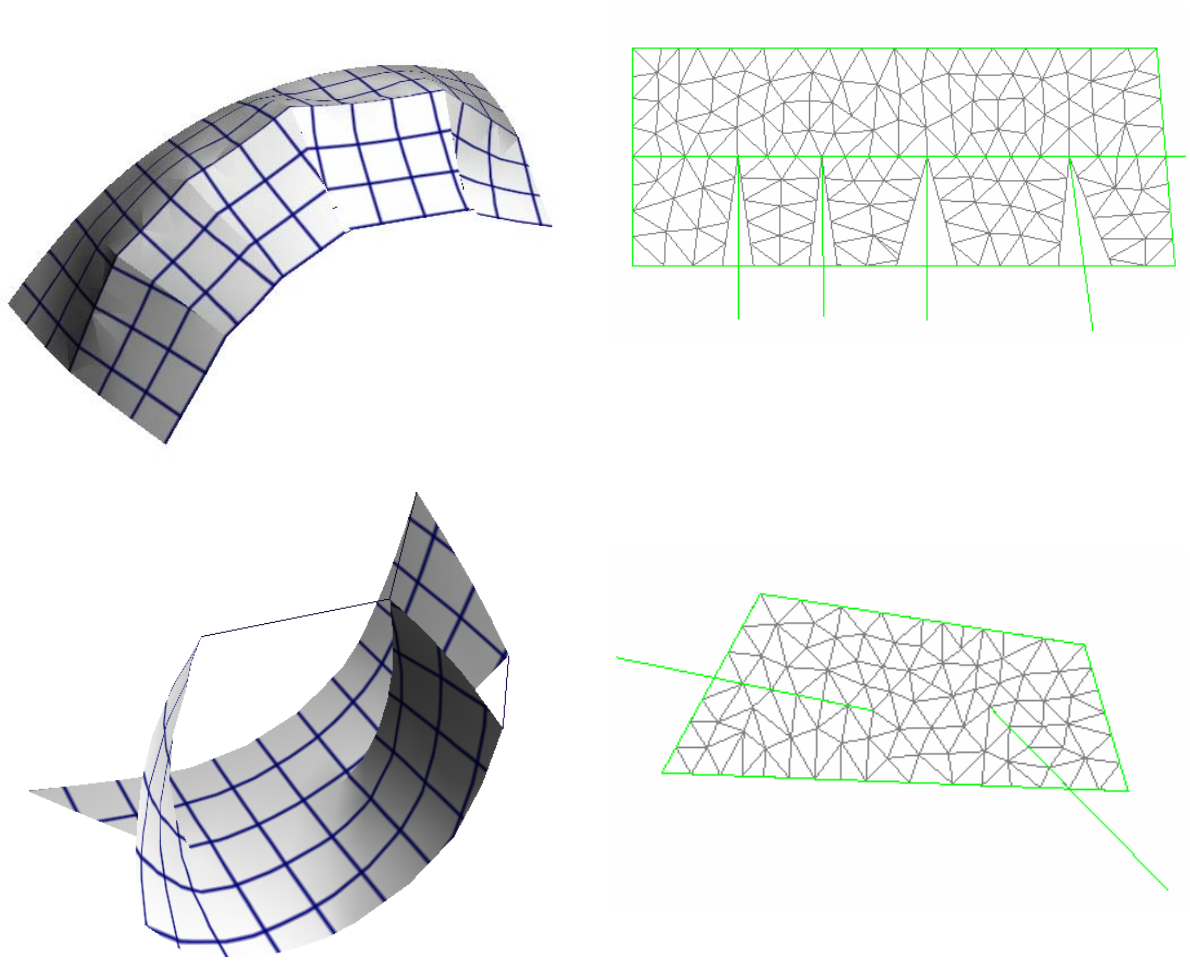

Figure IX-27: Shapes defined through sheet features

3. Fitness Heuristics and Goals

Loosely stated, the goal of the generative rationalization approach is to best approximate an ideal design surface with an assembly of sheets, whose geometric behavior correctly anticipates that of actual of actual construction materials. Additional desired behaviors may be anticipated. The resulting rationalized assembly should correctly interpret *intentional* features in the design model, including sheet boundaries, creases and continuity breaks (we recognize that such features may appear in the design model, but may not be intended in the final form). Other qualities, dictated by constructibility requirements, may be desired in the generated assembly as well. The fabrication process may dictate maximum or minimum sheet dimensions, or straight sheet edges. Our rationalization scheme should be able to incorporate such requirements, either as part of the schema of sheet shapes, or as goals of the generative process.

In order to determine fitness of a sheet assembly to these goals, we establish two types of metrics on the shape:

- Metrics on the shape of the assembly, relative to design surfaces
- Metrics of intrinsic and extrinsic properties of the shape relative to constructibility requirements

In our rationalization application, such metrics have application as weights or, more appropriately, weight fields, on features in parametric space, as discussed in Section VIII.B.2 above.

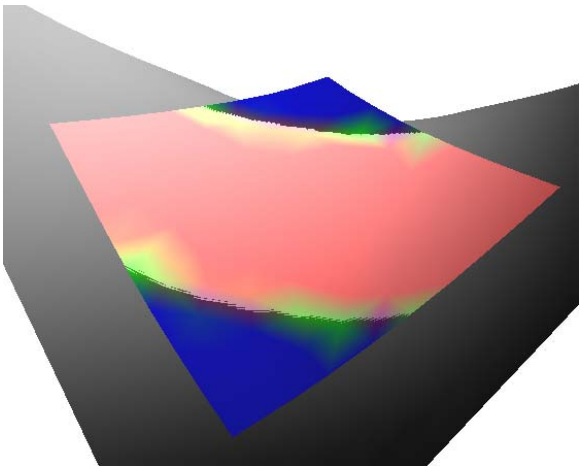

Figure IX-28:Distance metric on sheet

The most elemental metric of assembly fitness is distance between a design surface and the assembly. If the produced assembly is close to the design surface within some minimal tolerance at all points, then the generated assembly is a successful approximation of the design surface. Larger, non-trivial deviations between design and resulting surfaces may be accepted as part of the rationalization process; in these circumstances other heuristics such as surface smoothness may come into play. Distance is measured between each vertex of each sheet in the assembly. The distance between a vertex and each element of the design surface is computed; the closest of these distances is deemed the correct measure of the distance function. This computed distance to the closest design object is also used as the input to the attractor force computation. Distances between vertices locations in $\mathbf{R}^3$ and design elements are computed based on the design element type. For example, the distance between a vertex $\mathbf{v}$ and a sphere centered at $\mathbf{c}$ of radius r is simply

$$d = |\mathbf{v} - \mathbf{c}| - r \qquad \text{(IX.1)}$$

The distance between a vertex and Bézier or NURBS surfaces are computed by determining the point on the surface whose surface normal passes through the vertex[64]. Similar computations between points in $\mathbf{R}^3$ and Euclidean elements are well documented[13].

The attractor force is the simulated approximation of fastening strategies between sheet elements and an underlying substrate or sub-framing system. An inordinately large attractor force between sheets and design elements can guarantee close distances between input and generated elements, as the mesh is “squashed” down onto the surface. However, such large scale forces will both result in unrealistic simulation results, since the force will exceed the capabilities of real fasteners, and will overwhelm the computed internal forces of the sheet material, producing unrealistic deformations of the surface material. To address this condition as a simulation heuristic, we may of course limit the attractor force to some limit guided by an understanding of the capabilities of fastening elements.

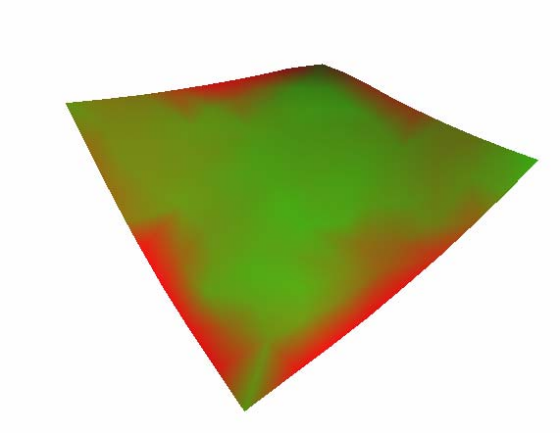

Figure IX-29:Strain map

We may also check the assembly for realistic configurations by analyzing the internal strain of the sheet elements. A heuristic is used in the simulator that checks relative lengths of triangle edges against the undeformed length of the sheet in its flattened reference configuration in parametric space. A readout is produced graphically of this relative deformation; these results are available as a heuristic to be used by the generative scheme.

Surface curvature is another key metric of the shape of a surface. It was established in Section V.D.2 that the gaussian curvature map of a surface is sufficient to fully describe its shape. Hence, equivalence of gaussian curvature between a design shape and a resulting rationalized shape dictates that these two representations have the same shape, and we may draw on this relative measure of localized gaussian curvature as a metric of a rationalized complex in representing a design shape. Of course, the rationalization operations will generally be intended to reduce surface curvature in the rationalized surface relative to the design surfaces, but we will still find this relative metric of use in describing the correspondence of the resulting surface relative to its pre-rationalized form.

Computation of gaussian curvature on the design shapes is achieved as described in Section V.D. The gaussian curvature of a sphere is trivially $1/r^2$, and invariant over the sphere. The

localized curvature of a Bézier surface is derived from the 1st and 2nd derivatives of the mapping function in (V.62).

Determination of the gaussian curvature of the discretized mesh is more problematic, since the triangulation is only C^0 continuous at triangle edges, hence the 1st and 2nd derivatives of the surface are unavailable at the triangle boundaries. Various techniques have been described for approximating the gaussian curvature and principal directions on a mesh[22,37 56,]. The simplest and most robust approximates the curvature at a vertex P_0 as:

$$\kappa_G \cong \frac{2\pi - \sum_{j=1}^{\#f} \theta_j}{\sum_{j=1}^{\#f} A_{V_j}}$$

where θ_j is the interior angle of triangle j neighboring P_0 , and A_{V_j} is the Vornoi region area of P_0 on j , defined as:

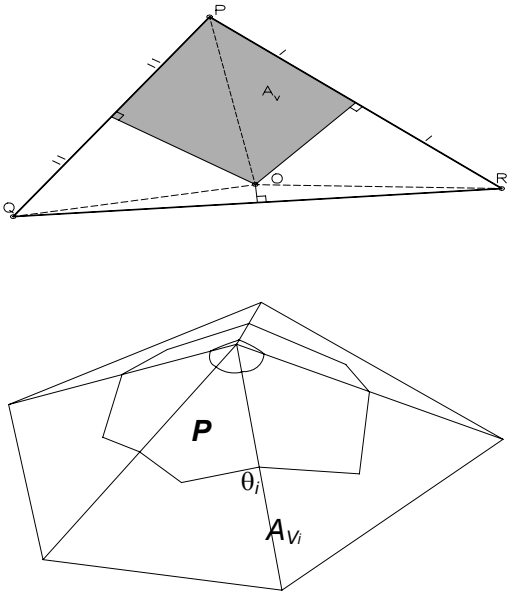

Figure IX-30:Gaussian curvature approximation on triangulated meshes

$$A_{V_j} = \frac{1}{8}\left(|PR|^2 \cot\angle Q + |PQ|^2 \cot\angle R\right) \qquad \text{(IX.3)}$$

or the area of the region of triangle j bounded by P, the midpoints of PR and PQ, and the circumcenter O at the intersection of the perpendicular bisectors of PR and PQ.

In generative examples described below, this representation of local gaussian curvature on the triangulation will be drawn to impose global curvature on the surface complex.

4. Initial Shape

A grammar requires an initial shape *I* as the starting point of transformations operations. In the materials based rationalization approach, the input shape is a starting complex of one sheet, best aligned with the design surfaces by attraction forces. The materials simulator is robust in its ability to align sheet materials with design surfaces, regardless of the starting location of the sheet. In the current version of the generative solver, the initial sheet's shape and location is provided by user input. This aligned shape – produced by running the materials solution toward convergence, provides the initial shape *I* of the grammar.

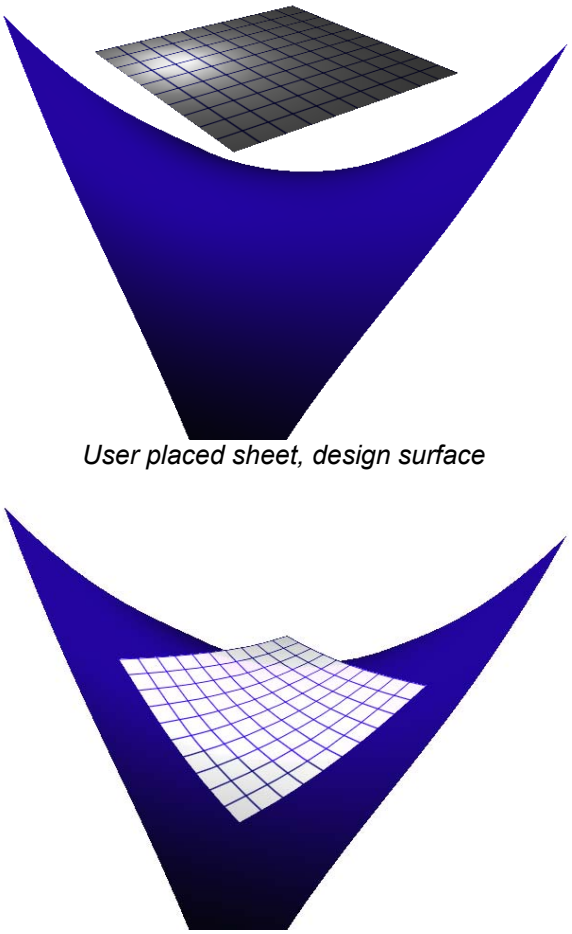

User placed sheet, design surface

Figure IX-31: Input shape to grammar, after initial convergence of the simulator

Improved strategies are possible for providing computationally generated an input shapes with closer affinity to the design surface. There has been substantial research in texture mapping applications to provide flattened meshes that minimize distortion of the shape[17, 22, 30, 75, 92]. This approach has also been targeted toward design applications[93]. Several of these approaches apply physics and / or energy based solutions to minimize distortion in these flattened triangulations. These approach are similar to the materials modeling approach presented in this thesis, but applied "in reverse" to provide a mapping function of the form $\mathbf{R}^3 \rightarrow \mathbf{R}^2$. The $\mathbf{R}^3$ triangulation is initially flattened into $\mathbf{R}^2$, in a topologically consistent (non-self intersecting or overlapping) manner. Energy penalties are determined for deformations of the $\mathbf{R}^3$ triangles in $\mathbf{R}^2$. An energy minimizing search is run, providing a best fit configuration of the parametric space triangulation, and determining (u, v) coordinates for the vertices of the mesh. In our application, this now parameterized mesh could then be applied to the design surface as a starting point for the sheet in $\mathbf{R}^3$. The simulation can then be run to convergence, providing the initial shape of the starting sheet.

5. Transformations

Chapter VIII provided the framework for grammars on manifolds, and established the basis for conducting generative operations on surface complexes. Details for applying this framework to the rationalization of surfaces have been described in this chapter. With this framework in hand, we are provided the ability to perform generative rationalization of sheet assemblies, in the parametric space of the sheets, and in the graph of the sheet complex, without incurring the complexity of performing operations on the embedded, curved surfaces themselves.

Figure IX-32 summarizes this strategy. The parametric space assembly of sheet boundaries and features in Figure IX-32A is mapped into R^3 through the material deformation function, resulting in the sheet configuration of Figure IX-32B. Fitness heuristics are determined on the sheets configuration in R^3 (Figure IX-32C). These heuristics are mapped back into the parametric / feature space through the inverse mapping function F^{-1} (Figure IX-32D), and serve as a "weight field" on features in parametric space. Production rules transform the shape composed of the parametric space features (Figure IX-32E), resulting in changes to the sheet boundary or other topological characteristics of the sheet. The transformed sheet is again mapped back into world space (Figure IX-32F) by the mapping function, solved over the simulation time. The simulation is allowed to converge to steady state after each production rule application. Once convergence is detected, the next production rule of the grammar is fired.

The cycle is repeated until the sheet configuration has satisfied the performance requirements, at which point the weight field – now within satisfactory ranges - results in terminal shapes of the grammar, and the iterations terminate.

With this framework and strategy in place, the unbounded range of shapes in Euclidean 2-space, and production rules constructed on these shapes, are available for application to surface rationalization. In the subsequent sections of this thesis, a few example applications are explored.

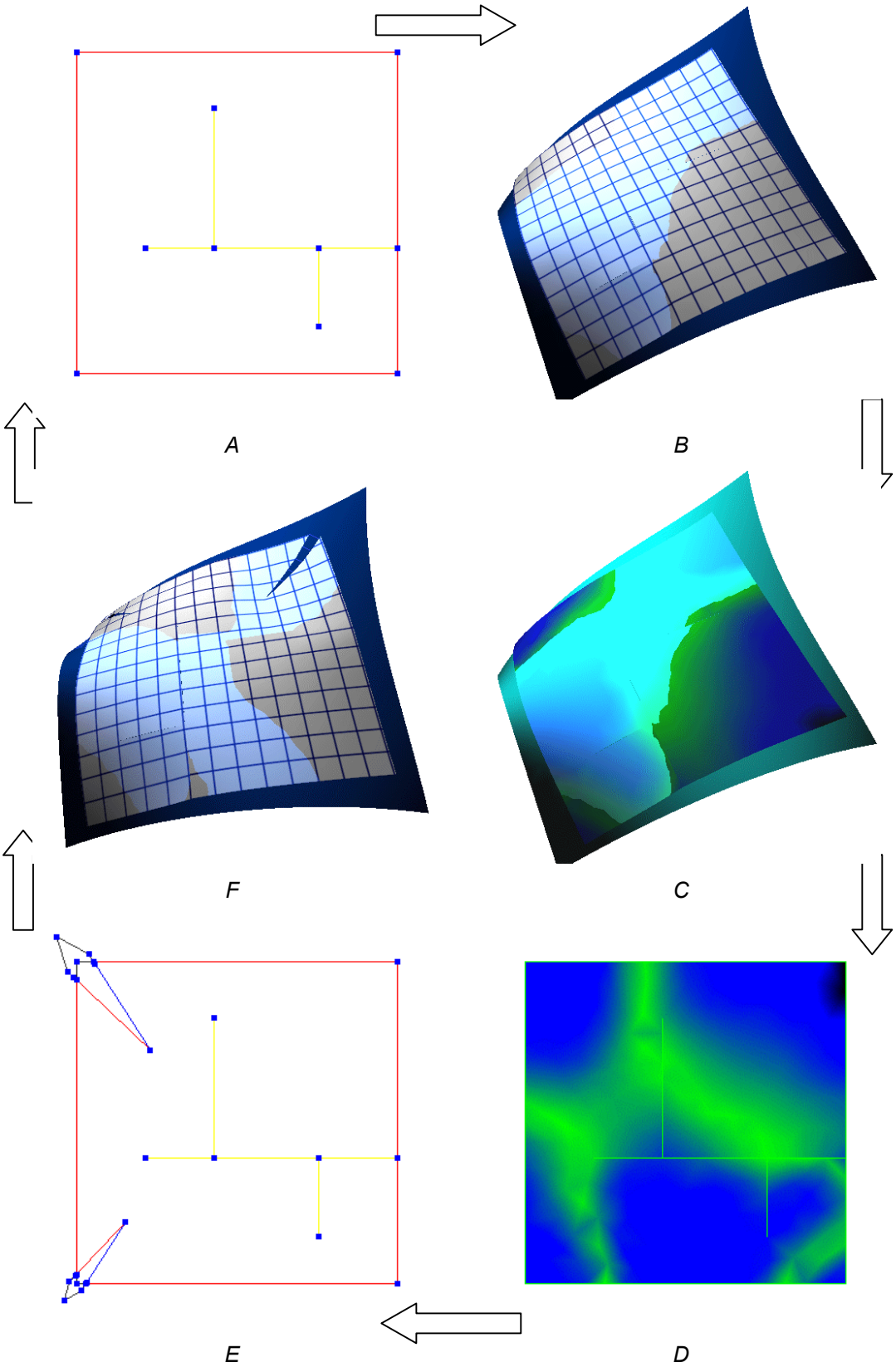

Figure IX-32: Generative Rationalization Scheme

6. Rectangle Grammars

A. Disney Concert Hall

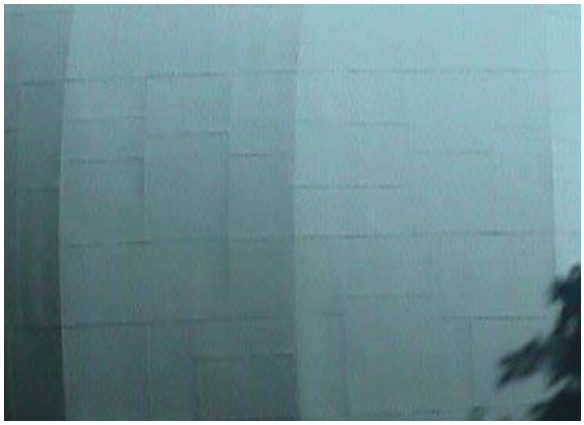

B. Experience Music Project

C. Weatherhead

D. Guggenheim Bilbao

Figure IX-33: Surface patterns of rectangular sheets

Construction assemblies of rectangular sheets represent a broad category of interest in Gehry projects. Many projects have been clad with sheet elements of approximately rectangular elements. The Experience Music Museum, Guggenheim Bilbao, Disney Concert Hall and Weatherhead projects are examples. Frequently, multiple cladding subsystems on a project have this property, including back panel and cladding elements, and possibly other elements as well (insulation, waterproof barrier, etc.). This section describes a materials simulation based grammar of rectangular sheet elements, their possible organizations and rationalization through variation of sheet sizes.

In the grammars that we develop, rectangles will represent the base shape of all grammar production rules. A rectangle is, of course, a region of $\mathbf{R}^2$ bounded by four linear features, two running horizontally, two vertically. We may thus define a rectangle as the 4-tuple of lines < l_1, l_2, l_3, l_4 >, where l_1 and l_2 are horizontally oriented and l_3 and l_4 are vertical. The horizontal and vertical pairs of features are joined by topological identification of their end points. We may define the linear features as parametric functions on their end points:

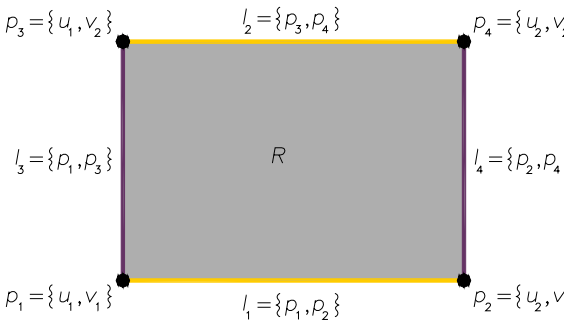

Base rectangle shape and boundary features
Figure IX-35

$$
\begin{aligned}
l_1 &= F(p_1,p_2) = p_1 + t_1(p_2 - p_1) \mid t_1 \in (0,1) \\
l_2 &= F(p_3,p_4) = p_3 + t_2(p_4 - p_3) \mid t_2 \in (0,1) \\
l_3 &= F(p_1,p_3) = p_1 + t_3(p_3 - p_1) \mid t_3 \in (0,1) \\
l_4 &= F(p_2,p_4) = p_2 + t_4(p_4 - p_2) \mid t_4 \in (0,1)
\end{aligned}
\qquad \text{(IX.4)}
$$

If we limit the grammars under consideration to those on orthogonally oriented rectangles, we may fully describe the instantiation of the rectangle in parametric space by two *u* parameter values {u_1, u_2} and two *v* values {v_1, v_2}. The vertex locations are determined by the permutations of these values:

$$
\begin{aligned}
p_1 &= \{u_1, v_1\} \\
p_2 &= \{u_2, v_1\} \\
p_3 &= \{u_1, v_2\} \\
p_4 &= \{u_2, v_2\}
\end{aligned}
\qquad \text{(IX.5)}
$$

We wish to, at least initially, develop grammars which only operate on such orthogonally oriented rectangles, and whose production rules only result in the generation of such rectangle. Furthermore, cladding and patterning grammars presume that the field of a surface under consideration is wholly covered with such rectangular elements, i.e. there are no gaps in the field or regions where non-rectangular shapes appear. For production rules to

define a closure operator on orthogonally oriented rectangles, all resulting shapes of production rules in the grammar must produce rectangles.

We thus define the closure operators (addition, subtraction, product) on rectangles, in such a way that all compositions of packed rectangles are admitted, and only packed rectangular configurations are produced. As a conventional grammar or $\mathbf{R}^2$ shapes and boundaries, problems begin to emerge.

Consider the subtraction operations shown in Figure IX-36, adhering to the operations on shapes and their boundaries as defined by Earl[24]. The configuration shown in Figure IX-36A produces a valid configuration of rectangles. However, the configuration in Figure IX-36B does not. In order for subtraction operations on rectangles to provide a closure operator on rectangles, we may and in fact must define a new subtraction operation specific to this class of objects, shown in Figure IX-36C. This rule results in the production of up to four rectangles, as demonstrated in Figure IX-36D.

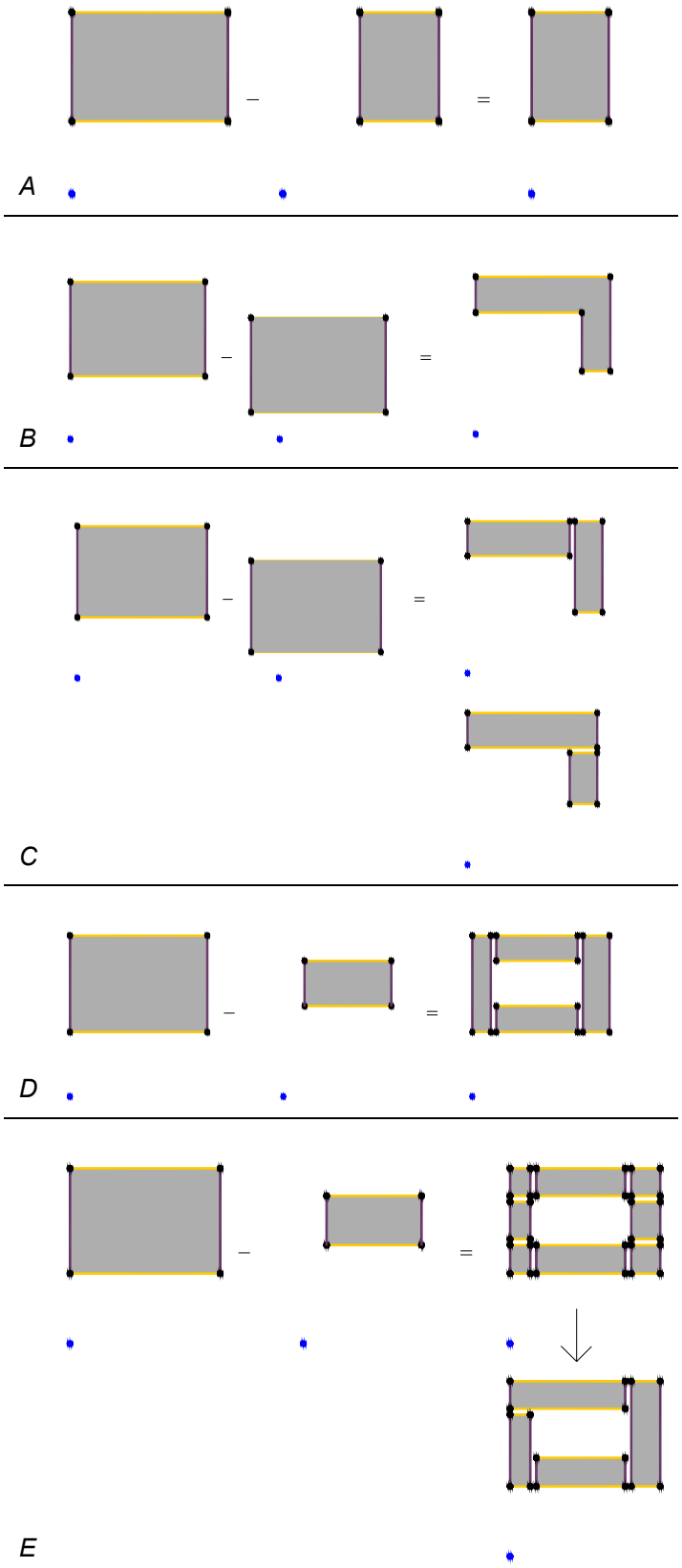

Figure IX-36: Rectangle subtraction operations

Furthermore, the resulting production is ambiguous, since either the resulting top or right rectangle can extend into the upper right corner.

The most unambiguous resolution of this condition is to resolve the production into the (8) possible resulting rectangles, then draw on subsequent union operations to select valid combinations of these rectangles, as shown in Figure IX-36E. We may define the subtraction operation on rectangles as an operation that takes an operator and operand rectangles, and returns (8) rectangles in the configuration shown in Figure IX-36E, of which, depending on the configuration of the input rectangles, any of the returned rectangles may be the empty shape ∅.

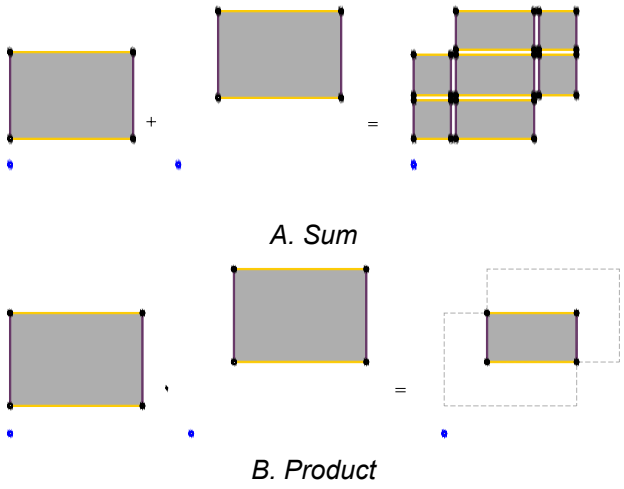

Figure IX-37: Rectangle Boolean operators

Similar considerations must be made for the sum operator (+), shown in Figure IX-37A. The product operator (•, Figure IX-37B) and subshape relation (<) are no different than those on more general $\mathbf{R}^2$ regions and their boundaries.

The Boolean operations on rectangles suggest the definition of alternatives to the subdivision grammars proposed in Section IX.A. One limitation of the recursive subdivision approach is that localized, non optimal configurations typically crop up, since each subdivision operates only on a local region without the possibility of performing operations across these recursively defined regions. The grammars shown in Figure IX-38 operate in an integer parametric space $\mathbf{I}^2$. Starting with a space populated with rectangle cells of unit side, the approach selects candidate rectangles to be extended in some direction, as well as subdivided. Heuristics are applied to determine whether the new configuration is an improvement on the prior rectangle assembly. This approach can still result in local optima, but configurations are not rigidly limited by the structuring of prior decisions. In this example, a simulated annealing approach has been applied, where locally non-optimal changes to the rectangle organization are stochastically applied, with a probability that decreases over time.

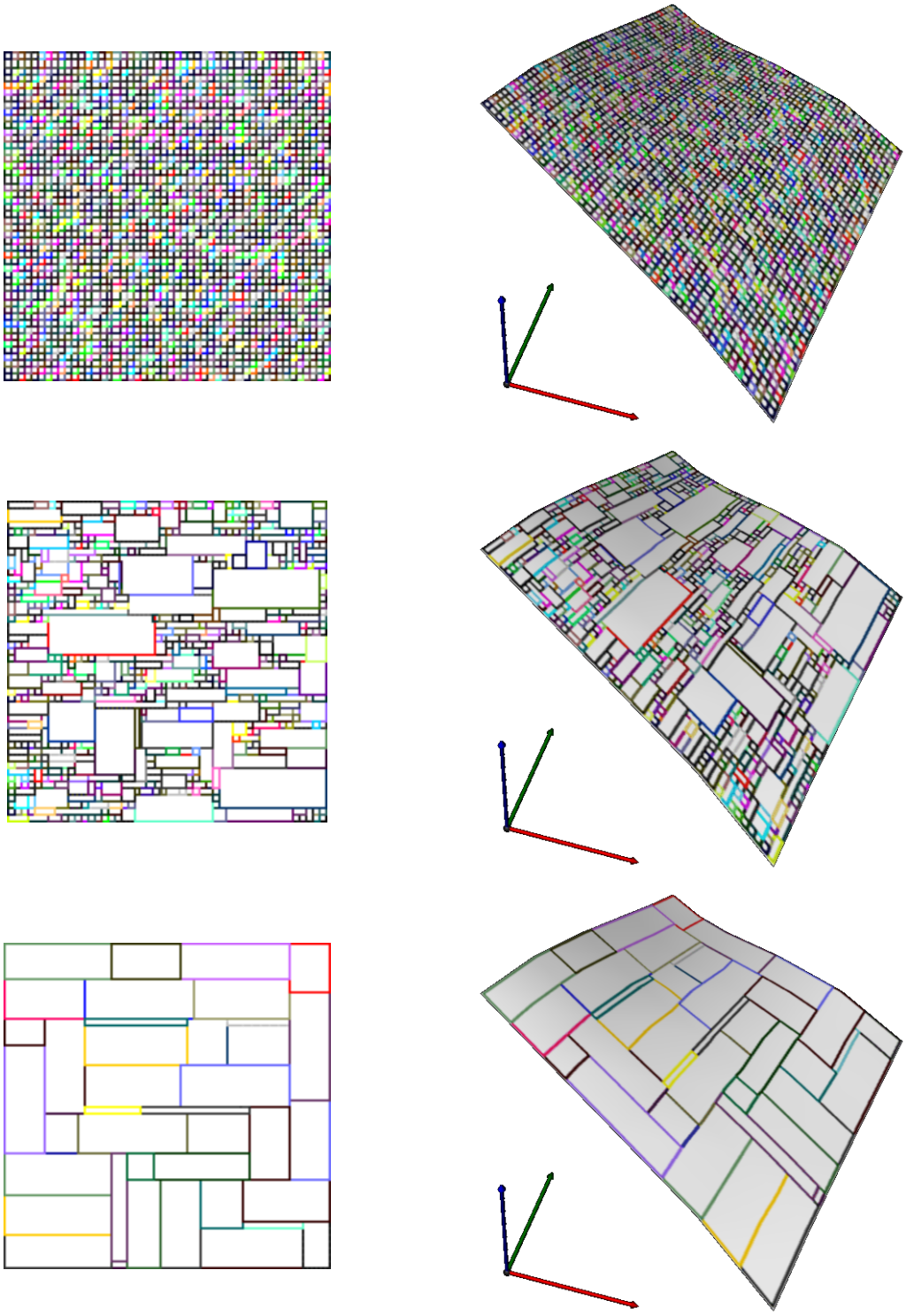

Figure IX-38: Mapping of the parametric space rectangle grammar

Feature behaviors

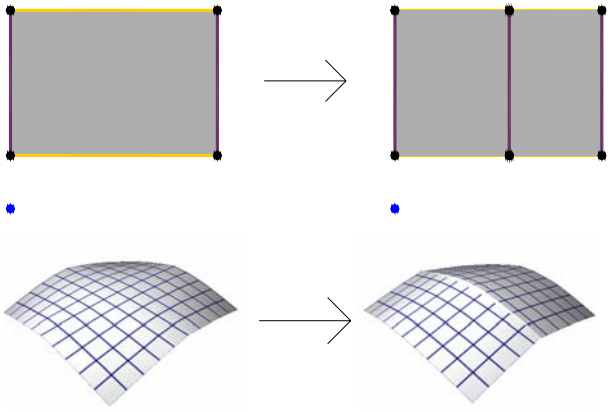

Figure IX-39: Basic rectangle split operation

Our basic notion of splitting the assembly at sheet edges, introducing surface discontinuities at sheet edges (Section IX.B.2) provides an initial strategy for surface rationalization. In practical constructibility applications, it is appropriate to imagine small scale surface discontinuities between sheets, discontinuities which are addressed in fabrication by overlapping sheets. These discontinuities locally relieve the stress on the surface induced by the macro scale surface curvature, as described in Section I.A.

Figure IX-39 suggests an extension of this strategy, where the splitting operation is accompanied by a behavior on rectangle edge features, that attempts to repair the gap between sheets induced by the combined actions of sheet splitting and localized surface curvature. We can extend our definition of the rectangle object to accommodate rectangles with feature behaviors of the types shown in Figure IX-25. Symmetries of these features then join neighboring rectangles, according to the rules defined in Section IX.B.2

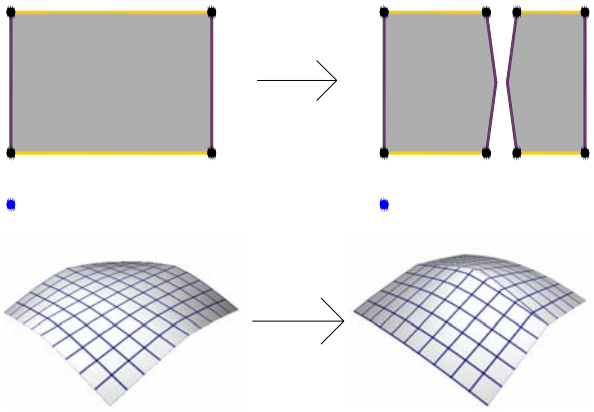

Figure IX-40: Basic rectangle split operation

The placement of surface discontinuities in the rationalized surface assembly was identified as the most important mechanism by which surface rationalization occurs. Our generative approach needs to include a strategy that makes best use of these features in generating a rationalized surface responding to the design surface. The previous discussions of surface curvature and approximations of the surface curvature of meshes provide some guidance.

As a point of departure for this discussion, we consider the implications of design surface curvature on splitting discontinuities in the rationalized shape. Figure IX-41 shows sheets mapped to attractor surfaces with positive and negative curvature. Split continuities are introduced on the sheet, while the ends points of the split are bound together. The identical feature produces *opposing* effects at the discontinuity (Figure IX-41C). Positive curvature surfaces result in the surface splitting open, and the edges of the discontinuity moving apart in space. Negative curvature results in the edges overlapping in space. These effects are most pronounced at the mid point of the split.

If we are interested in repairing the sheet at the discontinuity, we adjust the split feature's shape, by adding material to close the gap in the positive curvature case, and removing material to reduce the overlap in the case negative curvature. Figure IX-41D shows this strategy in the parametric space of the sheet, while Figure IX-41E shows the resulting sheet configuration in $\mathbf{R}^3$.

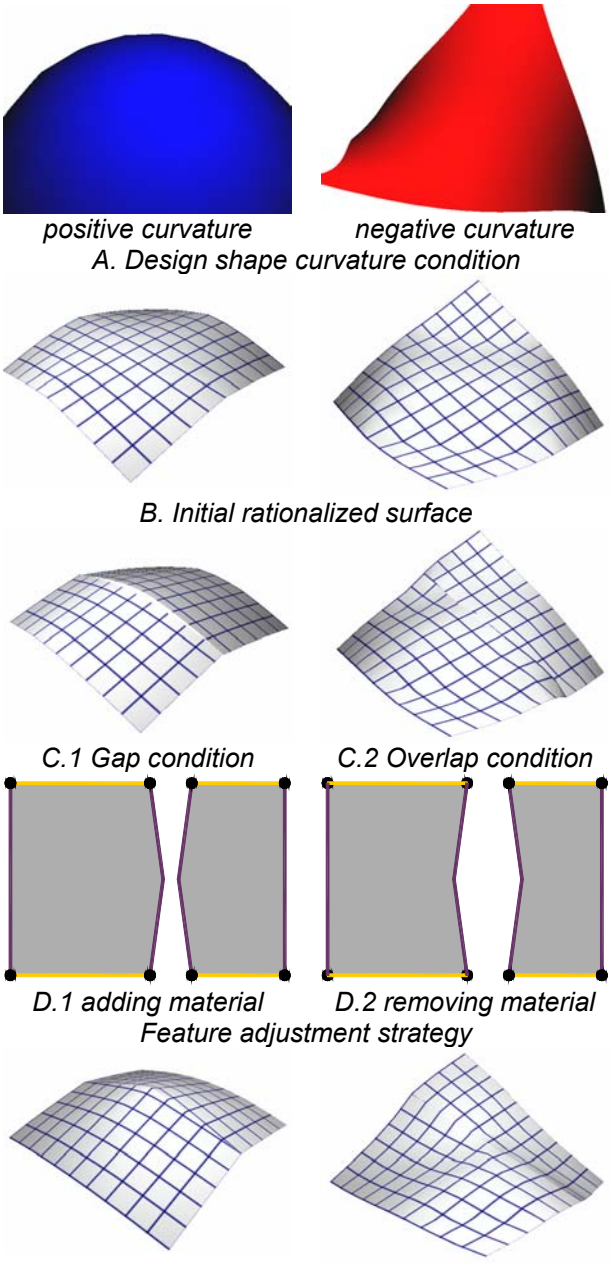

Figure IX-41: Feature generation response to design shape curvature

This understanding can be drawn on in if we are interested in inducing curvature into the shape of the sheet assembly. For conditions where we want to impose positive curvature, we introduce convex features, bulging outward from the respective boundaries of the sheets on

either side of the feature. For conditions where negative curvature is desired, we introduce a concave feature pair.

The discussion of gaussian curvature approximation on meshes (Section IX.B.3) provides the differential geometric analysis of this phenomenon. Consider the sheet conditions at the vertex of the split feature in Figure IX-41D.1. The interior angles are somewhat less than 180 degrees, in turn the sum of these two angles will be less than 360 degrees, or 2π radians. In the $\mathbf{R}^3$ configuration, the two features are joined together. If we assume negligible angular deformation of the sheets in $\mathbf{R}^3$ the numerator of Equation (IX.2) will be > 0, and the resulting gaussian curvature κ_G will be positive. In Figure IX-41D.2, the opposite effect occurs. The sum of the interior angles is now > 2π, corresponding to a negative curvature condition. At any other point along the edge the line feature pairs are straight and the angles sum to 2π, so the numerator (IX.2) – hence the induced gaussian curvature – is 0 . At the ends of the feature, the angles do not sum to 2π, but these vertices are open along the exterior boundary of the sheets so the above discussion does not apply. In practice, the material solution will result in some stretching of the material as a result of the sharp curvature discontinuity at the mid vertex, and curvature will propagate along the feature to a certain extent.

We may draw on this observation to derive a strategy for inducing gaussian curvature into the mesh through the shapes of paired edge features. We sample the gaussian curvature of the design surface corresponding to the closest point on the design surface to a given mesh vertex. Substituting (IX.3) into (IX.2), using small angle approximation, and drawing on the symmetries of Figure IX-42, we derive an equation for the induced angle:

$$\beta \cong \frac{\pi\gamma}{1+\gamma} \qquad \text{(IX.6)}$$

where

$$\gamma = \frac{\kappa_G l^2}{8}$$

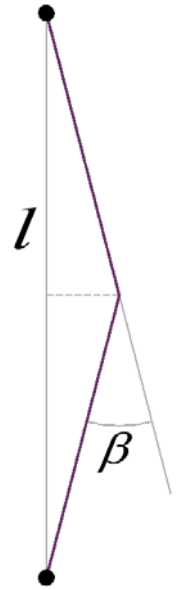

Figure IX-42: Curvature – angle relationship

This angle will be curve the edges toward the body of the

mesh regions in the case of positive gaussian curvature, and away from the body of the case of negative curvature. Figure IX-42 illustrates this strategy.

The constructs defined in this section allow many possible schemes for rationaling surface assemblies into valied configurations of material sheets. Figure IX-43 shows results of this approach, where several of subdivision grammars have been applied to test surfaces.

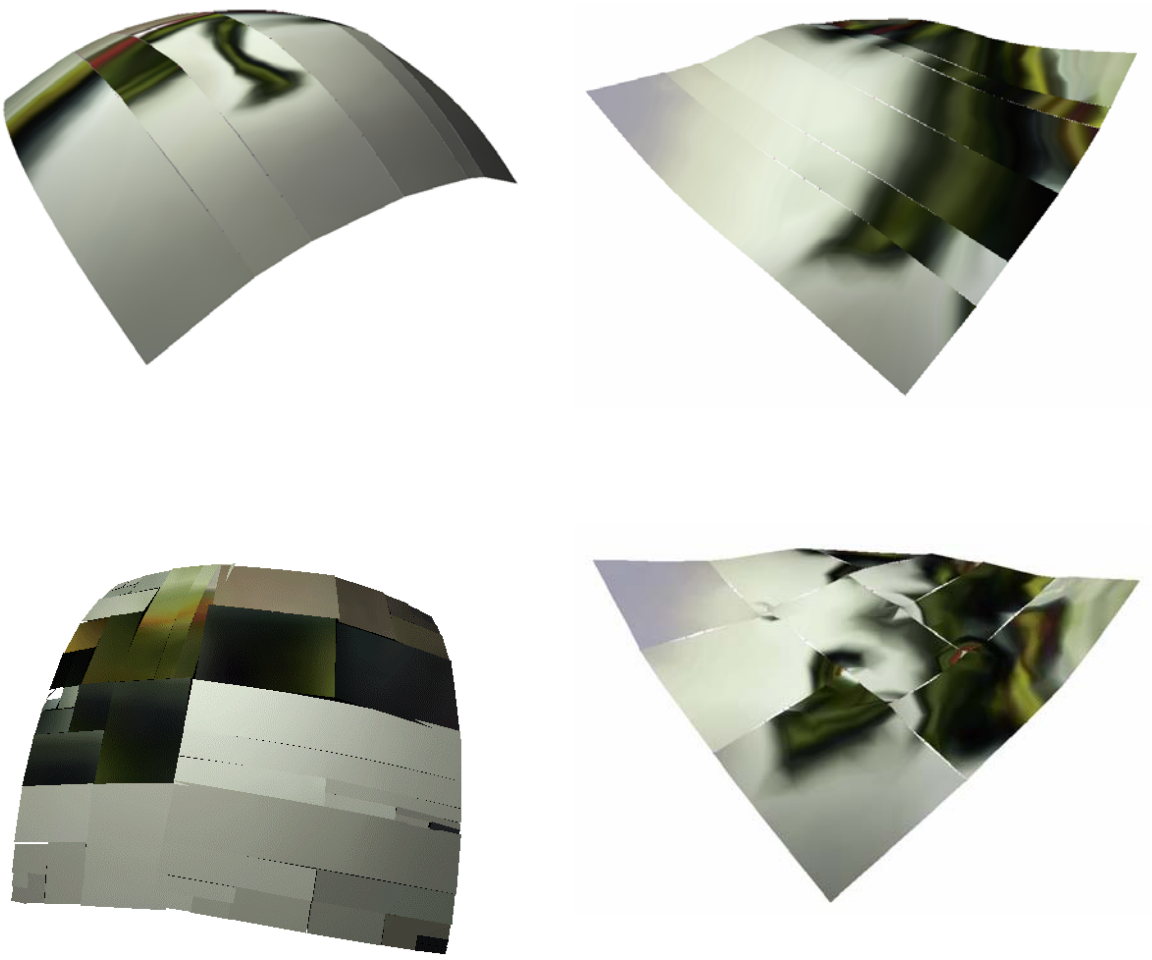

Figure IX-43: Applications of the materials based rationalization grammars

CONCLUSION

This thesis has documented efforts to describe computationally one aspect of Gehry's architecture: a set of paper surface forms whose nature is defined by the intersection of a broad set of aesthetic, material and fabrication intentions. A geometric definition of these surface forms has been developed within the framework of shape grammars. With this vocabulary of shapes and operations on shapes defined in a computationally rigorous manner, it has been possible to develop applications, operating within the space of paper surface configurations, which automate the solution of certain design and constructibility problems. This inquiry has deliberately avoided attempting to formalize the more elusive, evocative elements of Gehry's design intentions, focusing rather on the design development decisions regarding the constructibility of forms, for which explicit geometric rules are often defined. The automation of repetitive, lower level design operations associated with the propagation of system design decisions across the variations in project geometry is deemed to be of great value to the firm's process. At the same time, these rationalization decisions can have substantial impact on the project design intent, in addition to their more direct implications on building performance and fabrication economies, and are positioned within the broad scope of design decisions resulting in the ultimate development of the project form.

It is suggested that this specific inquiry of surface forms is indicative of broader opportunities for computation in design theory and practice. Gehry's ambitious formal explorations have resulted in new vocabularies of architectural forms. In order to realize these forms, explicit descriptions of these vocabularies must be developed to communicate design intent across the spectrum of building activities. Digital media present broad new capabilities that can allow new design intentions to be communicated in a formally rigorous manner.

However, this rewriting of the rules of architectural communication can not be undertaken in a thoughtless manner. Computing methodologies bring an inherent structure and logic to the products and processes they support. This explicit structuring renders transparent the underlying assumptions for their construction, and allows these assumptions to be critically assessed. At the same time, the definition of any formal descriptive structure unambiguously not only defines a class of intentions admissible in this framework, but also imposes limits to intentions admissible in the framework, and by implication suggests a world of possibility for which the framework has no application. A firm understanding of these qualities of

computation, integrated with a rigorous understanding of the conventions and historical development of building process, must be achieved for computing applications to appropriately serve design. When computational structures are inappropriately applied, the structuring of a computational framework limits descriptive capabilities in critical and disadvantageous ways. Alternatively, when a synergy between the logic of computation and that of the activities of design is achieved, the result is not simply tools to support existing processes, but rather the disclosure and critique of the supported process and, perhaps, the identification of new opportunities and avenues for design.

`

BIBLIOGRAPHY

1. AISC, Manual of Steel Construction: Allowable Stress Design, 9th Edition. AISC, Chicago, IL, 1989.

2. Alexandrov, P.S. Combinatorial Topology. Dover Publications, NY, 1960.

3. Aumann, G. Interpolation with Developable Bézier Patches. Computer Aided Geometric Design, 8:409-420, 1991.

4. Baraff, D., Witkin, A., and Katz, M. An Introduction to Physically Based Modeling. Siggraph Course Notes, 1997.

5. Baraff, D., and Witkin, A. Large Steps in Cloth Simulation. SIGGRAPH '98 Proceedings.

6. Bennis, C., Vezien, J., Iglesias, G., and Gagalowicz, A. Piecewise Surface Flattening for Non-Distorted Texture Mapping. Computer Graphics (Proceedings of SIGGRAPH 91) **25** 4, 1991: 237-246.

7. Bishop, R., and Goldberg, S. Tensor Analysis on Manifolds. Dover Publications, NY, 1980.

8. Borischenko, A., and Tarapov, I. Vector and Tensor Analysis with Applications. Dover Publications, NY, 1979.

9. Boddului, Ravani. Design Of Developable Surfaces Using Duality Between Plane And Point Geometries. Computer Aided Design **25** (1993): 621-632.

10. Ibid, p. 622.

11. Boddului, Ravani. Geometric Design and Fabrication of Developable Surfaces. ASMD Advanced Design Automation **2** (1992),: 243-250.

12. Bonola, R. Non-Euclidean Geometry. Dover Publications, NY, 1955.

13. Bowyer, A., and Woodwark, J. A Programmer's Geometry. Butterworth's, London, 1983.

14. Ibid, p. 104.

15. Breen, D. A Particle Based Model for Simulating the Draping Behavior of Woven Cloth. doctoral dissertation, Rensalaer Polytechnic Institute, 1993.

16. Burry, MC. Parametric Design and the Sagrada Familia. Architecture Research Quarterly, UK, 1996.

17. Campagna, S., and Seidel, H. Parameterization of Meshes with Arbitrary Topology. In Image and Multidimensional Digital Signal Processing 1998: 287-290.

18. Ceccato, C., Glymph, G., Shelden, D., et. al. A Parametric Strategy for Freeform Glass Structures Using Quadrilateral Planar Glass Facets. Submitted, Acadia 2002 Conference Proceedings.

19. Chalfant, J. Analysis and Design of Developable surfaces for Shipbuilding. Masters Thesis in Naval Architecture and Mechanical Engineering, MIT, 1997.

20. Chen, Q. Simulation of Wind Around the Stata Complex at MIT. Research report, 1999.

21. Colomina, B. The House that Built Gehry. in Ragheb, 2001: 300-321.

22. Desbrun, M. Meyer, M., Alliez, P. Intrinsic Parameterization of Surface Meshes. Eurographics 2002, **21** 2.

23. DeSimone, V., and Roorda, D. Structure as Art. Civil Engineering, June 2002: 40-47.

24. Earl, C.F. Shape Boundaries. Environment and Planning : Planning and Design 24: 669-687.

25. Earl, C.F. Generated Designs: Structure and Composition. Artificial Intelligence in Engineering Design **13**, 1999: 277-285.

26. Feynman, C. Modeling the Appearance of Cloth. Masters Thesis, MIT, 1986.

27. Friedman, M., and Ragheb, J. (ed). Frank Gehry, Architect, Exhibition Catalog. Guggenheim Museum Publications, NY, 2001.

28. Foley, J., VanDam, A, et. al. Computer Graphics Principles and Practice, 2nd Edition. Addison Wesley, NY, 1990.

29. Ibid: 521-523.

30. Floater, M. Parameterization and Smooth Approximation of Surface Triangulations. Computer aided Geometric Design **14** 3, 1997: 231-250.

31. Fuller, R. Buckminster. Synergetics. Macmillan Publishing, NY, 1982: 701-717.

32. Gasson, P. Geometry of Spatial Forms. Ellis Horwood Limited, NY, 1983: 312-319.

33. Frank O. Gehry & Associates. Exterior Closure Metal Systems Bid Package. Experience Music Project, Seattle Washington, May 20, 1997.

34. Glymph, J., informal conversations, 1997-2002.

35. Grimm, C., and Hughes, J. Modeling Surface with Arbitrary Topology Using Manifolds. SIGGRAPH '95: 359-368.

36. Guggenheimer, H. Differential Geometry. Dover Publications, NY, 1977.

37. Hamann, B. Curvature Approximation for Triangulated Surfaces. In G. Farin, et. al., editor, *Geometric Modeling*, Springer Verlag, 1993, p139-153.

38. Heath T. (trans). The Thirteen Books of Euclid's Elements. Dover Publications, NY, 1956.

39. Henle, M. A Combinatorial Introduction to Topology. Dover Publications, NY, 1979.

40. Haymaker, J. and Fischer, M. Challenges and Benefits of 4D Modeling on the Walt Disney Concert Hall Project. CIFE Working Paper #64, Stanford University, Stanford, CA, 2001.

41. JaeHong, L. Frank O. Gehry, Museums and Cultural Institutions 1984-1996. Korean Architects, Seoul, 1996.

42. Ibid: 17.

43. Jänich, K. Topology. Springer-Verlag, Berlin, 1980.

44. Kostof, S. A History of Architecture: Settings and Rituals, Oxford University Press, 1985: 651,702.

45. Krishnamurti, R. The Arithmetic of Shapes. Environment and Planning B **7**, 1980: 463-484.

46. Krishnamurti, R. The Construction of Shapes. Environment and Planning B **8**, 1980: 5-40.

47. Kreysig, E. Differential Geometry. Dover Publications, NY, 1981.

48. ibid: 179-180.

49. ibid: 185.

50. Lang, Roschel. Developable (1,n) Bézier Surfaces. Computer Aided Geometric Design **9** 1992: 291-298.

51. Lewis, S. Structural Steel Detailing Neutral File: Electronic Data Interface Between Structural Engineers and Fabricators. Fluor Daniel internal report.

52. Lindsey, B. Digital Gehry, Material Resistance, Digital Construction. Basel: Birkhauser, 2001.

53. Marsden, J. and Hughes, T. Mathematical Foundations of Elasticity. Dover Publications, NY, 1983.

54. Mayer, Gerhard. Personal interview on Weatherhead project. Conducted June 15, 2002.

55. McCullough, M. Abstracting Craft: The Practiced Digital Hand. MIT Press, Cambridge, MA, 1997: 229.

56. Meyer, M., Desbrun, M. et. al. Discrete Differential-Geometry Operators for Triangulated 2-Manifolds. Submitted, found at http://www.multires.caltech.edu/pubs/diffGeoOps.pdf, 2002.

57. Mitchell, W. J. Roll Over Euclid. In Ragheb, 2001: 353-364.

58. Mitchell, W. J. The Logic of Architecture : Design, Computation, and Cognition. MIT Press, Cambridge, MA, 1990.

59. Ng, H., Grimsdale, R. Computer Graphics Techniques for Modeling Cloth. *IEEE Computer Graphics and Applications*, 1996: 28-41.

60. O'Neill, B. Elementary Differential Geometry, 2nd Edition. Academic Press, 1997.

61. ibid: 58.

62. ibid: 87.

63. Packard, R. (ed). Architectural Graphic Standards, 7th edition, John Wiley & Sons, NY., 1981: 325-328.

64. Piegl, L., and Tiller, W. The NURBS Book, 2nd Edition. Springer, NY, 1997.

65. ibid: 233-234.

66. Post, N. and Daniels, S. Plum Job in Seattle Lifts Haze Over Technology. Engineering News Record, February 28, 2000: 76-83.

67. Pottman, Farin. Developable Rational Bézier and B-spline Surfaces. *Computer Aided Geometric Design* **12**, 1995: 513-531.

68. Pottman, Wallner. Approximation Algorithms for Developable Surfaces. Computer Aided Geometric Design 16 (1999), 539-556.

69. Press, W.H., Flannery, B.P., Vetterling, W.T. Numerical Recipies. Cambridge University Press, 1986.

70. ibid: 83-89.

71. Provot, X. Deformation Constraints in a Mass-Spring Model to Describe Rigid Cloth Behavior. Proceedings Of Graphics Interface, 1995: 147-154.

72. Ragheb, J. F., Editor. Frank Gehry, Architect. New York: Guggenheim Museum Publications, 2001.

73. Roe, A. Cleveland Gets a Case of Gehry's Totally Unreserved Architecture. Engineering News Record, May 27, 2002: 44-45.

74. Rogers, D. An Introduction to NURBS, with Historical Perspective. Kaufman, San Francisco, 2001.

75. Sheffer, A., and De Struler, E. Surface Parameterization for Meshing by Triangulation Flattening. Proceedings of the 9th International Meshing Roundtable, Sandia National Laboratories, 2000: 161-172.

76. Shewchuk, J. An Introduction to the Conjugate Gradient Method Without the Agonizing Pain. Technical Report CMU-CS-TR-94-125, Carnegie Mellon University, 1994.

77. Shewchuk, J. Triangle: Engineering a 2D Quality Mesh Generator and Delaunay Triangulator. First Workshop on Applied Computational Geometry, Association for Computing Machinery Philadelphia, PA, 1996: 124-133.

78. Stiny, G. Introduction to Shape and Shape Grammars. Environment and Planning B **7**, 1980: 343-351.

79. Stiny, G. Shapes are Individuals. Environment and Planning B **9**, 1982: 359-367.

80. Stiny, G. What is a Design? Environment and Planning B **17**1990: 97-103.

81. Stiny, G. Two Exercises in Formal Composition. Environment and Planning B **3**, 1976: 187-210.

82. Stiny, G. Weights. Environment and Planning B **19**, 1992: S49-S78.

83. Stiny, G. Shape Rules: Closure, Continuity and Emergence. Environment and Planning B **19**, 1994: 413-430.

84. Stiny, G., and Gips, J. Production Systems and Grammars: a Uniform Characterization. Environment and Planning B **7**, 1980: 399-408.

85. Stiny, G., and Gips, J. Shape Grammars And The Generative Specification Of Painting And Sculpture. Information Processing **71**, 1972: 1460-1465.

86. Stiny, G., and Mitchell, W J. The Grammar of Paradise: on the generation of Mughul gardens. Environment and Planning B **7**, 1980: 209-226.

87. Struik, D. Lectures on Classical Differential Geometry, 2nd Edition. Dover Publications, NY, 1961.

88. Synge, J., and Schild, A. Tensor Calculus. Dover Publications, NY, 1978.

89. Terzopolous, D., J. Platt, A. Barr and K. Fleisher. Elastically Deformable Models. Computer Graphics, V **21** 4, 1987: 205-214.

90. Trudeau, R. Introduction to Graph Theory. Dover Publications, NY, 1993.

91. Sedgewick, R. Algorithms in C. Addison Wesley, NY, 1990

92. Wang, C., Chen, S., and Yuen, M. Surface Flattening Based on Energy Model. Accepted, Computer Aided Design.

93. Wang, C., Chen, S., Fan, J., and Yuen, M. Two-dimensional trimmed Surface Development Using a Physics-based Model. in Proceedings of the 25th Design Automation Conference, 1999.

94. Weil, J. The Synthesis of Cloth Objects. Computer Graphics, 20, 1,1986: 49-54.

95. Yeh, B. Obtaining data from complex physical models. FOG/A research document 11039802, 1998.

96. Futagawa, Y. (ed). Frank O. Gehry: 13 Projects Since Bilbao. GA Document 68, A.D.A. EDITA, Tokyo, Japan, 2002.

97. Meek, DS and Walton, DJ. Approximation of Discrete Data by G^1 Arc Splines. Computer Aided Design, **24** 6, 1992.